INFRARED SPECTRA OF LATE-TYPE STARS

Thesis by

Jay Albert Frogel

In Partial Fulfillment of the Requirements

for the Degree of

Doctor of Philosophy

California Institute of Technology

Pasadena, California

1971

(Submitted January 28, 1971)

To My Parents

for Constant Encouragement

and Love

"In attempts at physical interpretation of these variables, the emphasis would seem to belong on conformity rather than on individual variation."

Paul W. Merrill, 1952

ACKNOWLEDGEMENTS

Prof. W.L.W. Sargent, H.M.P., once asked me: "Why don't you look into infrared astronomy?" This thesis is a partial result of that inquiry.

Prof. G. Neugebauer made this thesis possible by allowing me to use the infrared spectrometer and photometer and making available to me the facilities of the IR lab. He has instilled in me what I consider to be a proper, critical attitude toward data and their interpretation. Also, Gerry gave me one of his 100-inch runs when the 60-inch was down.

I have had several interesting and stimulating conversations with my adviser Prof. G. Münch. He pointed out to me the importance of turbulence in late-type stars and the fact that the path length of formation of a CO line will be considerably greater than that of a metallic line. He directed me to some important references and suggested several improvements to a first draft of this thesis.

Dr. A. R. Hyland taught me most of what I know abour IR spectroscopy. He suggested the observation of long period variable stars as a thesis project and helped considerably in the initial data reduction. He gave generously of his observing time when inclement weather prevented me from observing all of the variables during my runs. He took me on as a collaborator on a spectroscopic survey of late-type giants and supergiants and left me to finish the project when he returned to Australia. The spectra of Lalande 21185 and Wolf 359 were obtained during his 200-inch runs. We have had innumerable conver-

sations, relevant and otherwise, which often resulted in ideas for new ways of approaching an understanding of the data we have accumulated. Harry gave me encouragement, moral support, and friendship. I am grateful for everything.

Dr. E.E. Becklin taught me how to use the IR photometer and observed with me for several nights on the 24-inch to make sure I knew what I was doing. He has often patiently listened while I expounded my latest theory.

Harvey Butcher, Dr. Ian Glass, Paul Harvey, Ken Hultman, Alex Law, Frank Porter, Ed Ritz, Bob Toombs, Henry Tye, and Glen Veeder assisted in various ways with the observations.

Dr. T. Hilgeman provided me with some of his computer programs and suggested several ways of handling the data and provided assistance in the early stages of observing.

G. Forrester has been mostly responsible for keeping all of the electronics in working order. I am especially grateful to him for this.

I would like to thank Prof. J.L. Greetstein for a useful discussion about stellar evolution and stellar abundances.

V.G. Kunde provided me with some useful computations of CO absorption profiles and I have had several interesting discussions with him about molecular absorption. Dr. D. Carbon provided me with some model atmosphere calculations. Dr. J. Auman's talk in Tucson led me to investigate possible abundance differences between variables and non-variables. Dr. R.I. Thompson gave me material in advance of publication. Dr. S. Price provided me with some details

of his CN absorption calculations.

I acknowledge support from a NDEA Fellowship, a NASA Traineship, and a G&A.

Finally, I thank Eugene Hancock and Gary Tuton and Mario Jacquez for their general attitude.

ABSTRACT

Spectra have been obtained in the 2μ atmospheric window with a resolution of 32 and 65 Å of late-type dwarfs, giants, supergiants, and long period variables.

In the non-variable stars, the first overtone band of CO at 2.29μ shows a systematic increase with both increasing luminosity and decreasing temperature. This increasing strength is interpreted as arising from an increase in turbulence and a decrease in atmospheric opacity. The 1.87μ band of H_2O appears only in stars of spectral type M6 and later. The observed strength of this band is considerably weaker than that predicted by model atmospheres. Strong bands of $C^{13}O^{16}$ are visible in most of the stars, and they are interpreted as indicating a number ratio $[C^{12}/C^{13}] < 10$.

Variations in the strengths of the H_2O and CO bands were measured in 18 long period variables as well as variations in the continuum flux at 2.25μ, f(225). There is a phase lag between the visual and f(225) light curves in the sense that the maximum of the latter occurs after that of the former. The size of the lag is directly proportional to the range at 2.25μ. The molecular absorption bands are stronger in the variables than in the non-variables of the same spectral type. The value of $[C^{12}/C^{13}]$ for the variables is comparable to that for the non-variables.

There is evidence for differences in the value of [O/C] among the variable stars. NML Tau seems to have a value similar to that of U Ori, a typical M-type variable. R Aur, T Cas, χ Cyg, and RS Lib appear to have abnormally low values of [O/C].

A model involving the motion of a shock wave through the star's atmosphere is discussed as a possible means of explaining variations in both visual and infrared spectra.

The evolutionary history of and the effect of convective mixing in late-type stars is discussed and it is concluded that: 1.) the value of $[C^{12}/C^{13}]$ indicates that mixing has occurred; 2.) the degree of mixing may be greater in the non-variables than in the variables; 3.) the observations are not inconsistent with a high value of [O/C] in most of the stars observed, i.e. $[O/C] \sim 2$.

TABLE OF CONTENTS

PAPER I

PAPER II

SUMMARY

This thesis consists of two papers, the first of which will be published jointly with A. R. Hyland.

The data include a large number of spectra in the 2μ atmospheric window at a resolution of 32 or 65Å of late-type dwarfs, giants, supergiants, and long period variables. Photometry at 1.25, 1.65, 2.2, and 3.5μ was obtained for most of the objects. The spectra were corrected for telluric absorption and were calibrated on an absolute flux scale by comparison with early-type stars. The photometry was used to set up a temperature scale based on the J-L color.

The three main features of the spectra are the strong band of H_2O at 1.87μ, the strong first overtone band of CO at 2.29μ, and the numerous weaker absorption features. In the non-variable stars the strength of the CO band shows a strong increase with both decreasing temperature and increasing luminosity (Fig. 10a, Paper I). The water band is visible only in giants later than M5, is not visible in supergiants as late as M4, and is visible in the M8 dwarf Wolf 359 (Fig. 12, Paper I). The numerous weak absorption features also tend to increase in strength with decreasing temperature and increasing luminosity. Some of these have been identified as blends of atomic absorption lines. None, however, can be positively associated with any molecular absorption lines. In particular, absorption due to CN, SiO, and TiO seem to be absent from the spectra presented here (Figs. 8 and 9, Paper I).

Strong isotopic bands of $C^{13}O^{16}$ are visible in nearly all of the stars and have been interpreted as indicating a number ratio $[C^{12}/C^{13}] < 10$ (Fig. 11, Paper I). This value seems to be independent of spectral

type and luminosity for the giants and supergiants.

The increased band strengths observed in cooler and more luminous stars is interpreted as being due to a combination of decreased atmospheric opacity and increased turbulence in the region of band formation. It is noted that the variation with luminosity is opposite to that observed by Eggen (1967) in the near infrared. There is strong evidence that the band absorption cannot be characterized by a unique set of physical parameters. The strength of the 1.87μ H_2O band is considerably weaker than that predicted by model atmosphere calculations (Fig. 17).

The presence of strong $C^{13}O^{16}$ bands is interpreted as evidence for mixing of the surface material with material which has been processed through the CNO cycle. The surface abundances of C and O relative to H would then be expected to be considerably below the solar value. This may be reflected in the weakness of the H_2O band.

Eighteen variable stars were observed with varying degrees of completeness over all or part of their cycles. The variations of the continuum flux at 2.25μ, f(225), and the strengths of the CO and H_2O bands were studied in some detail. The variations of these quantities are out of phase with one another and with the visual light curve. The order in which the various maxima generally occur is visual, f(225), CO and H_2O. The phase lag between the visual and f(225) light curves is directly proportional to the range at 2.25μ and increases with decreasing mean temperature.

The maximum absorption strength of the H_2O band in each star is inversely proportional to the temperature at the time of maximum strength and seems to be a continuation of the mean relation established

for the non-variable stars in Paper I except that the variables have systematically stronger water absorption than the non-variables of the same spectral type or temperature (Figs. 3 and 5, Paper II). The maximum CO strength, on the other hand, increases only slightly if at all with decreasing temperature at the time of maximum strength. The difference between the variables and non-variables is in the same direction as for the H_2O band but it is not as great. The minimum CO band strength for each variable decreases with decreasing temperature (Figs. 3 and 5, Paper II). The mean value of the ratio $[C^{12}/C^{13}]$ for the variables is comparable to and perhaps slightly stronger than the value for non-variables of the same spectral type (Fig. 6, Paper II.

Four of the variables observed show evidence for a lower value of [O/C] than the remainder. These are R Aur, T Cas, χ Cyg, and RS Lib. Other authors have also observed that the first three stars have some S-type characteristics. Arguments have been given to show that NML Tau has a [O/C] value characteristic of other M-type long period variables, and in particular is quite similar to U Ori and does not possess S-type characteristics as has been claimed by some authors.

Observations of absorption and emission lines in visual spectra have been summarized. A schematic model involving a shock front propagating upward from the photosphere was discussed and was seen to account for the general behavior of the visual spectra. This model is essentially a synthesis of ideas proposed by other authors.

The increased continuous opacity at longer wavelengths and the finite time required for a disturbance to move from lower to higher layers could be an explanation for the fact that the phase lag between the

visual light curve and that at another wavelength increases as the wavelength is increased. That the H_2O absorption maximum always occurs after the CO maximum suggests that the region responsible for the H_2O absorption is higher than that in which the CO absorption primarily occurs. This might be expected since H_2O becomes fully associated at a much cooler temperature than CO (Fig. 9, Paper II).

The maximum absorption strength of CO and H_2O for a given star seems associated with a hotter temperature than occurs at minimum absorption strength, the opposite of the temperature-band strength relation observed between different stars (Paper I). This is interpreted as indicating that phenomena associated with the stars variability, for example an increase in the turbulence due to passage of the shock, dominate the molecular absorption spectrum. The observed rapidity of the rise to maximum strength of the H_2O band compared to the CO band, may arise from the H_2O being in a higher, less dense region where the effect of the shock may be greater than in more dense regions.

A comparison of the observations with model atmospheres (Fig. 10, Paper II) again indicates that the H_2O bands predicted by the models are too strong. It is suggested that radiation pressure may seriously affect the distribution of the H_2O molecules.

Observational and theoretical results bearing on the evolutionary history of and abundances in late-type stars are discussed and evaluated. It is concluded that observed band strength differences between the variables and the non-variables may be due to differences in the amount of convective mixing that has occurred in these stars as suggested by Auman (1970). As is the case with lithium, a small percentage of late-type

giants might have anomalously strong CO bands since, theoretically, they would not be expected to have undergone convective mixing (Wallerstein 1966) . It is also concluded that the observations presented here and by others are not inconsistent with a high value of [O/C] for most of the late-type stars rather than a value close to unity as has been suggested by some authors.

PAPER I

LATE-TYPE DWARFS, GIANTS, AND SUPERGIANTS

(with A. R. Hyland)

I. INTRODUCTION

A survey of astronomical literature published prior to the early sixties indicates a dearth of both theoretical and observational work on stars of spectral type later than K. Problems encountered in any theoretical treatment of these stars are especially severe. Knowledge of molecular absorption coefficients under conditions appropriate to stellar atmospheres is poor, and values of disassociation constants, especially for polyatomic species, are uncertain. Departures from the usually assumed conditions of LTE, plane-parallel structure, and dynamical stability are probably large. Particle condensation and mass loss play important roles but are little understood.

The last few years have seen a rapid growth of infrared observational techniques allowing intensive investigation of the spectral region where cool stars emit most of their energy. The observations of Pettit and Nicholson (1933) stood almost alone for several decades. Now, the measurement of radiation in the atmospheric windows longward of one micron have not only indicated new classes of objects, but have given new impetus to theoretical investigations of the old ones, namely late-type giants, supergiants, and long period variables.

The purpose of the present series of papers is to present medium resolution spectra, mostly in the 2μ window, of a large number of objects which emit a significant amount of their radiation in the infrared region. A preliminary, semi-quantitative analysis will be attempted in the context of what is known about these stars from other investigations.

Since there are strong bands of H_2O and CO in this region (and CN in the carbon stars), it is hoped that the observations will be able to serve as a guide to future theoretical work on the atmospheric structure and evolution of these stars. The spectra were obtained with an 0.5-meter Ebert-Fastie spectrometer operating at a resolution of 65Å/mm. The advantages of this instrument and the resolution employed are the number of objects which can be observed in a relatively short amount of time and the ease with which the spectra can be corrected for telluric absorption and be calibrated on an absolute flux scale. The main disadvantage is that while individual vibrational bands are well resolved, the rotational lines of molecules as well as closely spaced atomic lines are not, making identification difficult.

The present paper will be limited to non-variable giants and supergiants of normal chemical composition. Paper II will discuss observations of long period variable stars of types M and MS. Papers III and IV will consider stars of types C and S respectively. Observational techniques and the reduction procedures used will be discussed in detail here. Succeeding papers will be referred to as little as possible but free use will be made of results obtained in previous papers. No attempt has been made to provide a complete historical bibliography. Only those papers which directly influenced the author's thinking will be referred to.

II. OBSERVATIONAL TECHNIQUE

The spectra discussed in this and succeeding papers were obtained with an 0.5-m focal length Ebert-Fastie spectrometer used at the Cassegrain foci of the 60, 100, and 200-inch telescopes of the Hale Observatories. A physical description of the spectrometer has been given previously by McCammon, Münch, and Neugebauer (1967). This section, therefore, will be concerned primarily with a description of the observational techniques, the absolute calibration, and the elimination of telluric absorption features. The latter is most important as the major sources of error are due to incorrect or incomplete removal of such features.

A. Standard Procedure

Unless it is noted otherwise in the Journal of Observations, the instrumental set up and operating procedure described below were used during all observing runs. A circular entrance aperture of 4mm was used, thus making the spectrometer essentially slitless. Most of the objects were bright enough to allow the use of a 0.5 mm exit slit giving a resolution of 32.5Å with the grating used. This required that the seeing disc of a star be less than 0.5 mm, which corresponds to 4" on the 60", 2.5" on the 100" and 1.3"on the 200". If the seeing disc approached 1mm, a 1mm exit slit was used with a resulting resolution of 65Å and a gain of a factor of 2 in signal strength. For objects bright enough to be seen at a low enough amplifier gain to suppress all sky emission, two successive scans would be taken with a rapid scan on

empty sky after each object scan to check the level of background noise and to establish the zero level.

The scanning rate was 336 Å/min with an RC time constant of 0.5 sec on the signal amplifier. The time required between setting on one object, obtaining the spectra and setting on the next object averaged 40 min. If the object was faint enough so that sky emission would make a noticeable contribution to the total signal, the scans would be taken in the signal and reference beams alternately so that, when added together, the sky contribution would vanish. Although the monitor channel mentioned by McCammon, et al (1967) was available, it was not used in any quantitative manner. However, any systematic change in this reference level of more than a few percent was sufficient reason for rejecting the spectral scan. In general, the random noise fluctuations in the reference level ~~was~~ were considerably less than this for nearly all of the objects discussed in this paper. It was necessary to place all of the objects quite accurately in the aperture as the response of the detector was not flat over its area. Guiding had to be done very accurately as any motion in declination translated into a systematic wavelength shift, since this direction was perpendicular to the dispersion of the grating. Figure 1 shows two successive scans of the same object in the region of the CO bands. Both signal and reference channel are displayed.

B. Calibration

The primary standard used in the reduction of the spectra was α Lyrae. Its atmosphere in the 1.6 and 2μ region was assumed to be

Fig. 1. - Raw data from the chart recorder showing the region of the C0 bands on two consecutive scans of the same star and an early-type standard.

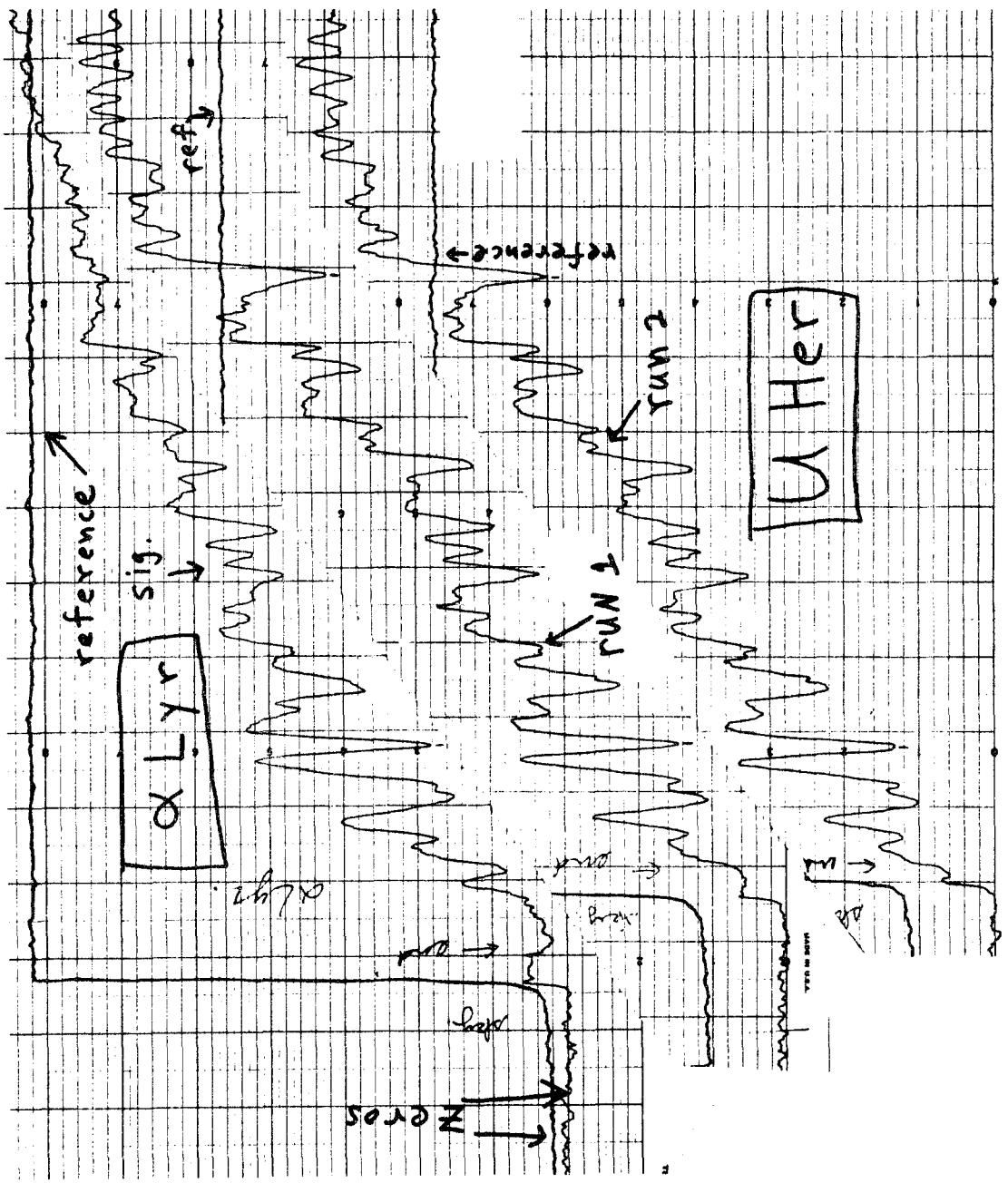

Figure 1.

that given by Gehlich (1968). The absolute flux of α Lyr was taken to be that given by Becklin (private communication). Secondary standards were α C Mi and α C Ma. The atmosphere of the former was determined empirically by averaging together scans obtained on several nights which had been reduced using α Lyr by the procedure to be described. The atmosphere of α C Ma was assumed to be the same as α Lyrae's. The latter's spectral type is AOV; the former's is AlV. A scale factor of .55 in log F_λ was applied to the atmosphere of α C Ma to take into account its being brighter than α Lyr. Spectra of stars reduced using α C Mi and α C Ma are virtually identical to the same spectra reduced with α Lyr. On a few nights, especially during the first quarter of 1969, the scans of these three standards were unusable. It was then necessary to use scans of these standards taken on some other night with very similar transmission characteristics. That this condition held, was determined by using non-variable stars which were in common to both nights, e.g. α Ursae Majoris. The error introduced by this procedure generally was less than 2 per cent in the most important spectral regions, i.e. from 2.0 - 2.4μ.

C. Telluric Absorption Features

Telluric absorption features show considerable variations in strength. The night to night variations in stars observed at the same air mass are often greater than the variations due to a difference of one air mass on any given night. From 2.09 to 2.27μ the atmosphere is essentially transparent except for some isolated absorption bands. Beyond 2.27μ, telluric H_2O bands become very strong. On any given

night, they may absorb 7 percent of the flux per air mass in this region. Shortward of 2.09μ telluric CO_2 bands become the principle absorber. The absorption in the center of the band at 2.0μ may be as great as 15 percent per air mass on any given night. Between the bands the absorption was considerably less and it was found that even when the band centers were poorly corrected the intensity between the bands provided a fair indication of the true intensity.

Because of the great sensitivity of the CO_2 bands to atmospheric extinction, the effectiveness of their removal from a stellar spectrum provided an excellent measure of how well the rest of the spectrum was corrected. By observing the standards and the objects at near equal air masses it was found that the region of the stellar CO bands could be corrected for atmospheric extinction to better than 5 percent and usually to better than 2 percent. Occasionally in some of the spectra presented here and in succeeding papers, the region of the telluric CO_2 band will appear excessively noisy. This is due to a slight wavelength shift between the standard and the object, not to poor correction. Improper correction will always make itself known by causing CO_2 bands to appear either in absorption or emission in the stellar spectrum. Spectra which are especially poorly corrected for telluric features will be noted in the Journal of Observations. Figure 2 is an example of two spectra of the same object on the same night but at different air masses.

D. Data Reduction

The scans were recorded in three ways: 1) a chart recorder

Fig. 2. - Two scans of αC Mi taken on the same night but with secant Z differing by 0.9. On this night the S/N ratio was down by more than a factor of 2 from usual as a less sensitive detector was in use.

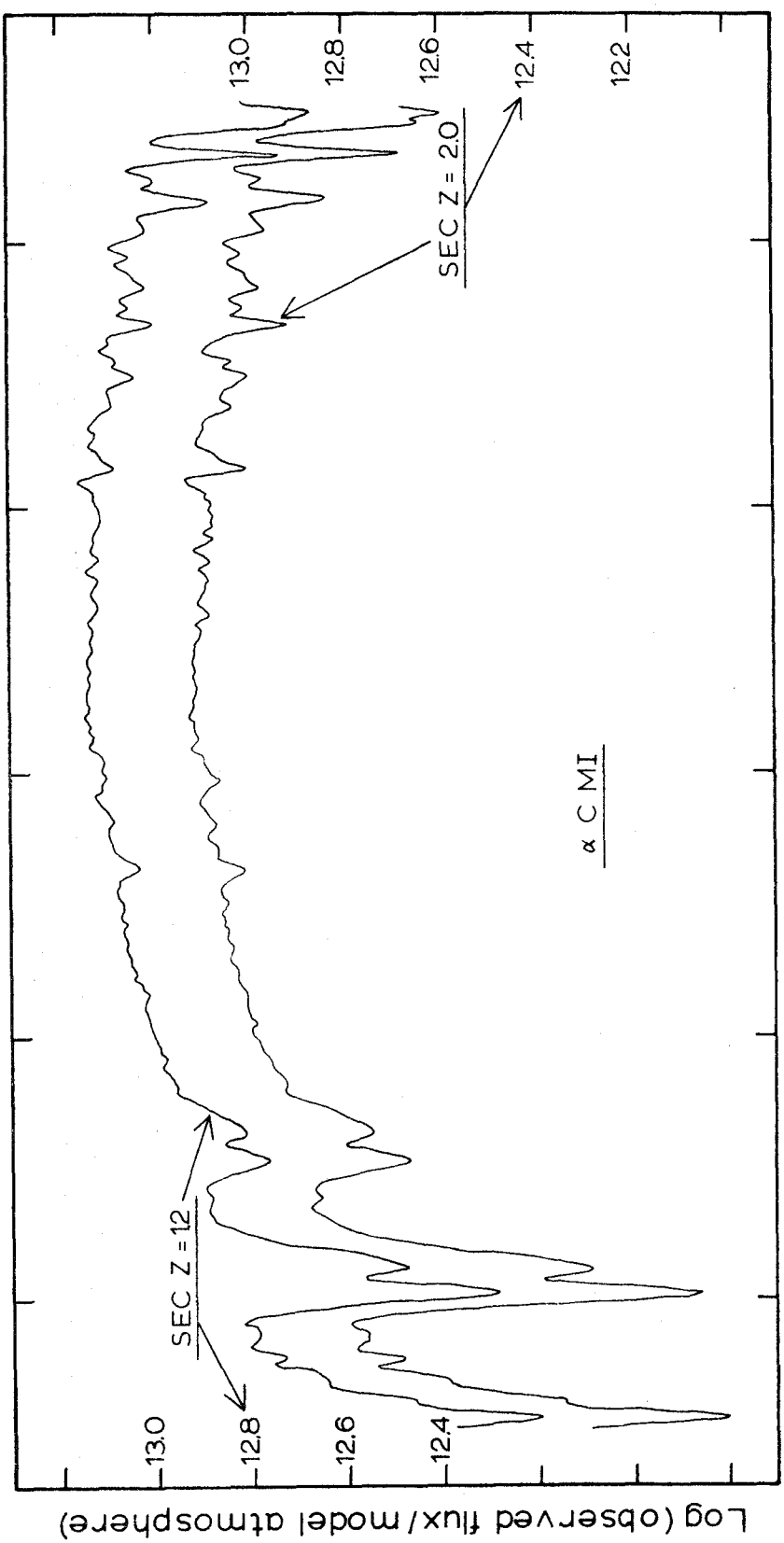
Log (observed flux/model atmosphere)
13.0
12.8
12.6
12.4
12.2
SEC Z = 12
SEC Z = 2.0
α C MI
2.0
2.1
2.2
2.3
2.4
λ (microns)

Figure 2.

which directly displayed the amplified outputs of signal and monitor channel; 2) a digital counter and printer with an integration time of 1.0 sec. and a recycle time of .2 sec.; 3) a digital magnetic tape recorder which sampled the output of the signal amplifier every .3 sec. When the output of system "3" was averaged in blocks of 4 points, the result was found to be identical to that of system "2". It was, therefore, possible to use these two systems as backups for one another. The first system was used primarily to judge the quality of the scans and to align individual scans with respect to wavelength as there was no absolute wavelength calibration on the individual scans. This alignment could usually be done to within 1 data point, or about 6 Å.

Two scans of each standard star taken at a gain of G_s db. were averaged together to get the observed, monochromatic signal strength for the standard, $I_s(\lambda)$. This function includes both the instrumental response and the telluric absorption features. The instrumental sensitivity function was then computed according to

$$S^*(\lambda) = \frac{I_s(\lambda)}{F_{MA(\lambda)}} \, 10^{-G_s/20}$$

where $F_{MA}(\lambda)$ is the appropriate calibrated model atmosphere. The function $S^*(\lambda)$ was then convolved with the response function of the exit slit of the spectrometer to eliminate high frequency noise (Westphal 1965). The only stellar feature in the scan of α Lyr, α C Mi, and α C Ma is B_γ at 2.1656μ. This line was removed by hand to give a final $S(\lambda)$. Individual scans of a star taken at a gain G would then be

averaged together to yield $I(\lambda)$. A final, calibrated spectrum for the star with atmospheric and instrumental effects removed was obtained according to

$$F(\lambda) = \frac{I(\lambda)}{S(\lambda)} \; 10^{-G/20}$$

If G was sufficiently high to introduce high frequency noise, $F(\lambda)$ would also be convolved with the appropriate slit response function. On the 60 inch telescope it was possible to get two very good scans at 32.5 Å resolution of an object of 0.0 magnitude at 2.2μ in 35 min. To conserve time and achieve a good S/N ratio, a 1 mm exit slit with a resulting resolution of 65 Å was used for objects fainter than K = 0.5.

An example of the effect of convolving a scan with the slit response function is shown in Figure 3. Tables 1 and 2 are the Journal of Observations for all of the spectra of late type stars which are discussed in this paper. The columns are self-explanatory.

With regard to resolution, the spectra presented in this paper may best be compared with those given by Johnson and co-workers (Johnson, Coleman, Mitchell, and Steinmetz 1968; Johnson 1968; Low, Johnson, Kleinmann, Latham, and Geisel 1970; Johnson and Mendez 1970). They obtained stellar spectra over the wavelength range from 1 to 4μ using a Fourier transform spectrometer having a resolution of 8 cm^{-1}. Such a comparison of objects in common to this paper and the papers of Johnson, et al indicates that the quality of the spectra presented here is equal to the quality of those obtained by Johnson, et al in terms of signal to noise ratio and removal of telluric

Fig. 3. - A reduced spectrum of α Boo before and after convolution with the slit function.

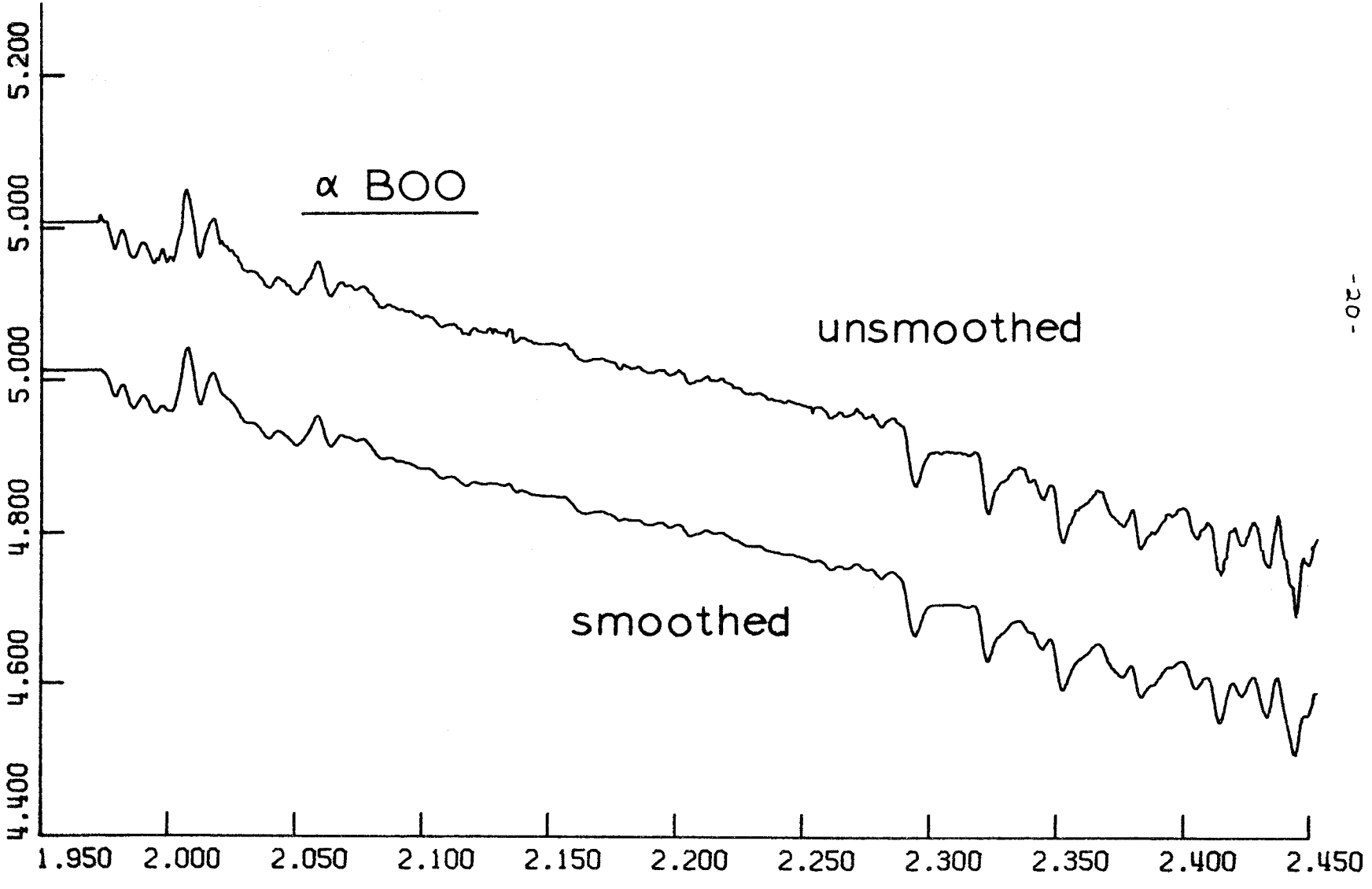
α BOO
unsmoothed
smoothed
5.200
5.000
5.000
4.800
4.600
4.400
1.950
2.000
2.050
2.100
2.150
2.200
2.250
2.300
2.350
2.400
2.450

Figure 3.

TABLE 1

LATE-TYPE GIANTS - OBSERVATIONS

Star	HR	IRC	Spectral Type	Date	Tele-scope	Exit Slit	Remarks
α Aur	1708	+50139	G5-8 III	1969 Dec. 19	60"	0.5mm	
γ Tau	1346	+20074	K0 III	1968 Oct. 4	100	0.5	a, b
δ Tau	1373	+20076	K0-1 III	1968 Oct. 4	100	1.0	b
β Gem	2990	+30194	K0 III	1969 Mar. 27	60	0.5	
α U Ma	4301	+60208	K0 II-III	1969 Mar. 27	60	0.5	
β Cet	188	-20010	K1 III	1969 Dec. 20	60	0.5	
α Ari	2538	+20038	K2 III	1968 Oct. 3	60	0.5	a
β Oph	6603	00317	K2 III	1969 Sep. 26	60	1.0	
α Boo	5340	+20270	K2 IIIp	1970 Apr. 25	100	0.5	c
δ And	165	+30014	K3 III	1968 Oct. 4	100	0.5	
β U Mi	5563	+70125	K4 III	1969 Mar. 27	60	0.5	
α Lyn	3705	+30210	K5 III	1969 Dec. 19	60	0.5	
α Tau	1457	+20087	K5 III	1970 Feb. 22	60	0.5	c
3 C Vn	4690	+50217	M1 III	1969 Dec. 19	60	1.0	f
2 Peg	8225	+20512	M1 III	1969 Sep. 28	60	0.5	d
ϰ Ser	5879	+20284	M1 III	1969 Mar. 27	60	0.5	
ν Vir	4517	+10245	M1 III	1969 Mar. 28	60	0.5	c, d
λ Aqr	8698	-10588	M2 III	1969 Sep. 26	60	0.5	
α Cet	911	00038	M2 III	1969 Jan. 29	60	0.5	
3 Aqr	7951	-10548	M3 III	1969 Sep. 28	60	0.5	
μ Gem	2286	+20144	M3 III	1969 Dec. 19	60	0.5	
30 Psc	9089	-10608	M3 III	1969 Sep. 26	60	0.5	

ρ Per	921	+40054	M4 II-III	1968 Oct. 4	100	0.5
51 Gem	2717	+20175	M4 III	1969 Dec. 19	60	0.5
U Del	7941	+20481	M5 II-III	1969 Sep. 26	60	0.5
R Lyr	7157	+40334	M5 III	1969 Sep. 25	60	0.5
---	4267	+10235	M5 III	1969 Dec. 20	60	0.5
---	4949	+20254	M5 III	1970 Mar. 24	60	0.5
R Z Ari	867	+20051	M6 III	1969 Nov. 22	60	0.5
Y U Ma	---	+60220	M7 II-III	1969 Mar. 2	60	0.5
" (2)	---	"	"	1969 Apr. 26	60	0.5
B K Vir	---	00220	M7	1969 Apr. 27	60	0.5
" (2)	---	"	"	1969 May 24	60	0.5
S W Vir	---	00230	M7	1970 Feb. 22	60	0.5
R T Vir	---	+10262	M7	1970 Feb. 21	60	0.5
R X Boo	---	+30257	M8	1969 Apr. 24	60	0.5
" (2)	---	"	"	1969 Apr. 27	60	0.5

See end of Table 2 for explanation of remarks

TABLE 2

LATE-TYPE HIGH LUMINOSITY STARS AND DWARFS - OBSERVATIONS

Star	HR	IRC	Spectral Type	Date	Tele-scope	Exit Slit	Remarks
ε Gem	2473	+30164	G8 Ib	1969 Nov. 19	60	1.0	
ζ Cep	8465	+60344	K1 Ib	1969 Dec. 20	60	0.5	
γ' And	603	+40034	K3 II	1969 Nov. 22	60	0.5	
o'C Ma	2580	-20112	K3 Iab	1970 Feb. 20	60	1.0	
η Per	834	+60099	K3 Ib	1969 Nov. 22	60	0.5	
ζ Aur	1612	+40110	K5 II+eb	1969 Nov. 19	60	1.0	
σ C Ma	2646	-30072	M0 Iab	1969 Mar. 3	60	0.5	c, d
5 Lac	8572	+50433	M0 Iab+B	1968 Oct. 4	100	0.5	
---	1009	+60117	M0 II	1969 Nov. 19	60	1.0	
B U Gem	2197	+20136	M1 Ia	1969 Nov. 19	60	1.0	
T V Gem	2190	+20134	M1 Iab	1969 Mar. 2	60	1.0	d
A Z Cyg	---	+50351	M2 Ia	1969 May 30	60	1.0	
V V Cep	8383	+60333	M2 epIa	1969 May 23	60	0.5	
μ Cep	8316	+60325	M2 Ia	1970 Mar. 25	60	0.5	
α Sco	6134	-30265	M1-2 Iab	1969 May 24	60	0.5	
α Ori	2061	+10100	M1-2 Iab	1969 Oct. 28	60	0.5	
W Y Gem	---	+20135	M2 Iab	1969 Nov. 19	60	1.0	e
119 Tau	1845	+20112	M2 Ib	1969 Oct. 26	60	0.5	
---	1155	+70046	M2 IIa	1969 Oct. 26	60	0.5	
π Aur	2091	+50156	M3 II	1969 Dec. 19	60	0.5	

K γ Cyg	---	+40415	M4 Ia	1969 May 30	60	1.0	
B C Cyg	---	+40409	M4 Ia	1969 Apr. 27	60	0.5	
U Y Sct	---	-10422	M4 Ia	1969 May 24	60	1.0	d
X Y Lyr	7009	+40323	M4-5 Ib-II	1969 June 1	60	0.5	
δ^2 Lyr	7139	+40331	M4 II	1969 June 1	60	0.5	c
U X Aur	---	+50138	M4 II	1969 Mar. 3	60	1.0	f, d
α Her	6406	+10324	M5 Ib-II	1969 Mar. 27	60	0.5	
R V Hya	---	-10199	M5 II	1969 Jan. 30	60	0.5	
W Tri	---	+30047	M5 II	1969 Nov. 19	60	1.0	
V Eir	---	-20049	M6 II	1969 Jan. 29	60	0.5	
" (2)	---	"	"	1969 Mar. 2	60	0.5	
Lalande	21185	---	M2 V	1969 June 22	200	1.0	
Wolf	359	---	dM8	1969 Jan. 1	200	2.0	e

a. 1 scan, 3 revs

b. poorly corrected

c. 1 scan

d. noisy

e. 4 scans, 12 revs

f. 3 scans

absorption features. The spectra presented here are more useful for detailed, quantitative analysis because the response function of the spectrometer has been removed and each spectrum has been calibrated on an absolute scale. Finally, it is noted that Johnson and co-workers find B_γ in emission in many objects whereas in this paper it is found only in absorption in some of the earlier type stars with no evidence of emission in any of the spectra presented here. A close examination of the spectrum of IRC +10216 (Becklin, et al 1970) and other unpublished spectra of objects which apparently have thick circumstellar dust shells and which have otherwise featureless spectra (eg V Cyg, Z C Ma, and late stages of Nova Ser 1970), indicates that the B_γ region is also featureless. This lends confidence to the correctness of the reduction procedure employed here and suggests that the apparent emission observed by Johnson and co-workers at 2.1656μ may be due to their helium reference line at 1.0833μ, half of the B_γ wavelength.

E. Temperature Scale

Johnson (1966) has given a calibration of effective temperatures and intrinsic colors for dwarfs, giants, and supergiants. He found the I-L color provides a sensitive index of the effective temperature for most stars. Since magnitudes in the I band (.9μ) could not be measured with the photometer used in the present study, the J-L color was used. Infrared magnitudes at 1.25, 1.65, 2.2, and 3.5 μ on the system of Johnson and Low (Johnson 1964) were measured for about 30 late type stars. The results agreed with Johnson's (1966) mean J-L,

spectral type relation except for the M4 and M5 giants. The intrinsic colors of these stars were modified to agree with the present results. Table 3 lists magnitudes determined for stars which have not been published elsewhere.

For giants later than M6, the colors and temperatures of Mendoza and Johnson (1965) were used as modified by Smak (1966). The mean relations for these stars fits smoothly onto those determined for giants earlier than M6. Table 4 gives finally adopted relations for mean J-L color and temperature as a function of spectral type for late giants. The results of Johnson (1966) indicate that these should also apply to late-type supergiants. Figure 4 graphs the relation between temperature and J-L color for ease of use.

The stars whose colors were determined for the present study were, in general, observed only once. A reasonable upper limit to the error in a J-L measurement is .1 for the fainter stars. The resulting error in the temperature may be read directly from Figure 4. Recently, Nather, McCants and Evans (1970) measured the angular diameter of λ Aqr (M2III). The effective temperature indicated was 3250° - 3450°K. This agrees reasonably well with the temperature that would be determined from the mean relation used here. Also, it was assumed that the colors of the giants and dwarfs are unaffected by interstellar reddening. The colors of the supergiants, on the other hand, are seriously affected by reddening.

TABLE 3

PHOTOMETRIC RESULTS

HR	Name	Spectral Type	J	H	K	L
2473	ε Gem	G8 Ib	0.97	0.38	0.25	0.10
6418	π Her	K3 II	0.80	0.12	-0.03	-0.13
7192	λ Lyr	K3 II	2.53	1.86	1.72	1.36
5563	βU Mi	K4 III	-0.36	-1.10	-1.22	-1.32
7405	α Vul	M0 III	1.48	0.71	0.53	0.37
4690	3 C Vn	M1 III	2.10	1.28	1.15	1.06
2197	BU Gem	M1 Ia	2.22	1.30	1.04	0.69
2190	TV Gem	M1 Iab	2.23	1.35	0.98	0.54
---	AZ Cyg	M2 Ia	2.45	1.49	1.13	0.68
8383	VV Cep	M2 Ia	0.94	0.11	-0.14	-0.48
---	WY Gem	M2 Iab	3.32	2.39	2.10	1.86
---	RW Cyg	M3 Ia	2.02	0.89	0.47	-0.09
2286	μ Gem	M3 III	-0.72	-1.61	-1.86	-2.03
---	UY Sct	M4 Ia	2.48	1.42	0.86	0.21
---	KY Cyg	M4 Ia	2.08	---	0.18	-0.59
---	BC Cyg	M4 Ia	2.02	0.85	0.30	-0.27
2717	51 Gem	M4 III	0.96	-0.07	-0.36	-0.66
7941	U Del	M5 II-III	0.8	-0.07	-0.38	-0.63
---	RV Hya	M5 II	1.78	0.84	0.48	0.18
4267	---	M5 III	0.31	-0.60	-0.82	-1.06
---	V Eri	M6 II	0.89	-0.09	-0.42	-0.85
7886	EU Del	M6 III	0.08	-0.82	-1.11	-1.31
---	X Her	M6 III	-0.26	-1.13	-1.43	-1.75
---	RV Boo	M6	1.14	0.22	-0.06	-0.35
---	Y U Ma	M7	0.64	-0.24	-0.61	-0.99
---	BK Vir	M7	0.42	-0.49	-0.85	-1.18
---	SW Vir	M7	-0.46	-1.41	-1.78	-2.14
---	RT Vir	M8	0.17	-0.75	-1.13	-1.52
---	RX Boo	M8	-0.57	-1.55	-1.96	-2.34

TABLE 4

ADOPTED COLOR TEMPERATURE - SPECTRAL TYPE RELATION FOR GIANTS *

Spectrum	J - L	Te
G5	.66	5010
G8	.71	4870
K0	.76	4720
K1	.81	4580
K2	.86	4460
K3	.95	4210
K4	1.03	4010
K5	1.12	3780
M0	1.14	3660
M1	1.19	3600
M2	1.21	3500
M3	1.26	3300
M4	1.33	3100
M5	1.40	2950
M6	1.53	2800
M7	1.68	2550
M8	2.08	2150
M9	2.35	1900
M10	2.68	1650

* See Johnson (1966) for supergiant relation.

Fig. 4. - The adopted (J-L), temperature relation.

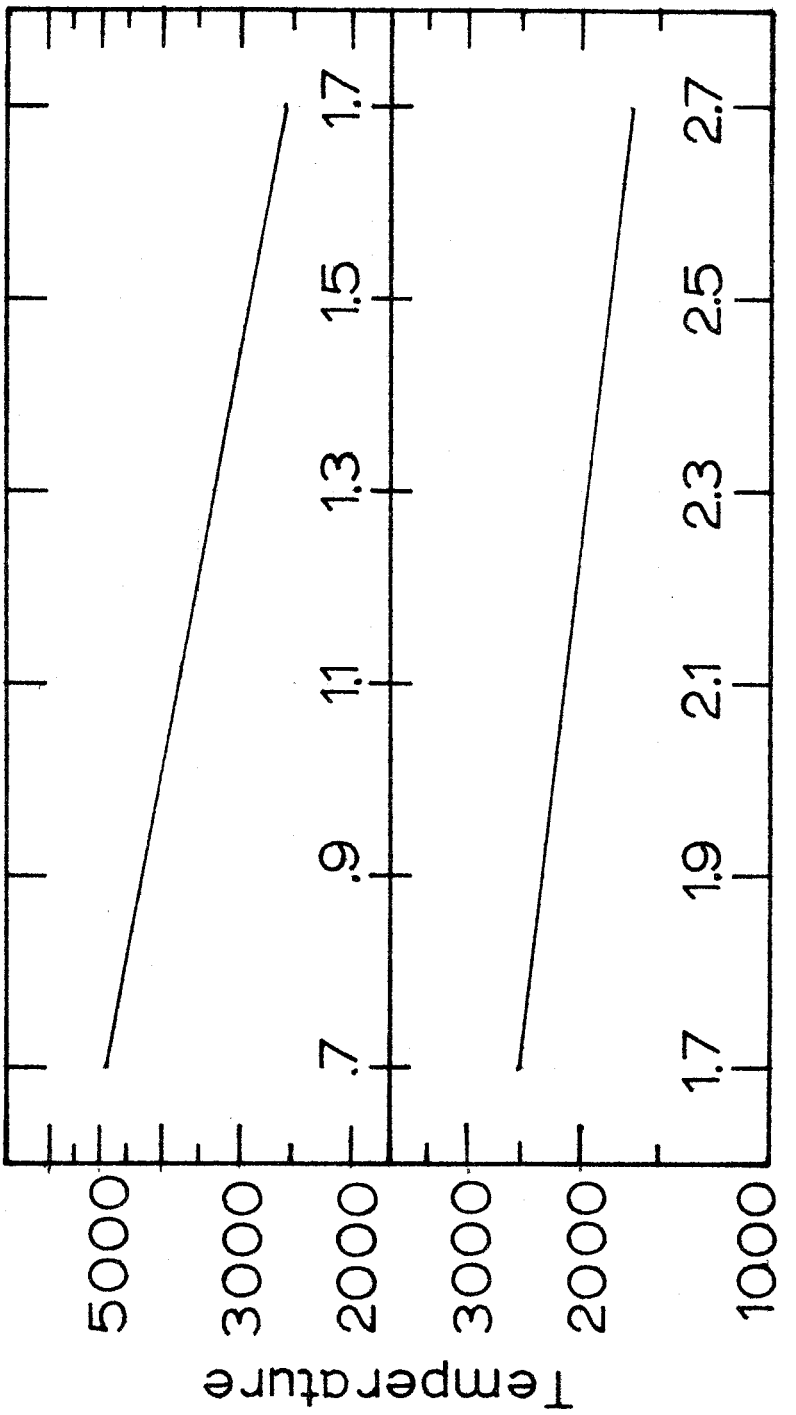
Temperature
5000
3000
2000
3000
2000
1000
.7
.9
1.1
1.3
1.5
1.7
1.7
1.9
2.1
2.3
2.5
2.7
(J-L)

Figure 4.

III. The Spectra -- Weak Absorption Features

A. Positions

The determination of the position of the true continuum of the stars studied here is made difficult by the presence of a great many overlapping absorption features in the 2μ region. However, the weakness of most of these features in the late G and early K stars allows one to use the intensity peaks to define a "pseudocontinuum" which probably does not differ from the true continuum by more than a few percent. For the spectra from which telluric absorption features were removed most successfully, the continuum was found to be best represented by a straight line in the 1.95 - 2.45μ region (the spectra are given in terms of log F_λ vs. wavelength). By comparisons with stars of successively later spectral types, it was possible to locate the continuum up to M8, the latest type considered in this study. One problem encountered was due to the presence of stellar H_2O which acts as a source of continuous opacity for normal giants later than M6. A second difficulty was the presence of a feature at 2.22μ which, in the later giants and in many of the class II and I stars seemed to lie above the continuum defined by the rest of the spectrum. This is certainly a true stellar feature and not due to incorrect removal of telluric absorption. As it is not clear if this is an emission feature or a region of the continuum which is free from overlapping absorption features, this particular feature was ignored when determining the level of the continuum.

Having determined the continuum level, ten high quality spectra representing types from G5 - M5 were chosen as a basis for determining the wavelengths of the most prominent absorption features. These stars were α Aur, β Gem, α Ari, β U Mi, α Lyn, α Tau, λ Aqr, μ Gem, π Aur, and R Lyr. All are class III stars except for π Aur which is class II. If the same feature appeared on at least four of the spectra it was considered to be real and its wavelength was determined by averaging its positions on all of the spectra on which it could be detected. In all cases, the wavelength of the center of the absorption feature was measured. The main error in determining the position of a feature arises from guiding and seeing effects at the telescope. Eye estimates were made of the strengths of the absorption features: w - weak, just detectable, with an equivalent width, W(λ), of about 1 Å; m - medium, clearly present with W (λ) about 2-4Å; s - strong, the strongest features seen in K stars, with W(λ) about 5 Å; vs - very strong, the strongest features in the M stars, with W (λ) of about 8 Å. Strengths were not assigned to features in the region of the first harmonic vibration-rotation bands of CO because of the great effect these bands have on everything else in the region. Table 5 is a list of positions of features from 2.08 to 2.40μ. The error in these positions is about 10 Å. The strengths are typical for stars of type M2-3 III. Inspection of the spectra indicates that there are also a number of distinct features shortward of 2.08μ, but these may occasionally be confused with terrestrial CO_2 bands. Figure 5 is the spectrum of π Aur with the positions of the features from Table 5 indicated.

Fig. 5. - A spectrum of π Aur with the positions of the features listed in Table 5 indicated.

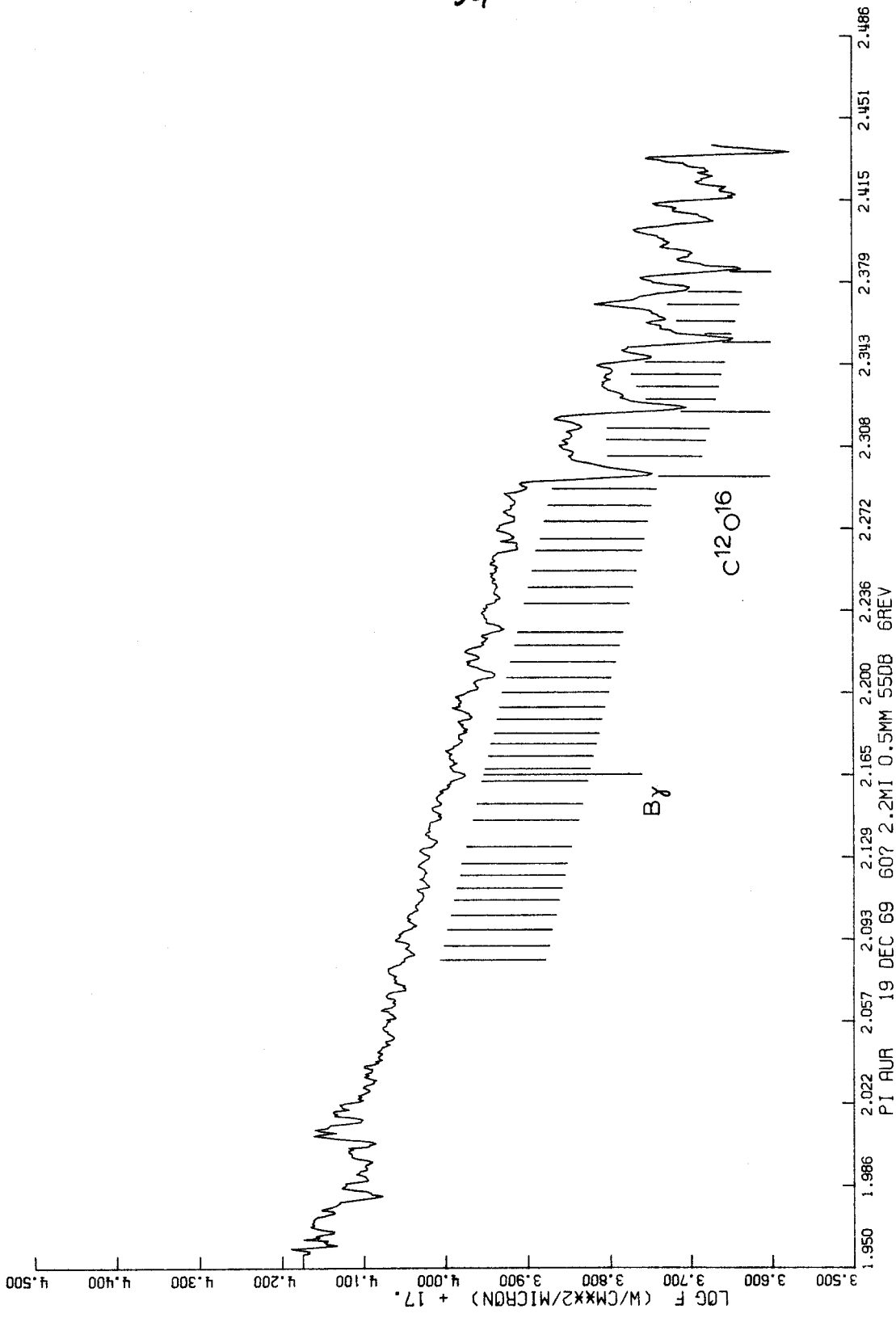
LOG F (W/CM**2/MICRON) + 17.
3.500
3.600
3.700
3.800
3.900
4.000
4.100
4.200
4.300
4.400
4.500
1.950
1.986
2.022
2.057
2.093
2.129
2.165
2.200
2.236
2.272
2.308
2.343
2.379
2.415
2.451
2.486
PI AUR 19 DEC 69 60? 2.2MI 0.5MM 550B 6REV
Bγ
C12O16

Figure 5.

TABLE 5

POSITIONS OF ABSORPTION FEATURES

Wavelength (microns)	Strength	Comments
2.085	S	
2.091	M	
2.098	M	
2.104	W	
2.111	S	
2.116	M	
2.121	M	
2.127	M	
2.134	M	
2.146	W	
2.153	W	
2.163	S	
2.165	-	$B\gamma$
2.168	M	
2.173	M	
2.179	M	
2.183	S	
2.189	M	
2.195	W	
2.201	S	
2.207	VS	
2.214	W	
2.222	M	
2.227	VS	
2.240	S	
2.247	M	
2.254	W	
2.263	VS	
2.268	M	
2.275	M	
2.282	M	
2.290	M	
2.295		$C^{12}O^{16}$
2.304		
2.311		
2.316		
2.324		$C^{12}O^{16}$
2.329		
2.334		
2.340		
2.345		$C^{13}O^{16}$
2.354		$C^{12}O^{16}$
2.358		
2.363		
2.370		
2.376		$C^{13}O^{16}$
2.385		$C^{12}O^{16}$

The spectra of stars of the latest M types present a different appearance from stars of earlier type, the transition occuring around M 5-6. First, is the strong depression of the continuum beginning at 2.17μ, increasing toward shorter wavelength. This is due to absorption by the 1.9μ band of H_2O. Benedict, Bass and Plyler (1954) noted that this band, which at room temperature extends from about 1.80 to 1.96μ, is broadened to extend from 1.7 to 2.2μ at a temperature of about 3000° K. This broadening is what is observed in stars. The second difference may best be described as a blending of some of the medium and strong features resulting in an overall reduction of the number of distinct features counted compared to earlier M stars. Figure 6 shows in detail the spectral region from 2.00 to 2.20μ for a sequence of M stars. The two phenomena discussed above are readily seen. The strengths of features lying in the broad 1.9μ H_2O band are measured with respect to the local continuum level rather than the level obtained by straight line extrapolation from longer wavelengths. Figure 7 illustrates the increase in relative numbers of strong absorption features as we pass from early to late spectral types.

The appearance of the weak absorption features in the supergiants approximately corresponds to their appearance in giants having the same CO band strength. In some of the supergiants, however, the number of features appear to be less, but those that are present are quite strong. Generally, an M2 supergiant spectrum closely resembles an M 7-8 giant spectrum except for the absence of the 1.87μ water band in the supergiant spectrum. The spectra of the later supergiants

Fig. 6. - The spectral region from 2.00 - 2.20μ for a sequence of M giants showing the appearance of the 1.87μ water band and a general strengthening of the weak absorption features.

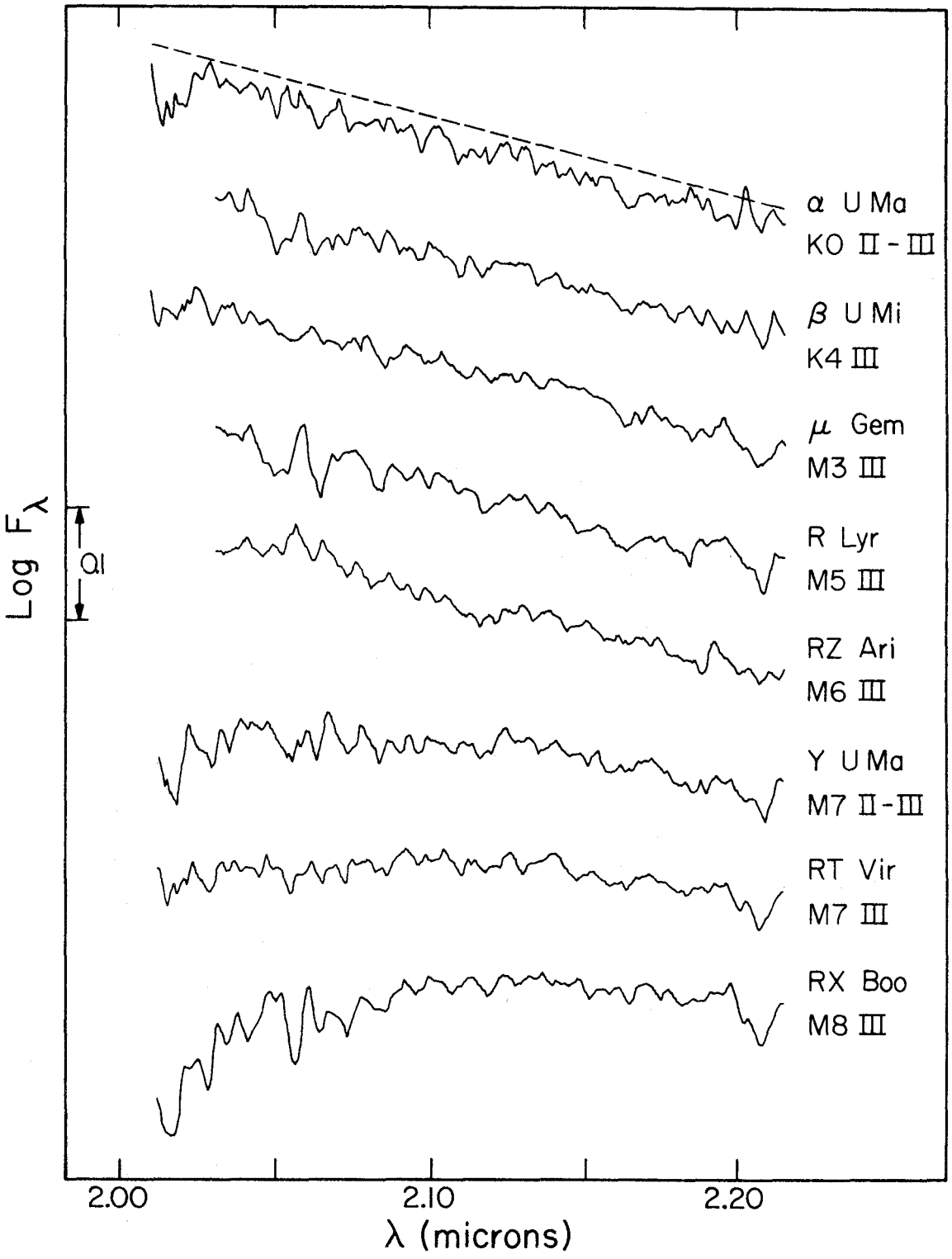
α U Ma
KO II - III
β U Mi
K4 III
μ Gem
M3 III
R Lyr
M5 III
RZ Ari
M6 III
Y U Ma
M7 II-III
RT Vir
M7 III
RX Boo
M8 III
Log F λ
0.1
2.00
2.10
2.20
λ (microns)

Figure 6.

Fig. 7. - A series of histograms showing the increase in the relative number of strong absorption features in the later giants.

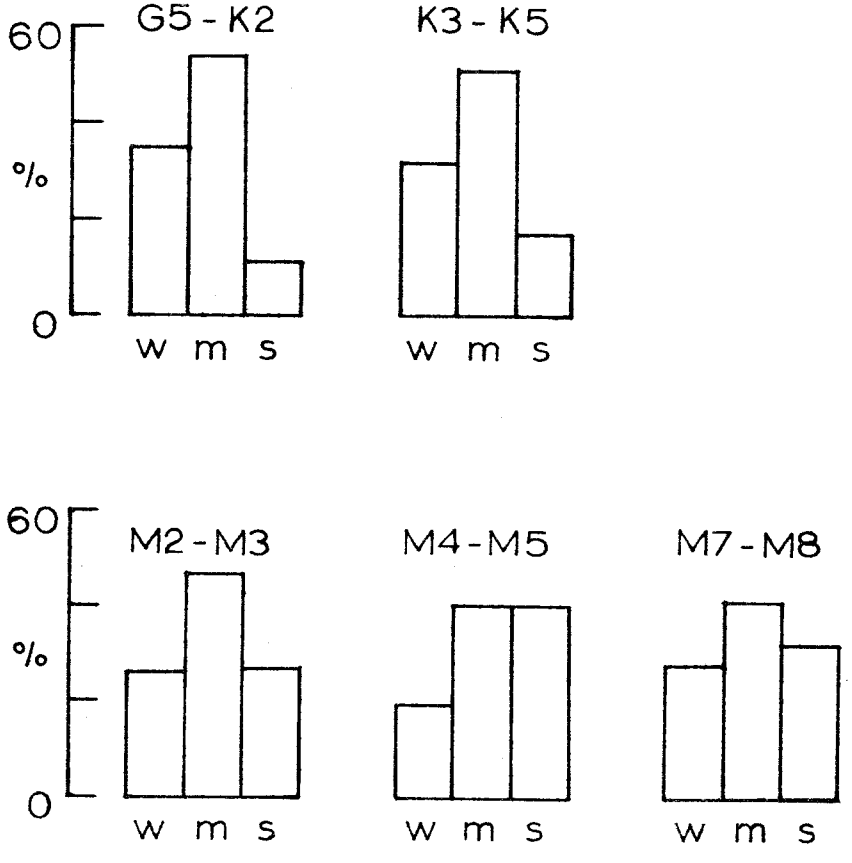

Figure 7.

presented here have a lower signal to noise ratio and resolution than the earlier supergiants and it is difficult to resolve the weaker features. Considering the fact that most of the absorption features remain unidentified, it is not felt to be worthwhile to pursue any discussion of differences between the giants and supergiants or between individual stars.

B. Atomic Lines

Table II of Spinrad and Wing (1969) provides a basis for the identification of atomic lines in the spectra presented here. Their table is made from a high resolution spectrum of α Ori obtained by P. and J. Connes. Table 6 contains the strongest features listed by Spinrad and Wing. Column 1 is the line identification, if any; column 2 is the excitation potential of the ground state; column 3 contains the estimated (Spinrad and Wing) intensities of the lines in α Ori; column 4 is based on the measured equivalent width in the solar spectrum and the intensity ratio α Ori/sun; column 5 is from ν_{vac} (cm^{-1}) given by Spinrad and Wing; column 6 is the wavelength of the feature in the spectra presented here with which the atomic line or blend of lines is identified, and column 7 is the approximate equivalent width of this feature in the typical M3 III star μ Gem. The strengths of the features in this star are representative of early to middle M stars.

Due to the limited resolving power of the Ebert-Fastie spectrometer employed here, an absorption feature must have an equivalent width of at least 1 Å to be detected. Therefore, most of the absorption

TABLE 6

ATOMIC LINES FROM SPINRAD AND WING

Element	Excitation (eV)	Intensity (α Ori)	W_λ (α Ori)	Wavelength (microns)	IDENTIFICATION HERE Wavelength (microns)	W_λ (Å)	Remarks
Ca I	1.90	VS	2.1	1.978		3.0	a
Ca I	4.62	MS	.3	1.982			
Ca I	3.91	S	.5	1.986			a, b
Ca I	1.90	VS	.7	1.992			
Si I	6.73	MS	.3	2.092			d
---	---	MS	---	2.094			c
---	---	MS	.4	2.106	2.111	1.8	b
Al I	4.08	MS	.2	2.109			
Al I	4.09	S	.5	2.116	2116	~1	b
Mg I	6.73	MS	.2	2.123	2.127	~1	b
---	---	MS	.4	2.126			
---	---	M	---	2.129			c
Si I	6.22	MS	.3	2.135			d
---	---	MS	---	2.157			c
---	---	MS	---	2.181			d
Si I	6.72	M	.2	2.182			d
Si I	6.72	M	.5	2.188	2.189	~.9	
Ti I	1.74	S	.1	2.190			
---	---	S	---	2.201	2.201	~2	
---	---	MS	---	2.202			

Element	Excitation (eV)	Intensity (α Ori)	W_λ (α Ori)	Wavelength (microns)	IDENTIFICATION HERE Wavelength (microns)	W_λ (Å)	Remarks
---	---	VS	---	2.205			
Na I	3.19	VS	.9	2.206			
Si I	6.73	M	.1	2.206	2.207	4.5	
Si I	6.73	M	.1	2.207			
Na I	3.19	S	.5	2.209			
---	---	M	---	2.209			d
---	---	M	---	2.211			d
---	---	S	----	2.221			c
---	---	S	---	2.223			
---	---	S	---	2.227			
---	---	S	---	2.227	2.222 2.227	~5	
Fe I	6.44	M	---	2.230			
Ti I	5.15						
---	---	S	---	2.232			
---	---	S	---	2.238			d
---	---	S	---	2.244	2.247	~1	
Ti I	4.90	MS	---	2.247			
Ca I	4.68	S	.8	2.261			
Fe I	4.99	S	1.4	2.262			
Ca I	4.68	S	1.0	2.263	2.263	~4	
---	---	MS	---	2.263			
Ca I	---	S	---	2.265			

					IDENTIFICATION HERE		
Element	Excitation (eV)	Intensity (α Ori)	W_λ (α Ori)	Wavelength (microns)	Wavelength (microns)	W_λ (Å)	Remarks
---	---	M	---	2.266			d
Si I	6.62	M	.1	2.267			d
Mg I	6.72	MS	.3	2.281			c

a. Region of strong atmospheric absorption

b. Identification uncertain

c. no identification

d. Line lies on the wing of an absorption feature

features listed in Table 5 can be identified only with groups of closely spaced atomic lines from Table 6. It is interesting to note that four of the strongest features which have been identified as blends of atomic lines, namely those at 2.201, 2.207, 2.227, and 2.203μ are weak or medium in early K giants but all become strong or very strong in late M giants. On the other hand, four unidentified features at 2.085, 2.111, 2.103, 2.183μ which are of comparable strength to the identified features in the earlier giants, donot show such a systematic increase in the latest spectral types.

C. Molecular Lines

Tsuji (1964), Vardya (1966), and Vardya (quoted by Spinrad and Wing 1969) have investigated theoretical molecular abundances in late-type stars. Their results are similar except that Vardya found SiO and HCl to be of comparable abundance to H_2O. The results of these authors will be used as a guide in searching for molecular absorption features in the spectra presented here. No attempt was made to make a complete search of the literature concerning molecular spectra. Herzberg (1950) was referred to for a great deal of empirical data. Therefore, this discussion should be regarded as preliminary.

Three of the most abundant molecules in cool stars are H_2, N_2, and O_2, all of which are homonuclear. Dipole radiation in infrared vibration rotation bands is strongly forbidden for such molecules. The intensity of permitted quadrupole radiation is typically 10^{-9} that of dipole radiation of ordinary molecules (Herzberg 1950). H_2, the most abundant molecule in stars cooler than 3600° K, is the most likely to be

detected. The spectrum has been given by Rank, et al (1962) and relevant wavelengths are given in Table 7.

Spinrad (1966) reported the identification of the first-overtone quadrupole bands of H_2 in several stars, but this identification is now doubtful because of his inability to detect the much stronger 1-0 bands in a high resolution spectrum taken by Connes of α Ori (Spinrad and Wing 1969). In the 2μ window, the two strongest bands should be S(1) and S(3), the latter lying in a region of strong terrestrial water absorption.

Table 5 indicates that there are features of medium strength (~ 2 Å) at λ = 2.121 and 2.222μ, agreeing with the positions of the S(1) and S(0) lines, respectively. This coincidence of position does not indicate identification, however, for several reasons. First, the S(1) line should be considerably stronger than the S(0) line, and the S(2) line should be present in comparable strength to the S(0) line. Neither of these things are found to be true. Second, the feature at 2.121μ is one of those mentioned earlier which is not present in the spectra of the M7 and M8 stars. Third, the inability of Spinrad and Wing to detect the lines in a high resolution spectrum of α 0ri makes it doubtful that they will be present in stars of similar spectral type, but lower luminosity. Also, the difference in gas pressure between giants and supergiants is insufficient to cause the pressure-induced dipole absorption of H_2 discussed by Rank, et al. (1962).

The OH molecule reaches an abundance comparable to H_2O at a temperature of 2500° K (Tsuji 1964). The first overtone (9, 7) red

TABLE 7

POSITIONS OF MOLECULAR BANDS

MOLECULE	TRANSITION	BAND HEAD (Å air)	REFERENCE
H_2	Q(1)	24066	a
	S(0)	22233	
	S(1)	21218	
	S(2)	20338	
	S(3)	19576	
OH	(8, 6)	20003	b
	(9, 7)	21514	
HCl	(5, 3)	19259	c
	(6, 4)	20087	
	(7, 5)	20986	
	(8, 6)	21963	
	(9, 7)	23031	
	(10, 8)	24202	
HF	(1, 0)	22266	c
	(2, 1)	23364	
	(3, 2)	24531	
NO	(7, 4)	19018	c
	(8, 5)	19330	
	(9, 6)	19654	
	(10, 7)	19988	
	(11, 8)	20334	
	(12, 9)	20692	
	(13, 10)	21063	
	(14, 11)	21447	
	(15, 12)	21846	
SiO	(4, 0)	20514	c
	(5, 1)	20720	
	(6, 2)	20930	
	(7, 3)	21144	
	(8, 4)	21362	
	(9, 5)	21584	
	(10, 6)	21811	
	(11, 7)	22042	
	(12, 8)	22277	
	(13, 9)	22517	

MOLECULE	TRANSITION	BAND HEAD (Å air)	REFERENCE
TiO	(5, 0)	20312	c
	(6, 1)	20505	
	(7, 2)	20702	
	(8, 3)	20903	
	(9, 4)	21107	
	(10, 5)	21315	
	(11, 6)	21528	
	(12, 7)	21745	
	(13, 8)	21966	
	(14, 9)	22192	
CN	(2, 4)		d
	R_{11}	21440	
	R_{22}	21320	
	Q_{11}	21600	
	R_{21}	21060	
	(3, 5)		
	R_{11}	22410	
	R_{22}	22270	
	Q_{11}	22570	
	R_{21}	22000	
$C^{12}O^{16}$	(2, 0)	22936	e
	(3, 1)	23227	
	(4, 2)	23525	
	(5, 3)	23830	
	(6, 4)	24141	
	(7, 5)	24461	
	(8, 6)	24788	
$C^{13}O^{16}$	(2, 0)	23449	e
	(3, 1)	23740	
	(4, 2)	24037	
	(5, 3)	24341	
	(6, 4)	24652	

a. Rank, et al (1962)
b. Wallace (1962)
c. This paper
d. Thompson and Schnopper (1970)
e. Kunde (1967)

degraded band head lies at 2.151μ (Wallace 1962). There is no evidence for a band at this position in the spectra presented here.

The calculations of Vardya (1966) have indicated that HCl is an abundant molecule in all stars later than M0. Using the constants given by Herzberg (1950) the positions of the first overtone, red degraded band heads of this molecule were calculated (Table 7). The (6, 4) band lies in the atmospheric CO_2 band. Table 5 indicates that there are three absorption features close to the positions of the (7, 5), (8, 6), and (9, 7) band heads. It is not clear that these features can be attributed to HCl bands since the former tend to be blue-degraded.

Spinrad and Wing (1969) report the identification on Connes' spectrum of weak lines due to HF in the 2.3μ region of α Ori. The positions of the first few heads of the fundamental band of HF using the constants given by Herzberg (1950) have been calculated. These positions are given in Table 7. The bands are too weak to be detectable with the resolution used in this study.

The maximum abundance of NO, about 10^{-4} that of CO, is found in stars with a $T_e = 2800^\circ$ (Tsuji, 1964). The positions of the band heads of the second overtone band have been calculated, again using the constants of Herzberg (1950) (Table 7). It is clear that only the band heads (11, 8) and higher could easily be detected on the spectra here. These are expected to be too weak to be visible with the resolution used.

Laboratory spectra in the 2μ region of NH_3 and CH_4 are available (Kuiper and Cruikshank 1964). Unfortunately these spectra are at room temperature and high pressure. These molecules are most abundant in the coolest stars. Although some of the absorption features in

M6 - M8 stars correspond with the strongest features in the spectra presented by Kuiper and Cruikshank (Figure 8), the mild decrease in the strength of these features in the earlier spectral types is not what would be expected from the sharp decrease in the abundances of NH_3 and CH_4 as computed by Tsuji and Vardya. So again identification is doubtful.

Fertel (1970 a, b) has tentatively identified the third overtone band of SiO in infrared spectra of χ Cyg and Y C Vn. This identification has been questioned by Wing and Price (1970). As both of these stars presumably have an O/C ratio close to unity, bands of SiO should be stronger in the oxygen rich giants studied here. The positions of the red-degraded band heads of the $\Delta v = 4$ system were calculated using the constants given by Herzberg (1950). The wavelengths agree with those given by Fertel (1970 b) and are indicated in Figure 8. While there is some agreement between the expected positions and absorption features that are present, positive identification is by no means clear. Positions of TiO bands were also calculated from Herzberg (1950) and are given in Table 7 and indicated in Figure 8. The conclusion regarding the SiO bands applies here also.

Connes, et al. (1968) and Thompson and Schnopper (1970) have reported the identification of bands of the red system of CN in the spectra of carbon stars between 1.4 and 2.5μ . Observations of CN bands at shorter wavelengths have been reviewed by Spinrad and Wing (1969). The wavelengths of the band heads given in Table 7 are from Thompson and Schnopper. The theoretical calculations of Tsuji (1964)

Fig. 8. - Laboratory spectra of NH_3 and CH_4 compared with an observed spectrum of a M7 III star. Also indicated are the calculated positions of TiO and SiO band heads.

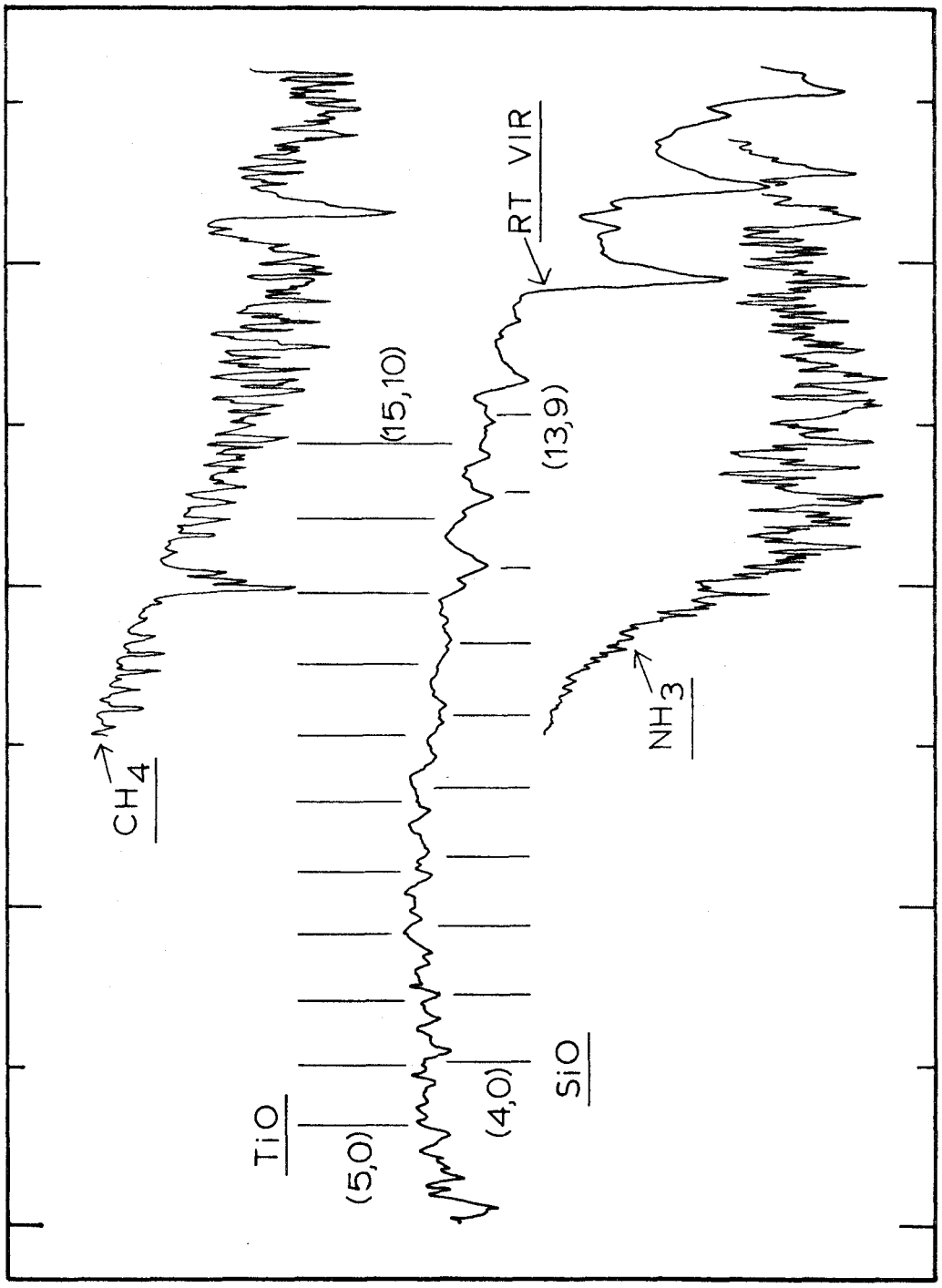

Figure 8.

for stars of solar composition indicate that the maximum CN abundance occurs in stars of $T_e \approx 4000^{\circ}K$ at which temperature it is typically 10^{-4} as abundant as CO. For cooler temperatures, [CN/CO] ("[ ]" signifies ratio of abundance by number) decreases rapidly. Wing and Spinrad (1970) have argued that "the red system of CN is probably the most important of all bound-bound sources of opacity in K giants, . . . " In Figure 9 is the spectral region containing the (1, 3), (2, 4), and (3, 5) band heads of the red CN system for the stars α Aur, α Boo, β U Mi, and U Hya. The latter is a carbon star whose spectrum in this region has also been published by Thompson and Schnopper. In addition to being able to identify the R_{21}, R_{22}, R_{11}, and Q_{11} band heads of the (2, 4) and (3, 5) transition which Thompson and Schnopper have done for U Hya, these four heads in the (1, 3) transition are also identified here. Comparing the spectrum of U Hya with the three oxygen rich giants we see that identification of any of the CN band heads in the latter stars is marginal at best. The absorption features centered at 2.134 and 2.227μ may correspond to the R_{22} band heads of the (2, 4) and (3, 5) transitions respectively. However, the feature at 2.134μ gets weaker in later spectral types whereas the one at 2.227 gets stronger.

Johnson and Méndez (1970) have identified broad absorption features at 1.95μ and 2.04μ in the spectra of giants and supergiants as due to CN. The spectrum of U Hya shown here, however, illustrates that this is not the appearance expected for the CN bands. Furthermore, these broad features correspond to the positions of exceedingly strong

Fig. 9. - Partial spectra of the M giants α Aur, α Boo, and βU Mi and the carbon star U Hya (reading from top to bottom). The calculated positions of the (1, 3), (2, 4), and (3, 5) bands of CN are indicated.

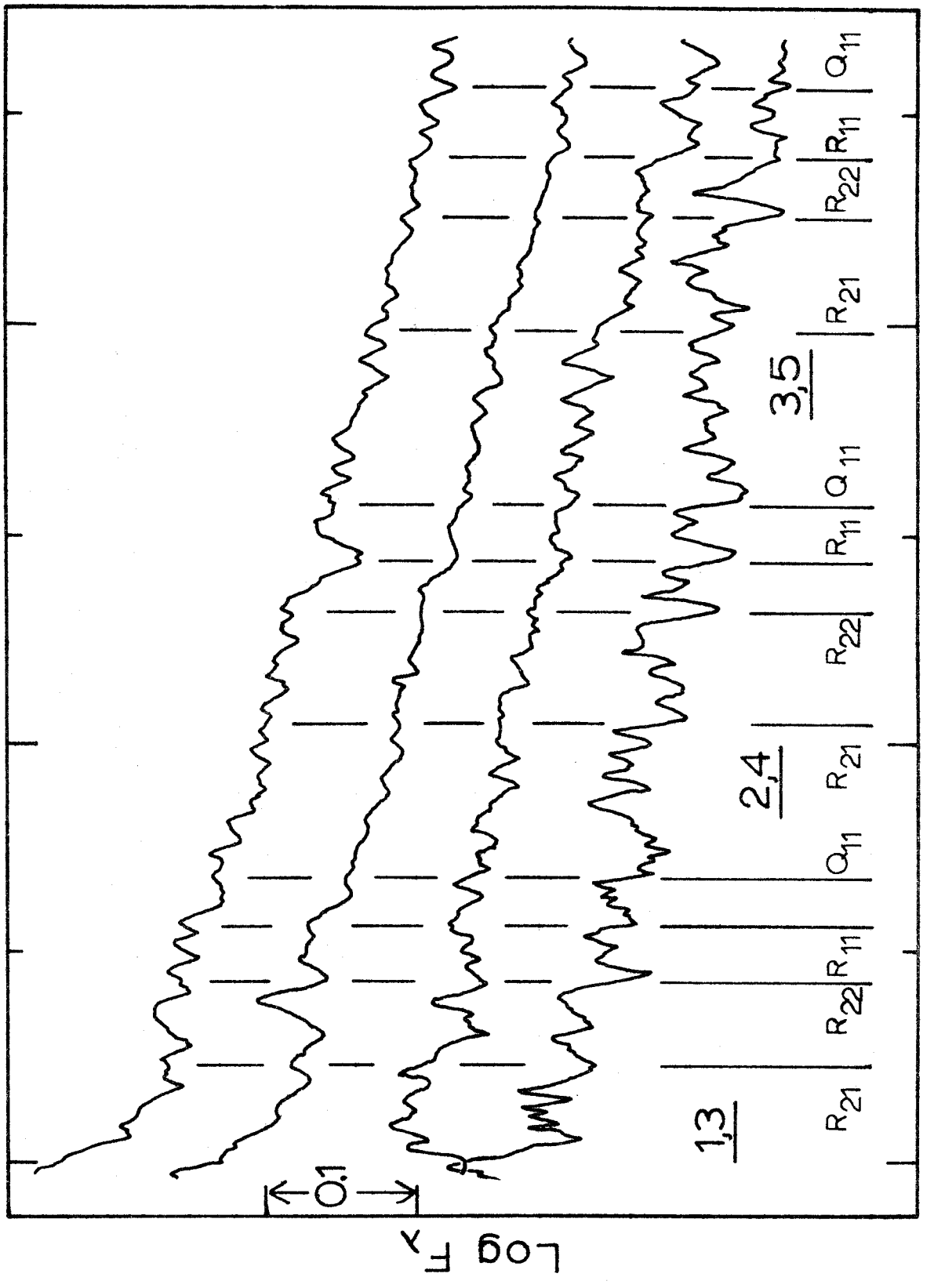

Figure 9.

telluric CO_2 bands and the appearance of these features identified with CN by Johnson and Méndez are suggestive of a slight undercorrection for the telluric absorption. Thus, while CN may be present in late-type giants and supergiants, the strength of its absorption bands in the 2μ region is such as to make identification on spectra with a resolution similar to those presented here doubtful.

IV. THE SPECTRA — CO AND H_2O

A. Carbon Monoxide

The two most important molecules in terms of apparent influence on the infrared spectra of late-type stars are H_2O and CO. The detection of broad absorption bands due to these molecules in infrared stellar spectra has been discussed by many authors (cf. Spinrad and Wing [1969] for a complete bibliography). The CO molecule will be discussed here and H_2O in the next section.

Carbon monoxide is a well understood diatomic molecule (Herzberg 1950). The infrared absorption spectrum of CO has been studied by Young (1966) and Kunde (1968, 1969). The wavelengths of the first overtone band heads of $C^{12}O^{16}$ and $C^{13}O^{16}$ are given in Table 7. The band heads of $C^{13}O^{16}$ in the 2.2μ region are visible in the spectra published by Johnson, et al (1968) and were positively identified in the spectra of normal late-type giants and supergiants by Johnson and Méndez (1970). They are also seen in the 1.6μ region in some of the spectra presented by McCammon, et al (1966). These isotopic bands are present in most of the spectra presented here which were taken at 32.5Å resolution.

For an estimate of the strength of the CO absorption in the 2μ spectra, the equivalent width of the absorption in the wavelength region from the (2, 0) up to the (5, 3) band head was measured using the continuum previously determined. This quantity will be referred to as W(CO). Measurement of the amount of absorption was cut off at the (5, 3) band

head to minimize contamination due to stellar water vapor which can become strong at longer wavelengths. This is not the true equivalent width of these bands for two reasons: individual rotational lines for these vibrational transitions extend beyond the longward limit considered; secondly, the overlapping of the individual lines results in non-linear contributions to the total absorption. The values obtained for W(CO) for all stars observed in this program are plotted in Figure 10a and tabulated in Tables 8a and 8b. In addition, for purposes of comparison with theoretical absorption profiles, the ratios $W_\lambda(2,0)/W_\lambda(3,1)$ and $W_\lambda(2,0)/W_\lambda(4,2)$ were measured. The quantity $W_\lambda(a,b)$ refers to the equivalent width measured from the wavelength of the (a, b) band head up to the wavelength of the (a+1, b+1) band head. All of these measurements were made with respect to the continuum previously determined. These quantities are given in Tables 8a and 8b.

A reasonable upper limit to the error in measuring W(CO) due to misplacement of the continuum is 30Å. The relative error for any two stars whose measured values of W(CO) differ by less than 80Å is considerably less than this. Also, for nearly all of the stars, errors due to improper correction of terrestrial absorption in the region over which W(CO) is measured are negligible for reasons discussed earlier. Thus, it is confidently felt that most of the scatter at a given spectral type in Figure 10 is real.

Possible contamination due to the presence of other molecular bands has not been taken into account. W(CO), in fact, includes a contribution from the (2, 0) and (3, 1) bands of $C^{13}O^{16}$. As will be seen

Fig. 10a. - The quantity W(CO) as a function of spectral type and luminosity for all of the stars observed.

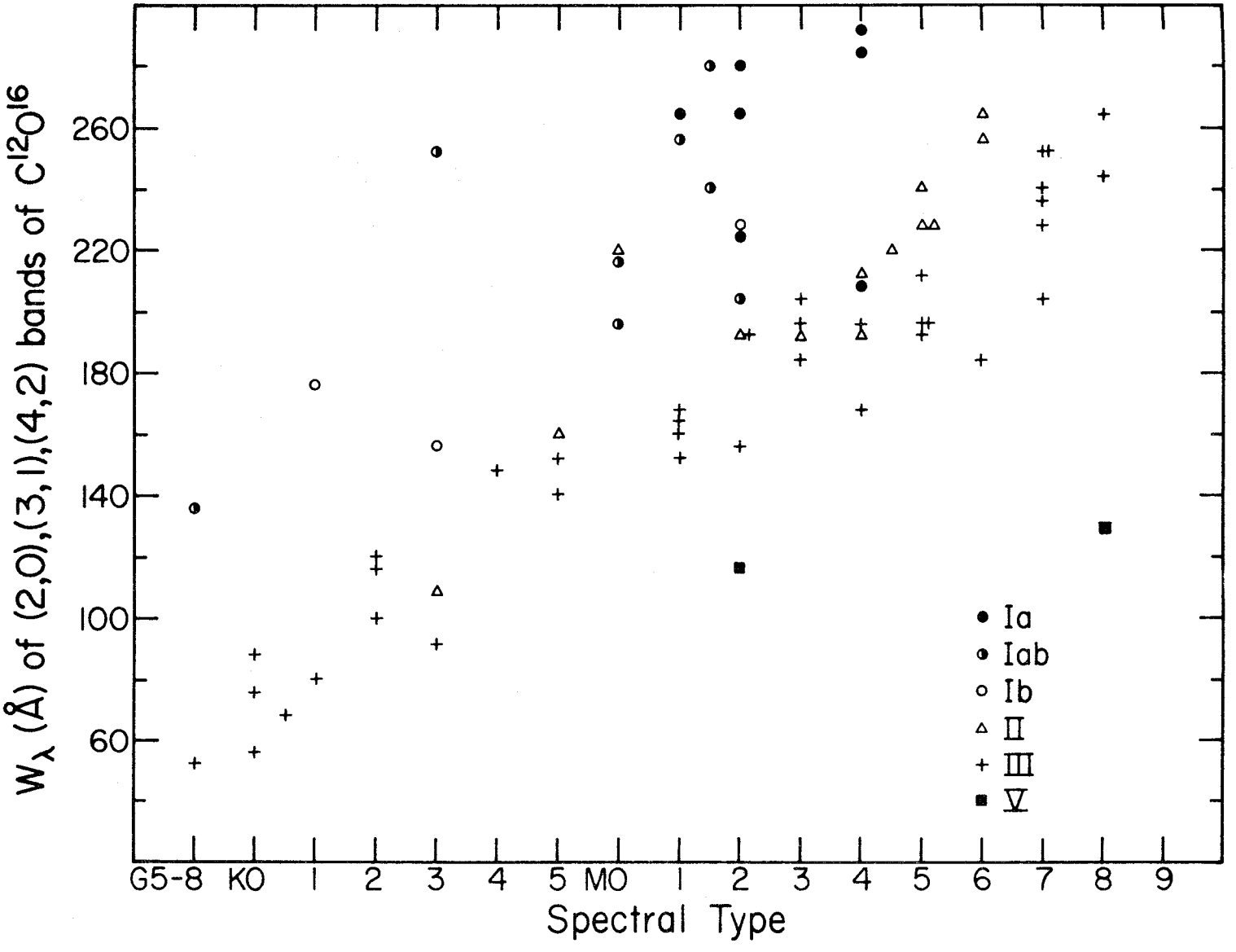
W_λ (Å) of (2,0),(3,1),(4,2) bands of $C^{12}O^{16}$
260
220
180
140
100
60
G5-8
K0
1
2
3
4
5
M0
1
2
3
4
5
6
7
8
9
Spectral Type
Ia
Iab
Ib
II
III
V

Figure 10a.

TABLE 8a

LATE-TYPE GIANTS -- BAND STRENGTHS

Star	Spectral Type	W_λ (Å) of CO bands				$[C^{12}/C^{13}]$	WV
		(2, 0)	(2, 0)+ (3, 1)+ (4, 2)*	(2, 0) / (3, 1)	(2, 0) / (4, 2)		
α Aur	G5-8 III	14	51	.81	.74	>6.3	.008
γ Tau	K0 III	13	58	.59	.58	4.8	-.002
δ Tau	K0-1 III	15	66	.57	.59	3.1	.008
β Gem	K0 III	20	76	.78	.68	>30.	.015
αU Ma	K0 II-III	23	90	.79	.63	3.1	.012
β Cet	K1 III	21	79	.80	.71	6.3	.002
α Ari	K2 III	19	115	.48	.35	9	.011
β Oph	K2 III	29	122	.73	.56	4.5	.010
α Boo	K2 IIIp	24	99	.74	.58	5.1	.009
δ And	K3 III	17	93	.48	.43	7.8	.003
βU Mi	K4 III	34	146	.73	.53	6.5	.010
α Lyn	K5 III	36	152	.69	.58	5.1	.010
α Tau	K5 III	29	138	.60	.47	9.8	.000
3 CVn	M1 III	37	158	.68	.54	>5.3	.010
2 Peg	M1 III	40	169	.67	.58	4.3	.019
ϰ Ser	M1 III	38	166	.65	.53	7.7	.013
ν Vir	M1 III	40	155	.74	.66	6.0	.007
λ Aqr	M2 III	47	194	.72	.57	4.0	.006
α Cet	M2 III	35	154	.67	.54	9.0	.002
3 Aqr	M3 III	49	197	.71	.61	5.1	.014
μ Gem	M3 III	43	184	.69	.54	5.3	.013
30 Psc	M3 III	49	205	.71	.55	4.6	.006
ρ Per	M4 II-III	36	168	.57	.51	2.9	.000
51 Gem	M4 III	46	198	.69	.54	3.8	.012
U Del	M5 II-III	52	211	.74	.60	5.6	.009
R Lyr	M5 III	46	191	.71	.59	3.5	.009
HR 4267	M5 III	44	196	.68	.52	4.3	.022

Star	Spectral Type	W_λ (Å) of CO bands				$[C^{12}/C^{13}]$	WV
		(2,0)	(2, 0)+ (3, 1)+ (4, 2)*	(2, 0) / (3, 1)	(2, 0)/ (4, 2)		
HR 4949	M5 III	47	197	.70	.57	4.9	.016
RZ Ari	M6 III	45	182	.73	.61	4.6	.016
YU Ma	M7 II-III	53	228	.68	.54	12	.008
" (2)	"	53	235	.65	.52	7.2	.029
BK Vir	M7	45	206	.64	.49	2.8	.038
" (2)	"	56	241	.70	.53	>4.6	.018
SW Vir	M7	56	252	.64	.51	4.8	.018
RT Vir	M7	57	251	.67	.52	6.3	.034
RX Boo	M8	63	263	.73	.56	8.1	.047
" (2)	M8	53	243	.64	.50	7.2	.060

* - this quantity is W(CO)

TABLE 8b

LATE-TYPE HIGH LUMINOSITY STARS
AND DWARFS -- BAND STRENGTHS

Star	Spectral Type	W_λ (A) of CO bands				$[C^{12}/C^{13}]$	WV
		(2, 0)	(2, 0)+ (3, 1)+ (4, 2) *	(2, 0)/ (3, 1)	(2, 0) / (4, 2)		
ε Gem	G8 Ib	33	135	.70	.58	5.1	.001
ζ Cep	K1 Ib	42	177	.70	.55	12	.005
γ' And	K3 II	29	106	.78	.72	—	.004
o'C Ma	K3 Iab	59	252	.69	.55	25	.020
η Per	K3 Ib	43	157	.82	.69	9.7	.015
ζ Aur	K5 II+eb	38	161	.70	.56	>6.0	.001
σC Ma	M0 Iab	54	215	.73	.62	10	.024
5 Lac	M0 Iab+B	45	195	.65	.56	6.7	.004
HR 1009	M0 II	50	220	.68	.52	>10	.008
BU Gem	M1 Ia	65	265	.72	.60	>8.0	.004
TV Gem	M1 Iab	61	257	.67	.59	4.6	.006
AZ Cyg	M2 Ia	54	224	.73	.57	5.7	.000
VV Cep	M2ep Ia	66	266	.75	.59	15	.015
μ Cep	M2 Ia	72	280	.74	.64	14	.007
α Sco	M1-2 Iab	73	282	.79	.63	7.2	.018
α Ori	M1-2 Iab	58	241	.73	.57	6.8	.003
WY Gem	M2 Iab	48	203	.66	.58	>3.5	.002
119 Tau	M2 Ib	54	229	.70	.56	11	.012
HR 1155	M2 IIa	45	192	.70	.54	13	.009
π Aur	M3 II	47	193	.71	.58	6.4	.014

Star	Spectral Type	W_λ (A) of CO bands				$[C^{12}/C^{13}]$	WV
		(2, 0)	(2, 0)+ (3, 1)+ (4, 2) *	(2, 0)/ (3, 1)	(2, 0)/ (4, 2)		
KY Cyg	M4 Ia	74	294	.74	.62	>8.1	-.003
BC Cyg	M4 Ia	67	285	.69	.56	7.1	.011
UY Sct	M4 Ia	55	209	.79	.64	>9.7	.013
XY Lyr	M4-5 Ib-II	52	218	.71	.57	10	.004
δ^2 Lyr	M4 II	46	194	.70	.56	12	.011
UX Aur	M4 II	53	211	.74	.60	10	.020
α Her	M5 Ib-II	52	228	.67	.53	9.6	.009
RV Hya	M5 II	54	227	.71	.56	>3.5	.007
W Tri	M5 II	56	241	.69	.53	>4.6	.017
V Eri	M6 II	60	254	.69	.57	6.4	.013
" (2)	"	60	263	.65	.54	8.5	.012
Wolf 359	dM8	--	~130	---	---	---	~.09
Lalande 21185	M2 V	21	116	.51	.40	>4	.012

* - this quantity is W(CO)

below, this contribution appears to be largely independent of spectral type. For stars with [O/C]> 1, contamination due to CN absorption in this region is negligibly small (Stephan D. Price, private communication). Based on the strength of the 1.87μ band, contamination due to the 2.7μ band of H_2O may also be considered to be negligibly small.

The most striking feature of Figure 10a is the clear dependence of W(CO) on spectral type and luminosity. Figure 10 b shows W(CO) as a function of J-L for those stars which were observed photometrically. Figure 10c is W(CO) as a function of the slope of the continuum in the 2μ region. The slope will be less affected by interstellar reddening than the J-L color. It is interesting to compare these results with those of Eggen (1967). He finds that absorption due to TiO in dwarfs is considerably stronger than that in giants of the same temperature, but that supergiants have the same TiO absorption as the giants. This is quite different from the behavior of the CO band strength. Eggen (1967) also finds a "slight but real variation in TiO absorption at a given temperature" which agrees with the CO observations. See Figs. 18 and 19 in the Appendix for a luminosity and temperature sequence of the spectra.

The results presented in Figures 10a, b, c suggest that a narrow band filter system which could measure the continuum and CO band strength in the 2μ region could be used, in conjunction with broad band infrared photometry, to provide a reasonably accurate two dimensional classification for late-type stars.

B. $[\, C^{12}/C^{13} \,]$

To estimate the ratio of equivalent widths of $C^{12}O^{16}$ and $C^{13}O^{16}$ features, the depths of the (2, 0) band heads of these two molecules

Fig. 10b. - The quantity W(CO) as a function of J-L and luminosity for all of the stars observed.

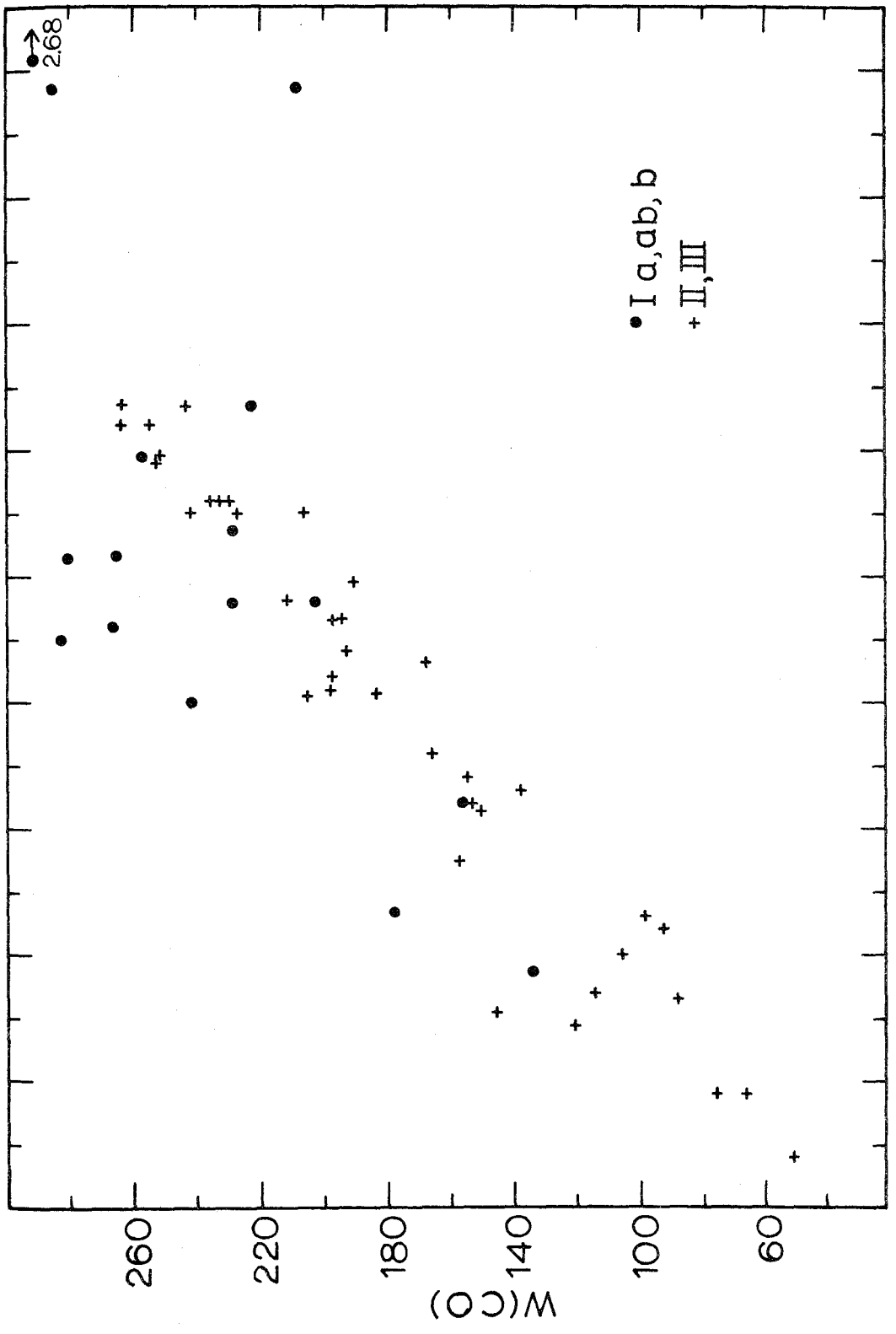
2.68
I a,ab, b
II,III
W(CO)
260
220
180
140
100
60
(J-L)
.5
.7
.9
1.1
1.3
1.5
1.7
1.9
2.1
2.3

Figure 10b.

Fig. 10c. - The quantity W(CO) as a function of slope of the continuum in the 2μ region for all of the stars observed.

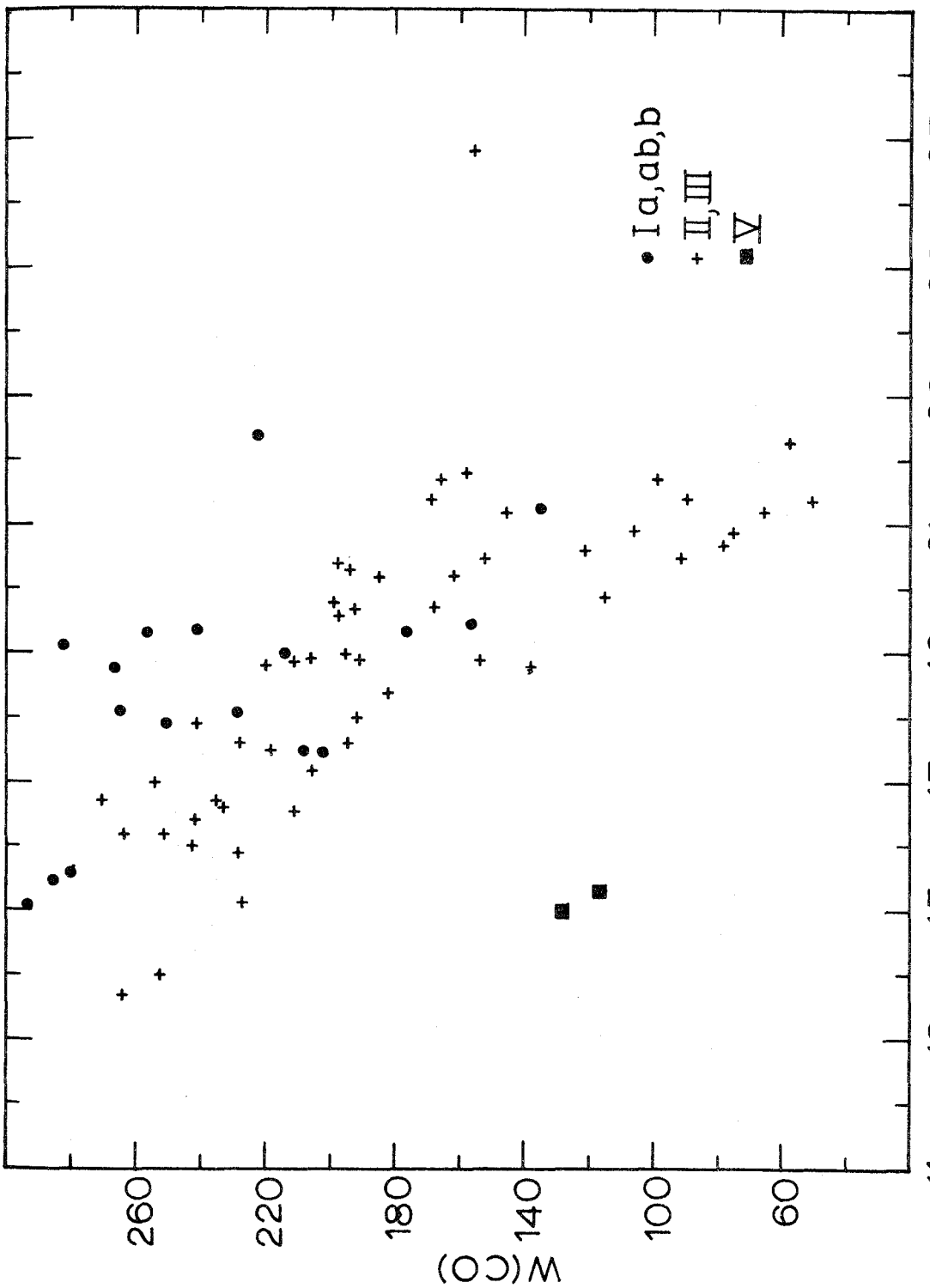
W(CO)
260
220
180
140
100
60
1.1
1.3
1.5
1.7
1.9
2.1
2.3
2.5
2.7
Log (F2.057μ / F2.343μ)cont.
• Ia,ab,b
+ II,III
■ V

Figure 10c.

have been measured. For the $C^{12}0^{16}$ band the previously defined continuum level was used. For the $C^{13}0^{16}$ band, a "local" continuum defined by the (3, 1) $C^{12}0^{16}$ band was used (see schematic below):

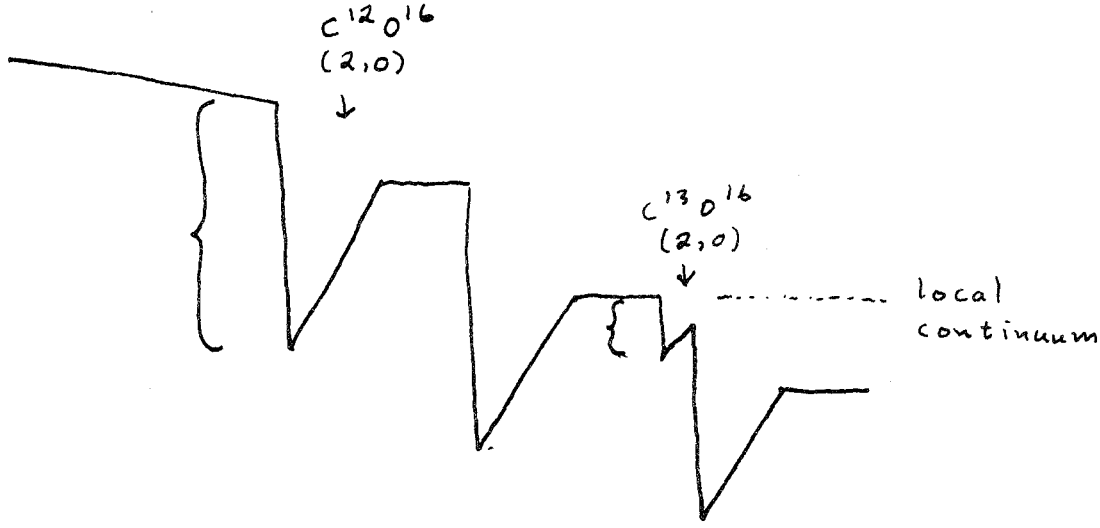

The high resolution spectra of Connes, et al (1968) indicates that in the region of the band heads there are about 10 individual lines per resolution element of the spectrometer employed here, so that the depth at the band head may indeed be considered as a reasonable measure of the absorption and, therefore, the depths may be interpreted to give an estimate of the ratio of equivalent widths. The strength of the $C^{13}0^{16}$ absorption will be systematically underestimated since the continuum with respect to which it is measured is formed at a higher level than the continuum used in measuring the $C^{12}0^{16}$ absorption. Also, this may result in a systematic underestimation of $C^{13}0^{16}$ in stars with the strongest CO absorption.

A ratio of equivalent widths normally yields a ratio of abundances if

the proper saturation correction is known. Thompson, et al (1971) have argued from a model atmosphere approach that the CO bands in carbon stars are unsaturated. On the other hand, Spinrad, et al (1971) have found large saturation effects in high resolution spectra. Neither of the arguments for the two possibilities are especially convincing, particularly in view of the large uncertainties in the theoretical interpretations and in corrections for turbulent broadening. Therefore, it has been somewhat arbitrarily decided to treat the equivalent widths as though they arise from the square root part of the curve of growth. Estimates of the $[C^{12}/C^{13}]$ ratio for the stars observed based on this assumption are presented in Figure 11 and Tables 8a, b. Nearly all of the observational error lies in deciding with respect to what level the depth of $C^{13}O^{16}$ should be measured. It is estimated that the maximum resulting error in the ratio of equivalent widths is typical a factor of 1.5, or a factor of 2 in the abundance ratios presented here. Visual inspection of the spectra indicates, however, that at least some of the scatter in Figure 11 is real.

C. Water Absorption

The wings of the 1.87μ H_2O band are relatively easy to observe in stars. At temperatures appropriate to a stellar atmosphere, the longward wing extends considerably beyond 2.0μ (Benedict, Bass, and Plyler 1954) thus separating it from telluric H_2O absorption. This broadening is due to the increased population of the higher energy states as discussed by Kuiper (1962) and Ferriso and Ludwig (1964 a, b).

Fig. 11. - The value of $[C^{12}/C^{13}]$ for all of the stars observed. The square root portion of the curve of growth was assumed as discussed in the text.

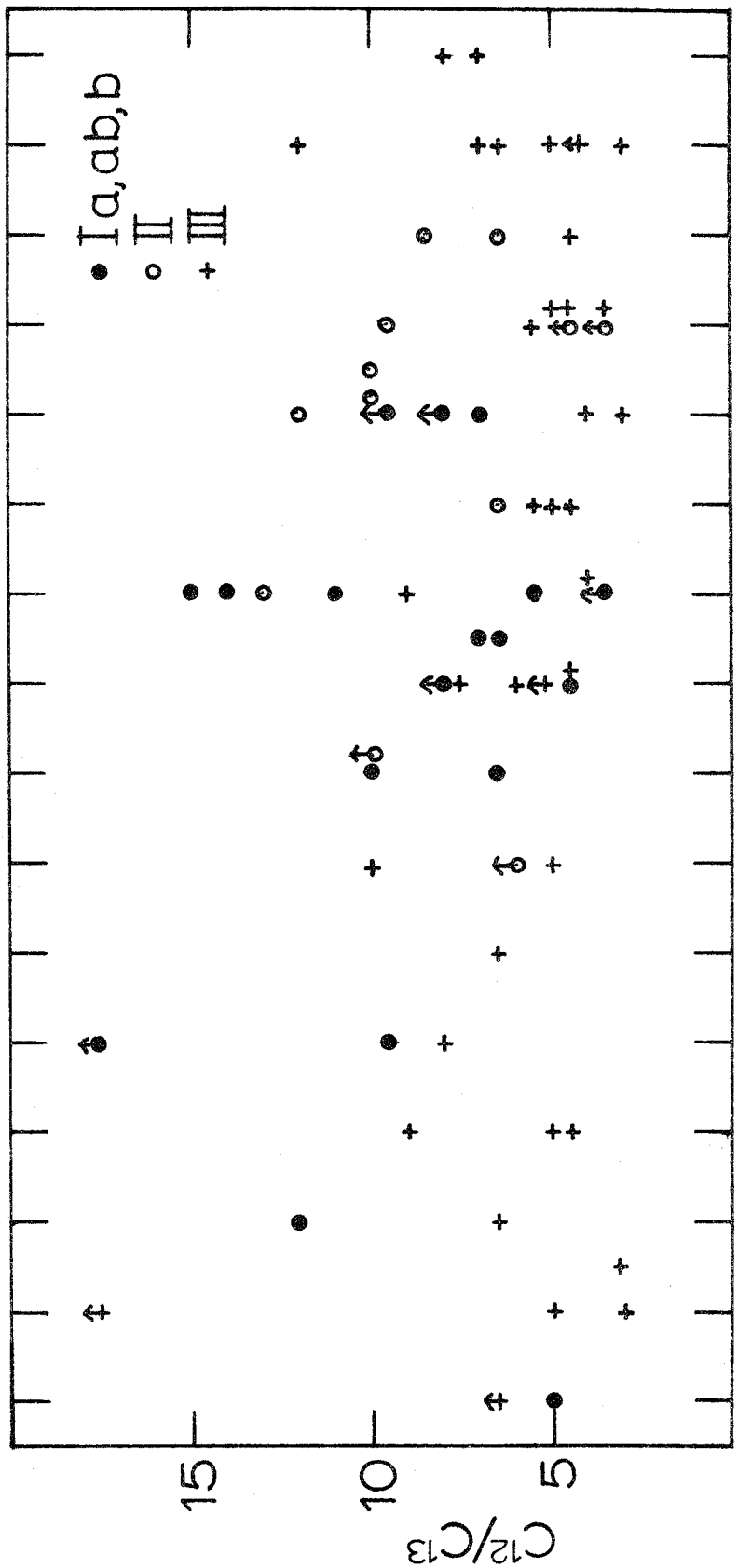
Ia,ab,b
II
III
C12/C13
15
10
5
G5-8 K0 1 2 3 4 5 M0 1 2 3 4 5 6 7 8
Spectral Type

Figure 11.

The extreme number of lines results in the water molecule acting as a source of continuous opacity. The profound effect that this molecule has on the emergent flux has been shown by Tsuji (1966) and Auman (1969).

A good measure of the water absorption was found to be the depression of the observed flux at 2.10 μ below that expected from an extension of the continuum determined in the manner described previously. In Tables 8a, b and Figure 12 the quantity

$$WV = \log \left(\frac{F_{\text{continuum}}}{F_{\text{observed}}} \right)_{\lambda = 2.10\mu}$$

is presented for the stars observed here. $F_{observed}$ represents a mean over 80 Å. The presence of discrete absorption features in this region causes WV to be > 0 even in the absence of any absorption due to water.

Figure 13 indicates the lack of any evidence of water absorption in normal giants and supergiants earlier than M6. This agrees with the observations of Spinrad and Wing (1969) made in the 1μ region and with the observations of Johnson, et al (1968) and Johnson and Méndez (1970). The presence of water in the small range irregular variables of types M7 and M8 observed here was previously found by Spinrad and Newburn (1965) in 1 μ spectra.

The above authors have pointed out that these findings contradict the results of Woolf, Schwarzchild, and Rose (1964) who claim to have found the 1.87 μ band of H_2O in the M giant ρ Per and the M supergiant α Ori. To facilitate comparison, Figure 13 shows the absolute flux of ρ Per as observed here and by Woolf, et al. Also compared are the spectra of μ Gem obtained in the two studies. Only the region of CO

Fig. 12. - The quantity WV, indicating the strength of the 1.87μ water band, for the stars observed here.

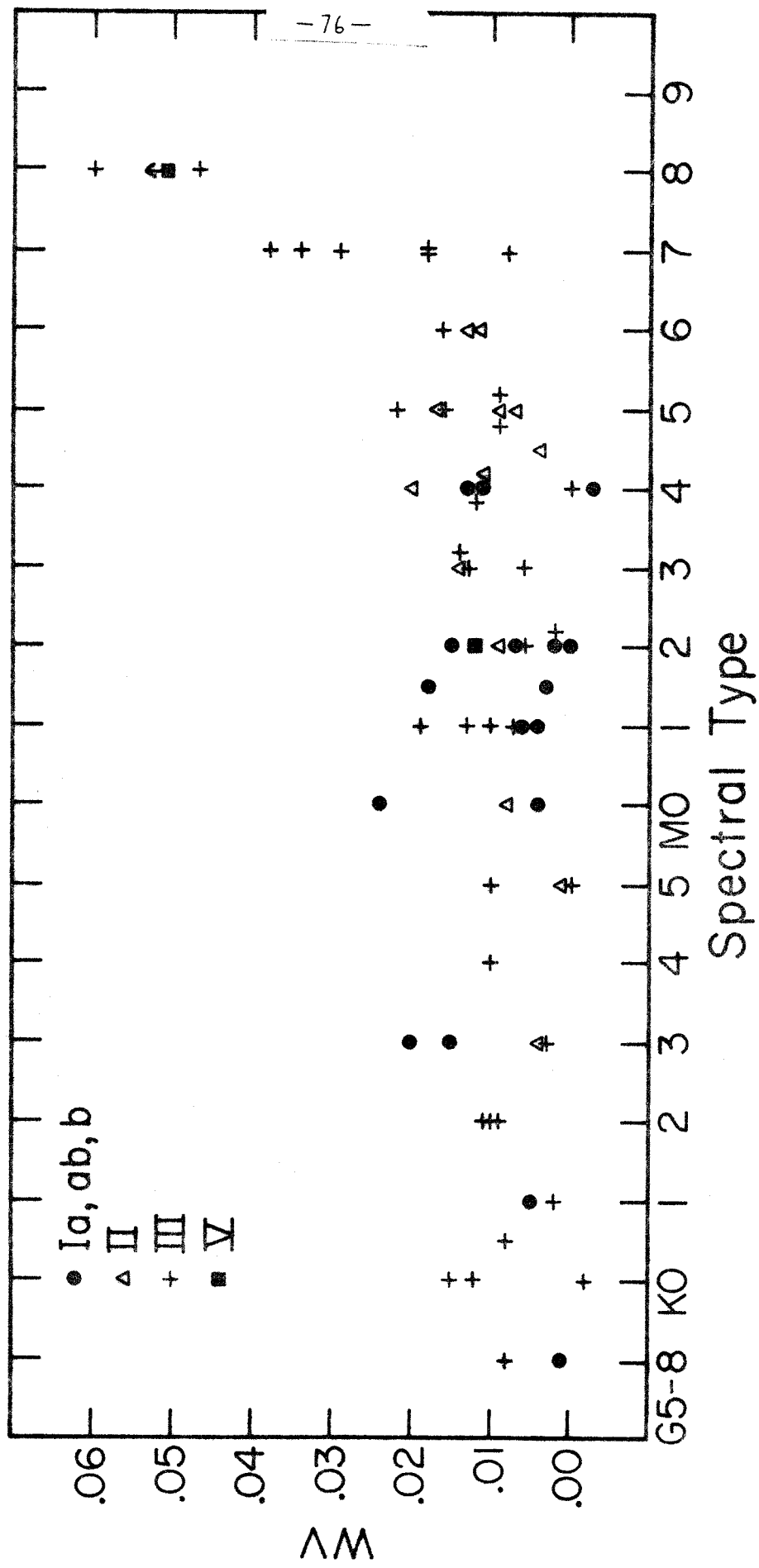
Ia, ab, b
II
III
V
WV
.06
.05
.04
.03
.02
.01
.00
G5-8
K0
1
2
3
4
5
M0
1
2
3
4
5
6
7
8
9
Spectral Type

Figure 12.

Fig. 13. - Spectra of μ Gem and ρ Per obtained here compared with the results of Woolf, Schwarzchild, and Rose (1964). The results of their detectors "A" and "B" are indicated. Only the region of the C0 bands is shown in detail on the spectra obtained here.

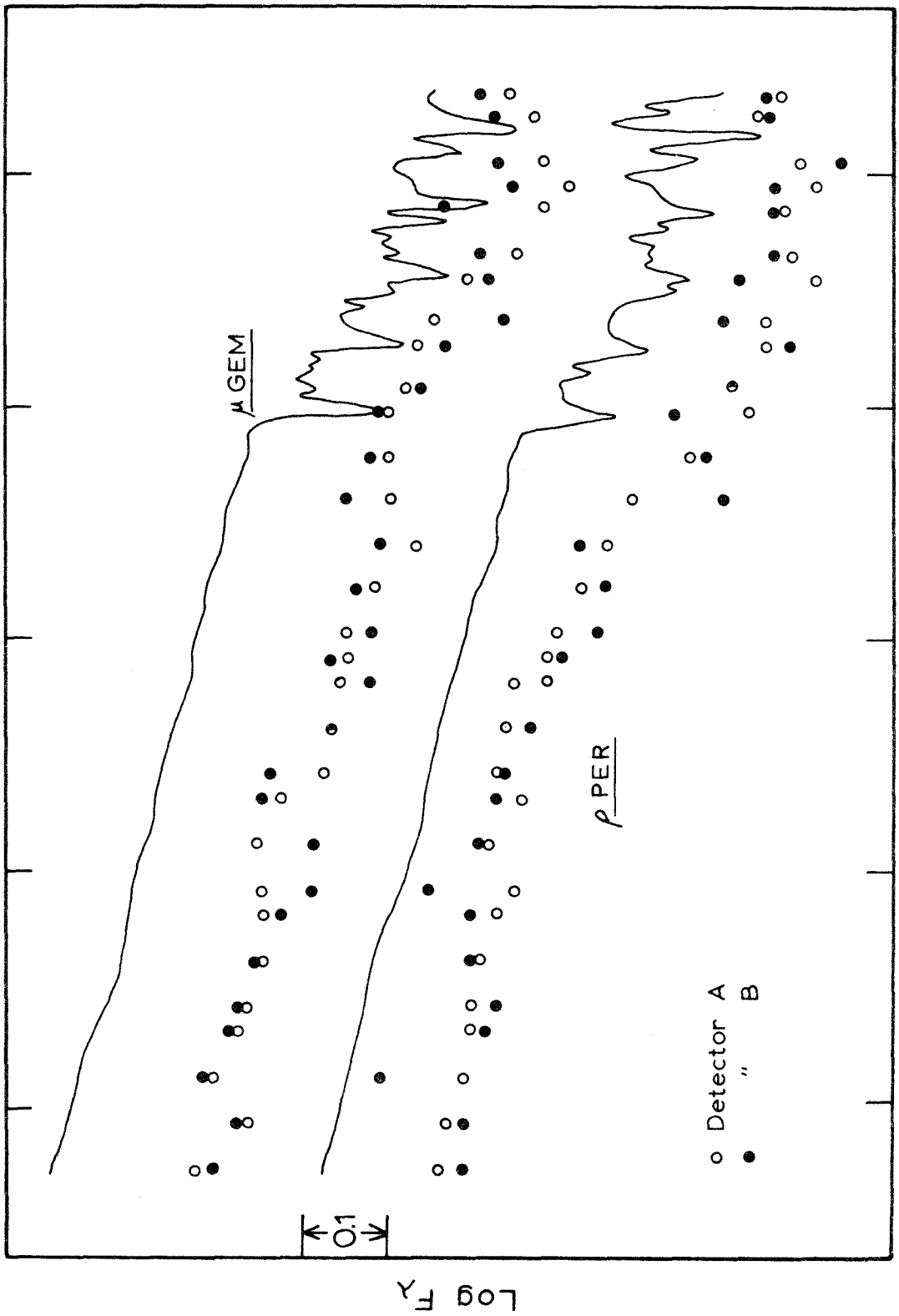

Figure 13.

absorption has been shown in detail on the spectra obtained here. Note that the outputs of detectors A and B of Woolf, et al. differ considerably in detail and that, as noted by Wing and Spinrad (1970), the only features whose presence can be confirmed in this spectral region are those due to CO. Since the 1.4μ H_2O band is weaker than the 1.9μ band (Ferriso and Ludwig 1964a,b), the lack of any evidence for the latter band in ρ Per or μ Gem makes the identification of the 1.4μ feature with H_2O suggested by Woolf, et al, doubtful. Wing and Spinrad (1970) suggested that the 1.4μ feature may be a CN band.

The strongest band of H_2O is the fundamental vibration-rotation band at 2.7μ . It has an integrated intensity which is typically ten times greater than the band at 1.9μ (Ferriso and Ludwig 1964a, b). However, the experimental studies by Ferriso and Ludwig indicate that for the temperatures considered here, absorption by the 2.7μ band would have a negligible effect on spectra shortward of 2.4μ . Longward of 2.4μ absorption by telluric H_2O becomes significant. The broadening effect associated with high temperatures and discussed in connection with the 1.87μ band, occurs only on the long wavelength wing of the 2.7μ band (Ferriso and Ludwig 1964 a, b).

V. DISCUSSION

A. Interpretation of CO Band Strength

The most outstanding feature of the spectra of the stars presented here is the variation in strength of the first overtone CO band with temperature and luminosity. In general, the integrated band intensity of CO will be determined by four parameters: the temperature, pressure, column density of CO, and the microturbulent velocity of the gas. The Doppler half-widths of the individual rotational lines increases with increasing temperature, and, as shown by Kunde (1967, 1968), the effect of changing the population of the different vibration-rotation levels by changing the temperature is to cause the integrated band intensity of the first overtone band to increase with increasing temperature. The pressure operates vis-á-vis collisional broadening in a manner which will increase line widths with increasing pressure. Since pressure decreases with increasing luminosity and both pressure and temperature decrease with advancing spectral type, these two parameters cannot account for the observed behavior of the CO bands. Making the reasonable assumption that the association of CO is complete for stars later than K0 (Schadee 1968), model atmosphere calculations by Auman (1969), Goon and Auman (1970) and Carbon (private communication) indicate the amount of CO above the photosphere does not change in any systematic manner over the temperature range considered here. The logarithm of the projected number densities of CO above $\tau_\nu = 0.3$ at $\lambda = 4.6\mu$ for a sequence of giant and supergiant atmospheres taken from the data of Goon and Auman is presented in Table 9. As will be discussed below,

TABLE 9

CO ABUNDANCES FROM GOON AND AUMAN

TEMPERATURE (^{o}K)	g (cm-sec^{-2})	log N(CO) (cm $^{-2}$)
4000	2.0	22.2
4000	1.0	22.6
3500	1.5	22.2
3500	0.5	22.9
3000	1.0	21.6
3000	0.0	22.2
2500	0.0	22.2
2500	-1.9	22.1
2000	-1.0	22.5
2000	-2.0	22.5

Fig. 14. - Theoretical absorption profiles of CO using the parameters given in Table 10.

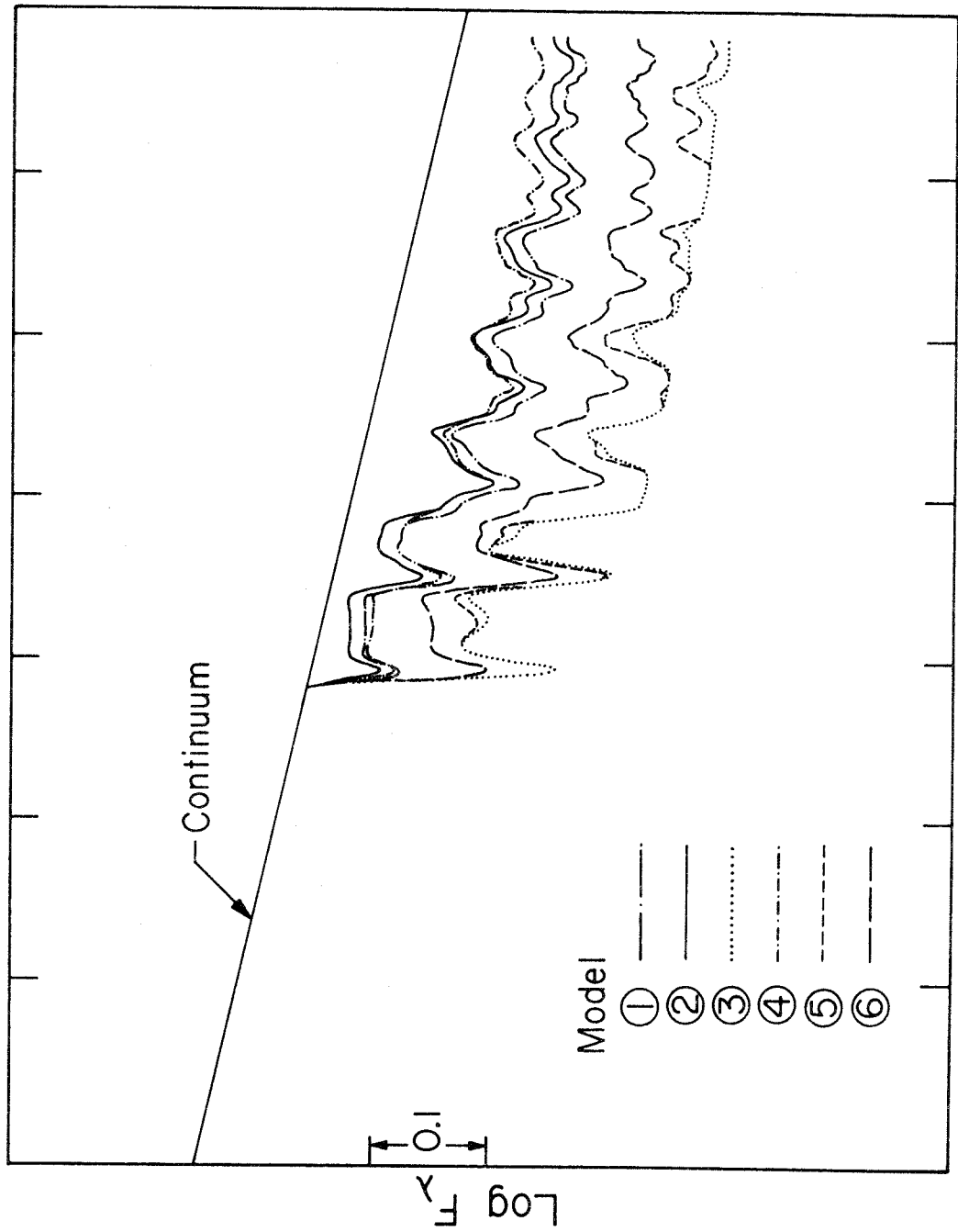
Continuum
Model
① ② ③ ④ ⑤ ⑥
2.20
2.25
2.30
2.35
2.40
2.45
λ (microns)
Log F_λ
1.0

Figure 14.

TABLE 10

CO MODELS FROM KUNDE

MODEL	TEMPERATURE (^{o}K)	PRESSURE (mb)	TURBULENT VELOCITY (cm/sec)	DENSITY OF CO (gm/cm^2)
1	3000	1	0.0×10^5	100
2	3000	.01	0.0×10^5	100
3	3000	1	8.0×10^5	100
4	2000	1	0.0×10^5	100
5	2000	1	8.0×10^5	100
6	3000	1	0.0×10^5	1000

the emergent fluxes predicted by these atmospheres are in serious disagreement with the observations with regard to the strength of the H_2O absorption features. Thus it is not clear how much weight should be attached to their results.

Observationally there is little evidence for any large scale changes in the continuous opacity which would result in a change in CO band strengths. As noted in a previous section, the main change in appearance of the spectra in the region shortward of the (2, 0) CO band is a general strengthening of the absorption features with advancing spectral type. As the identified features seem to be low excitation atomic lines, the observed strengthening may be interpreted as due to an increase in population of the appropriate atomic energy levels. Some calculations done by V. G. Kunde (private communication) using a Milne-Eddington model indicate that the CO absorption coefficient increases relative to the continuous absorption coefficient as cooler stars are considered. This is the same as Auman's (1967) result concerning the H_2O absorption coefficient.

In Figure 14 some results of Kunde's calculations are presented and show the effects of varying physical parameters on a CO absorption spectrum. A single slab model was chosen to represent the reversing layer, and the continuum is that given by the 2 μ spectrum of α Orionis. The continuous opacity was not considered here. The various sets of parameters used to characterize the reversing layer are in Table 10. In all cases the boundary temperature was taken to be 1500°K and a $[C^{12}/C^{13}]$ ratio of 10. The great effect of changing the turbulent

velocity is very evident.

What are typical values for the microturbulent velocity in late-type giants? In her study of the lithium abundance in these stars, Merchant (1967) obtained values between 2 and 3 km/sec for early M giants and between 3 and 4 km/sec for early M supergiants. Rosendhal (1970) finds microturbulent velocities on the order of 10 km/sec in A supergiants, but, in summarizing the observational data, he concludes that the value decreases sharply for Ia stars later than G0-G2 with probably similar behavior in the less luminous giants and supergiants. All of these values, however, are based on measurements of very strong metallic lines which have f values that typically are many orders of magnitude greater than the f values for the individual lines arising from different rotational states of C0. From the theoretical line intensities tabulated by Kunde (1967) and the data given by Rosendhal for Ti II, a typical value of $f_{Ti}/f_{CO} = 3 \times 10^7$ is found. (Note that the g values for different vibrational levels are all equal to 1). Oscillator strengths for C0 calculated by Schadee (1968) based on observations of Goldberg and Müller (1953) are in good agreement with the theoretical values of Kunde. Now the observations reported by Montgomery, et al (1969) indicate that the equivalent widths of the strong C0 lines in α Boo are comparable to the strong Ti II lines observed by Rosendhal in A supergiants -- several tenths of an Ångstrom. Assuming that most of the Ti in an A supergiant is in the form Ti II, that C0 is completely associated in α Boo, and that the atomic abundances do not differ too greatly between the two stars, it is found that the path length required in α Boo to produce a C0 line is roughly 100 times greater than the path length required to produce a Ti II line of comparable strength

in an A supergiant. If, as some authors believe, α Boo is metal deficient, then the path length becomes even greater. Since the distinction between micro-and "macro" turbulence is based on the size of the turbulent eddies relative to that of the line forming region, it is reasonable to conclude that velocity fields usually considered to arise from macroturbulence in late-type stars will affect the equivalent width of the CO bands as if they were microturbulent velocities. Although the observational evidence is scanty, it seems that at least for G and K supergiants these large scale velocities are an order of magnitude greater than the microturbulent velocities noted above (Kraft (1960).

The theoretical calculations of Kunde (1967) indicate that the average spacing of lines arising from both $C^{12}O^{16}$ and $C^{13}O^{16}$ in the region of the (2, 0), (3, 1) and (4, 2) bands of $C^{12}O^{16}$ is 2 Å. The high resolution (~0.5Å) spectrum of α Ori presented by Connes et al (1968) indicates that individual lines strongly overlap, are very deep, and have Doppler widths of 1-2Å which in this spectral region correspond to velocities of 13-20 km/sec. The strong overlapping of the lines suggest that pressure and Lorentz broadening will have little effect on the equivalent widths of the CO bands.

It is instructive to attempt to represent the CO band with a modified Elsasser model. Let S and δ be the mean line intensity and line spacing, respectively. Following Goody (1964), define the following dimensionless parameters:

$$\chi = \nu/\delta$$
$$y = a_D/\delta$$
$$u = Sa/a_D\sqrt{\pi}$$

where a is the amount of CO in gm cm^{-2} and a_D is the Doppler width. The equivalent width of the band may then be written as

$$\frac{W_\lambda}{\delta} = \int_o^\infty \left\{ 1 - \exp\left(- \sum_i \left[u \exp\left(-\frac{\chi_i^2}{y^2} \right) \right] \right) \right\} d\chi$$

where the summation is over the number of lines considered in the model. Except for very high densities and turbulent velocities, six lines were found to be sufficient to illustrate the effects of various model parameters. Figure 15 shows log (W_λ/δ) as a function of log a for various values of the turbulent velocity. For small values of a the curves merge into the linear curve of growth for weak lines. For large values of a, the pure Doppler lines become saturated and the flat part of the curve of growth obtains. Increasing the turbulent velocity removes the saturation until the overlapping of the lines causes complete absorption over the whole region. This is an exaggeration of the true state of affairs since the various sequences of overlapping lines are not all of the same strength and the lines are not evenly spaced. However, it is clear that by the time saturation becomes great enough for the Lorentz wings to be important under normal circumstances, they will not make a contribution here because of the deep, turbulent broadened Doppler cores. Some of the computed line profiles are shown in Figure 16. Those with no turbulent broadening are much too narrow when compared with the high resolution spectrum of α Ori (Connes, et al 1968), and those with ξ_t > 13 km/sec are too broad. The profile with ξ_t = 6.5 km/sec and "a" between .15 and .46 gm/cm^2 does, in fact, bear a fair resemblance to the lines in α Ori. Reference to Table 9 indicates that these values are between those calculated by Goon

Fig. 15. - Curve of growth for the modified Elsasser band model discussed in the text for various values of the turbulent velocity, ξ_t. N(CO) is the column density of CO, W_λ the equivalent width in Angstroms, and δ is the line spacing in Angstroms.

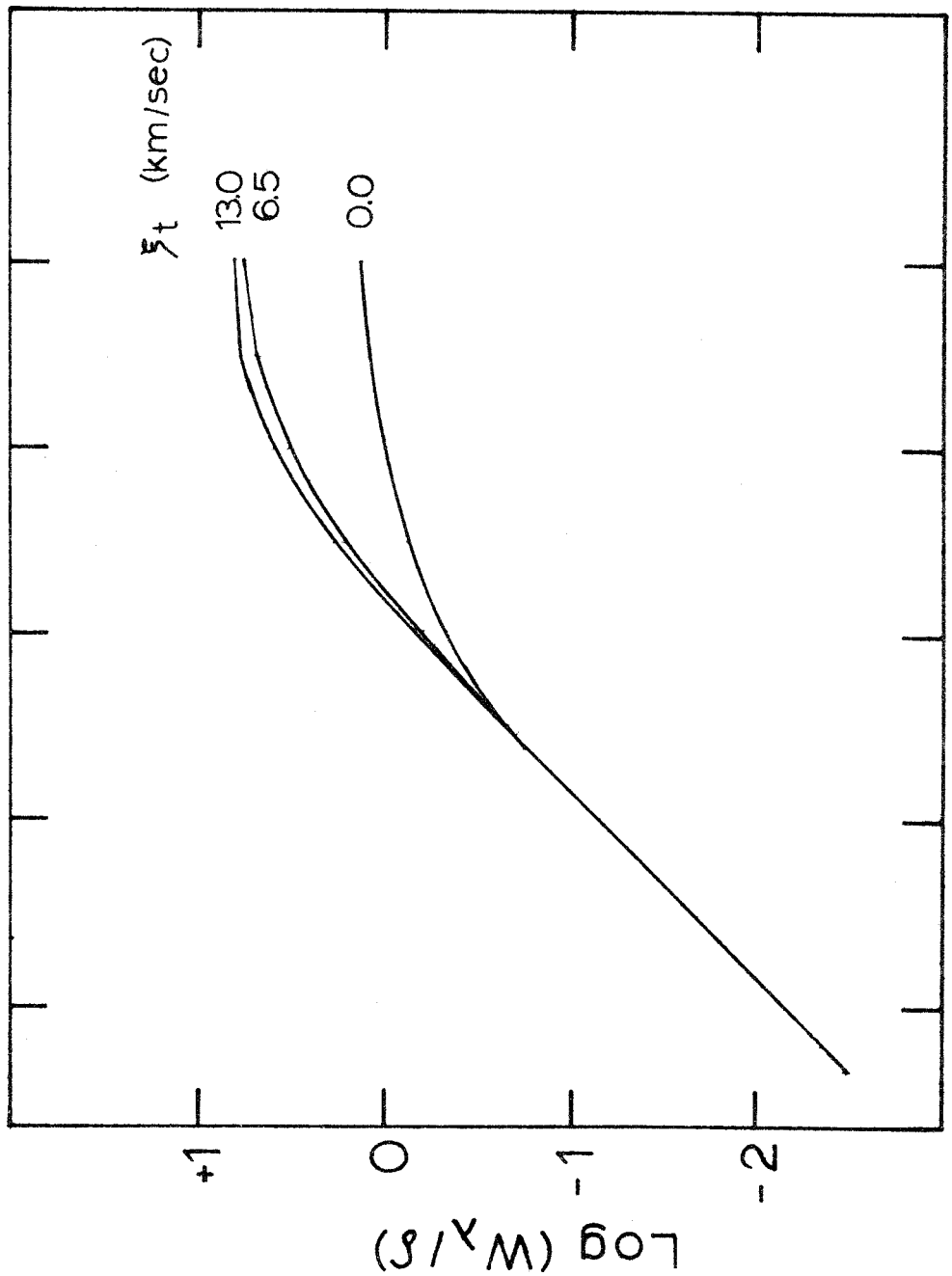

Figure 15.

Fig. 16. - Calculated line profiles for different values of the parameters defined in the text. From top to bottom, the values of log N(CO), (cm^{-2}), are 21.0, 21.5, and 22.0. The profile with $\xi_t = 6.5$ km/sec and log N = 21.5 (cm^{-2}) is considered to be similar to the high resolution spectra of α Ori.

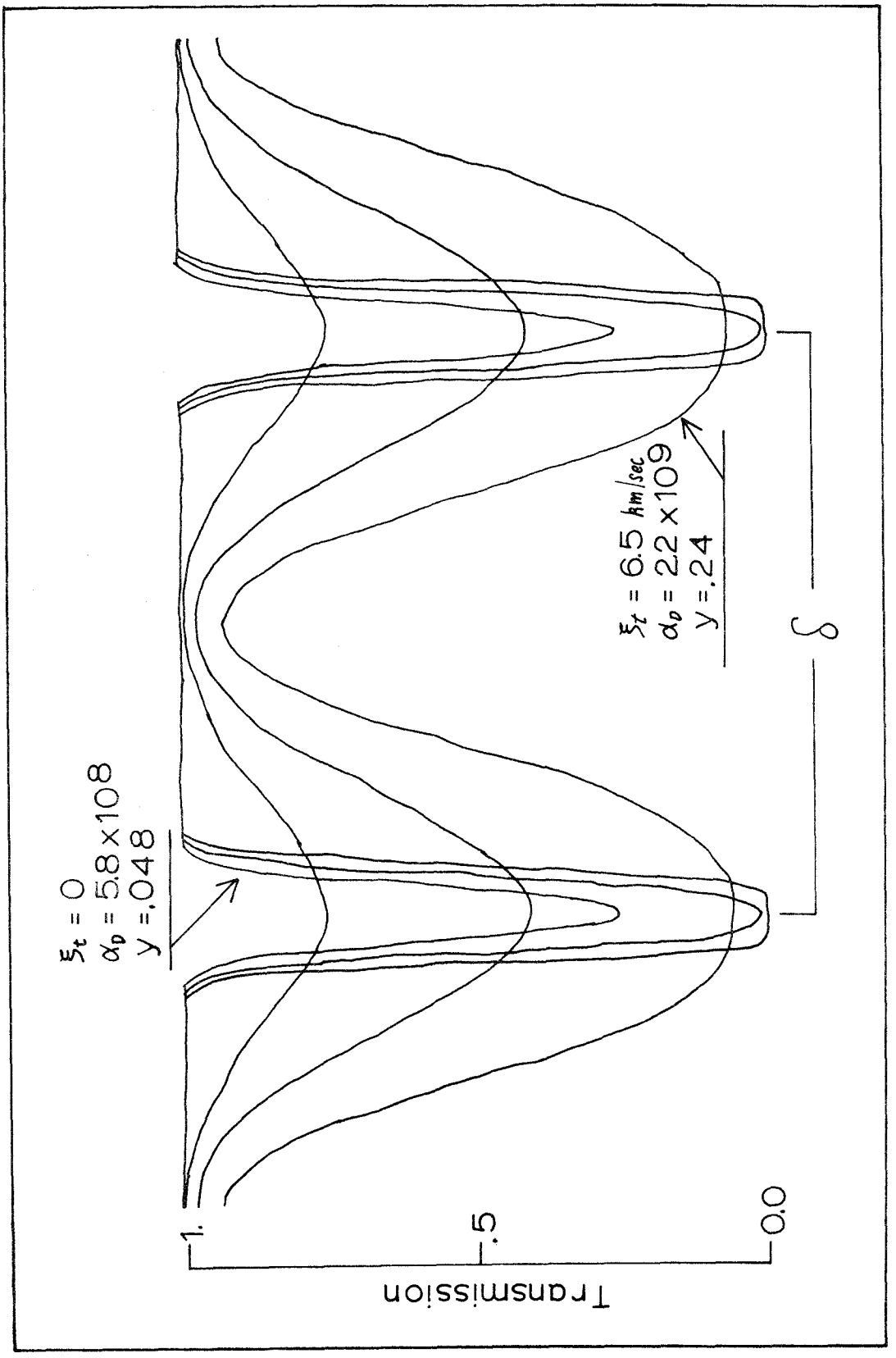
Transmission
1.
.5
0.0
$\xi_t = 0$
$\alpha_D = 5.8 \times 10^8$
$y = .048$
$\xi_t = 6.5$ km/sec
$\alpha_D = 22 \times 10^9$
$y = .24$
δ

Figure 16.

and Auman for giant and supergiant stars with Te = 3000°K.

Schadee (1968) has computed theoretical band strengths for several molecules in G and K stars. In his figure 2 the strength of the CO band is plotted as a function of spectral type. Going from G5 to K5 the strength should increase by about a factor of three. This is slightly less than what is observed here (Figure 10). However, his diagram also indicates a general levelling off of the CO band strength as late K stars are approached whereas what is observed is an almost steady increase from G5 to M8. The equivalent widths given by Montgomery et al (1969) for α Boo, a K3 III star indicate that saturation is beginning to set in. Thus for normal metal stars of M0 and later, saturation is probably large and the effects of turbulence cannot be neglected when computing theoretical band intensities. Even for the late K models considered by Schadee, turbulence should be taken into account. This would have the effect of causing his values of the band strength to increase more strongly with advancing spectral type.

The suggestion that turbulence could account for the difference in strength of the CO bands between giants and supergiants was made by Woolf, Schwarzchild, and Rose (1964). Sequences of cooler temperature and higher luminosity are also sequences of lower surface gravity which would favor an increase in large scale gas motions. As has already been discussed, these large scale motions are expected to greatly influence the CO absorption coefficient. Using the crude band model discussed here, a turbulent velocity on the order of 10 km/sec seemed to apply to α Ori. This agrees with the conclusion of Spinrad, et al (1971).

A final possibility to be considered in accounting for variation in CO band strength is that the assumption of similar chemical composition is incorrect. As will be discussed in Paper II, observational and theoretical evidence lend support to the interpretation of late-type giant stars (not necessarily supergiants) as stars that are evolving to the left in an HR diagram. It is possible, therefore, that there is a systematic variation in the degree to which these stars have mixed their surface material with material which has undergone nuclear processing. Such mixing could also account for the large discrepancy in predicted and observed water absorption strengths as discussed below. This suggestion was made by Auman (1970).

B. Comparison With Model Atmospheres

Detailed model atmospheres which include some molecular opacity sources have been calculated by Tsuji (1966) and Auman (1969). Tsuji used an analytic expression to account for opacity due to the water molecule whereas Auman treated the individual line in a statistical fashion. Auman (1969) gives a detailed critique of the model atmosphere approach to cool stars and cautions against comparing theory with observation. Such a comparison is made, however, in Figure 17. Also shown are the results of a line blanketed model of α Boo (Duane Carbon, private communication). The hotter models agree quite well with the observations as do the dwarf models. The agreement gets progressively worse for the cooler giants and supergiants, primarily due to the lack of any water absorption in these stars.

Various explanations for the lack of H_2O absorption are discussed

Fig. 17. - A comparison of models calculated by Auman (1969) with a schematic representations of the spectra obtained. The temperatures are assumed to be those implied by the visual spectral types. The dots indicate the line blanketed model of α Boo provided by D. Carbon.

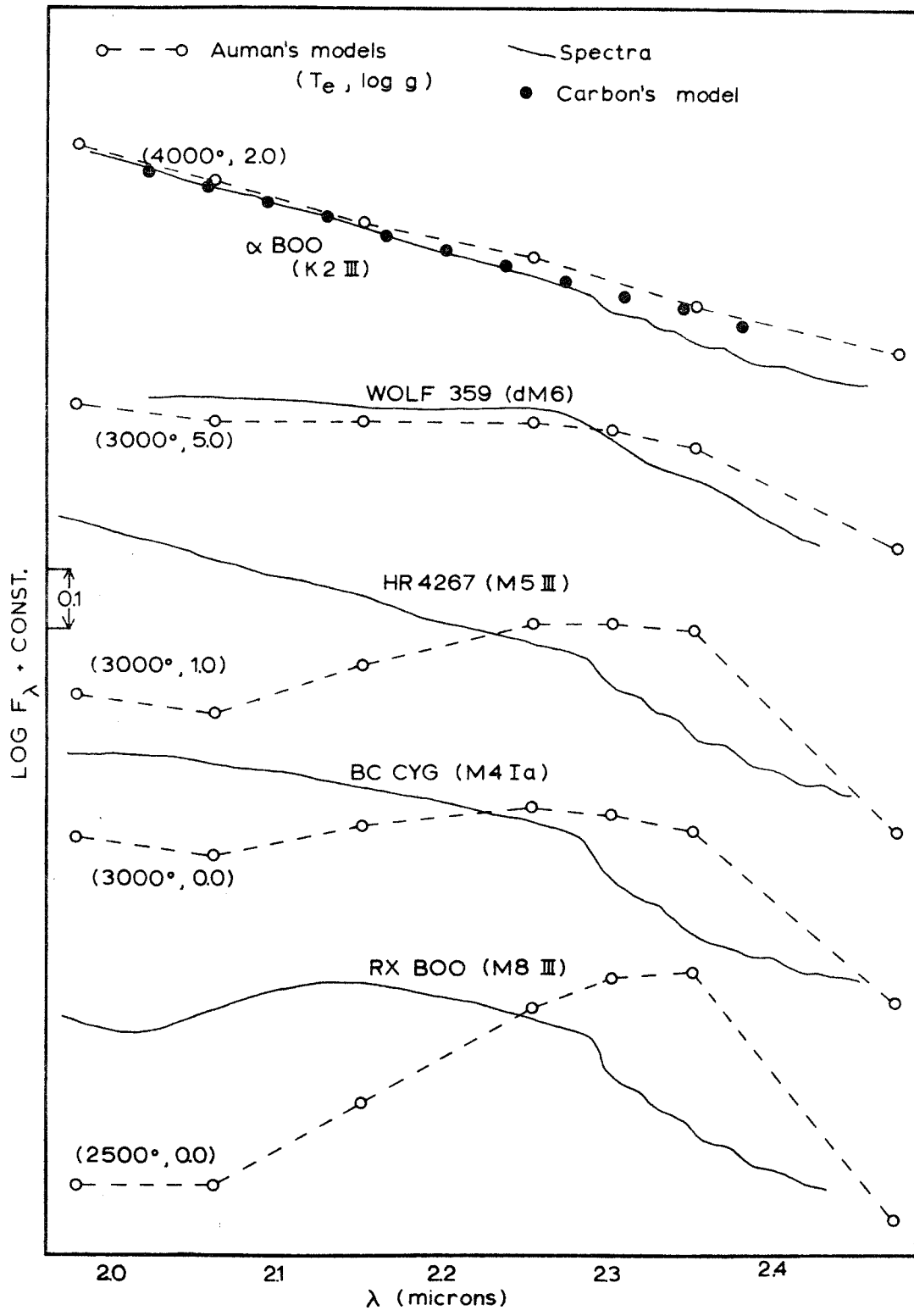
Auman's models
(Te , log g)
Spectra
Carbon's model
(4000°, 2.0)
α BOO
(K2 III)
WOLF 359 (dM6)
(3000°, 5.0)
HR 4267 (M5 III)
0.1
(3000°, 1.0)
BC CYG (M4 Ia)
(3000°, 0.0)
RX BOO (M8 III)
(2500°, 0.0)
LOG Fλ + CONST.
2.0
2.1
2.2
2.3
2.4
λ (microns)

Figure 17.

in the literature (Spinrad and Vardya 1966, Spinrad and Wing 1969, Goon and Auman 1970, Auman 1970) and are gone into in more detail in Paper II. One of the conclusions of Paper II is that the observations of the late-type giants and supergiants presented here can be interpreted as evidence for the idea that these stars have already descended from the red giant tip (Iben 1965), are burning helium in their cores, and have a surface abundance rich in nitrogen but deficient in oxygen and carbon. Thus the surface abundance of H_2O and CO should be considerably lower than that expected if the star had a solar abundance. The most convincing evidence for mixing is the presence of strong $C^{13}O^{16}$ bands in the spectra of nearly all of the stars observed here. The difficulty in determining a reasonably accurate value for the C^{12}/C^{13} ratio has already been discussed, and in view of this difficulty, it is not felt worthwhile to pursue in any quantitative fashion the question of how much mixing has taken place.

APPENDIX

Fig. 18. - A typical sequence of giant stars illustrating the manner in which the spectra change with temperature. The $C^{12}O^{16}$ and $C^{13}O^{16}$ band heads are indicated. Note B_γ in absorption in the G and K stars.

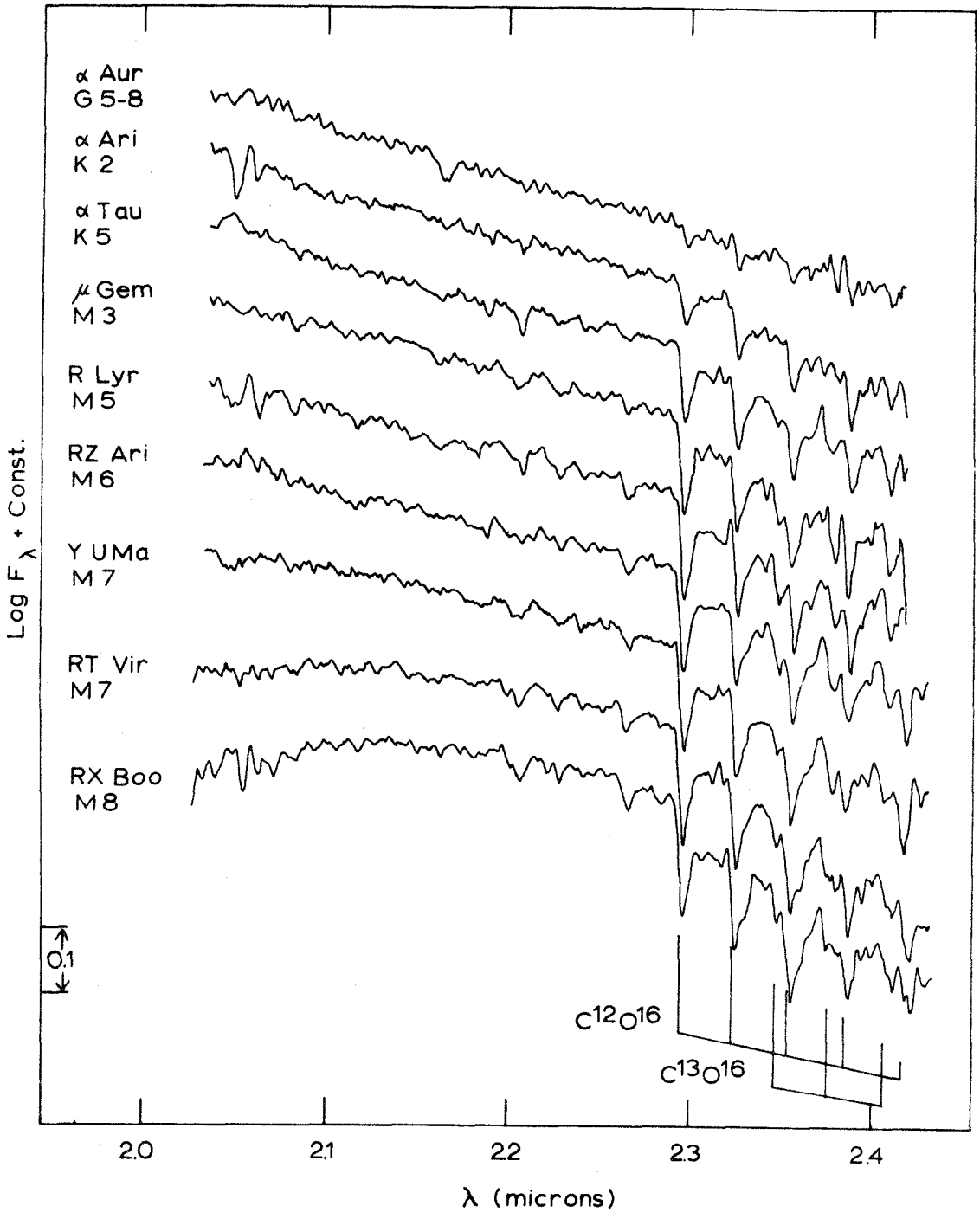
α Aur
G 5-8
α Ari
K 2
α Tau
K 5
μ Gem
M 3
R Lyr
M 5
RZ Ari
M 6
Y UMa
M 7
RT Vir
M 7
RX Boo
M 8
0.1
Log F λ + Const.
C12O16
C13O16
2.0
2.1
2.2
2.3
2.4
λ (microns)

Figure 18.

Fig. 19. - A sequence of stars of different luminosities but all class M2. The telluric CO_2 bands have not been well corrected in μ Cep.

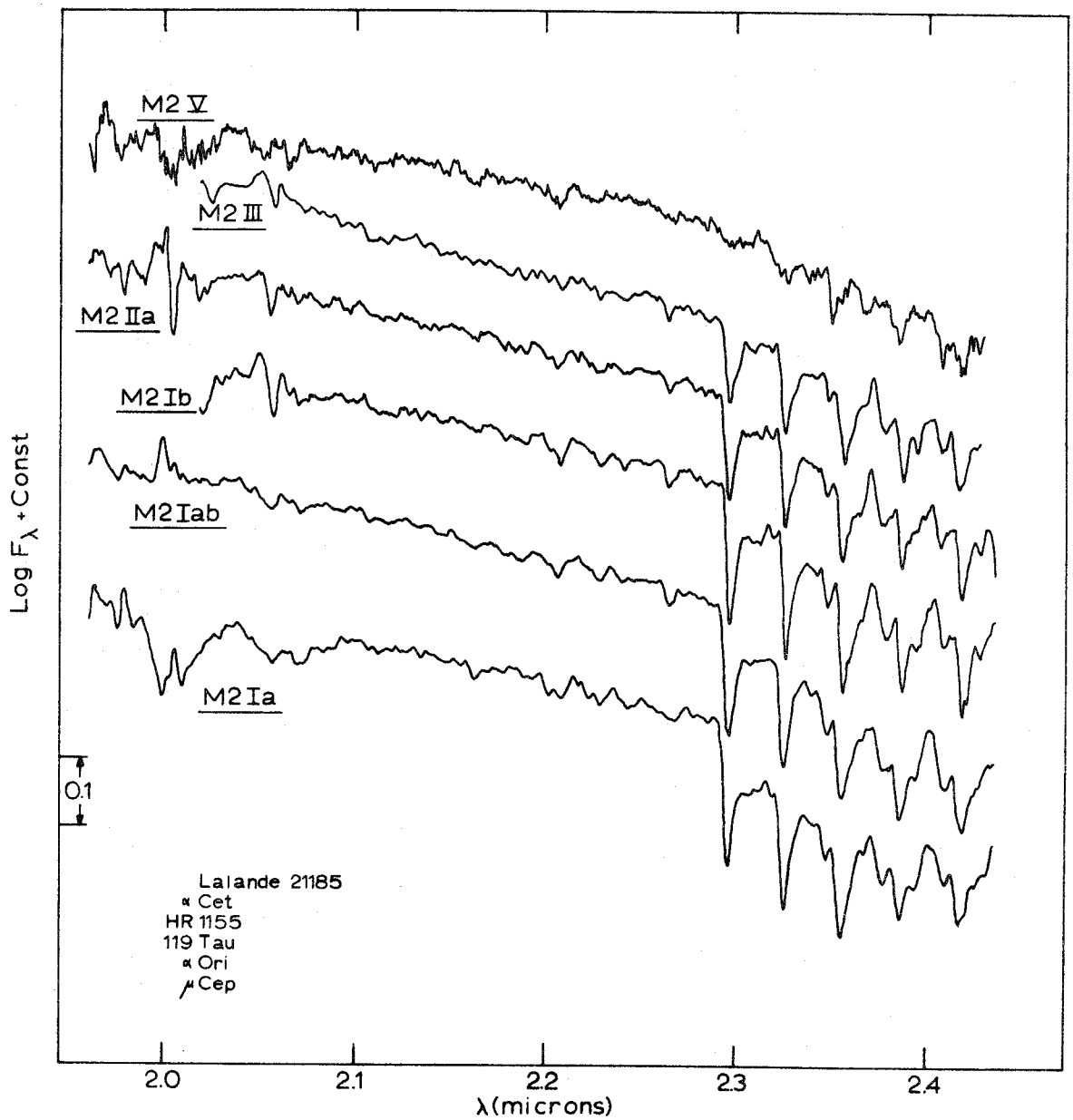
M2 V
M2 III
M2 IIa
M2 Ib
M2 Iab
M2 Ia
0.1
Log F_λ + Const
Lalande 21185
α Cet
HR 1155
119 Tau
α Ori
μ Cep
2.0
2.1
2.2
2.3
2.4
λ(microns)

Figure 19.

The spectra on the succeeding pages are primarily those of supergiants which have not been published before. They should be compared with the sequence of giants in Fig. 18. The caption on the bottom of each figure tells the name of the star, the date of observation, the telescope used, wavelength, the size of the exit slit, the amplifier gain, the scanning speed, and the number of scans which were averaged together. The range in strengths of the CO features, even for stars of the same spectral type, is clearly evident.

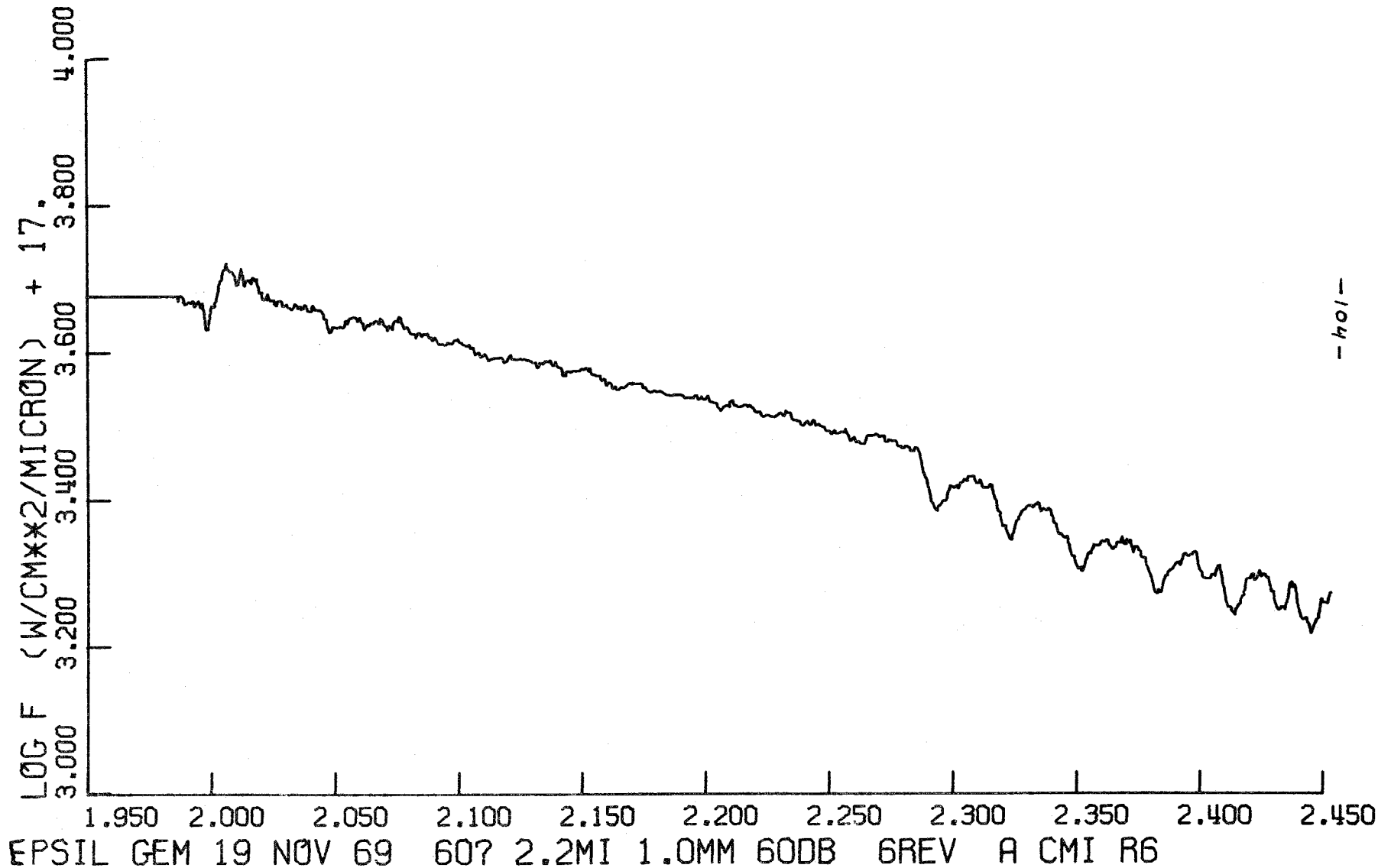
LOG F (W/CM**2/MICRON) + 17.
3.000
3.200
3.400
3.600
3.800
4.000
1.950
2.000
2.050
2.100
2.150
2.200
2.250
2.300
2.350
2.400
2.450
EPSIL GEM 19 NOV 69 607 2.2MI 1.0MM 60DB 6REV A CMI R6

Figure 20.

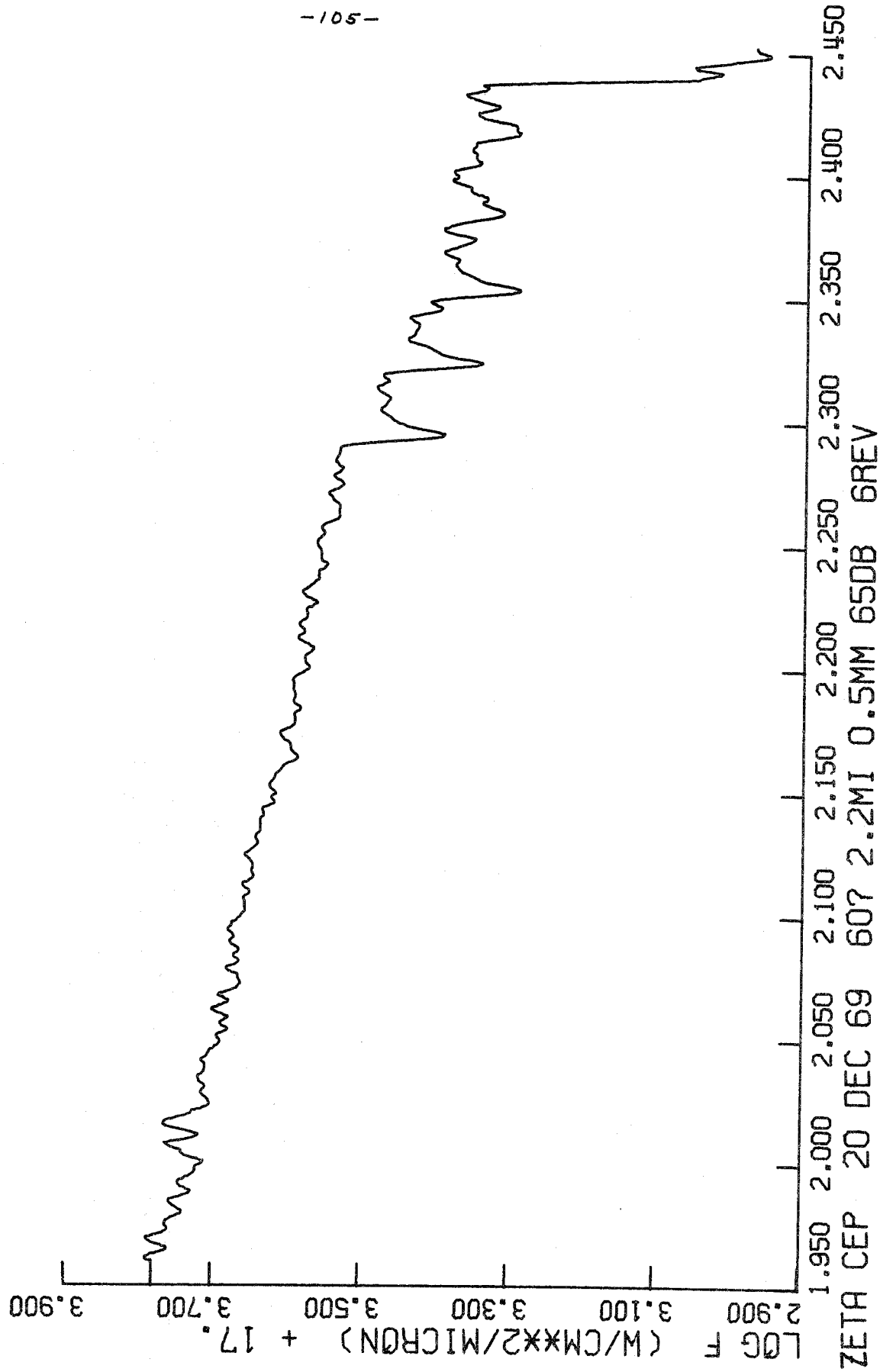
ZETA CEP 20 DEC 69 607 2.2MI 0.5MM 650B 6REV
LOG F (W/CM**2/MICRON) + 17.
1.950
2.000
2.050
2.100
2.150
2.200
2.250
2.300
2.350
2.400
2.450
2.900
3.100
3.300
3.500
3.700
3.900

Figure 21.


LOG F (W/CM**2/MICRON) + 16.45
2.500
2.700
2.900
3.100
3.300
3.500
1.950
2.000
2.050
2.100
2.150
2.200
2.250
2.300
2.350
2.400
2.450
0MIP CMA 20 FEB 70 60? 2.2MI 1.0MM 60DB 6REV 2 SCANS A CMA

Figure 22.

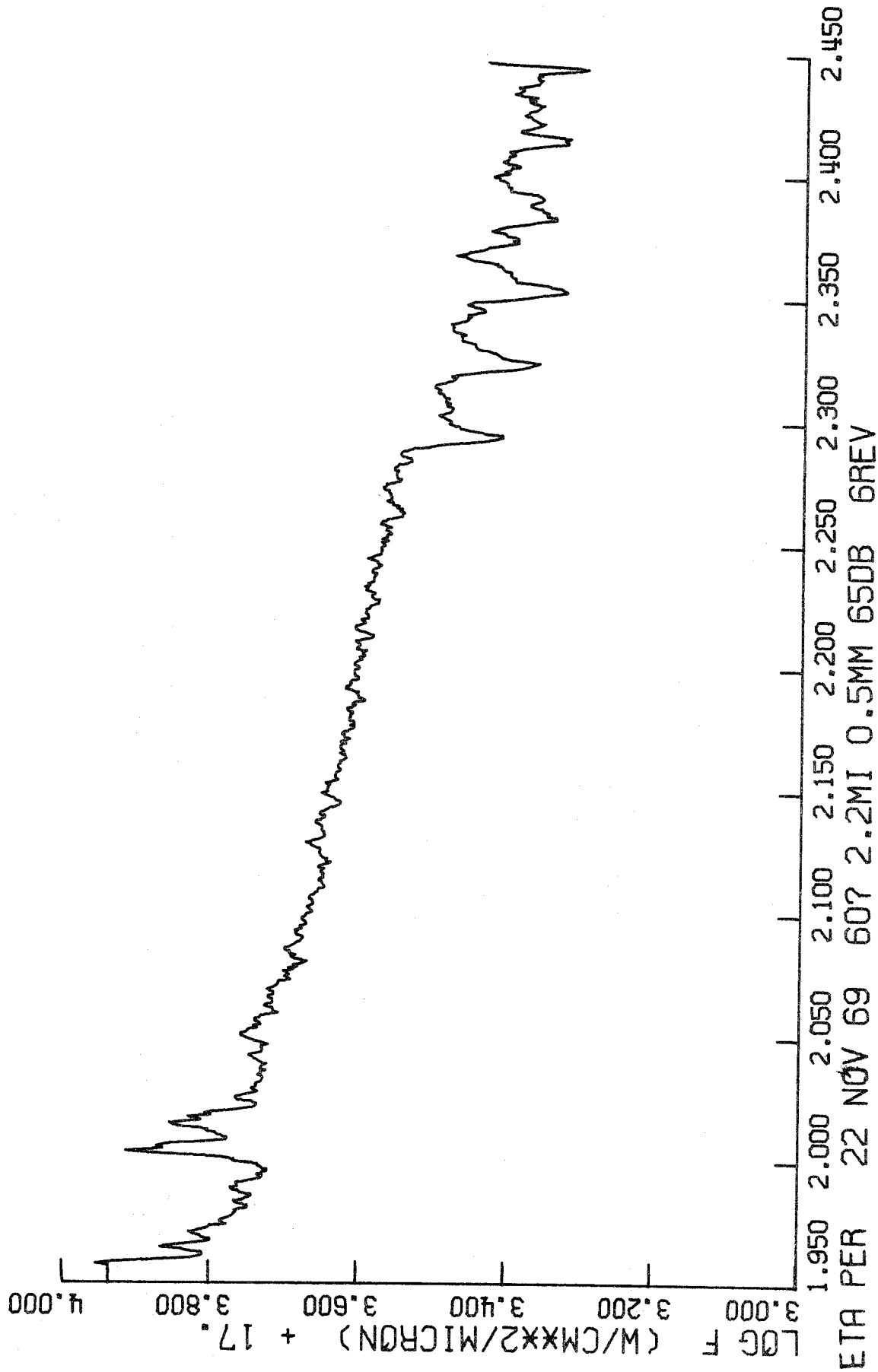
LOG F (W/CM**2/MICRON) + 17.
3.000
3.200
3.400
3.600
3.800
4.000
1.950
2.000
2.050
2.100
2.150
2.200
2.250
2.300
2.350
2.400
2.450
ETA PER 22 NOV 69 607 2.2MI 0.5MM 650B 6REV

Figure 23.

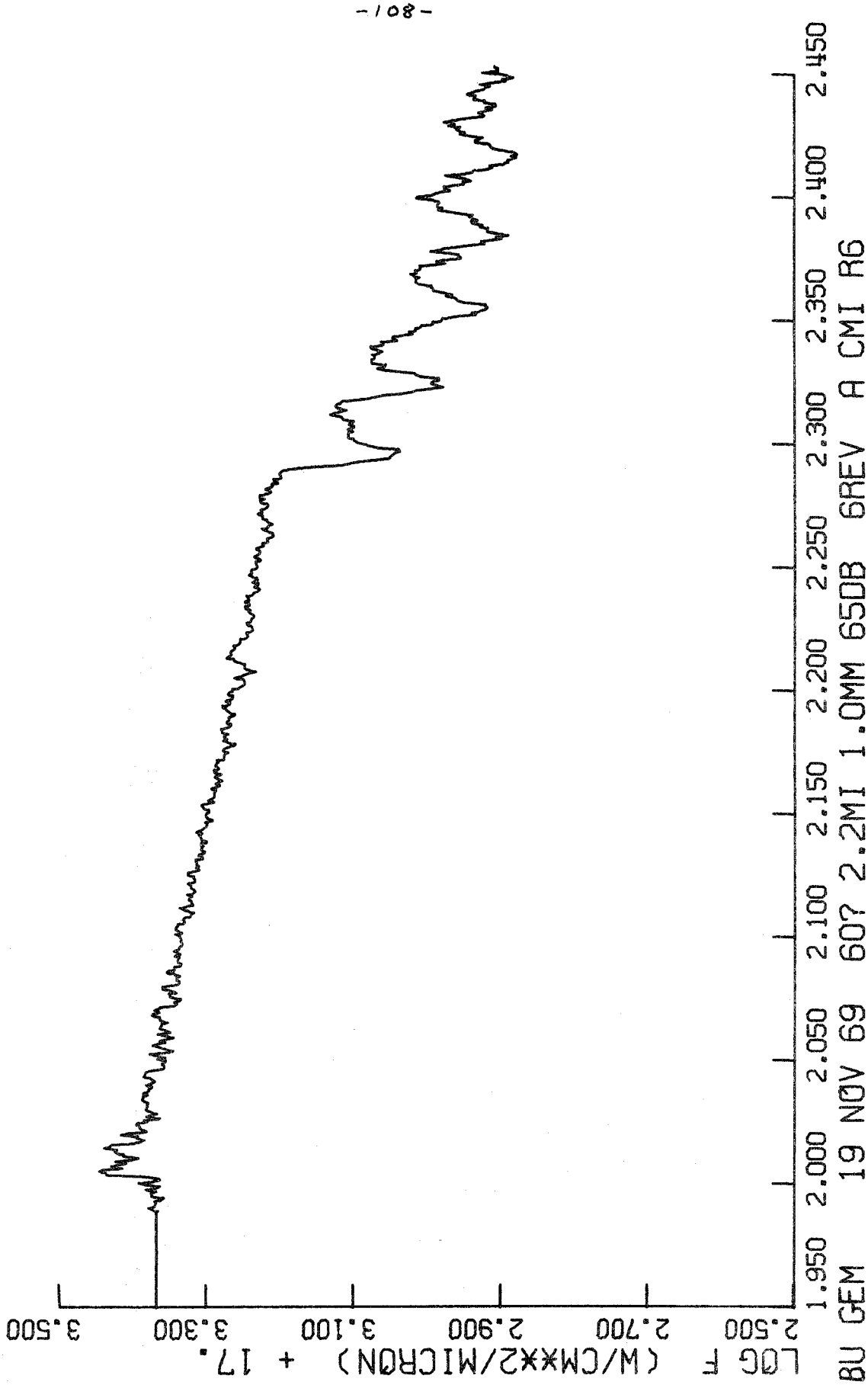
BU GEM 19 NOV 69 60? 2.2MI 1.0MM 650B 6REV A CMI R6
LOG F (W/CM**2/MICRON) + 17.
1.950
2.000
2.050
2.100
2.150
2.200
2.250
2.300
2.350
2.400
2.450
2.500
2.700
2.900
3.100
3.300
3.500

Figure 24.

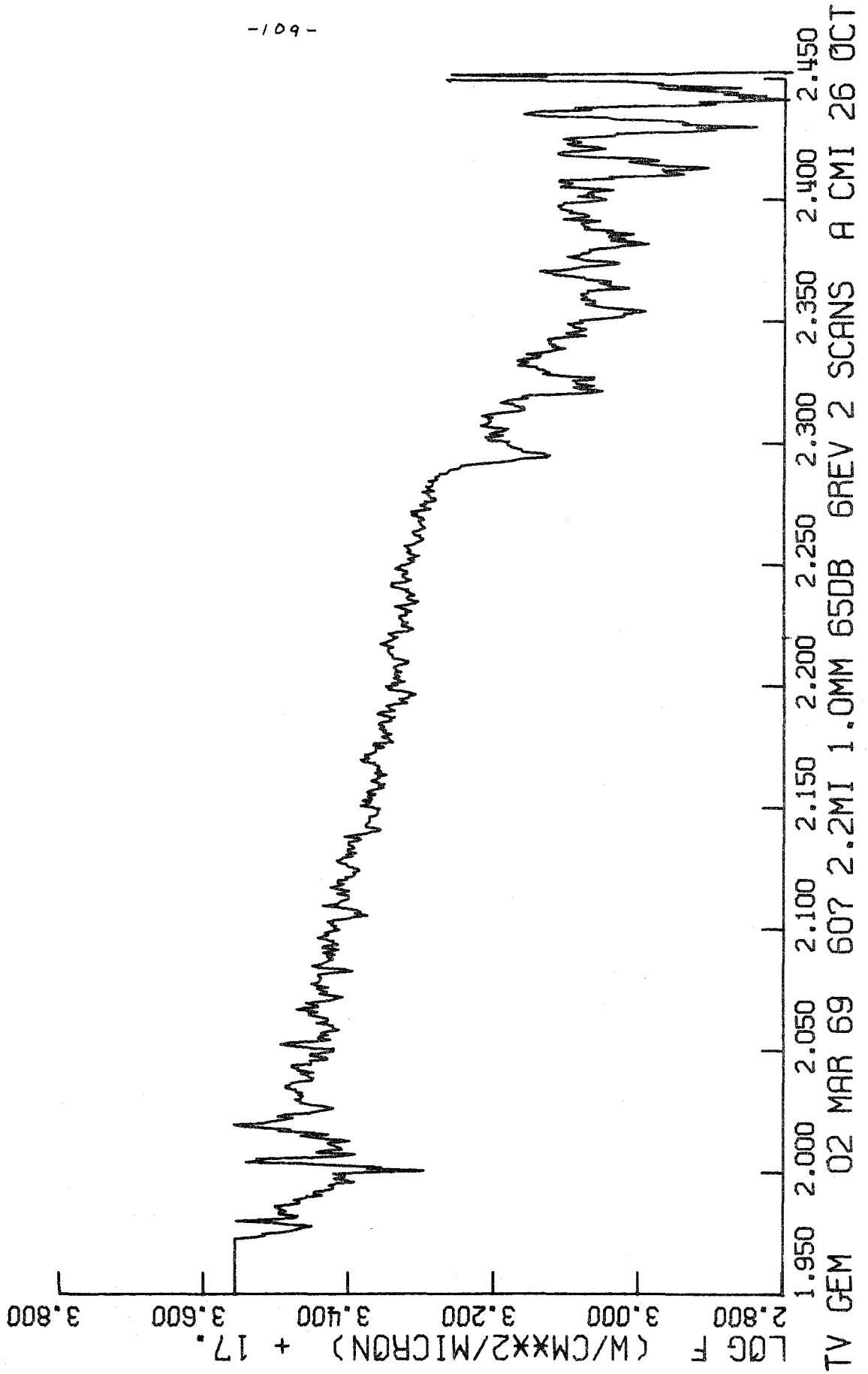
TV GEM 02 MAR 69 607 2.2MI 1.0MM 65DB 6REV 2 SCANS A CMI 26 OCT
LOG F (W/CM**2/MICRON) + 17.
2.800
3.000
3.200
3.400
3.600
3.800
1.950
2.000
2.050
2.100
2.150
2.200
2.250
2.300
2.350
2.400
2.450

Figure 25.

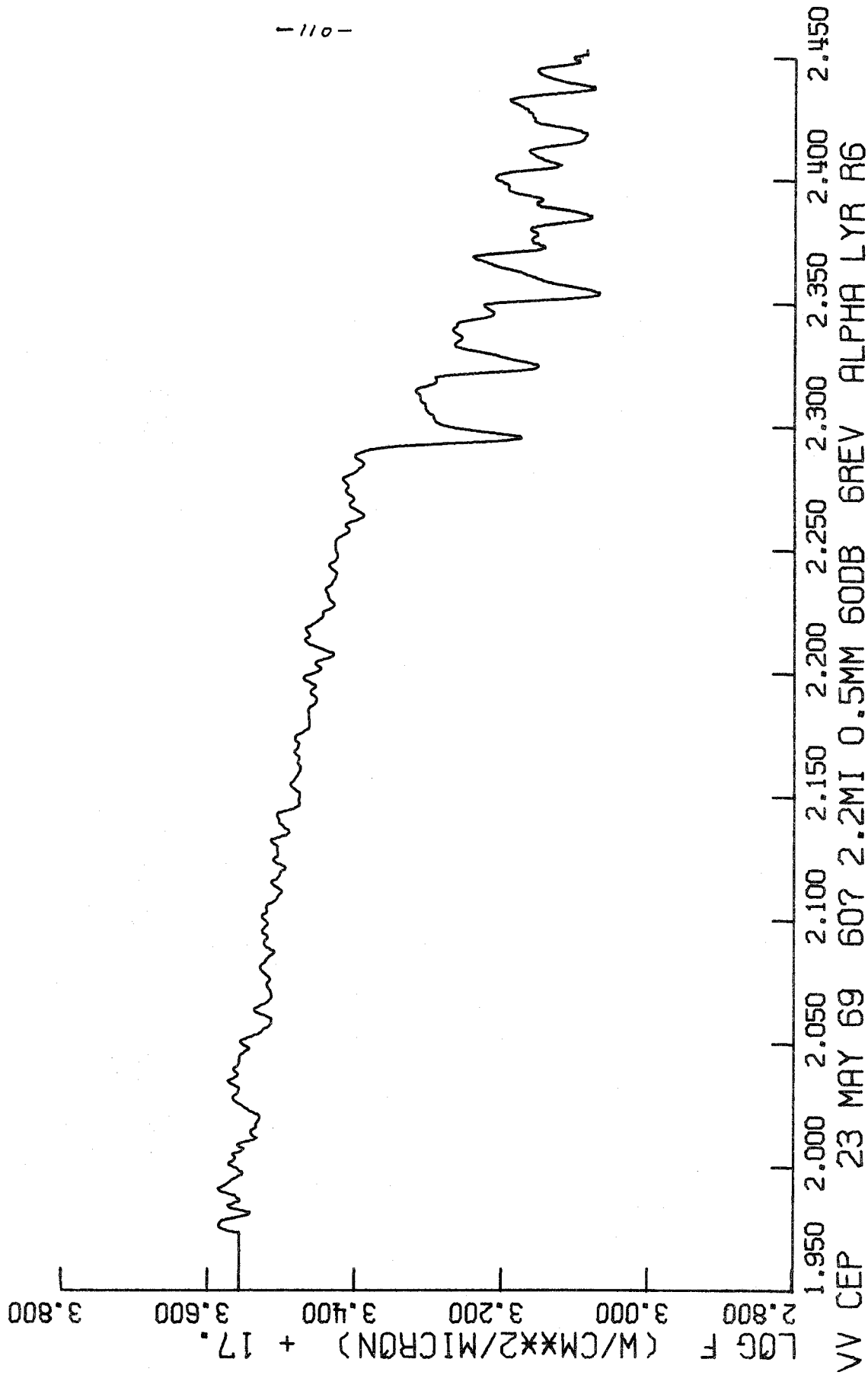
VV CEP 23 MAY 69 607 2.2MI 0.5MM 60DB 6REV ALPHA LYR R6
LOG F (W/CM**2/MICRON) + 17.
2.800
3.000
3.200
3.400
3.600
3.800
1.950
2.000
2.050
2.100
2.150
2.200
2.250
2.300
2.350
2.400
2.450

Figure 26.

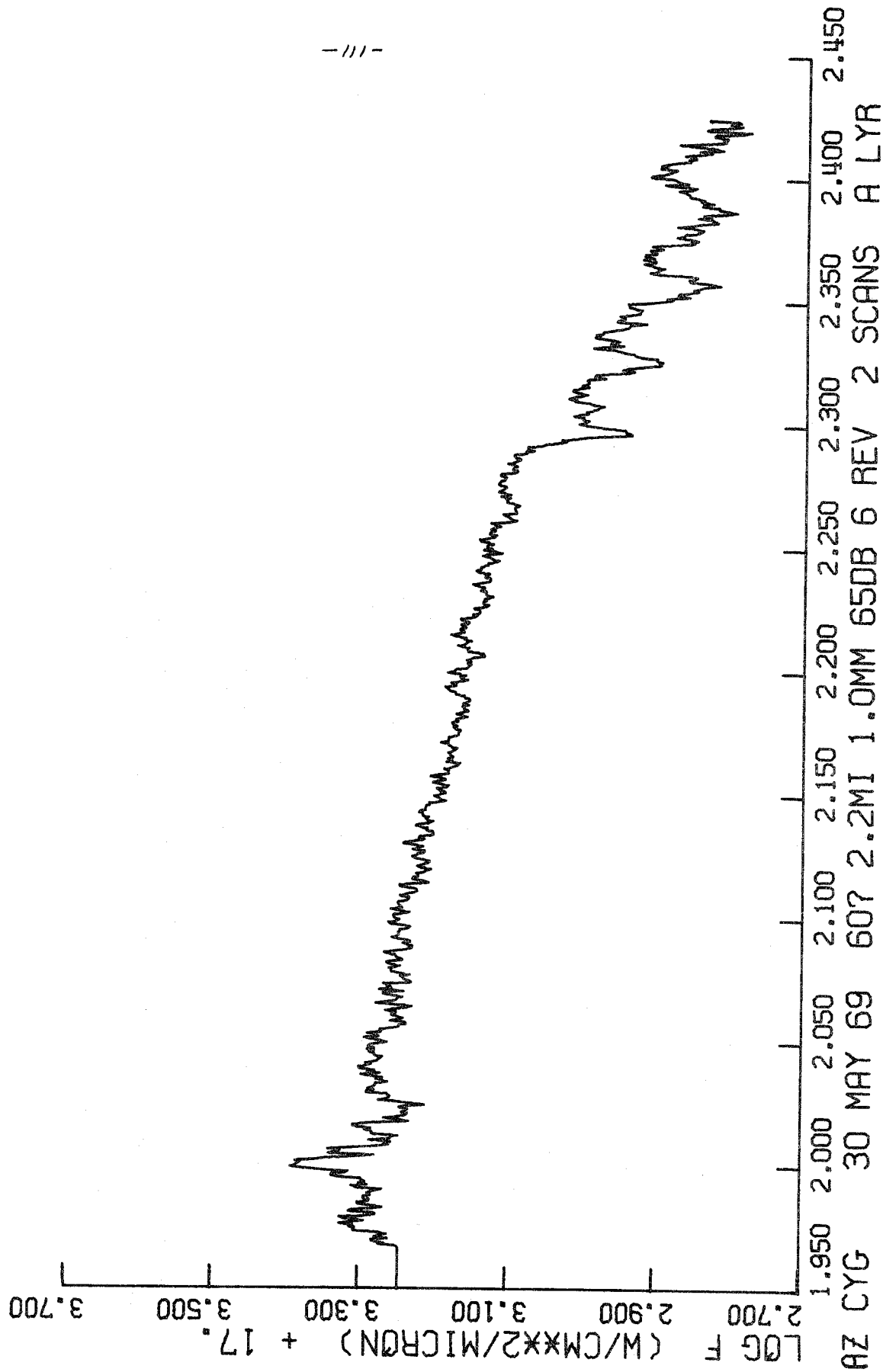
AZ CYG 30 MAY 69 607 2.2MI 1.0MM 65DB 6 REV 2 SCANS A LYR
LOG F (W/CM**2/MICRON) + 17.
1.950
2.000
2.050
2.100
2.150
2.200
2.250
2.300
2.350
2.400
2.450
2.700
2.900
3.100
3.300
3.500
3.700

Figure 27.


LOG F (W/CM**2/MICRON) + 17.30
2.500
2.700
2.900
3.100
3.300
3.500
1.950
2.000
2.050
2.100
2.150
2.200
2.250
2.300
2.350
2.400
2.450
WY GEM 19 NOV 69 607 2.2MI 1.0MM 65DB 12REV 4 SCANS A LYR R9

Figure 28.

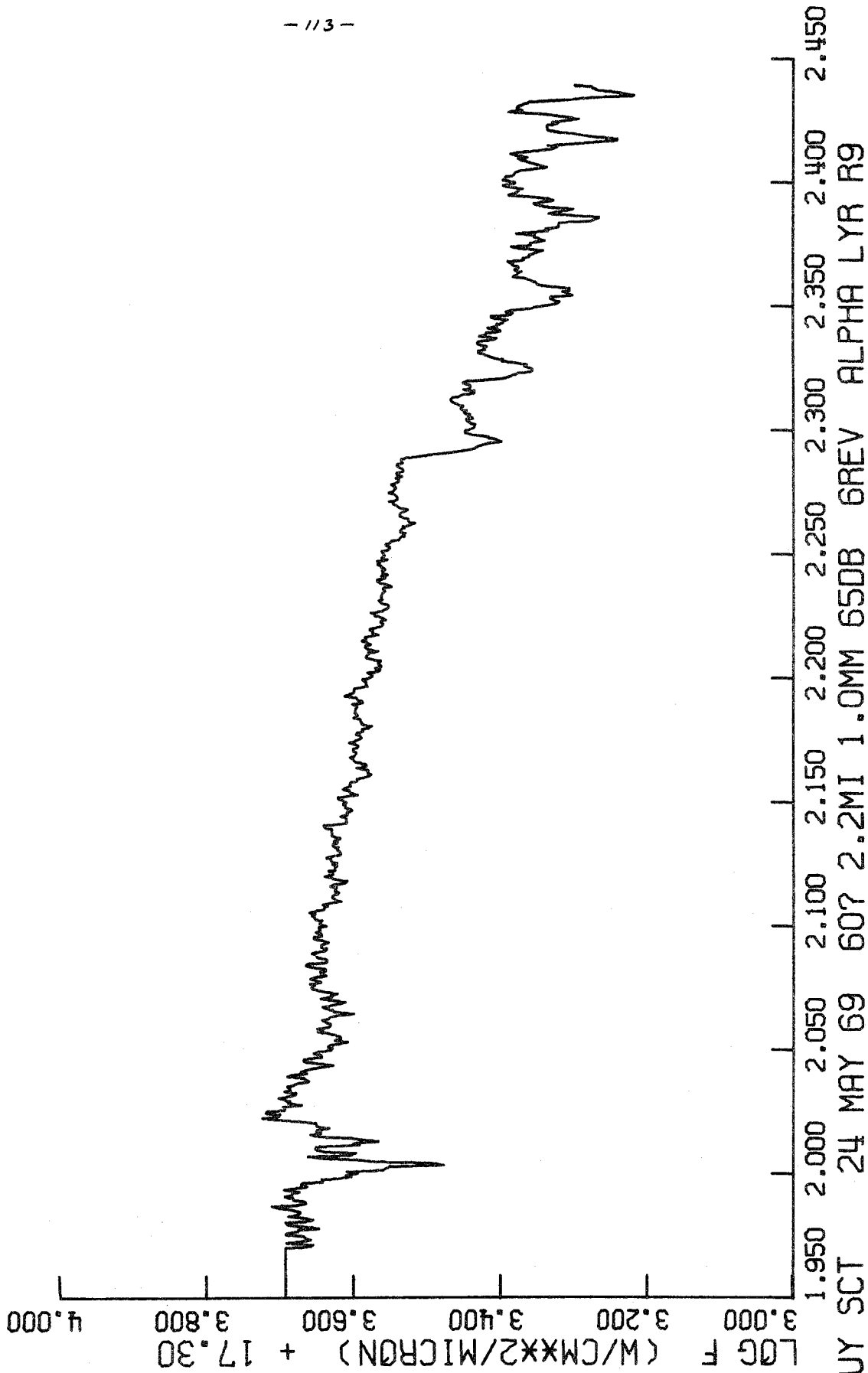
UY SCT 24 MAY 69 607 2.2MI 1.0MM 650B 6REV ALPHA LYR R9
LOG F (W/CM**2/MICRON) + 17.30
3.000
3.200
3.400
3.600
3.800
4.000
1.950
2.000
2.050
2.100
2.150
2.200
2.250
2.300
2.350
2.400
2.450

Figure 29.

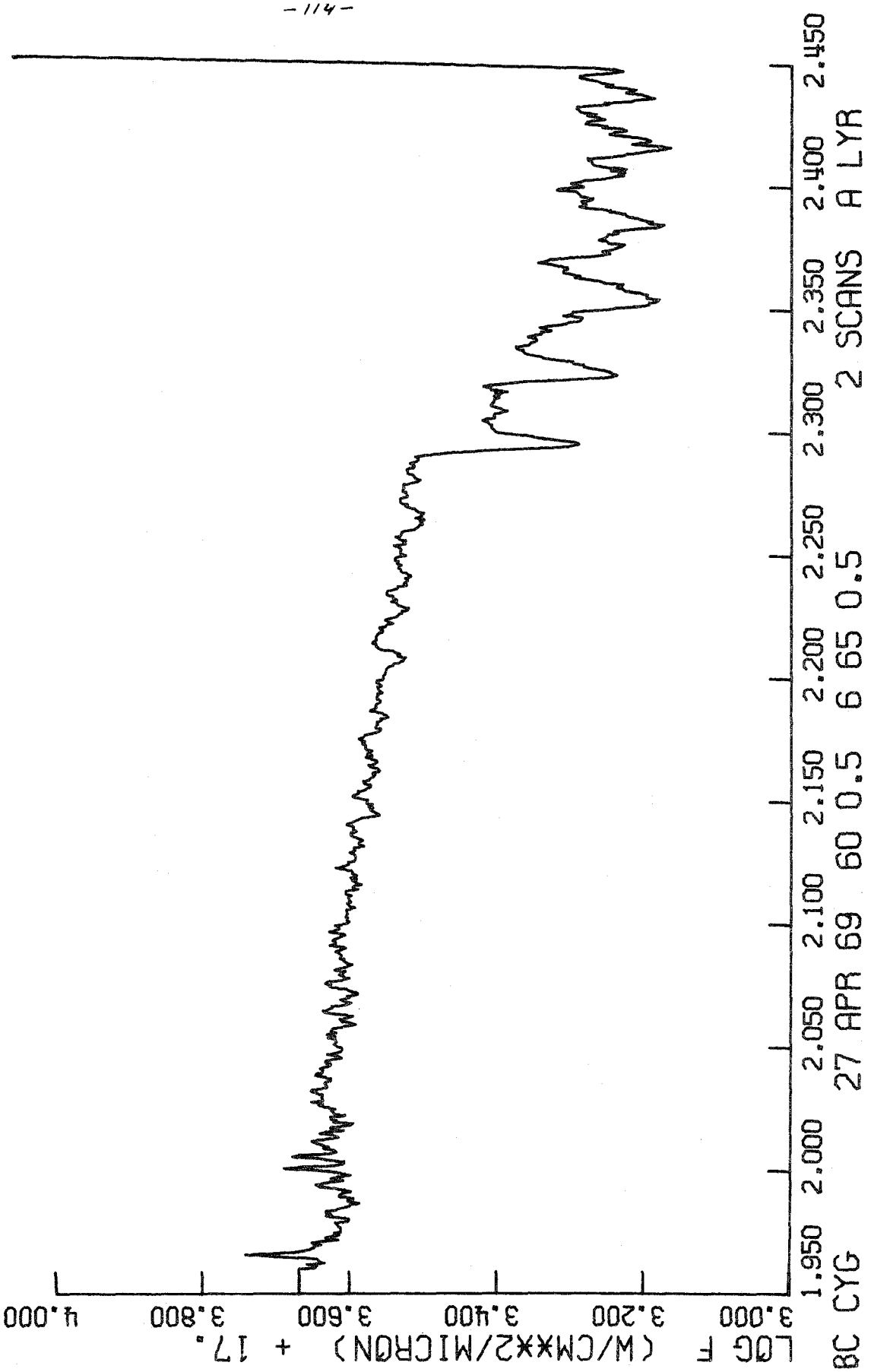
BC CYG
27 APR 69 60 0.5 6 65 0.5
2 SCANS A LYR
LOG F (W/CM**2/MICRON) + 17.
3.000
3.200
3.400
3.600
3.800
4.000
1.950
2.000
2.050
2.100
2.150
2.200
2.250
2.300
2.350
2.400
2.450

Figure 30.

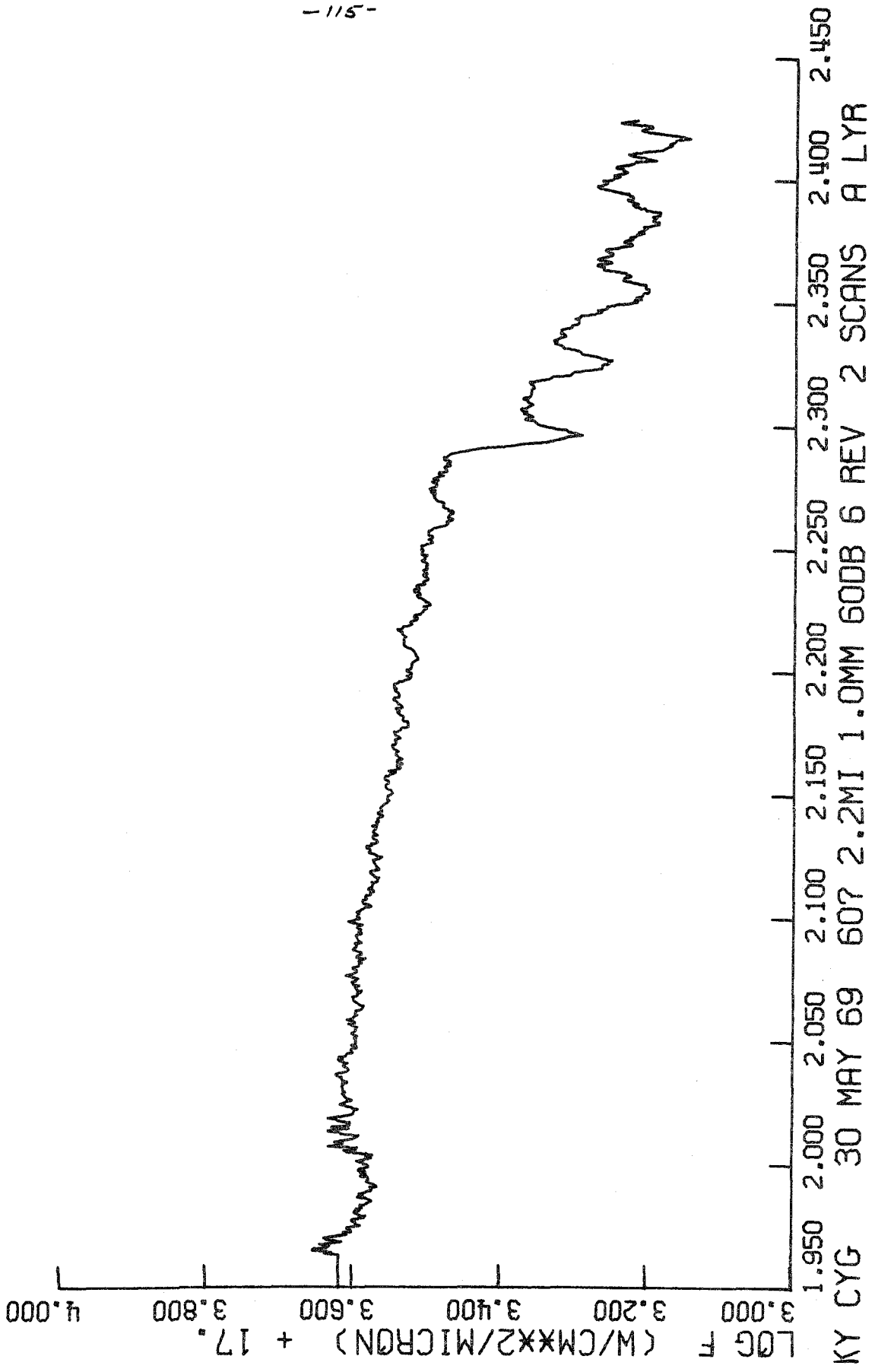
KY CYG 30 MAY 69 607 2.2MI 1.0MM 600B 6 REV 2 SCANS A LYR
LOG F (W/CM**2/MICRON) + 17.
3.000
3.200
3.400
3.600
3.800
4.000
1.950
2.000
2.050
2.100
2.150
2.200
2.250
2.300
2.350
2.400
2.450

Figure 31.

ALPHA HER 27 MAR 69 60? 2.2MI 0.5MM 350B 6 REV 2 SCANS A LYR 26 MAR
1.950 2.000 2.050 2.100 2.150 2.200 2.250 2.300 2.350 2.400 2.450
LOG F (W/CM**2/MICRON) + 17.0μ
μ.500 μ.700 μ.900 5.100 5.300 5.500

Figure 32.

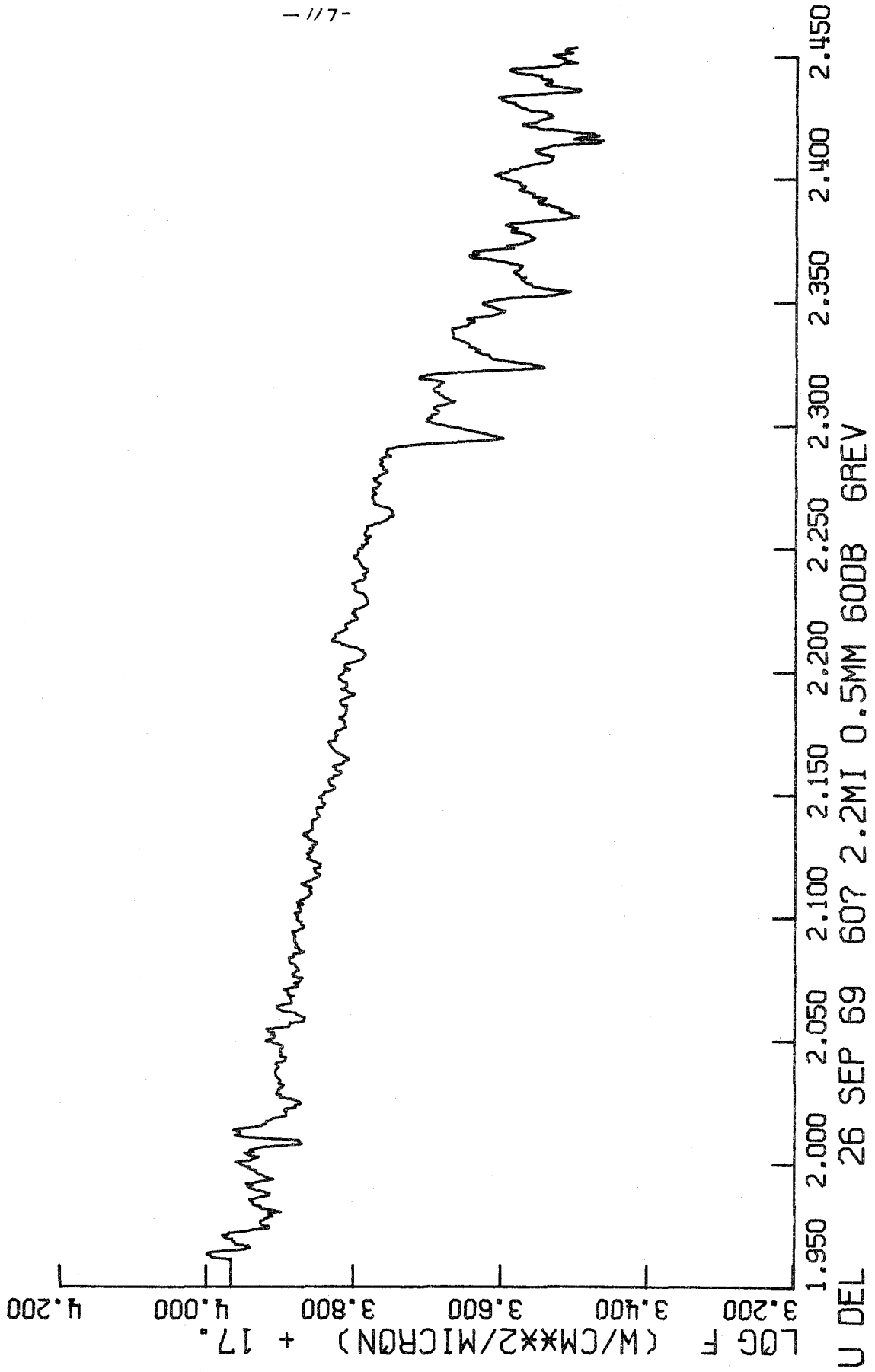
U DEL
26 SEP 69 607 2.2MI 0.5MM 600B 6REV
LOG F (W/CM**2/MICRON) + 17.
3.200
3.400
3.600
3.800
4.000
4.200
1.950
2.000
2.050
2.100
2.150
2.200
2.250
2.300
2.350
2.400
2.450

Figure 33.

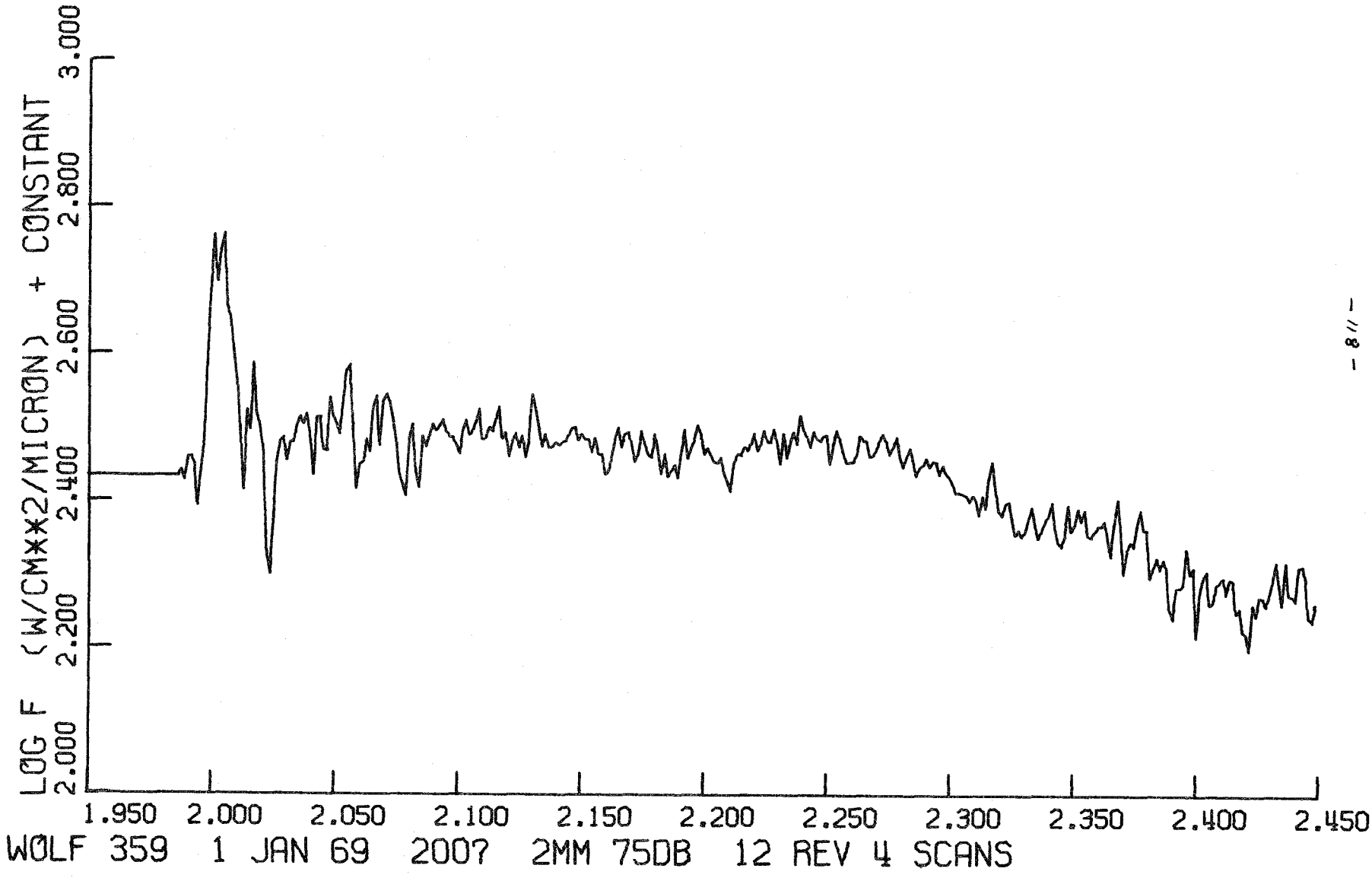
LOG F (W/CM**2/MICRON) + CONSTANT
2.000
2.200
2.400
2.600
2.800
3.000
1.950
2.000
2.050
2.100
2.150
2.200
2.250
2.300
2.350
2.400
2.450
WOLF 359 1 JAN 69 2007 2MM 75DB 12 REV 4 SCANS

Figure 34.

REFERENCES

Auman, Jr., J. 1967, Ap. J. Suppl., 14, 171.

_____. 1969, Ap. J., 157, 799.

_____. 1970, talk given at Conference on Late-Type Stars, Tucson.

Becklin, E. E., Frogel, J. A., Hyland, A. R., Kristian, J., and Neugebauer, G. 1969, Ap. J. (Letters), 158, L133.

Benedict, W. S., Bass, A. M., and Plyler, E. K. 1954, J. Research NBS, 52, 161.

Connes, P., Connes, J., Bouigue, R., Querci, J., Chauville, J., and Querci, F. 1968, Ann. d'Ap., 31, 485.

Eggen, O. J. 1967, Ap. J. Suppl., 14, 307.

Ferriso, C. C., and Ludwig, C. B. 1964, J. Chem. Phys., 41, 1668.

_____. 1964, J. Q. S. R. T., 4, 215.

Fertel, J. H. 1970, Ap. J. (Letters), 159, L7.

_____. 1970, Ap. J. (Letters), 162, L75.

Gehlich, U. K. 1968, Diplomarbeit Universität Hamburg (to be published).

Goldberg, L., and Müller, E. A. 1953, Ap. J., 118, 397.

Goody, R. M. 1964, Atmospheric Radiation: I. Theoretical Basis (Oxford: Oxford University Press).

Goon, G., and Auman, Jr., J. R. 1970, Ap. J., 161, 533.

Herzberg, G. 1950, Molecular Spectra and Molecular Structure: I. Spectra of Diatomic Molecules (Princeton: Van Nostrand).

Iben, Jr., I. 1965, Ap. J., 142, 1447.

Johnson, H. L. 1964, Bol. de los Obs. Ton. y Tac., 3, 305.

_____. 1966, Ann. Rev. Astr. and Ap., 4, 193.

_____. 1968, Ap. J. (Letters), 154, L125.

Johnson, H. L., Coleman, I., Mitchell, R. I., and Steinmetz, D. L. 1968, Comm. Lun. and Planet. Lab., 7, 83.

Johnson, H. L., and Méndez, M. E. 1970, Astron. J., 75, 785.

Kraft, R. 1960, in Stellar Atmospheres, ed. J. L. Greenstein (Chicago: University of Chicago Press).

Kuiper, G. P. 1962, Comm. Lun. and Planet. Lab., 1, 179.

Kuiper, G. P., and Cruikshank, D. P. 1964, Comm. Lun. and Planet. Lab., 2, 141.

Kunde, V. G. 1967, NASA Goddard Space Flight Center, Document X-622-67-248.

_____. 1968, NASA Technical Note, NASATN D-4798.

_____. 1969, Ap. J., 158, 1167.

Low, F. J., Johnson, H. L., Kleinmann, D. E., Latham, A. S., and Geisel, S. L. 1970, Ap. J., 160, 531.

McCammon, D., Münch, G., and Neugebauer, G. 1967, Ap. J., 147, 575.

Mendoza, V., E. E. and Johnson, H. L. 1965, Ap. J., 141, 161.

Merchant, A. E. 1967, Ap. J., 147, 606.

Montgomery, E. F., Connes, P., Connes, J., and Edmonds, Jr., F. N. 1969, Ap. J. Suppl., 19, 1.

Nather, R. E., McCants, M. M., and Evans, D. S. 1970, Ap. J. (Letters), 160, L181.

Pettit, E., and Nicholson, S. B. 1933, Ap. J., 78, 320.

Rank, D. H., Rao, B. S., Sitaram, P., Slomba, A. F., and Wiggins, T. A. 1962, J. of O.S.A., 52, 1004.

Rosendhal, J. D. 1970, Ap. J., 160, 627.

Schadee, A. 1968, Ap. J., 151, 239.

Smak, J. 1966, Acta Astr., 16, 1.

Spinrad, H. 1966, Ap. J., 145, 195.

Spinrad, H., and Vardya, M. S. 1966, Ap. J., 146, 399.

Spinrad, H., and Wing, R. F. 1969, Ann. Rev. Astr. and Ap., 7, 249.

Spinrad, H., Kaplan, L. D., Connes, P., Connes, J., and Kunde, V. G. 1971, (to be published).

Thompson, R. I., and Schnopper, H. W. 1970, Ap. J. (Letters), 160, L97.

Thompson, R. I., Schnopper, H. W., and Rose, W. K. 1971, Ap. J., (to be published).

Tsuji, T. 1964, Ann. Tokyo Obs., 9, 1.

Tsuji, T. 1966, P.A.S.J., 18, 127.

Vardya, M. S. 1966, M.N.R.A.S., 134, 347.

Wallace, A. 1962, Ap. J. Suppl., 7, 165.

Westphal, J. A. 1965, Ap. J., 142, 1663.

Wing, R. F., and Price, S. D. 1970, Ap. J. (Letters), 162, L73.

Wing, R. F., and Spinrad, H. 1970, Ap. J., 159, 973.

Woolf, N. J., Schwarzchild, M., and Rose, W. K. 1964, Ap. J., 140, 833.

PAPER II

LONG PERIOD VARIABLES

I. INTRODUCTION

This paper is an extension of the study begun in Paper I to the coolest M-type stars -- the long period variables. In view of limitations on observing time, and a desire to observe a star over as much of its cycle as possible, a rather homogeneous group of variables was selected. With the exceptions of RS Lib and BG Ser, all of the stars have periods greater than 300 days. They are among the brightest variables in the sky and thus have long records of optical observations, allowing comparisons with the observations presented here. No pure S or C stars were observed for this particular program. Occasionally it was necessary to observe a star at a large hour angle and in these cases correction for atmospheric absorption was not very successful. Careful examination of the resulting data, however, has indicated that no systematic errors have been introduced.

The variations of luminosity and band strengths which have been observed contain many clues about the internal structure and composition of these stars. A limited and uncertain theoretical understanding of these stars limits the ability to understand and interpret these clues. The interpretations which are suggested should be regarded as schematic and preliminary and by no means unique. They are interpretations which now seem physically plausible.

II. THE OBSERVATIONS

A. Preliminary Remarks

The two features which dominate the spectra of the Mira-type variables in the 2μ region are the first overtone vibration-rotation band of CO and the 1.87μ band of H_2O. The procedure used in estimating the strength of these features is the same as described in Paper I. W(CO) is a measure of the equivalent width of the (2, 0), (3, 1), and (4, 2) bands of CO. WV is a measure of the optical depth in the 1.87μ band of H_2O and is defined by

$$WV = \log \left(\frac{F_{cont}}{F_{obs}}\right)_{\lambda = 2.10\mu}$$

where F_{obs} is the observed flux and F_{cont} is the expected continuous flux in the absence of water vapor.

In Paper I it was shown that the continuum for non-variable giants in the absence of water vapor was well represented by a straight line on a log F_λ, λ plot, and that the slope changed slowly with temperature. Inspection of the spectra of the Mira variables presented here which have small amounts of water vapor indicates that the same holds true. In particular, the spectrum of χ Cyg near minimum, which is probably close to the lower limit of temperature of the stars observed and which has little water vapor, has a continuum determined by the peaks between absorption features that closely approximate a straight line with a slope not greatly different than that of much hotter stars. Some of the Miras near phases of maximum H_2O absorption had almost no region of the spectrum left which was not affected by either the 1.87μ band or the

CO bands. In these cases spectra taken at earlier phases were used as a guide in drawing the continuum. This method is good as long as there are no unknown sources of continuous opacity which would make their appearance coincident with the appearance of strong water absorption. As a check on this method, W(CO) and WV were also calculated using upper and lower limits for what might be called still reasonable values for the slope of the continuum. In extreme cases W(CO) changed by 30% and WV by .04. The general characteristics described below, however, remained unchanged. In particular, the relative variations with time of WV, and W(CO) were unaffected.

After the continuum was determined in this manner, a comparison was made with the 1.6μ spectra which were taken at the same time as the 2.2μ spectra for a few of the stars. In cases of both strong and weak H_2O absorption, a straight line extrapolation of the continuum from the 2.2μ region to the 1.6μ region agreed very well with the observed flux level in the latter region. Also, in cases where the broad band colors were available and these were relatively unaffected by strong molecular absorption, the continuum determined from these colors agreed well with the continuum determined from the spectra alone.

On some of the spectra there is one wide (~100Å) feature whose peak is consistently higher than the rest of the spectrum by as much as .05 in log F_λ. On these spectra, the <u>slope</u> of the continuum would be well determined ignoring this feature, but the <u>level</u> of the continuum was set by the top of this feature. If this is in fact a broad emission feature, then the values of WV and W(CO) will have been systematically

overestimated. Evidence for this is discussed below. Again, however, this has no effect on the various points which will be made.

As discussed by Frogel (1970), the variations of flux in the 2.25μ region is characteristic of the total-luminosity light curve of the long-period variables discussed here. This flux is determined directly from the calibrated spectra and hereafter will be referred to as f(225). A comparison of standards (α Lyr, αC Mi, αC Ma) run on the same night but at different zenith distances indicates that the difference in log F_λ over the range 2.10 - 2.38μ is less than .01 for differences of secant Z less than .4 and is about .02 for differences of secant Z of about 1.0. The differences become greater than this in the centers of strong atmospheric bands as discussed in Paper I. The 2.25μ region in particular is free of such bands, and the formal errors assigned to log f(225) are (+.02, -.01). Similar errors apply to the quantity WV in addition to errors arising from the positioning of the continuum as discussed above. Large differences in the zenith distance between the variable and standard arose from the necessity of observing the variable over as much of its cycle as possible. This also caused larger errors in the determination of W(CO) than in the case of the stars discussed in Paper I. Careful visual inspection of the data indicates, however, that the results obtained are not affected in any systematic fashion.

Finally, it should be pointed out that the errors in a single measurement W(CO) and WV will often be greater than the change in these quantities from one observation to the next. Visual examination of the individual spectra indicates, though, that the relative changes

between succeeding observations are in almost all cases correctly given. Therefore, the various dependencies of one quantity upon another should be regarded as firmly established.

B. The Temperature Scale

The establishment of a color temperature scale for the non-variable giants was discussed in Paper I. The main difficulty in extending it to the Mira variables was a lack of photometric observations over a substantial part of the period for most of the variables studied here. In fact, many of the variables have been observed photometrically only once during the course of the spectroscopic program. To get around this difficulty, the following procedure was adopted. For those stars which had more than one measurement of the (J-L) color, the change in (J-L) was plotted as a function of the change in log f(225) and a best-fit straight line was drawn through the points (Figure 1). As best as could be determined from the observations, an increase in (J-L) was always correlated with a decrease in log f(225). So, tentatively, it would seem that the bluest color (or maximum color temperatures) coincides with maximum flux at 2.25μ . The error in one determination of J-L is about 0.1. The scatter in Figure 1 is about the same. Using an observed value of Δ log f(225), and at least one observed value of J-L, the mean relation defined in Figure 1 yields a color temperature with an error on the order of $\pm$ 100°K since the cool temperatures of the Miras are relatively insensitive to changes in (J-L). The two points with the greatest Δ (J-L) are observations of NML Tau. They have not been used in determining the mean relation

Fig. 1. - The change in log f(225), as measured from the spectra, versus the change in J-L color between two observations. The mean relation adopted is shown. Points from Mendoza's data (1967) as explained in the text are indicated by circles.

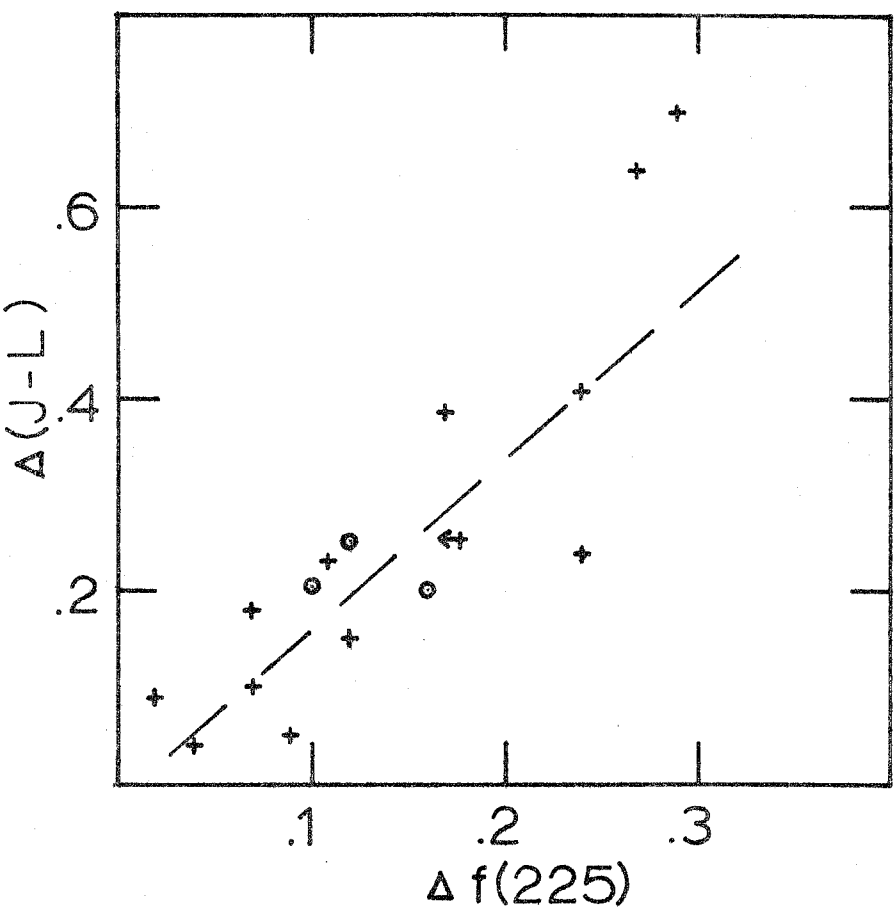

Figure 1.

since the effect on the colors of the extensive circumstellar shell surrounding the object (Hyland, et al 1971) is not well known.

The internal consistency of the above procedure may be checked by comparing observed values published by Mendoza (1967) with predicted values for J-L at the same phase. For $(J-L)_{Mendoza} < 2.5$, two out of twelve comparisons differ by .2. The rest differ by .1 or less. The observations of χ Cyg near minimum ($J-L > 2.5$) are redder by .4 than the predicted values, but for these colors the temperature difference is less than 150°K. For three stars which were observed photometrically only once in the present study, R Cnc, R Leo, and L Mi, the observations were combined with those of Mendoza taken during different cycles. Assuming that the value of log f(225) does not change significantly from cycle to cycle at the same phase, three points indicated as circles were plotted in Figure 1. These agree with the mean relation previously established. The predicted J-L colors at minimum light agree with the adopted color-spectral type relation as discussed in Paper I. The predicted colors at maximum infrared light, however, are redder, for most of the variables, than those given by the color-spectral type relation. This effect agrees with the observations of variable stars near maximum light of Mendoza (1967), and is not due to the method of extrapolation.

In Table 1 maximum and minimum values of the temperature are compared for those variables in common to this study and that of Pettit and Nicholson (1933). While the values for T_{max} agree within the errors expected, the values for T_{min} determined here seem to be systematically hotter than those of Pettit and Nicholson. This reflects

TABLE 1

STAR	FROM PETTIT AND NICHOLSON		PRESENT STUDY	
	T_{max}	T_{min}	T_{max}	T_{min}
R Aql	2300	1900	2400	2100
R Aqr	2300	1700	2300	1850
R Cnc	2300	1700	2500	2100
χ Cyg	2200	1650	2300	1800
R Leo	2200	1800	2400	2000
R LMi	2300	1800	2300	1950
o Ceti	2600	1900	2400	2000
X Oph	2400	1900	2600	2300

the fact that the temperatures determined for the latest spectral types from multicolor photometry (e.g. Mendoza 1967) differ from the temperatures determined by the radiometric observations of Pettit and Nicholson (e.g. Smak 1964). Fujita, et al (1964) have determined an excitation temperature scale based on strengths of observed molecular and atomic lines. This scale is about 200°K hotter still than that based on multicolor photometry. Perhaps, when strong molecular absorption spectrum under stellar conditions are better known, the infrared colors could be corrected in the same manner that Smak (1964) has corrected the UBV colors for the effects of TiO bands.

The highly extended atmospheres and the large scale mass motions which are believed to occur in them may render the concept of "effective temperature" useless for these late type stars and instead require that detailed temperature structure be specified. Keeley (1970) and Goon and Auman (1970) have pointed out how crucial such knowledge of the temperature structure is both for analysis of the pulsation of long period variables and their molecular abundances. In what follows, "temperature" will always refer to (J-L) color temperature determined in the manner discussed above. The limitations and shortcomings of this scale should be kept clearly in mind.

C. Variations of Flux and Molecular Band Strengths

The behavior of the 2.25μ light curve and the strengths of the absorption bands of CO and H_2O tend to follow certain general patterns in the Miras which have been observed:

(1) The range in brightness at 2.25μ is related to the phase lag between the visual and the 2.25μ maximum and to the mean temperature during the cycle in the sense that the stars of larger range and cooler temperature tend to have a larger phase lag.

(2) The maximum strengths of H_2O absorption bands are correlated with the temperature at these maxima in the sense that the strongest maxima are associated with the coolest temperatures at the times of maxima. The CO bands may show a weak correlation in the same sense.

(3) The greatest values at minimum H_2O strength are found in the stars having the coolest temperature at minimum band strength. The opposite is true for the minimum CO band strength.

(4) The phase of maximum CO strength ranges from about 0 in those stars having the earliest 2.25μ maximum to .5 in those having the latest 2.25μ maximum. The minimum CO strength occurs between .6 and .95 and usually coincides with the 2.25μ minimum.

(5) The values for the phase of maximum H_2O strength tend to cluster around 0.45 with the latest phase tending to be associated with the coolest temperatures and thus, by 2 above, with the greatest strengths. Minimum strength usually occurs between .8 and .2.

(6) The H_2O maximum occurs at the same time as or after the CO maximum, never before, except for the ambiguous case of X Oph.

(7) The shape of the 2.25μ light curve is generally symmetric with some evidence for a shorter rise time than fall time and for a broader minimum than maximum.

(8) The strength of the CO bands seem to increase faster than they decrease with maximum and minimum being generally of the same shape.

(9) The H_2O strength generally has a markedly steeper rise than fall with a broad minimum ($\sim$.2 of total period) and narrow maximum. The stars having the largest variation in strength tend to have both narrow maxima and minima.

The most notable exceptions to the above are T Cas, R Aur, and RS Lib which have anomolously strong CO and o Ceti which has anomolously weak CO for their respective temperatures. Also χ Cyg, R Aur, RS Lib and T Cas have anomolously weak H_2O for their temperatures. These statements may be made independent of temperature: χ Cyg, T Cas, R Aur, and RS Lib have CO band strengths that are much stronger than one would expect from their H_2O band strengths when compared with the other variables. Also, U Ori shows only a small variation in strength of the CO bands in comparison with the large observed variation of the H_2O band.

While the maximum observed strength of CO in R Aqr and NML Tau is probably close to the true maximum value, neither of these stars were observed over a large enough part of their cycles to place anything but a lower limit on their maximum H_2O strengths. In addition, R Cas has been observed only three times spectroscopically. It seems to have a very strong 1.87μ H_2O band, in agreement with the observation of Johnson and Méndez (1970). S CrB was observed once. It had a spectrum similar to that of R Aql when the latter is at the same phase.

The individual observations of band strength and log f(225) are depicted graphically in the appendix as are several examples of the spectra. The most important of the relations which have been described are illustrated in Figures 2-4. The relevant data on maximum and minimum band strengths, phases, etc., are given in Table 2a, b, c. In Figure 5 the mean relation of band strength versus temperature for the giants discussed in Paper I is compared with mean relation of maximum band strength versus temperature for the variables as determined by excluding those stars which apparently have anomolous band strengths. Except for the jump discontinuity, the run of strengths from late G to late M type stars is remarkably consistent. The discontinuity in part can be attributed to the manner in which the level of the continuum of the variables was chosen as described earlier, and in part is real.

As pointed out above, the variation of minimum C0 band strength with temperature and spectral type is quite different from its variation of max. strength. The minimum value of W(C0) decreases steeply with decreasing minimum temperature. Three stars which depart most strongly from this mean relation are χ Cyg, U Ori, and NML Tau. All three of these also show a large range in luminosity, but a small range in the W(C0) parameter. χ Cyg is an MS star with very weak H_2O whereas U Ori and NML Tau apparently have normal H_2O and, as discussed later, are probably pure M stars. Visual comparison of the spectra having the weakest minimum value of W(C0) (e.g., o Ceti, U Her, and R LMi) with spectra of early K stars having similar values of W(C0) indicate striking differences. Whereas band heads of the (6, 4) transition are

Fig. 2a. - The range in log f(225) versus the phase lag between the visual and 2.25μ light curves in the sense Max (2.25) - Max (vis.).

Fig. 2b. - The range in log f(225) versus the mean temperature over a variable's cycle.

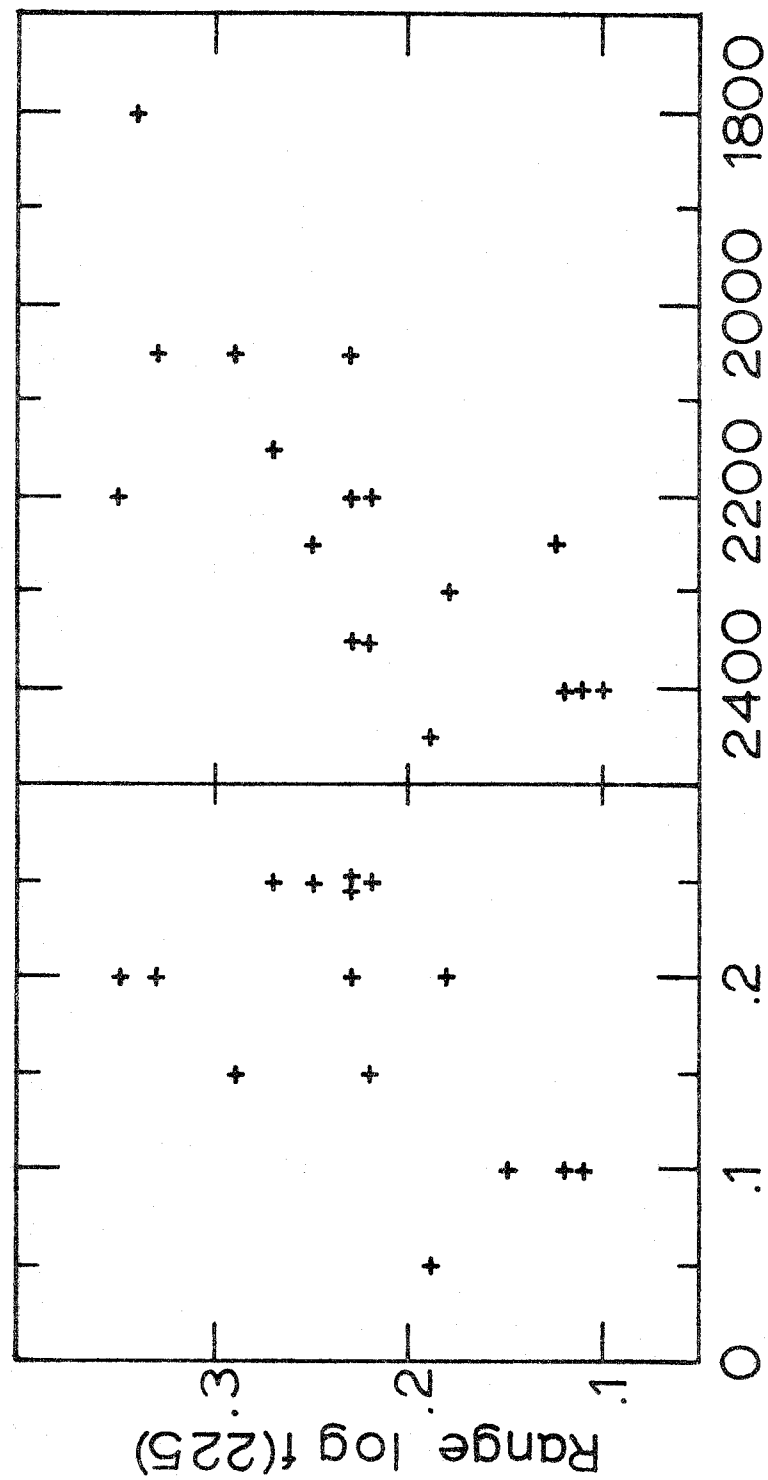

Figure 2a.

Figure 2b.

Fig. 3a. - The observed maximum and minimum strengths of the first overtone CO bands (as measured by W(CO)) versus temperature at the time of observation. R Aur, T Cas, χ Cyg, and RS Lib are marked as MS stars.

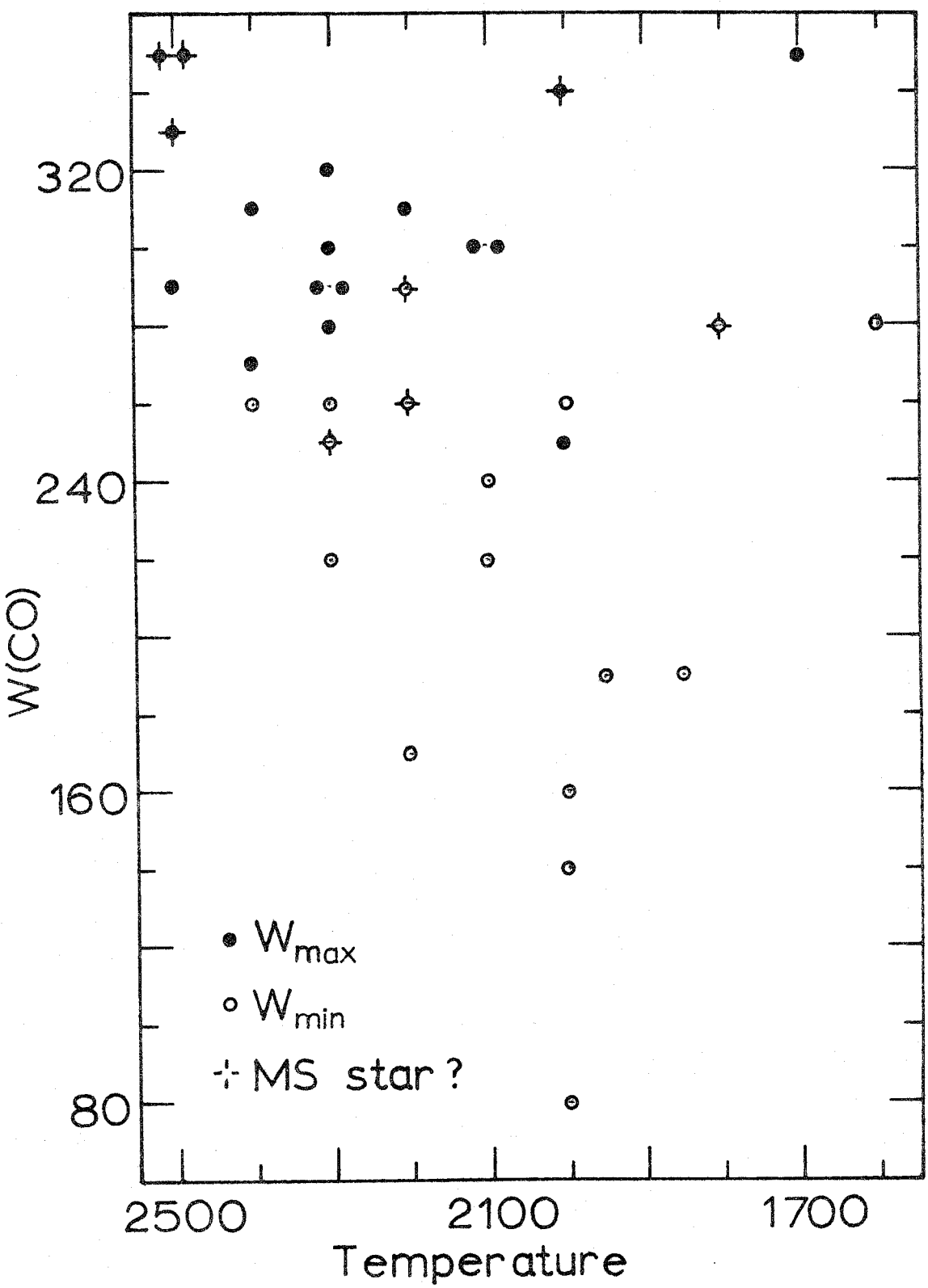
320
240
160
80
W(CO)
2500
2100
1700
Temperature
W max
W min
MS star ?

Figure 3a

Fig. 3b. - The observed maximum and minimum strengths of the 1.87μ H_2O band (as measured by WV) versus temperature at the time of observation. R Aur, T Cas, χ Cyg, and RS Lib are marked as MS stars.

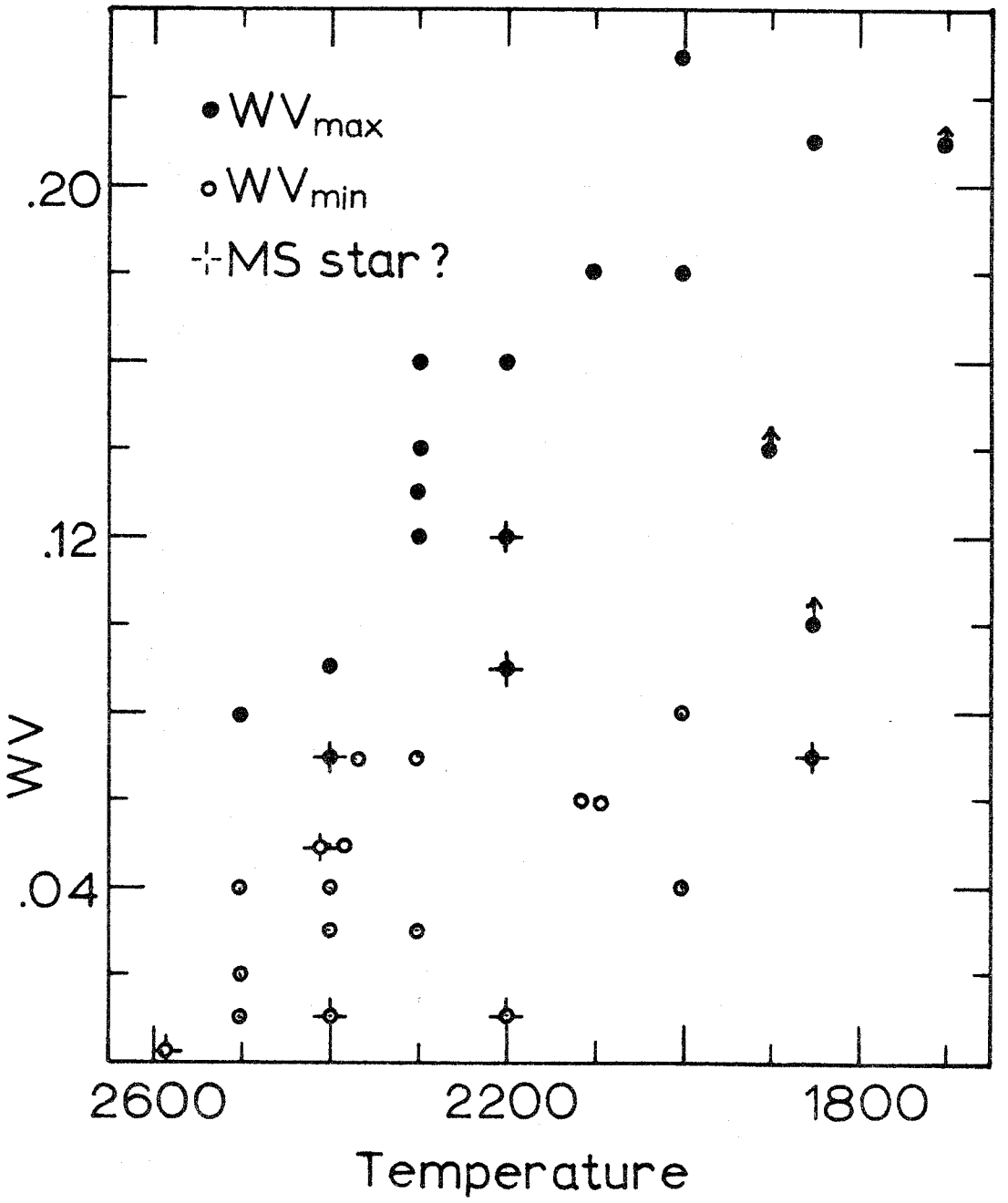

Figure 3b

Fig. 4a. - Phase of the maximum observed values of WV and W(C0) versus the phase of the observed f(225) maximum. The phase is measured with respect to the maximum of the visual light curve.

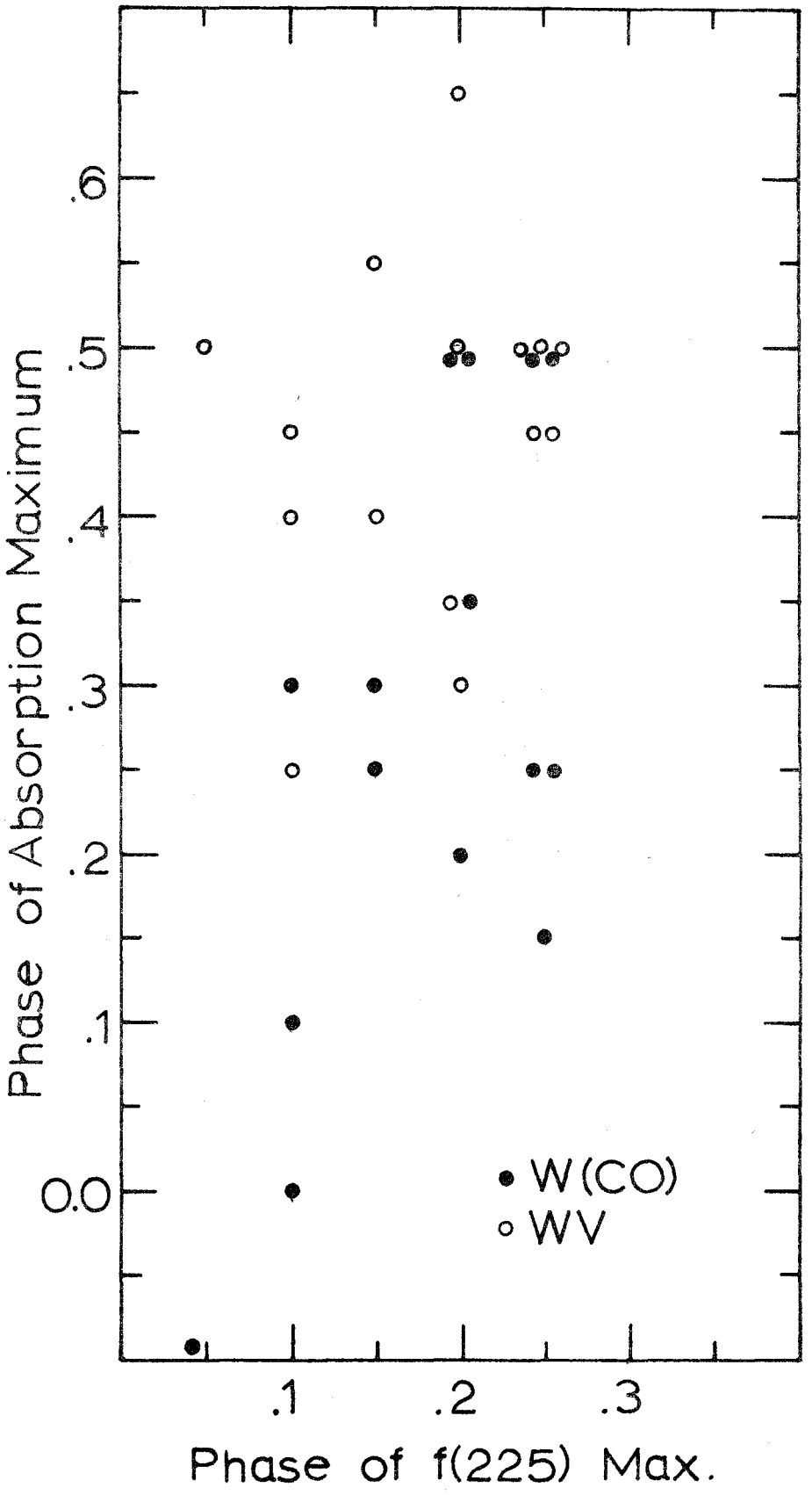
Phase of Absorption Maximum
.6
.5
.4
.3
.2
.1
0.0
.1
.2
.3
Phase of f(225) Max.
W(CO)
WV

Figure 4a

Fig. 4b. - The phase difference between the absorption and f(225) maxima versus the phase of the f(225) maximum. All phases are measured with respect to the maximum of the visual light curve.

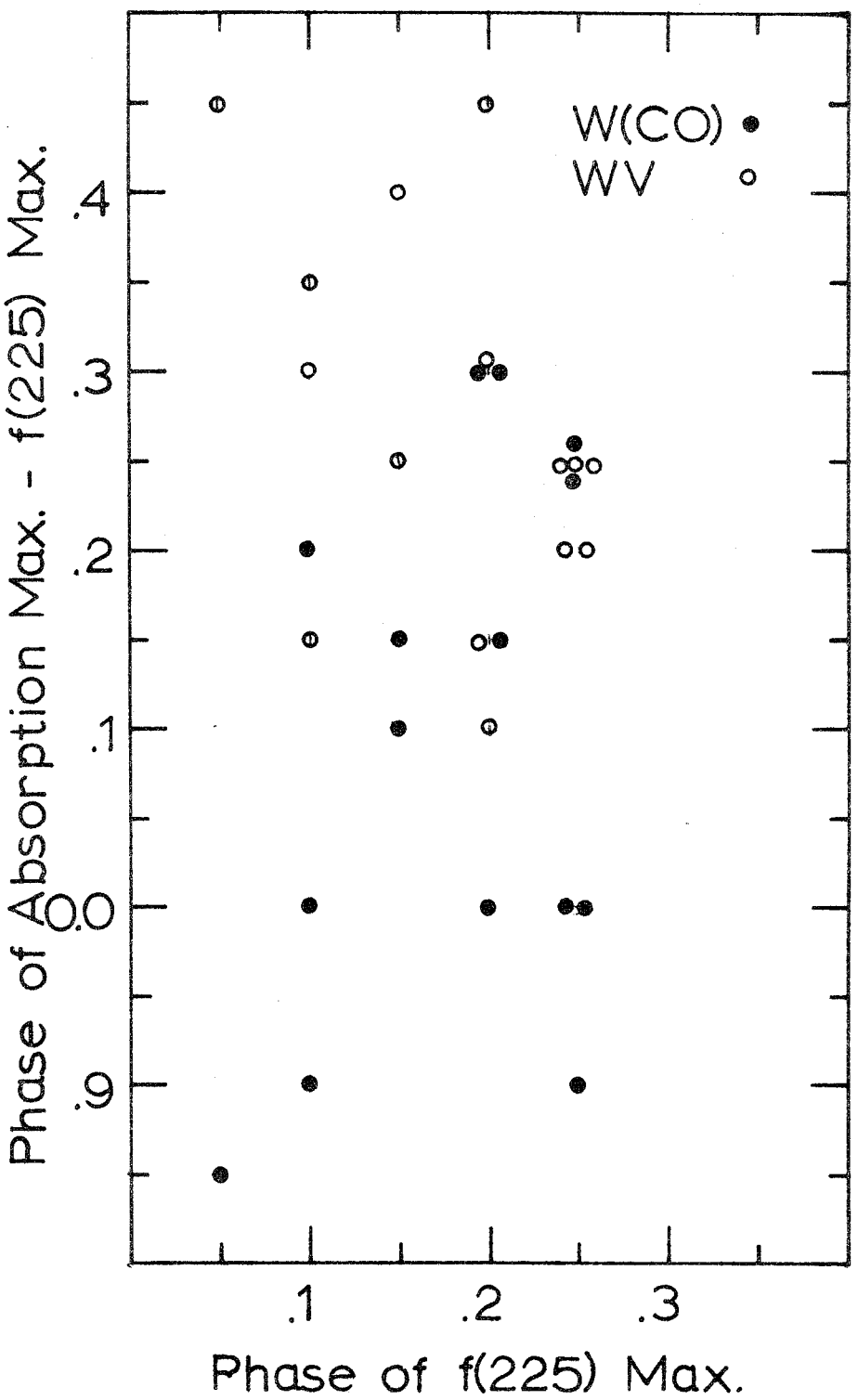
W(CO)
WV
Phase of Absorption Max. - f(225) Max.
.4
.3
.2
.1
0.0
.9
.1
.2
.3
Phase of f(225) Max.

Figure 4b.

Fig. 5. - The mean relation of the quantities WV and W(CO) versus color temperature for the normal giants is from Paper I. The mean relations for the Miras at times of maximum absorption are from Figs. 3a and 3b.

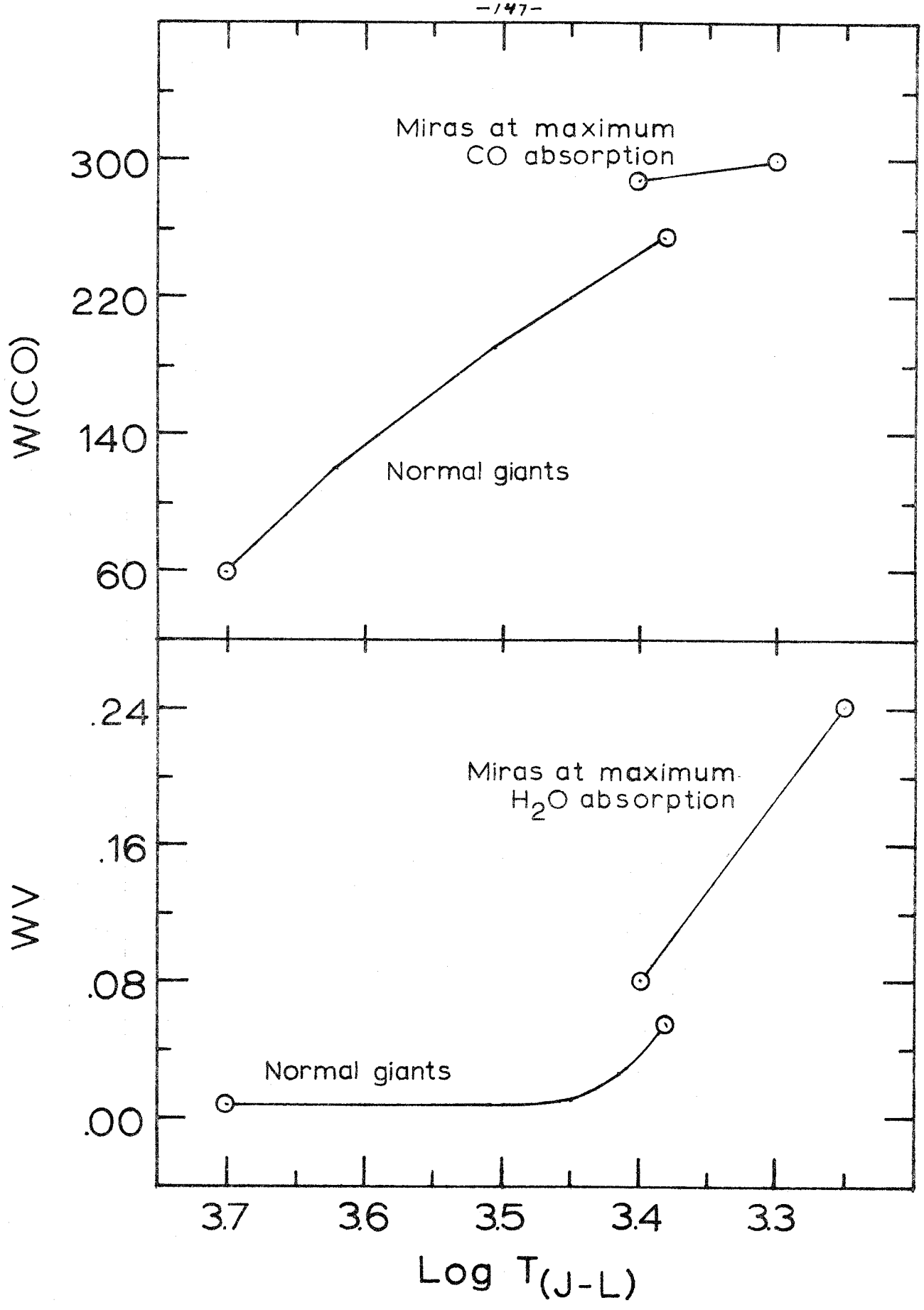
Miras at maximum
CO absorption
300
220
140
60
W(CO)
Normal giants
.24
.16
.08
.00
WV
Miras at maximum
H_2O absorption
Normal giants
3.7
3.6
3.5
3.4
3.3
Log $T_{(J-L)}$

Figure 5.

TABLE 2a LIGHT CURVE DATA

Star	VISUAL LIGHT CURVE		log $F_{\lambda = 2.25\mu}$					Remarks
	Period (Days)	Spectral Type (range)	Range	MAXIMUM		MINIMUM		
				Phase	Temperature	Phase	Temperature	
R Aql	300	M6.5-M8	.15	.1	2400°K	.6	2100°K	
R Aqr	387	M7 -M9	>.33	.2	2300	--	~1850	b
R Aur	457	M6.5-M8	.22	~.15	2600	.55	2100	b
R Cas	431	M7 -M10	--	--	---	--	---	b
T Cas	445	M7.5-M8.5	.11	.1	2500	.75	2300	
T Cep	390	M6.5-M9	.12	~.1	2500	.7	2300	
R Cnc	362	M6.5-M9	.18	.2	2500	.8	2100	
χ Cyg	407	M7 -M10(S)	.29	.15	2300	.8	1800	
U Her	406	M6.5-M9	.23	.2	2200	.85	1850	
R Leo	312	M7 -M9	.22	.25	2400	.85	2000	
R L Mi	372	M7 -M9	.27	.25	2300	.8	1950	
RS Lib	217	M7 -M8	.23	.25	2500	.75	2200	
Mira	332	M5.5-M9	.23	.25	2400	~.75	2000	
X Oph	334	M6.5-M8	.19	.05	2600	.55	2300	
U Ori	372	M6.5-M9	.35	.2	2400	.8	1950	
BG Ser	143	M6 -M8	.1	--	2500	--	2300	a
R Ser	357	M6.5-M9	.25	<.25	2500	.85	2000	
NML Tau	550 ?	M8 -M10 ?	.33	--	2000 ?	--	1600 ?	a, b

a. Visual light curve not available
b. Not observed over full cycle

TABLE 2b

1.87μ H_2O BAND ABSORPTION

	MAXIMUM OBSERVED			MINIMUM OBSERVED		
	$\log\left[\frac{F_{cont}}{F_{obs}}\right]_{\lambda=2.10u}$	Color Temperature	Phase	$\log\left[\frac{F_{cont}}{F_{obs}}\right]_{\lambda=2.10\mu}$	Color Temperature	Phase *
R Aql	.14	2300°K	.45	.05	2400°K	.95
R Aqr	>.10	1850	>.3	.06	2100	0.1
R Aur	.09	2200	.4	~.00	2600	<.1
R Cas	>.14	<1900	<.7	--	---	--
T Cas	.07	2400	~.4	.01	2400	~0.0
T Cep	.08	2500	.25	.01	2500	<0.0
R Cnc	.16	2300	.35	.03	2400	.9
χ Cyg	.07	1850	.55	.01	2200	<0.0
U Her	.21	1850	.5	.06	2100	.05
R Leo	.13	2300	.45	.07	2300	<.1
R L Mi	.18	2100	.5	.04	2000	
RS Lib	.12	2200	.45	.05	2400	<.1
Mira	.18	2000	.5	.03	2400	<.3
X Oph	.12	2300	.5	.02	2500	.05
U Ori	.23	2000	.65	.07	2400	.15
BG Ser	.09	2400	--	.03	2300	--
R Ser	.16	2200	.5	.04	2500	<.2
NML Tau	>.21	1700 ?	--	.08	2000 ?	--

* In cases of broad minima, the phase is that just before the steep rise begins.

TABLE 2c FIRST OVERTONE C0 BAND ABSORPTION

	MAXIMUM OBSERVED			MINIMUM OBSERVED		
	W(C0)	COLOR TEMPERATURE	PHASE	W(C0)	COLOR TEMPERATURE	PHASE
R Aql	290	2300	.3	220	2100	.6
R Aqr	280	2300	.2	190	1850	.9
R Aur	350	2500	.25	290	2200	.6
R Cas	>260	---	--	<240	---	--
T Cas	330	2500	0.0	250	2300	.75
T Cep	290	2500	~.1	220	2300	.7
R Cnc	300	2300	.35	170	2200	.9
χ Cyg	340	2000	.3	280	1800	.8
U Her	300	2100	.5	190	1950	.95
R Leo	270	2400	.25	160	2000	.75
R L Mi	300	2100	.25	140	2000	.85
RS Lib	370	2500	.15	260	2200	.75
Mira	250	2000	.5	~ 80	2000	.95
X Oph	320	2300	.9	260	2300	.6
U Ori	310	2200	.5	260	2000	~.9
BG Ser	290	2300	--	260	2400	--
R Ser	310	2400	.5	240	2100	.75
NML Tau	>350	1700 ?	--	280	1600 ?	--

clearly visible in the hot K stars, the band heads of the (4, 2) transition and higher are indistinct and washed out in these very cool Miras. Thus, the expected decrease of band strength with decreasing temperature may finally be apparent here. In χ Cyg all of the high level band heads remain distinct and strong, nearly independent of the phase of the star. Although the high level band heads are weaker and more washed out in U Ori and NML Tau at minimum strength than they are at maximum, the difference is not as extreme as, for example, in U Her. In particular, the sharp and deep drop observed just longward of the (2, 0) and (3, 1) band heads remains visible in these two stars, whereas in the other cool Miras it is not present. It is as if the atmospheres of the three stars are highly transparent allowing one to see down to hotter levels. The absorption of the 2.7μ H_2O band at the time of minimum W(CO) in U Ori and NML Tau seems to be normal as far as can be inferred from the behavior of the 1.87μ band.

As the minimum value of WV occurs at about the time of maximum visual light, a plot of WV versus the earliest, visually determined spectral type indicates that the Miras generally have stronger water absorption than do the non-Mira giants of the same spectral type discussed in Paper I. In fact, from various sources of spectral type versus phase for the long period variables studied here, it seems that the water absorption is always stronger in the variables than the non-variables of the same spectral type. This is not true for the CO band strengths, however. The discrepancy in the color-spectral type relation between the Miras at maximum luminosity and the non-Mira giants may be due to the differences in the H_2O absorption since there is a water absorption

band in the band pass of the J filter. Except for χ Cyg, the stars with weak maximum values of WV are not as apparent when considering minimum values of WV.

D. Values of $[C^{12}/C^{13}]$

The measurement of the isotopic ratio $C^{12}O^{16}/C^{13}O^{16}$ proceeded in a manner similar to that discussed in Paper I. Again, it has been assumed as a "best compromise" that the square root portion of the curve of growth applies to the region of the band heads. Average values were obtained for each of the variables and are given in Table 3 and plotted in Figure 6 as a function of spectral type together with values for some of the late-type giants from Paper I. There is considerable variation for a given star over a cycle. This is probably attributable to the varying strength of the much stronger $C^{12}O^{16}$ bands which determine the local continuum for the $C^{13}O^{16}$ bands. Thus, as was the case with the non-variable giants, the values given here probably represent upper limits to the value of C^{12}/C^{13} for that portion of the curve of growth which is assumed to apply. They agree with the values quoted by Johnson and Méndez (1970) after allowing for the fact that these authors assumed that the linear portion of the curve of growth applies to the band heads. Note that two stars with MS characteristics, χ Cyg and T Cas, have the largest ratio. This may in part be due to their having very strong $C^{12}O^{16}$ bands. Again, it must be said that these ratios are probably quite inaccurate. The indication from Figure 6 that the variables may have a higher value of C^{12}/C^{13} than the non-variable giants must be regarded with caution.

Fig. 6. - The mean value of $[C^{12}/C^{13}]$ for each variable with the range in spectral type of the variable indicated. The square root portion of the curve of growth was assumed. Lack of room prevented plotting two more stars with $[C^{13}/C^{13}]$ and spectral type range of 7.1, 7.3, M6.5-9, and M7-8 respectively. Also indicated are $[C^{12}/C^{13}]$ values for very late giants from Paper I.

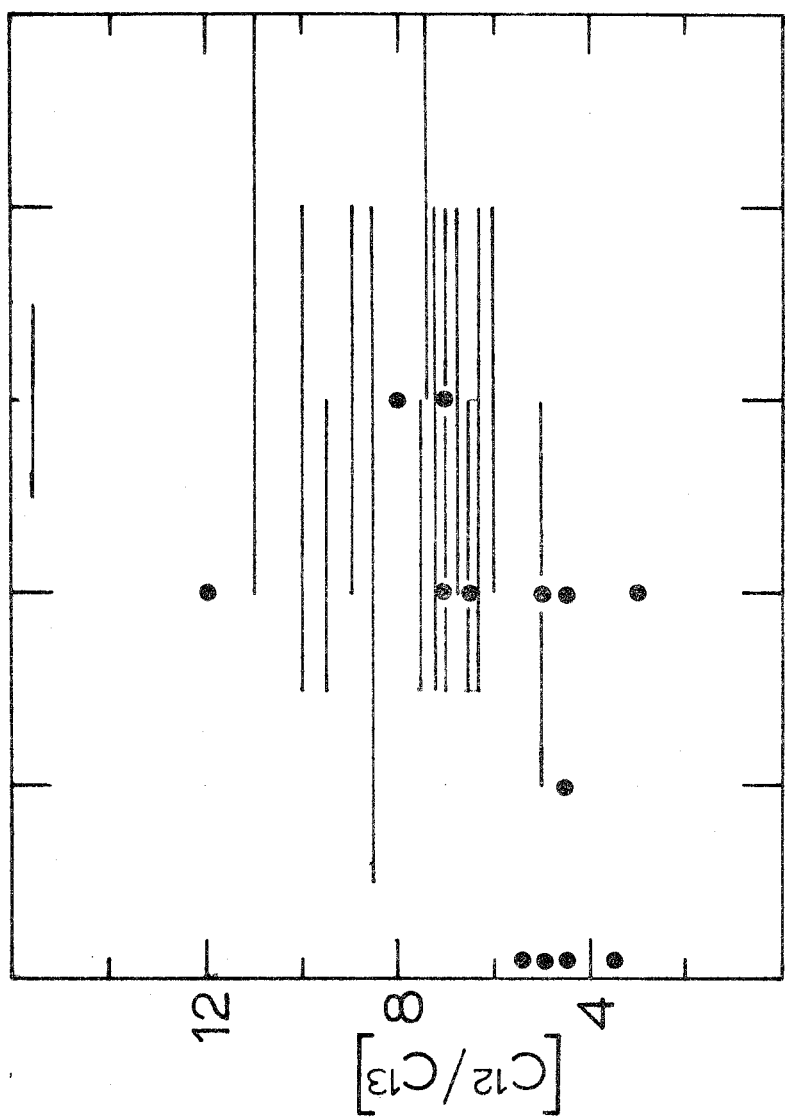

Figure 6.

TABLE 3

MEAN VALUE OF $[C^{12}/C^{13}]$

STAR	$[C^{12}/C^{13}]$
R Aql	6.7
R Aqr	9.0
R Aur	7.7
T Cas	15.8
T Cep	9.8
o Ceti	8.7
R Cnc	7.1
χ Cyg	10.8
U Her	6.7
R Leo	6.7
RS Lib	7.3
RL Mi	5.8
X Oph	9.3
U Ori	6.9
R Ser	7.1
BG Ser	4.8
NML Tau	7.3

III. THE VALUE OF [0/C] IN THE STARS OBSERVED

Merrill, Deutsch, and Keenan (1962) present evidence based on the relative band strengths of V0 6132λ and Ti0 6148λ that spectroscopic differences among certain Me variables are probably due to chemical composition differences. In particular, they conclude that R Aur and R Hya have band ratios closer to those of W And, a weak S star than to RL Mi, a pure M star. Also they conclude that atmospheric "opacity decreases as we go upward through the sequence RL Mi → R Hya → R Aur → W And." Spinrad and Newburn (1965) and Spinrad, Pyper, Newburn, and Younkin (1966) have suggested that on the basis of the strength of Zr0 bands near 9000Å, the M stars T Cas, T Cep, and possibly R Ser are of intermediate MS type. Spectra obtained in the red and near infrared by Terrill (1968), on the other hand, gave no evidence for any S characteristics in W And, T Cas, T Cep, or R Ser.

In addition to differences in heavy metal abundances, S stars are usually distinguished from M stars by a lower value of [0/C]. Spinrad, et al (1966) define a "spectral peculiarity index" which is designed to distinguish stars with weak S characteristics from pure M stars. It is possible to define an index A = W(C0)/1000 - WV based on the data obtained here which can pick out stars having anomalously strong or weak molecular bands. S stars should have H_2O bands weaker relative to their C0 bands at a given temperature than M stars. Also, their C0 bands may be slightly enhanced when compared with M stars of the same temperature because of lower

TABLE 4

SPECTRAL PECULIARITY INDEX

STAR	W(C0), WV MAXIMUM	W(C0), WV MINIMUM	CORRECTED MEAN VALUE
R Aql	.15	.17	.09
R Aqr	<.18	.13	~.15
R Aur	.26	.29	.25
R Cas	~.12	---	~.12
T Cas	.26	.24	.18
T Cep	.21	.21	.12
R Cnc	.14	.14	.07
χ Cyg	.27	.27	.26
U Her	.09	.13	.11
R Leo	.14	.09	.05
RL Mi	.12	.10	.06
RS Lib	.25	.21	.20
Mira	.07	.05	.02
X Oph	.20	.24	.15
U Ori	.08	.19	.11
BG Ser	.20	.23	.14
R Ser	.15	.20	.13
NML Tau	<.14	.20	<.16

atmosphere opacity (Merrill, Deutsch, and Keenan 1962). That a star may be characterized by a unique value of A may be seen from the table below. The values in the second column were obtained from the maximum observed values of W(C0) and WV while those in the third column were obtained from the minimum observed values. Except for U Ori, the differences between the two sets are generally comparable to the error in a single determination of either W(C0) or WV. Since the quantities WV and W(C0) vary differently with temperature, the mean dependence of these quantities on temperature was used to correct the value of A obtained by averaging the second and third column. The results are in the fourth column. The temperature of R Cas was assumed to be the same as U Her since the spectra of the former resemble those of the latter at the same phase. The minimum value of A has been taken as representative of R Aqr. The spectra of NML Tau over the observed part of the cycle are similar to those of U Ori. The latter is the only star observed for which the value of A at minimum band strength is significantly larger than the value at maximum band strength. It is expected, therefore, that the true mean value of A for NML Tau will be .02 or .03 lower than that given in column 4.

The four variables having the largest value of A are χ Cyg, R Aur, RS Lib, and T Cas. This may be interpreted as meaning that these four stars have the lowest value of [0/C] of those observed. Neither T Cep nor R Ser have values of A which would cause them to be distinguished from the rest of the variables. The observed C0 band strengths in those stars having apparantly lower values of [0/C]

provide no evidence that the value of [(0+C)/H] is significantly different from the other stars.

Wing, Spinrad, and Kuhi (1967) interpret observations of NML Tau as indicating that it is extremely cool and has S-type characteristics. In particular, their determinations of the band strengths of TiO and VO as a function of temperature (the latter quantity based on relative intensities of selected continuum points) from scans in the red and near infrared indicate that NML Tau lies between the mean relation for normal M stars (their "M sequence") and the region occupied by the extreme S stars R Gem and R And. Also, the λ9400 band of H_2O was invisible on a spectrum taken very close to maximum visual light, while in a spectrum taken about 2 months after maximum this band was weaker than that in a spectrum taken of o Ceti near minimum even though the former object had a redder energy distribution. Wing, et al observe strong water absorption in NML Tau only when its energy distribution is redder than that of any other star they have observed. They interpret the weakness of the oxide and water bands to mean that the O/C ratio may be as low as it is in R And. These authors also suggest that the lack of any observed enhancement of S-process elements in NML Tau may mean that this and the lowering of the O/C ratio are brought about by separate processes and that the occurrence of one does not require the occurrence of the other.

Other observations of NML Tau relevant to the present discussion were made by Mendoza (1967) and McCammon, Münch, and Neugebauer (1967). On the basis of broad-band photometry of a large selection of M, S, and C stars, Mendoza concluded that his

measurements were consistent with NML Tau being a very cool S star. McCammon, et al obtained scans of NML Tau in the 1.5 and 2.2μ region using the same instrument employed in the present study. These scans were obtained at the time of visual maxima in 1965 September and nearly coincided in time with the observations of Wing, et al. Although the scans of McCammon, et al were not corrected for effects of the earth's atmosphere, the extreme weakness of the water bands and the general shape of the scans led them to conclude that NML Tau resembled weak carbon stars rather than normal M-type Miras.

During the early fall of 1969 NML Tau was at maximum infrared light as indicated by unpublished 2.2μ photometry done at the Hale Observatories and by the value of f(225). On the basis of the observed variation in strength of the 1.87μ H_2O band during the period October 1968 to December 1969, and the general pattern followed by all of the other long period variables observed, it is confidently believed that the strength of this band was at or close to its minimum value for the cycle during August and September 1969. The spectrum of 1969 September 26 is nearly identical to the spectrum of U Orionis taken on 1969 November 21 even in regards to the appearance of the many weak absorption features (see Appendix). In general, it may be said that the spectra obtained of NML Tau are similar to those of U Ori at corresponding phases except that the CO and H_2O band strengths are generally slightly stronger in NML Tau than U Ori. It was also pointed out that NML Tau and U Ori are the only stars observed for which the A index becomes large for minimum values of the band

strength due to a large change in strength of the 1.87μ H_2O band while the CO band remains relatively constant during the cycle. Thus, the spectroscopic observations presented here are consistent with the interpretation of NML Tau as a cool, Mira-type variable, not unlike U Ori, with a "normal" O/C ratio.

Hyland, Becklin, Frogel, and Neugebauer (1971) present strong evidence for the presence of a large circumstellar shell surrounding NML Tau. There is no evidence to suggest that the reddening caused by such circumstellar shells, which seem to surround many infrared stars, follows the normal interstellar reddening law. Therefore, any temperature determination based on either broad or narrow band colors such as used in this present study or in the work of Wing, Spinrad, and Kuhi (1967) will be incorrect. If one were to assume that NML Tau is <u>not</u> reddened, then using a mean $M_V = -1$ (Smak 1966) at maximum visual light and a maximum $m_V = 12$ (Wing, et al), NML Tau would be at ~4000pc. Since $b^{II} \approx -31^\circ$, its distance below the plane of 2000 pc would be highly atypical of normal long period variables with periods in excess of 400 days (Smak 1966).

There are two explanations for the observed disparity in minimum H_2O absorption strengths in 1965 and 1969. It is possible that between March and August of 1969 the strength of the 1.87μ band had a deep, sharp minimum comparable to that deduced from the spectrum of McCammon, et al (1967). Alternatively, the minimum band strength may vary considerably from cycle to cycle. There is some suggestion that this is true in some of the other stars observed (see Figures in Appendix). Furthermore, the 1.87μ band in several variables which

are considered to be of pure M type (eg. R Cnc) have very weak strengths at minimum. Neither of these possibilities would alter the conclusion that NML Tau has a O/C ratio comparible to that of other normal, oxygen-rich Miras.

Keenan (1954) and Merrill, Deutsch, and Keenan (1962) have suggested that W And has S type characteristics which cause its spectrum at maximum to be similar to that of χ Cyg. Wing, Spinrad, and Kuhi (1967), on the other hand, claim that this star lies on their "M sequence", thus implying a normal O/C ratio. Terrill (1969) also has classified it as pure type M from his red and near infrared spectra. The spectrum presented here was obtained two months before visual minimum. ~~Photometric~~ Photometric observations made ten days before the spectrum was obtained indicate a color temperature of 2200°K. The spectrum obtained of U Ori on 1969 November 21, three months before its minimum, is most similar to that of W And in regards to the strength of the 1.87μ water band and the general appearance of most of the weaker features. Also, the predicted temperature of U Ori at this time was 2300°. The CO bands, however, are significantly stronger in W And than in U Ori. From this limited data, one can tentatively conclude that W And has water bands characteristic of a pure M star of similar temperature but enhanced CO bands characteristic of an MS star.

IV. DISCUSSION -- THE SPECTRAL VARIATIONS

A. Summary of Visual Observations

Studies of emission and absorption lines in long period variables have been done by many authors, e.g. Deutsch (1960), Deutsch and Merrill (1959), Feast (1963), Joy (1954), Maehara (1968), Merrill (1940, 1952a, b, c, 1960), Merrill, Deutsch, and Keenan (1962), Merrill and Greenstein (1956, 1958). Although the observed phenomena vary widely from star to star, and even from cycle to cycle of the same star, there are several general behavioral characteristics which emerge from the mass of accumulated data. Unfortunately there are very few cases where a particular variable has been observed in detail throughout an entire cycle. Joy's (1954) work on o Ceti is probably the most extensive that has been done on any single variable. That of Feast (1963) on S Ind is somewhat less so as it was incidental to a larger program. These authors compare their results with those obtained from the more limited observations of other stars and conclude that the behavior of Mira and S Ind is not atypical. It is interesting to note that velocity variations obtained from studies of the absorption and emission lines are difficult to interpret in terms of variations in the diameter of a long period variable.

Several of the above authors have suggested theories usually involving shock waves which qualitatively seem to provide reasonable explanations for some of the observed behavior. More quantitative theoretical work has been done specifically on long-period variables by Gorbatskii (1961), Kamijo (1962), and Keely (1970). It is the

purpose of the present section to briefly summarize the visual spectroscopic observations and their interpretations and to attempt to correlate these with the infrared spectroscopic observations reported in this paper.

Observations of absorption lines in long period variables are not as frequent as observations of emission features. Feast (1963) and Joy (1954) have found the mean absorption velocity generally reaches a maximum (i.e. highest recessional velocity) shortly after maximum visual light. In S Ind this peak seemed to be quite narrow. Observations of other stars are generally insufficient to detect the existence of such narrow peaks. The maximum absorption velocity varies from cycle to cycle by an amount comparable to the velocity variation within a single cycle. Joy finds evidence for a direct correlation between the maximum luminosity and maximum velocity in a given cycle.

It is well established that the displacement of absorption lines of neutral atoms increases algebraically with the excitation potential of the lower level of the line (Deutsch and Merrill 1959, Merrill and Greenstein 1956, Merrill 1960, Maehara 1968). Such asymmetries are visible in tracings of spectra of R Leo and R Hya (Merrill 1952a, b). The doubling of absorption lines has been studied in detail at times of light maximum in the Mira stars R And (Merrill and Greenstein 1958) and χ Cyg (Maehara 1968). Deutsch (1960) has reviewed other manifestations of these phenomena. The dependence of radial velocity on excitation potential, the asymmetries, and line splitting are usually

interpreted as being related phenomena due to an expanding circumstellar shell with the violet displaced component originating in the shell. The asymmetrical lines would be due to partially unresolved circumstellar lines, while the shortward displacements of the low excitation lines would be due to a totally unresolved shell line. The cooler temperatures prevailing in a shell would favor the low excitation potential lines. Several authors have commented on the fact that the shell lines have a remarkably consistent discrete velocity. Intermediate velocities giving evidence for acceleration are not observed. The recent work of Maehara (1969) and Tsuji (1968 and unpublished) points out that not all occurrences of line doubling can be interpreted as due to a shell. They have studied χ Cyg, R Cyg, and R And. Their findings are summarized by Fujita (1970): "Most absorption lines that were single at maximum phase appear with a violet displaced component at post-maximum phase.... The violet displaced component at post maximum phase is characterized by a higher excitation temperature ($T \approx 3000^{\circ}K$) as compared with the normal component ($T \approx 2000^{\circ}K$).... The zero-volt lines of KI, RbI, LiI, Y I, and Zr I have shortward components both at maximum and post maximum phases.... Emission lines of Hα and Ca II triplet are strong and displaced to the violet. Hα has an overlapping absorption at its normal position." In addition, these authors conclude that the shortward component of a double absorption line originates in a layer below that in which the longward component is found. The model proposed by these authors will be discussed below. Detailed studies as done by Maehara and Tsuji may be more feasible in S and

MS stars than in pure M stars because of a lower atmospheric opacity in the former stars as suggested by Merrill, Deutsch, and Keenan (1962).

Other phenomena associated with absorption lines in Mira variables have been discussed by Merrill, Deutsch, and Keenan (1962). They suggest that part of the line weakening observed in long-period variables (with respect to non-variables of the same spectral type) which have earliest spectral types later than M5 and are generally of low velocity and intermediate population (includes variables observed in the present study) can be explained by a metal deficiency of 10^{-1} in the variables. The rest could be due to variable continuous and molecular opacity.

Merrill (1940, 1960) has suggested that both spectral and light variations could be due at least in part to "veiling" by solid or liquid particles. This has been discussed by Smak (1966). Also Kamijo (1963) has concluded from a theoretical study that "the opacity due to liquid and solid particles is negligible" in late type giant stars. Fix (1969) and Wickramasinghe (1968) have shown, however, that under the right conditions, a large number of graphite particles will form and significantly affect the emergent flux. It is not clear, though, if the "right" conditions ever obtain in normal Mira stars.

Variations in velocity and intensity of hydrogen and metallic emission lines have been studied in considerable detail. The average behavior of the velocity of <u>all</u> emission lines as discussed by Feast (1963), is a decrease at or shortly after maximum light with a minimum (i.e. greatest velocity of approach) corresponding approximately in

time to the maximum absorption velocity. Feast points out that the observed minimum of emission line velocity in S Ind and that of the well observed cycle of U Ori in 1927 were very narrow and that such minima might easily have been missed in velocity measurements of other Me variables as is the case with the absorption velocities mentioned earlier. The practice of averaging together observations from several cycles would tend to smooth out narrow maxima or minima.

The emission lines of highest excitation potential, i.e. H and ionized metals, tend to appear first, usually before maximum light. As the light declines, large numbers of metallic emission lines begin to appear and increase in strength. Joy points out that without exception these lines are displaced shortward with respect to the absorption lines. The displacement decreases as they increase in strength in accord with the average behavior noted above. The emission lines usually disappear near minimum light. As is the case with the absorption lines, the emission lines with higher excitation potential show a strong tendency to have algebraically larger velocities compared with low excitation potential lines. Occasionally (Merrill 1952a, b) the H-emission lines show a continual outward acceleration whereas the metal lines follow the normal behavior. When the H lines first appear their relative intensities are usually anomalous and superimposed absorption lines are usually visible. After maximum light the Balmer decrement becomes normal (Merrill 1960). This is interpreted as indicating that the emitting layer initially lies below the reversing layer and does not rise above it until sometime after

light maximum. From his study of southern variables Feast (1963) derived a mean relation between the periods of the stars and the difference between their absorption and emission velocities (A-E). He found that for P > 200 days, (A-E) increases from 10 to 15 km/sec with a step up occuring around 325 days. The maximum value of (A-E) during any given cycle can be 20 km/sec greater than the mean value.

B. The Proposed Model

It has long been thought that the phenomena observed to occur in the atmospheresof long period variables could be accounted for at least in part by the action of shock waves. Qualitative models have been discussed by Merrill and Deutsch (1959) and Fujita (1970). Kamijo (1962) has discussed the progressive waves that are generated by non-adiabatic radial pulsations. Keeley (1970) has considered the energy which will be available to drive the atmosphere. The radius and luminosity of his theoretical model vary with time in a manner similar to that found for o Ceti by Pettit and Nicholson (1933). Since the radial velocity variations observed in the absorption and emission lines are inconsistent with what would be expected from volumn pulsation, it is suggestive that these velocity variations are almost completely determined by disturbances moving through the atmosphere. In this section the motion of a strong shock will be considered. The behavior of such a disturbance is relatively simple and the equations describing it have been discussed by Landau and Lifshitz (1959). A multilayered atmospheric model will be discussed based on the ideas of Merrill and Deutsch (1959) and Fujita (1970). The general behavior

of visual spectra can be understood on the basis of this model. An attempt will be made to understand the behavior of the infrared spectra presented in this paper. Finally, the energetics of the shock will be briefly considered and a mass loss rate of $\sim 10^{-5} M_{\odot}$/year will be seen to be consistent with the model.

Consider the instantaneous release of an amount of energy E at the origin of a spherical coordinate system (Figure 7). Let the gas of region (1) into which the resulting shock front moves be at rest in this coordinate system and have density ρ_1. All velocities will be measured with respect to region (1). At time t the front is at a distance r_o from the origin and is moving with velocity U_1. The gas directly in back of the shock has velocity V_2 and density ρ_2. At a point r* from the origin such that $\frac{r^*}{r_o} \to 0$, the velocity and density are V* and ρ^*. Landau and Lifshitz show that for a perfect gas the physical parameters are given by the following equations:

$$r_o = \xi_o \left(\frac{Et^2}{\rho_1}\right)^{1/5}, \quad U_1 = \frac{dr_o}{dt} = \frac{2\xi_o}{5}\left(\frac{E}{\rho_1 t^3}\right)^{1/5} \qquad 1.$$

$$V_2 = \frac{2U_1}{(\gamma+1)}, \quad \rho_2 = \rho_1 \frac{(\gamma+1)}{(\gamma-1)}, \quad p_2 = \frac{2\rho_1 U_1^2}{(\gamma+1)} \qquad 2.$$

$$\frac{V^*}{V_2} \sim \frac{r^*}{r_o}, \quad \frac{\rho^*}{\rho_2} \sim \left(\frac{r_*}{r_o}\right)^{3/\gamma+1} \qquad 3.$$

ξ_o is a constant of motion given by

$$\xi = r\left(\frac{\rho_1}{Et^2}\right)^{1/5}$$

Fig. 7. - This illustrates the parameters which characterize the shock disturbance.

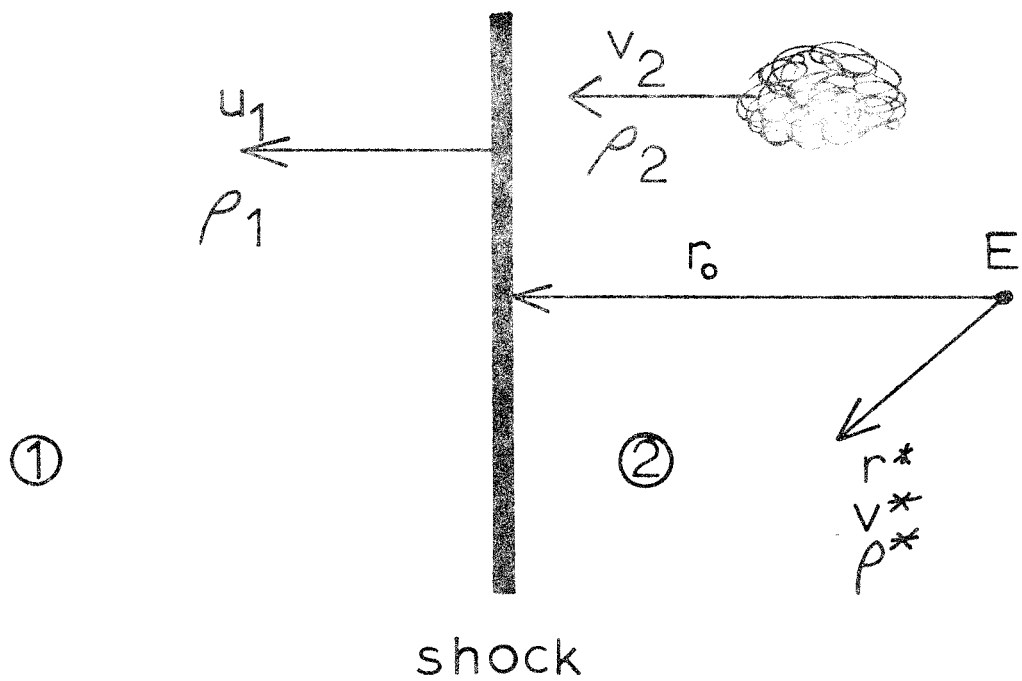

Figure 7.

Combining the ideas of Merrill and Deutsch (1959) and those summarized by Fujita (1970), the schematic model shown in Figure 8 is adopted:

Layer I is the top of the region in which most of the flux is carried by convection and layer II is the bottom of the reversing layer through which the shock has already passed. Layer III is the shock front itself with a region of heated gas behind it. Layer IV is the top of the reversing layer and is the undisturbed region into which the shock is moving. Layer V is the extended tenuous outer atmosphere (in the notation of Maehara [1968], layer IV is the "ℓ" layer and layer II is the "S" layer). Deutsch and Merrill did not consider a reversing layer to exist below the emitting region L III.

Parameters characterizing the star and its atmosphere may be obtained from the models of Auman (1969), Carbon (private communication) and Keeley (1970) and from the observations of eclipsing binaries reviewed by Wilson (1960). The average luminosity, mass and radius are taken to be 2×10^{37} ergs/sec, 4×10^{33} gm, and 2×10^{13} cm. so $g \approx 1$ cm sec^{-2}. In L I a typical density is 10^{-8} gm/cm^3. In the reversing layer a typical value of ρ is 10^{-12} gm/cm^3. The scale height of the reversing layer is small and the density will fall off quite rapidly as L V is approached. At one stellar radius above the surface this density may be 10^{-20} gm/cm^3. The scale height in this region is large and may be comparable to a stellar radius. The energy available for the shock phenomena is taken to be 10^{42} ergs.

The shock front is assumed to originate deep in LI and begins to emerge from it at the time of first appearance of emission lines,

Fig. 8. - Schematic model for a variable's atmosphere with a shock front moving through it.

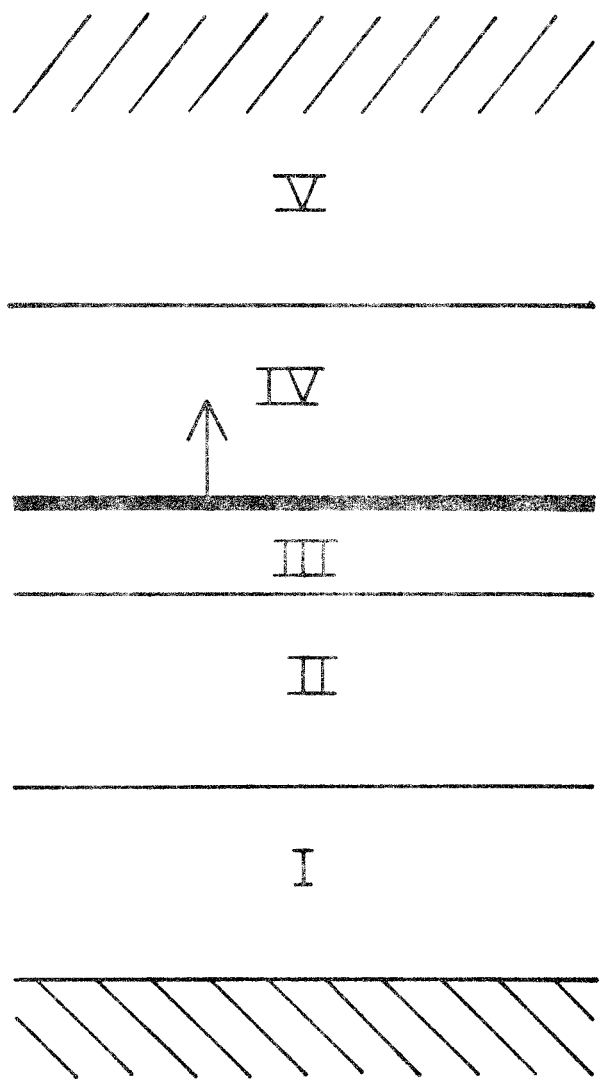

Figure 8.

two tenths of a period before maximum visual light (Joy 1954). The passage of the front is expected to have three effects on the gas -- an outward streaming motion (V_2) will be induced; the gas will be heated; turbulent motions will be increased. As the front crosses into L II its outward velocity increases, due to the large density gradient, and the temperature of the heated gas will increase causing the H-emission lines to become strong. From equations 1 and 2 it is seen that $\frac{dT}{T} = \frac{2du}{u}$. The emission lines will be severely affected by the overlying absorbing layers, in agreement with observation. Around the time of maximum light, the configuration illustrated in Figure 8 is reached. The gas in L II has undergone radiative cooling and is cooler than the photosphere but not as cool as L IV. This produces the doubling of absorption lines discussed by Maehara and Tsuji. The component arising in L II will be characterized by a higher excitation temperature and an outward velocity with respect to L IV. The emitting layer L III, as pointed out by Merrill and Deutsch (1959), must be optically thin in the continuum but optically thick in the lines so that the rate of radiative cooling will be proportional to the recombination rate which in turn is proportional to the square of the density. Using the typical values of the physical parameters for the reversing layer given above and a time scale of 10^7 sec, equations 1, 2, and 4 give $\xi_o = .5$, $u_1 = 1.6 \times 10^6$ cm/sec, $V_2 = 1.2 \times 10^6$ cm/sec, $T = 6 \times 10^3\,^oK$. This velocity agrees with the observed difference in absorption and emission line velocities. The gas at some distance behind the front will have cooled somewhat and lower excitation metallic emission lines will appear. Gravitational deceleration will cause these lines

to have algebraically greater radial velocities than the hydrogen lines, again in agreement with observations. The observed asymmetry of many emission lines may be due to unresolved absorption components.

Depending on the detailed density distribution within the star's atmosphere, the shock front will either continue to be accelerated as it rises, or will be decelerated by gravity. These two possibilities would result in the H-emission lines having a continually decreasing velocity, or an initially decreasing, but then an increasing velocity as the gas is decelerated.

The behavior of the absorption lines as the front moves further up into L IV is well illustrated in a series of post maximum spectra of χ Cyg by Maehara (1968). The component arising from L II increases in strength and velocity (algebraic) as more heated gas is added to this layer and it is decelerated by gravity (Tsuji (unpublished) has suggested that part of this increase could also be due to decreasing continuous opacity in the upper layers). The component arising from L IV decreases in strength, but maintains constant velocity as no precursor of the shock front can propagate into L IV ahead of the front itself. The emission velocities measured by Maehara seems to be anomalous in that they are algebraically greater than the absorption velocities of L II. The observed outward acceleration of the absorbing material which is often observed after the time of maximum light (e.g. Joy 1954, Feast 1963) could easily be caused by a blending of the L II and L IV components resulting in a blueward velocity shift as the L II component increases in strength. The asymmetric appearance of many absorption lines has been remarked upon in the references which have

been given.

At a considerable time after visual light maximum, the Balmer decrement is no longer affected by overlying absorption. This is usually interpreted as indicating that the emitting layer has risen above the reversing layer. Also at this time forbidden emission lines appear indicating a low density for the emitting layers. Further, the absorption lines now seem to show a maximum velocity of expansion. As the shock disturbance moves into L V the emission lines would be expected to fade away and the velocity of the absorption lines should tend to algebraically increase due to gravitational deceleration. This again agrees with the general behavior that is observed.

There is an important conceptual difference between the model proposed here and those considered by Merrill and Deutsch (1959) and Gorbatskii (1961). Merrill and Deutsch consider a "semi-static" model in which an absorbing layer always remains above the emitting layer because of energy losses in the lower levels of the atmosphere. Gorbatskii pictures the shock as moving rapidly through the atmosphere and ceasing to be influential shortly after the time of maximum light. The observations do not support these views. In particular, emission lines are seen to persist up until the time of minimum light at which time they seem to be above the reversing layer and their velocity with respect to the absorption lines is probably always supersonic, implying that shock phenomena exist throughout the pulsation cycle.

C. Interpretation of Broad Band Infrared Observations

The behavior of the infrared spectra of the variable stars

studied here is more difficult to understand quantitatively than the visual spectra. The resolution employed, 32Å, is too low to discern individual absorption lines from which a temperature and radial velocity could be derived. The much longer pathlength required for the formation of a molecular line as opposed to an atomic line implies that the characterization of molecular absorption features by a single set of physical parameters is a poor approximation. Keeping these caveats in mind, an attempt will be made to understand the variations of molecular band strengths in the context of the model discussed above.

There is strong evidence that the variation of spectral features and broad band flux get progressively out of phase with the visual light curve as one goes to longer wavelengths. Smak (1964) found that the minimum strength of TiO bands and maximum strength of H-emission occurs at or close to the time of maximum visual light. Pettit and Nicholson (1933) found that the maximum bolometric magnitude occurred after the maximum visual magnitude and that the range in bolometric magnitude was considerably less than the visual range. For six of their best observed stars, Pettit and Nicholson found the maximum bolometric magnitude to occur 0.14 phase later than maximum visual magnitude and to have a range of 0.89 mag. Five of these stars were observed by the present author: R Aql, χ Cyg, R Leo, R L Mi, and o Ceti. Averaged over one cycle, maximum f(225) occurred 0.20 phase later than the visual while the range was 0.58 mag. The m_b of Pettit and Nicholson is not corrected for stellar water absorption. On the basis of the variation of water absorption with phase found here, a correction

to m_b would tend to increase the phase lag and decrease the range. Terrill (1969) has evidence which suggests that the change in the M subtype of a long period variables classified from near infrared spectra "lags behind the change in visual light on the ascending branch of the light curve with respect to the descending branch." Hetzler (1936) finds that the light curve based on photographic photometry at 8500Å lags behind the visual light curve. Wing (1967) reports on narrow band photometry at 1.04μ of χ Cyg. He finds a phase lag of 50 days and a range of 2.5 mag. The range is larger than that given by f(225) probably because 1.04μ lies shortward of the black body peak for χ Cyg.

The explanation given by Wing to explain the phase lag is that the infrared radiation comes from the photosphere, the visual originates in higher layers, and the temperature variations of the two layers are out of phase. This idea is also suggested by Wing, Spinrad, and Kuhi (1967) to explain apparent "loops" in their diagrams of band strength versus color (see Figure 9). This picture implicitly assumes that the line blanketing due to metallic oxide bands is much greater in the visual than any opacity source in the red and infrared. Such a picture is difficult to understand, however, since it implies that the temperature and flux increase in the lower layers after they increase in the upper layers.

Wisniewski and Johnson (1968) found from multicolor photometry of Cepheids that the longer the wavelength, the greater the phase shift with respect to the visual light curve. The stars with the smallest phase shift also had the smallest infrared amplitudes in agreement

Fig. 9. - Here, the water vapor and carbon monoxide band strengths are plotted against one another for two well observed stars. Similar closed figures would result if the band strengths were plotted against f(225).

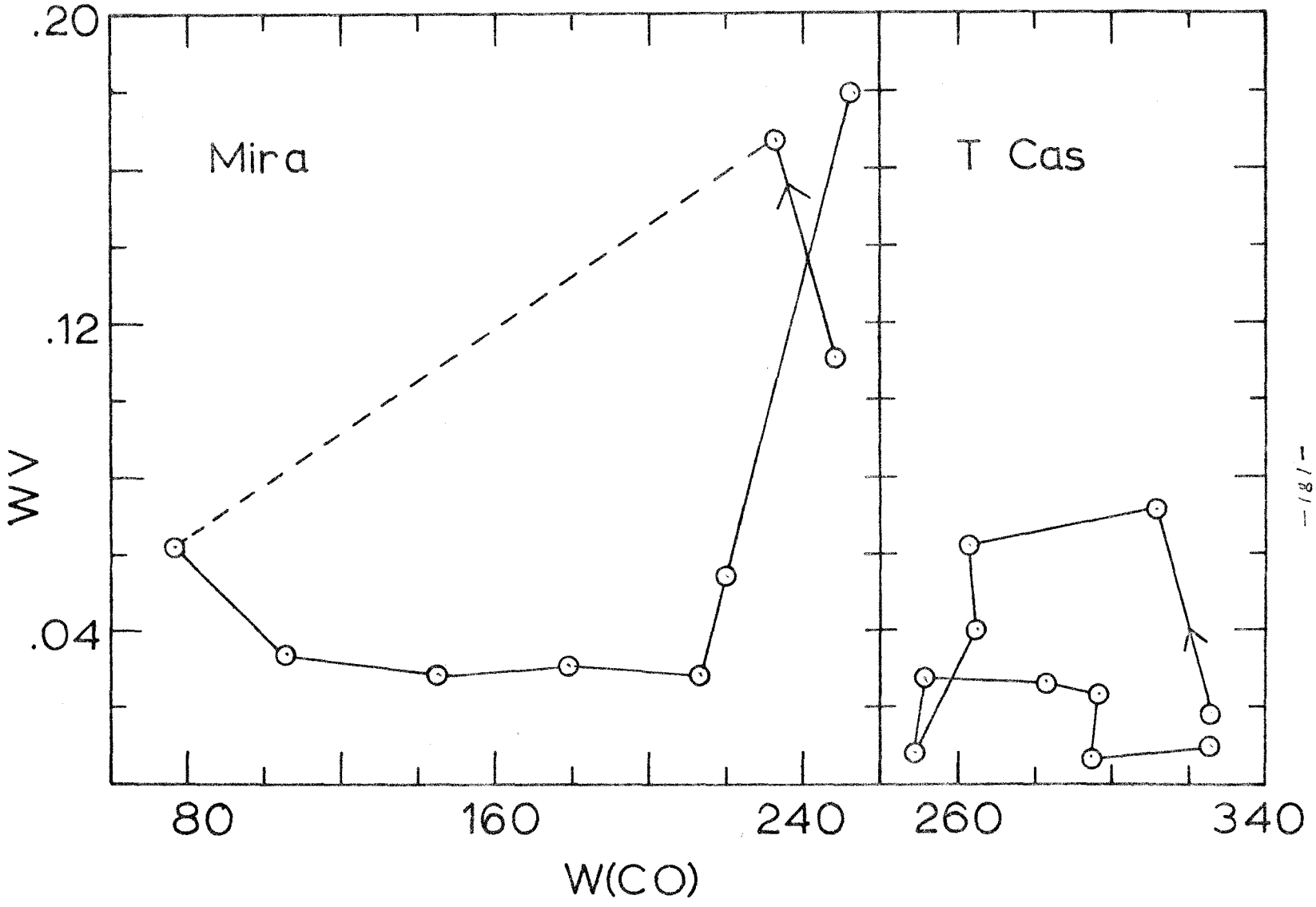

Figure 9.

Fig 89

with the results presented here. Finally, the bumps which appeared on the descending branch of the visual light curves of the Cepheids became the primary maxima at longer wavelengths.

All of these observations can be understood if the opacity increases with increasing wavelength (Noyes, Gingerich, and Goldberg 1966). In particular, the radiation in the visual band would be expected to be characteristic of the deepest layer which can be seen. The bump observed by Wisniewski and Johnson (1968) might be interpreted as an opacity anomoly which causes the visual radiation at that particular phase to be characteristic of a higher layer than otherwise. Keeley's (1970) theoretical results can be interpreted as predicting a phase lag for the longer wavelengths since he has shown the higher the layer considered, the longer it takes to respond to the disturbance which triggers the pulsation.

That temperature derived from atomic and molecular absorption features in the visual seem to be higher than temperatures based on broad band photometry could be attributed to the temperature gradient and the dependence on wavelength of the continuous opacity. The correlation of the phase lag between the infrared and visual light curves and the range of flux in the infrared can be understood as arising from scale differences between different stars. If a larger flux amplitude is indicative of a more energetic pulsation and larger disturbances propagating into the atmosphere, a more extended atmosphere might be expected. For normal, Me-type long period variables there is evidence that abnormally bright visual maxima are associated with abnormally strong emission line strengths, further suggesting a

correlation between the energy output and the magnitude of the shock disturbance.

D. Behavior of the CO Bands

The observed variations in the quantity W(CO) have already been discussed in Section II. C. Since the pathlength required for the formation of the CO lines is probably large compared to the thickness of the shock front (Paper I and Merrill and Deutsch 1959), and since CO is generally completely associated for the temperatures of the stars considered here, it is reasonable to assume that disassociation of CO by the heating due to the shock may be neglected compared to other factors influencing the strength of the absorption bands. The spectrum of o Ceti taken on 1969 October 28 near maximum infrared light, shows at least six $C^{12}O^{16}$ bands, thus being characteristic of a temperature around 3000°K (Young 1966, Kunde 1968). One taken near minimum infrared light, on the other hand, has a CO absorption spectrum more characteristic of about 2000°K (Young 1966, Kunde 1968). Since the times of maximum and minimum flux approximately correspond to the times of maximum and minimum temperature in the region responsible for the 2.25μ light, it is suggestive to explain the observed variation of W(CO) in a single star in terms of temperature variations in the region of band formation. Any observed delay between the time of maximum f(225) and maximum W(CO) can be attributed to a combination of factors. The region of band formation must necessarily lie above the emitting region, causing a lag in the temperature variations. This is the same effect which causes the phase shifts

between the various light curves. The delay may also in part be caused by the effects of the shock front, local heating and turbulence.

It should be noted that this temperature dependence of the CO absorption variation in any one star is different than the dependence observed for a group of stars of different temperatures. The differences of CO band strength from star to star are probably attributable to effects like those discussed in Paper I.

It was noted previously that the spectra of U Ori and NML Tau, two otherwise normal oxygen rich long period variables, have anomolously strong minima CO absorption strength for their respective temperatures. In particular, the first two vibrational bands seemed to be characteristic of a considerably higher temperature than the higher bands. A recent paper by Spinrad, et al (1971) studied a high resolution spectrum of α Ori. They compared the individual rotation lines of different bands with theoretical profiles calculated by Kunde. If the theoretical profiles were made to match the medium excitation rotational lines of the (2, 0) band ($6 \leq J < 80$), two important discrepancies were found. First, the lowest and highest excitation potential lines were overpopulated compared to the Boltzmann distribution which fit the intermediate lines. Spinrad, et al suggest that the lowest lines seemed to be characteristic of a rotational temperature of only a few hundred degrees. Second, the departure of the observed strengths of the higher, (3, 1), (4, 2), etc., vibrational bands from the strengths expected on the basis of a unique vibrational temperature increased with height above the ground state in the sense that the observed strengths were too weak. Other synthetic spectra computed by Kunde

(private communication) at a lower resolution illustrate the same effect when compared with spectra obtained in the present study, namely the observed strengths of the upper vibrational bands become progressively weaker when compared with the predicted strengths. Thus, the spectra of U Ori and NML Tau may be extreme cases of this. Spinrad, et al attribute this discrepancy to the fact that in a low density medium the vibrational relaxation time is significantly greater than the rotational relaxation time, implying that LTE probably does not obtain. It is not necessary, however, to invoke non-LTE effects to explain this discrepancy, for it could be due entirely or in part to temperature stratification effects in the atmosphere. Kunde's synthetic spectra were computed using a single slab model characterized by a unique temperature. As pointed out in Paper I, the very low f values of the CO bands implies a very long pathlength for formation. Now the f values are higher for the higher vibrational bands. Therefore these higher bands could form primarily at a higher level and be characteristic of a lower rotational temperature than the lower excitation bands.

The CO absorption spectrum of χ Cyg may be taken to be characteristic of those stars which apparently have a "low" O/C ratio, viz. T Cas, R Aur and RS Lib. The spectrum of χ Cyg on 1969 April 27 is remarkably similar to that of RT Vir on 1970 February 21 (Paper I). The latter star is an M7 III irregular variable of small amplitude. The colors (J-L) and spectral types (visual) of the two stars would normally be interpreted as showing χ Cyg to be 800°K cooler than RT Vir. If RT Vir is assumed to have a "normal" O/C ratio (i.e.

greater than χ Cyg) than the equality of strength of the 1.87μ water band in both stars could be interpreted as being due to the observed fact that this band increases in strength with decreasing temperature, and that the lower temperature compensates for the lower H_2O abundance in χ Cyg. The similarity of the high excitation CO bands, though, suggest that in χ Cyg they are formed at the same temperature as in R T Vir. The similarity of the many minor absorption features is also suggestive of a similar temperature and perhaps similar H/C ratios in both stars.

Finally, the CO absorption bands of o Ceti itself are peculiar. They seem to be abnormally weak for the indicated temperature (either by infrared colors or visual spectra). The minor absorption features also are weak when compared with spectra of other stars. Taken together, these two facts might indicate a higher atmospheric opacity than exists in the other stars.

E. Behavior of the H_2O Band

The variation of strength of the 1.87μ water band is complicated by the low disassociation energy of the H_2O molecule. As described before, the time behavior of this band may be characterized by a rapid rise to maximum strength, a slower decline, and a broad minimum. The variations are out of phase with the variations in both the CO band and the 2.25μ flux resulting in "loops" when the H_2O band strength is viewed as a function either of CO band strength or 2.25μ flux (Figure 9).

The fact that the maximum strength of the 1.87μ band <u>always</u>

occurs either at the same time as or after the CO band maximum and always after the 2.25μ flux maximum is interpreted as indicating that the mean level of formation of the water band lies above that of the CO band. Since the H_2O molecule reaches a maximum concentration only for $T \leqslant 2300^{\circ}K$ (Tsuji 1964, Vardya 1966), such a stratification might be expected on theoretical grounds. The relatively rapid rise in strength of the H_2O band is interpreted as indicating that it is more strongly influenced by the passage of the shock than is the CO band. Keeley's (1970) models lend support to this idea. The disturbance of any given layer with time becomes more and more asymmetric in the sense that rise time becomes much steeper than the fall time.

It is interesting to note that maximum H_2O absorption approximately corresponds to the time when the emission lines in the visual spectral region seem to be in the upper part of LIV (Figure 8), i.e. when they are free of overlying absorption. This can be taken to mean that the shock disturbance is now passing through the high region where the 1.87μ band is primarily formal. After maximum strength, the gas cools, the turbulence decays, and the band gets weaker.

Model atmospheres calculated by Auman (1969) have indicated that water absorption bands increase in strength as stars of successively cooler temperatures are considered, due to the declining relative importance of other opacity sources, and as the turbulence is increased. But as the variation of H_2O in a given star is similar to the variation of CO band strength, it is again felt that the variation for a given star with phase is not due to the same cause as the systematic variation from star to star which is characterized by stronger CO and H_2O bands

being associated with cooler temperatures. If it were, it would mean that the temperature variation in the molecular absorption region is about 180^{o} out of phase from the region where the continuum 2μ flux originates. This is physically implausible although not impossible. Also, it was previously noted that at maximum strength, the band structure of the CO absorption is characteristic of a higher temperature than it is at minimum strength.

If this schematic picture is correct, it means that for any single star, the variation of CO and H_2O band strength is dominated by the effects of temperature and turbulence on the molecular absorption coefficient directly, not by changes in continuous opacity. The difference between the resulting absorption spectra of the two molecules would primarily arise from differences in height of formation.

It has also been suggested (Frogel 1970) that the band variations may be due to injection of matter into cool regions where molecules may form thus increasing the column density of absorbing material. Such injection would be caused by the pulsation.

F. Comparison With Model Atmospheres

The model atmospheres constructed by Auman (1969) are the only ones made for late-type stars that consider water absorption in any detailed fashion. It is instructive to compare the observations made here with the models if only to indicate the direction in which the models must be corrected. In Figure 10 are plotted log $(F_{\lambda=1.67\mu}/F_{\lambda=2.3\mu})$ and log $(F_{\lambda=2.3\mu}/F_{\lambda=2.0\mu})$ as functions of effective temperature for a sequence of giants and supergiants from Auman's models

Fig. 10. - Shown here are the ratio of the maximum flux on either side of the 1.87μ H_2O band, log f(167)/f(230), and a measure of the depth of the 1.87μ band relative to the maximum flux longward of this band, log f(230)/f(200). The solid and dashed lines are the theoretical values for giants and supergiants respectively (Auman 1969). The dots in the lower figure represent the variables at maximum observed 1.87μ band strength. The possible MS stars R Aur, T Cas, χ Cyg, and RS Lib were excluded. R Aqr was excluded because of insufficient observations. In the upper figure are those stars for which spectra in the 1.6μ region were available, as discussed in the text, regardless of phase. These stars are R Aql, R Aqr, U Her, R Ser, o Ceti, Mira, U Ori, and NML Tau. The arrows indicate the direction in which the (J-L) color temperature was changing at the time of observation.

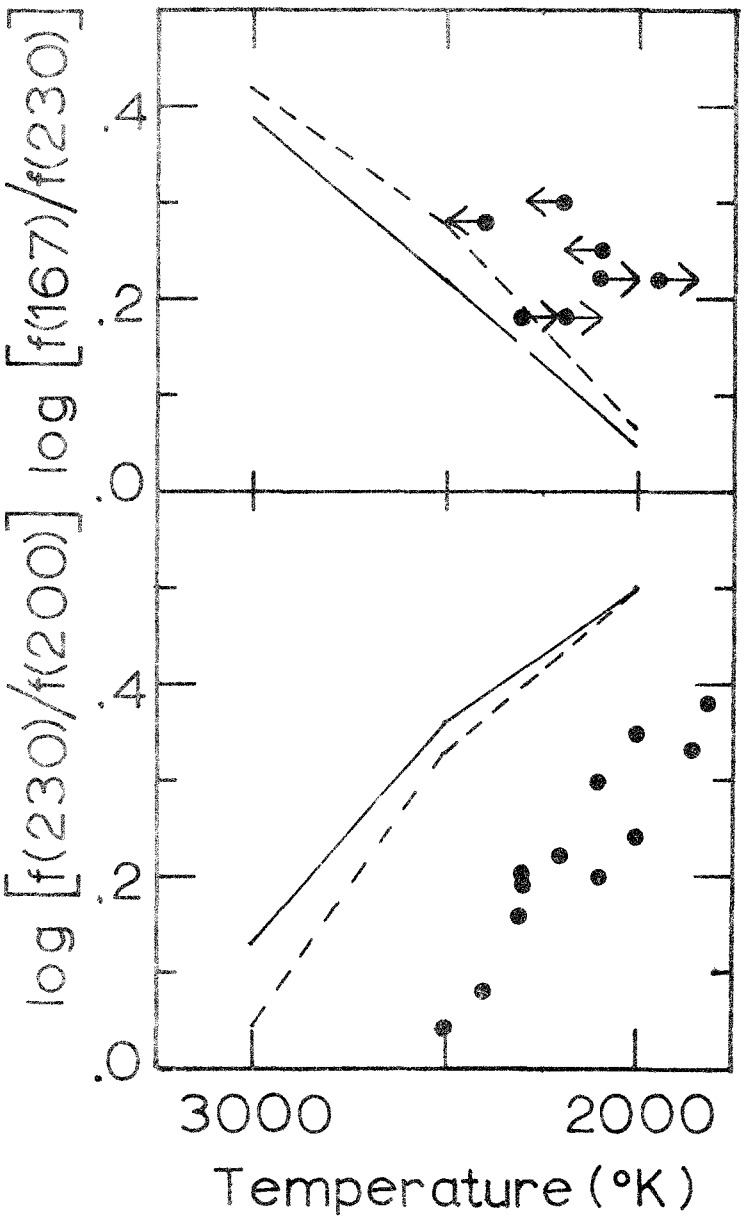

Figure 10.

(1969, private communication). The first quantity measures the ratio of the peak fluxes emitted on either side of the 1.87μ water band. The second quantity is a measure of the depth of this band. The crosses in this figure represent the maximum water absorption and corresponding color temperature for each star. The stars R Aql, R Aur, R Cas, T Cas, χ Cyg, and RS Lib were excluded either because of incomplete observations or because of evidence for an abnormally low value of O/C. The arrows represent those stars for which both 2.2 and 1.6μ spectra were available, regardless of phase. U Her and R Ser did not have 2μ spectra taken at the same time as the 1.6μ spectra, but a reasonable extrapolation from available data was made to obtain the 2μ quantities. The direction of the arrows indicate the direction in which the temperature was changing.

It is at once clear from Figure 10 that the predicted strengths of the bands are too great. Since the models were constructed assuming a turbulence parameter of 2 km/sec, whereas reasons have been given earlier for favoring a value of 10 km/sec, the predicted band strengths may even be underestimated. It is extremely unlikely that the color temperatures are in error by the amount necessary to bring the observed points into agreement with the predicted relation. That the observed points define a relation which is approximately parallel to the predicted one is encouraging, however,

Several factors can contribute to the incorrectness of the models. Auman (1969) performed his calculations treating the water opacity as a harmonic mean opacity. He has discussed the difficulties and probable incorrectness of such an approximation. A more correct approach,

suggested by Auman, is to use both a harmonic and a straight mean. He indicated that it was not at all clear how the calculated energy distribution would be changed by such an approach. A second factor is the possible importance of non-LTE effects. Calculations performed by Auman (1969) indicate that for Te $\leq 3000^{\circ}$K the pressures in the band forming regions of giants and supergiants are too low to allow either rotational or vibrational relaxation to obtain. Such an effect may have been observed in the CO bands as discussed above. Auman has also pointed out that convective motions may seriously affect the structure of the lower atmosphere. In addition, radiation pressure acting selectively on the H_2O molecule may severely affect the equilibrium distribution of this molecule. Such an effect was considered by Weymann (1962a) as a possible mechanism for mass loss. This will be investigated in detail in Section V. Finally, there is the problem of elemental abundances. Auman (1969) calculated two models in which the C/H ratio was increased and decreased by a factor of two. The model with the high carbon abundance ($O/C \approx 1.26$) had slightly weaker water bands. Spinrad and Vardya (1966) have suggested that the value of O/C in "oxygen rich" stars they measured is ~ 1.05. It is not clear what the emergent flux from a star with such a value of O/C would look like. The apparent existence of various O/C values among the stars studied here was discussed in a previous section. In particular, it is clear that χ Cyg, a very cool long-period variable, has almost no water. The abundance problem will be considered in more detail later.

G. Some Comments on Mass Loss

Deutsch and Merrill (1959) pointed out that their shock model led to a continuous outflow of matter from the star. Since the model considered here is basically similar, it leads to the same conclusion- stars in which strong shocks play an important role will have a high rate of mass loss. Using the model parameters given in Section IV. B. with $\rho \approx 10^{-12}$ gm/cm^3, V = 12 km/sec. and performing the same calculation as Merrill and Deutsch, upper limits for the rate of mass loss and the energy required may be derived by assuming that all of the matter in the region characterized by the parameters escapes. These values are 2×10^{42} ergs/year and 4×10^{-5} $M_\odot$/year. These are in reasonable agreement with high theoretical and observational values (Keeley 1970, Deutsch 1960). If two different heights are considered, then from mass conservation $\rho_1 V_1 r_1^2 = \rho_2 V_2 r_2^2$. In the reversing layer the density certainly falls off faster than r^{-2}, thus giving an expansion velocity increasing outward, possibly accounting for the algebraically lower velocities observed in the lowest excitation lines compared to lines of higher excitation potential. Above the reversing layer in the circumstellar envelope, the density may approximate the barometric law - $\rho \sim r^{-2}$, so that the expansion velocity will be independent of height, as it seems to be in α Her (Deutsch 1960, Weymann 1963). Tsuji (unpublished) has similarly proposed that the material in the circumstellar envelope is part of that material which was accelerated by the shock and subsequently ejected. He estimates a mass ejection rate for R And of 10^{-5} $M_\odot$/yr.

Gehrz and Woolf (1970) have associated large infrared excesses observed in RV Tau stars with the strong shock waves that are presumed to exist in their atmospheres, implying that the latter leads to mass loss. In a study of carbon stars (Frogel and Hyland, in preparation) it was found that the long period carbon variables have systematically weaker CO and CN bands in the 2μ region than do the irregular and semi-regular carbon variables. This was interpreted as being due to increased veiling by circumstellar material. Gillett, et al (1971) have reported that the long period variable carbon stars have higher infrared excesses than do the others. Presumably the shock phenomena is considerably stronger in the long period variables than in the others.

Gehrz and Woolf (1971) have considered the effects of radiation pressure on dust particles. They conclude that gas can be driven out of a star via coupling with the dust particles, and that this provides the dominant mechanism for mass loss in late type stars. There are several important examples, however, of considerable mass loss in late type stars without the accompanying infrared excess usually associated with a shell. Several strong microwave OH sources (eg R Aql, U Ori, U Her), and microwave H_2O sources (the same stars plus α Boo) have no measurable excess. The Se stars R And and R Cyg have high mass loss rates and no excess.

The observations of H_2O microwave emission from long period variables can be interpreted as indicating the presence of a considerable amount of water in the circumstellar environment of some of these stars. In particular, it was

found (Frogel 1970) that a necessary condition for H_2O microwave emission from the long period variables which were observed was a strong 1.87μ absorption band. As pointed out previously, stars with such strong absorption tend to be among those with the greatest 2.25μ flux variation and the greatest lag between visual maxima and 1.87μ absorption maxima. Thus again it seems that the two quantities phase lag and flux range are indicative of the magnitude of the disturbance in the stellar atmosphere.

The connection between long period variables having strong infrared H_2O absorption and OH microwave emission has been discussed in detail elsewhere (Hyland, Becklin, Frogel, and Neugebauer 1971). The observations and implications are similar to those of the H_2O sources and there is a considerable degree of overlap between the two sets of sources.

V. RADIATION PRESSURE

Since the absorption coefficient of the H_2O molecule is very large and nearly continuous in the 1-3μ region where the star emits its maximum amount of flux, (Tsuji 1966, Auman 1967, 1969) it was decided to investigate the effects of radiation pressure on the H_2O molecule. This was suggested as a possible mechanism for mass loss by Weymann (1962). The analytic representation of the absorption coefficient given by Tsuji (1966) based on the just-overlapping approximation is used. He has shown it to be in reasonable agreement with empirical results and should certainly be of sufficient accuracy to judge the importance of radiation pressure. The absorption coefficient per H_2O molecule is represented by

$$k_\omega = \sum_{n_1 n_2 n_3} \frac{\pi e^2}{mc^2} f_o^{n_1 n_2 n_3} \xi_{n_1 n_2 n_3}(\omega, T)\, \phi_{n_1 n_2 n_3}(T) \left[cm^2\right]$$

where

$$\phi_{n_1 n_2 n_3}(T) = \left\{ \prod_{j=1}^{3} \left[1 * \exp\left(- \frac{hcw_j}{kT} \right) \right]^{-nj} \right\} X$$

$$\left\{ 1 - \exp\left[- \frac{hc}{kT} (n_1 w_1 + n_2 w_2 + n_3 w_3) \right] \right\}$$

and

$$\xi(w, T) = \frac{hc|w-w_o|}{4kTB^*} \exp\left(\frac{-hc|w-w_o|^2}{4kTB^*} \right)$$

w_o is the band origin of the transition characterized by the n_i's; the w_i's are molecular constants taken from Herzberg (1945). The absorp-

tion due to the pure rotation band of H_2O was also considered but found to be negligible. The stellar radiation field was approximated by a black body. Thus, the net force acting on an H_2O molecule is given by

$$F_R = \frac{\pi}{c} \int_o^\infty k_\lambda B_\lambda (T) d\lambda$$

Using the sequence of models given by Auman (1969) and Goon and Auman (1970) and the relative concentration of H_2O given by Tsuji (1964), Table 5 was calculated. In this table, the radiation force, F_R, and the gravitational force, F_G, per gram and per molecule are compared for the sequence of models. An example of the radiation force per molecule in .1μ intervals for a temperature of 3000°K is given in Figure 11.

It might be thought that collisions with other molecules would rapidly smooth out any excess momentum transferred to the H_2O molecules via the radiation field. Michaud (1970) in a study of diffusion processes in peculiar A stars showed that this is not true: "A radiation force as large as a gravitational force causes diffusion through the same distance as the gravitational force, <u>independent</u> of t_c," where t_c is the time scale for a particle to transfer momentum received from the radiation field through collisions. What is crucial in judging the effects of radiation pressure on the H_2O molecule in late-type stars is convection and the turbulent velocity fields. While convection may be unimportant in the upper parts of the atmosphere, turbulence certainly is not. It is not at all obvious if these two effects will cancel out the action of the "negative gravity" field experienced

Fig. 11. - The radiation force per H_2O molecule in 0.1 micron intervals in cgs units is shown. Tsuji's (1966) analytic form of the absorption coefficient was used and the radiation field was taken to be that of a blackbody with $T_e = 3000^{\circ}K$.

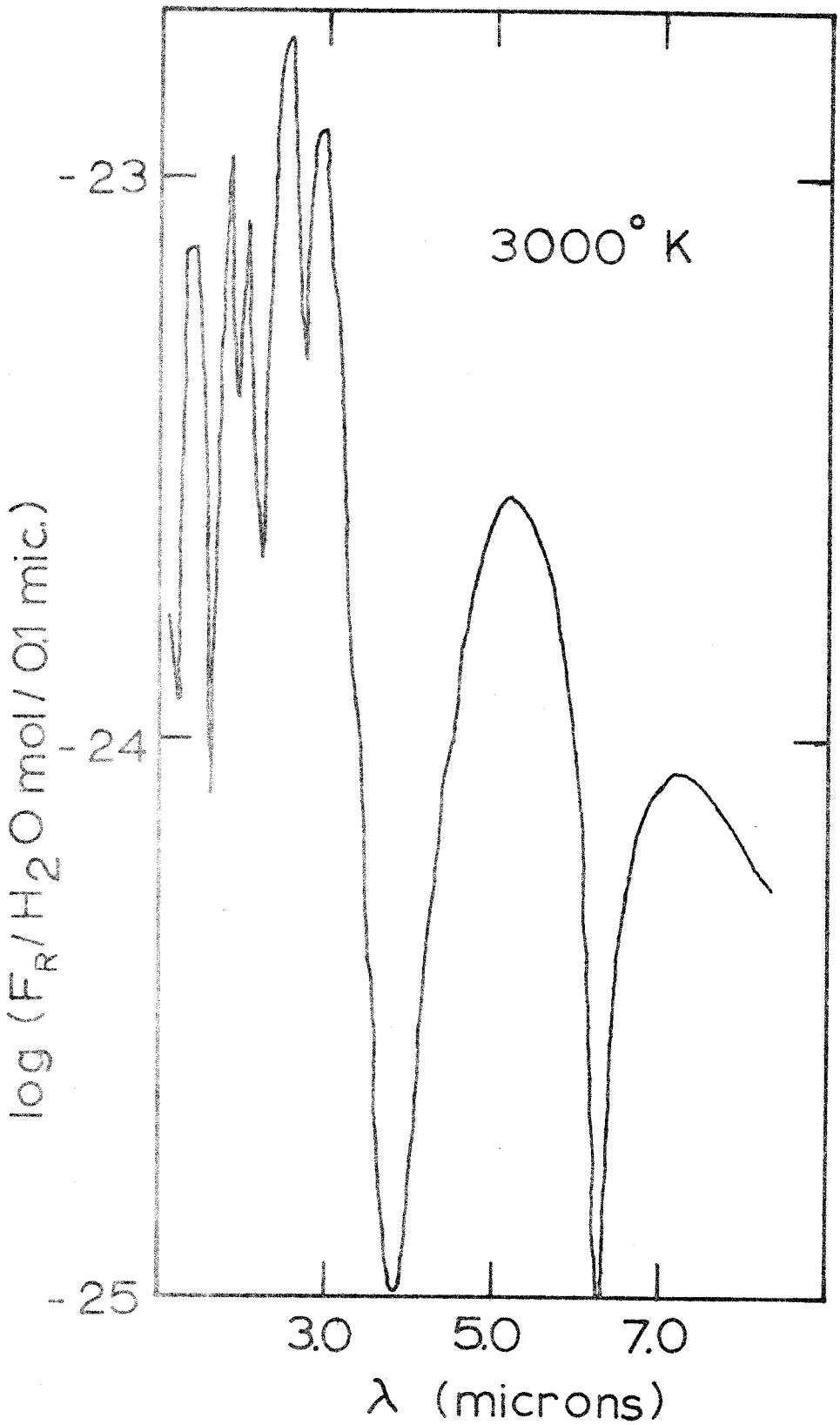

Figure 11.

TABLE 5

RADIATION PRESSURE CALCULATIONS

TEMPERATURE (°K)	F_R/mol.	F_G/mol.		log F_R/gm		log F_G/gm	
		giants	super-giants	giants	super-giants	giants	super-giants
4000	4.27×10^{-22}	3.0×10^{-21}	3.0×10^{-22}	-6.8	-8.1	2.0	1.0
3500	3.05	9.5×10^{-22}	9.5×10^{-23}	-5.3	-6.2	1.5	0.5
3000	2.06	3.0×10^{-22}	3.0×10^{-23}	-3.2	-4.4	1.0	0.0
2500	1.29	3.0×10^{-23}	3.0×10^{-24}	-2.7	-3.5	0.0	-1.0
2000	.71	3.0×10^{-24}	3.0×10^{-25}	-2.2	-3.1	-1.0	-2.0
1500	.31	(3.0×10^{-25})	(3.0×10^{-26})	(-2.0)	(-2.0)	(-2.0)	(-3.0)

by the water molecules. If the T = 2500°K model is considered, it is readily seen that a velocity of 10 km/sec is achieved in a time $t \approx 2 \times 10^5$ sec, which is short compared to the period of a typical Mira star, and over a distance of 8×10^{10} cm which is probably comparable to or smaller than the scale height of the lower atmosphere.

If radiation pressure acting on H_2O molecules is important, it will profoundly effect the distribution of these molecules. The scale height of the equilibrium distribution will be increased reducing the mean temperature for these molecules. This will cause model atmospheres to overestimate the importance of H_2O absorption and predict bands that are much stronger than observed. Also it will lead to increased selective loss of water molecules. This may be a contributing factor in those stars observed to have H_2O microwave emission. Finally, there may be coupling with the rest of the gas in the manner suggested by Gehrz and Woolf (1971) for dust grains. Table 5 indicates, however, that only for the extremely cool stars will the radiation force/gm of stellar material approach the gravitational force. This problem must be studied in more detail.

VI. DISCUSSION--ABUNDANCES AND EVOLUTION

Theories of stellar evolution make specific predictions as to the change in observed elemental abundances due to atomic burning and subsequent convective mixing. Observations of the abundances of H, C, N, O, and Li are important as they are relatively easy to make and should be considerably effected by the CNO cycle and helium burning. The evolutionary state and masses of the variable stars considered here and the giants and supergiants considered in Paper I are probably such that these two chains of reactions are the most important. This section will consider what bearing the observations reported here, in Paper I, and by other observers have on understanding the evolutionary history of late-type stars.

A. Work of Other Observers

Spinrad, et al (1966) and Spinrad and Vardya (1966) have combined observations of molecular band absorption from near infrared spectra and from Stratoscope II (Woolf, Schwarzchild, and Rose 1964) with model atmosphere calculations and arrive at values for relative number densities of $[O/C] \sim 1.05$, $[O/H] \sim 10^{-4}$-10^{-3}, and $[O/N] \sim 0.3$-3 for the M stars they considered. It is felt, however, that these results must be considered as being highly uncertain. The H_2O abundances for o Ceti and R Leo were determined by comparing the strengths of the stellar λ9400 and λ11000Å lines with the same lines due to terrestrial absorption and making corrections for temperature and saturation effects. The uncertainties introduced by assuming that molecular absorption features may be characterized by a unique set of physical parameters have been described elsewhere. The inability to confirm

the identification of H_2O in α Ori and ρ Per made by Woolf, et al (1964) in the Stratoscope II data has already been discussed in Paper I. Similar criticism's apply to the determinations of the CO abundance in M stars by Spinrad, et al (1966) and Spinrad and Vardya (1966). Finally the problems inherent in model atmosphere calculations have been summarized in this paper.

Goon and Auman (1970) and Auman (1970) have interpreted the discrepancy between the predicted and observed H_2O band strengths (Johnson, et al 1968), Johnson and Méndez 1970, Paper I) in late-type giants and supergiants as evidence for an O/C ratio close to unity. In addition, Spinrad, et al (1971) have been unable to find any H_2O lines in very high resolution 2μ spectra of α Ori. Auman (1970) has also interpreted the apparent difference in H_2O band strength between Miras and non-Miras reported here as being due to a lower O/C ratio in the former stars than the latter and attributed this ~~due~~ *to* differences in the amount of convective mixing that has occurred. Differences between observations and predictions of model atmospheres must be treated very carefully. In particular, although there may well be an abundance difference between late-type stars and the sun, it is by no means clear that this difference would entail a lower [O/C] ratio. In fact, differences in band strength between theory and observation could also be attributed to a general lowering of both O and C without reducing their ratio. Such an effect would be predicted from the equilibrium abundances of the CNO cycle and arguments in favor of this view will be presented below.

Schadee (1968) has shown abundances of oxygen-containing molecules become extremely sensitive to changes in the value of O/C when this quantity approaches unity. Abundance analysis of G and K giants by Greene (1969) and Conti, et al (1967) have been consistent with a solar or greater value for [O/C]. Thus it would be necessary to postulate some abrupt change in composition between K and M giants if Spinrad and Vardya's (1966) conclusions are correct. The continuous increase in observed CO band strength reported in Paper I would argue against any such abrupt change.

What is the evidence, if any, that would indicate that the stars considered here and in Paper I are highly evolved and should have surface abundances that would reflect some degree of mixing with CNO processed material? The remainder of this paper will be an attempt to answer this question.

Barbaro, et al (1966) have discussed evidence from old galactic and globular clusters which indicates that the long-period variables represent an extension of the giant branch of these clusters to higher luminosities ("giant branch" will refer to the steep, nearly vertical track that stars follow in a temperature-luminosity diagram immediately preceeding the onset of helium burning). From the main sequence turnoff point, ages of a few times 10^8 years and masses of 1-2 $M_\odot$ would be indicated for these stars, in agreement with masses derived from binary systems containing a long period variable. This is consistent with what would be expected from the velocity and space distribution of field long period variables with periods greater than 200 days as discussed by Feast (1963) and Smak (1966). Also, the lifetime

of these variables indicated by mass loss rates of 10^{-5} -10^{-6} $M_\odot$/ year is consistent with the evolutionary time scale for stars of a few solar masses at the tip of the red giant branch as discussed by Iben (1967, 1968).

Blanco (1964) has summarized the kinematical properties of the late-type giants. They appear to be similar to the Mira variables of long period, although there is some evidence that they are slightly younger. The G and K giants are also probably slightly more massive than the typical long period variable. The giants typically have masses of 3-4 $M_\odot$.

Inspection of the evolutionary lifetime diagrams calculated by Iben (1965, 1966) indicates that stars of 3 and 5 $M_\odot$ spend about 30 times as much time as a red giant <u>after</u> they leave the tip of the red giant branch (i.e. when they are evolving to the <u>left</u> in the HR diagram) then they do as a red giant <u>before</u> ascending to the giant tip (i.e. when they are evolving to the right). Cannon (1970), on the basis of a study of old galactic clusters, has inferred that a significant fraction of field red giants, in particular those around $M_V = 1$, $B - V = +1.0$, may have already gone up to the red giant tip and down and are now in the core helium burning stage. Unfortunately, evolutionary models do not predict the existence of giants much later than K0; these stars would all lie in the forbidden Hayashi region. Kippenhahn (1966) has pointed out that the theoretical position of the Hayashi line can be easily shifted to the right either by increasing the opacities or decreasing the mixing length in the stellar interiors. Such a change would not significantly alter the relative evolutionary lifetime calculated by Iben.

Iben's calculations predict the following for stars from 2.25 - 5 $M_{\odot}$. As the star begins to ascend the giant branch, a convective envelope begins to grow rapidly in depth. By the time the star reaches the tip of the red giant branch, the convective envelope includes about 80% of the mass and mixing with the material that has been processed through the CNO cycle occurs. The red giant tip marks the maximum extent of the convective envelope. As the star approaches the helium burning phase, the base of the convective zone recedes toward the surface. The abundances in this outer region remain fixed at the values reached at the tip of the red giant branch as the temperature and luminosity are too low for any significant nucleosynthesis to occur during the entire phase of helium burning. In particular, the surface abundances will be unaffected by what goes on in the core. Faulkner (1966) has also argued against mixing of material from the helium burning core with material of the envelope. Since the amount of CNO processed material that is mixed with the hydrogen rich envelope is only a fraction of the total amount of material in the envelope, the resulting envelope abundances will be intermediate between the initial main sequence values and the values that obtain when the CNO cycle is in equilibrium. The surface value of $[N^{14}/C^{12}]$ is increased by a factor of 3 over the main-sequence value, $[O^{16}/C^{12}]$ is increased by about 1.5, and $[N^{14}/O^{16}]$ by about 2. If $[C^{13}/C^{12}]$ is initially 0, it will become 1/27 (Iben 1966). From these models there is no way to reduce the value of [O/C] to ≈ 1. The temperature at which the CNO process takes place has to be $>40 \times 10^6$ °K, to get the equilibrium abundances of the CNO cycle such that [O/C] < 1. To get this value

in the surface abundance, it would be necessary to expel most of the hydrogen rich envelope. There is the possibility, of course, that stars which are massive enough to get an $[O/C] \approx 1$, lose a large quantity of mass, slowing down their rate of evolution and causing them to appear as less massive giants. It would be unlikely, though, that a large number of stars should be of just the right mass to have a resulting CNO equilibrium abundance such that $[O/C] \approx 1$.

Observations of Li depletion in late-type giants (Wallerstein 1966, Merchant 1967) provide further evidence for the interpretation of these stars as having already descended from the tip of the giant branch. Wallerstein notes that the lithium content of the G giants he looked at is significantly lower (nearly a factor of 100) than that of the F giants. This is in agreement with the consequences of Iben's (1965) conclusion that the G giants have been extensively mixed. The results of Bonsack (discussed by Iben) also indicate a very low lithium abundance in G and K giants. Merchant (1967) discusses her observations of lithium together with all other past observations and concludes that the general trend of decreasing lithium abundance with advancing spectral type is consistent with an increasing degree of convective dilution as a star evolves to the right in an HR diagram. She adds that it may be possible to associate the stars with the lowest lithium abundance with evolution to the left in the HR diagram and to attribute the spread in abundance at a given spectral type to a spread in the masses and previous histories of the stars. On the basis of the evolutionary lifetime quoted early, however, it would be expected that the majority of the giants should be evolving toward the left. Inspec-

tion of her Figure 8 indicates that the M giants may have significantly higher lithium abundances than some of the latest K giants.

A final clue concerning the evolutionary state of the red giants is the detailed abundance analysis by Greene (1969) of four K giants. He concluded that the HCNO abundances were consistent with cycling of some stellar material through the CNO cycle and subsequent mixing with surface material. The results of an analysis of K giants by Conti, et al (1967) are, on the other hand, ambiguous: some of their stars do seem to have anomalous abundances when compared with the color values.

B. Results of the Present Investigation

It is useful at this point to summarize the relevant observational results:

The absorption due to CO increases with advancing spectral type among the non variable giants. The supergiants tend to show greater absorption than the giants although there is some overlap, especially among the later types. The scatter in band strength at a given spectral type is real. There is no evidence for water absorption in the 1.87μ band except for stars of type M6 and later. When considered as a function of visually determined spectral type, the strength of this water band in the long period variables of apparently normal composition is significantly greater than in the non-variable giants. Values for the CO absorption when considered at the time of maximum visual light seem to be consistent with the non-variable giants, but values at the time of maximum CO absorption seem to be systematically greater

in the variables than the non-variables. The differences in the case of the CO bands are small. The weakness of the CO bands in the Mira and their relatively great strength in the MS-type stars is quite clear, though. The approximations and assumptions that have gone into estimating the $[C^{12}/C^{13}]$ ratio have already been discussed. Keeping these in mind, it may be tentatively concluded that this ratio remains relatively constant for all of the non-variable giants. It is probably the same in the supergiants as in the giants and may be higher in the variables than in the giants. But for all three classes of stars the $[C^{12}/C^{13}]$ ratio is certainly considerably lower than the solar value.

If all of the above results are correct, it is then interesting to speculate on the following interpretation of them. If the stars started their evolutionary history with a solar value of $[C^{12}/C^{13}]$, then, in the absence of any surface spallation reactions, the existence of a value considerably less than solar means that the original surface material has been mixed to some degree with material which has been processed through the CNO cycle. The relative constancy of this value in the non-variable giants may be an indication of the relative uniformity with which this mixing has taken place in all of these stars. A higher value of $[C^{12}/C^{13}]$ in the variables would be consistent with their location on the tip of the giant branch (Barbaro 1966) where, presumably mixing is not yet complete. The value found here, by Johnson and Méndez (1970) for $[C^{12}/C^{13}]$ based on the CO bands is considerably lower than the value suggested by Iben (1966). This may be due entirely to uncertainties in interpreting the relative strengths of the $C^{12}O^{16}$ and $C^{13}O^{16}$ features. The difference is not felt to be significant.

Greene (1970) has pointed out the large discrepancy between the value determined from the CO features and that determined from CN features.

Stronger CO and H_2O absorption in the variables would also be expected on account of incomplete mixing since [C] plus [O] will be greater although the ratio [C/O] may be similar. (The author first heard the suggestion that the degree of mixing may be greater in variables from Auman [1970].)

If, in fact, the giants are all uniformly mixed, then the trend of increasing CO absorption with advancing spectral type could be attributable to effects discussed earlier in this paper and Paper I. The supergiants with shorter lifetimes, also have a relatively higher probability of being found on different parts of their evolutionary tracks where, presumably, differing degrees of mixing will have influenced their surface abundances, thus accounting for the much larger range of absorption strengths. Wallerstein (1966) has suggested that if enough G and K giants are surveyed for lithium, about 5% of them should be found with strong lithium as these will be evolving to the right in the HR diagram. A similar test should be possible with regard to CO strength. Auman (1970) has suggested that perhaps the presence of enriched helium envelopes in the late-type non-variable giants cause them to be non-variable. Keeley (1970) has shown that it is the hydrogen ionization zone in a star that induces pulsational instability. Finally, it should be pointed out that the differences in band strengths between variables and non-variables may be due to effects associated with the pulsation phenomena alone.

In summary, Iben's evolutionary models for stars of a few solar masses predict that most late-type giants should be in the helium burning phase and should have undergone a certain degree of mixing. This mixing predicts increased [0/C] and $[C^{13}/C^{12}]$ ratios and decreased surface lithium, carbon, and oxygen abundances. Detailed abundance analysis of field giants tend to support this picture as do observations of giants in old clusters. Although these theoretical models cannot predict giants cooler than 4000°K, this does not seem to be a serious difficulty. There is evidence that the long period variables represent an extension of the red giant tip. The infrared spectra presented here and in Paper I can, with caution be interpreted as supporting this picture and in particular are suggestive of abundance differences between the variables and non-variables. There is, however, a general lack of understanding of very cool atmospheres and, in particular, the role played by dynamic phenomena. The evidence now seems to be quite strong that it is necessary to consider abundances which depart sharply from the traditional solar ones due to a certain admixture of material which has undergone at least hydrogen burning.

APPENDIX

Figs. 12 - 28. - This series of figures presents the data used in this paper. The H_2O and CO band strengths are measured by the quantities WV and W(CO) respectively. The flux at 2.25μ is measured by log f(225). WV, W(CO), and f(225) have been defined in the text. Also indicated are the times of visual maximum (M) and minimum (m). As an aid in associating the spectra which will be presented with these figures, 1969 January 1 was JD 2440222 and 1970 January 1 was JD 2440587.

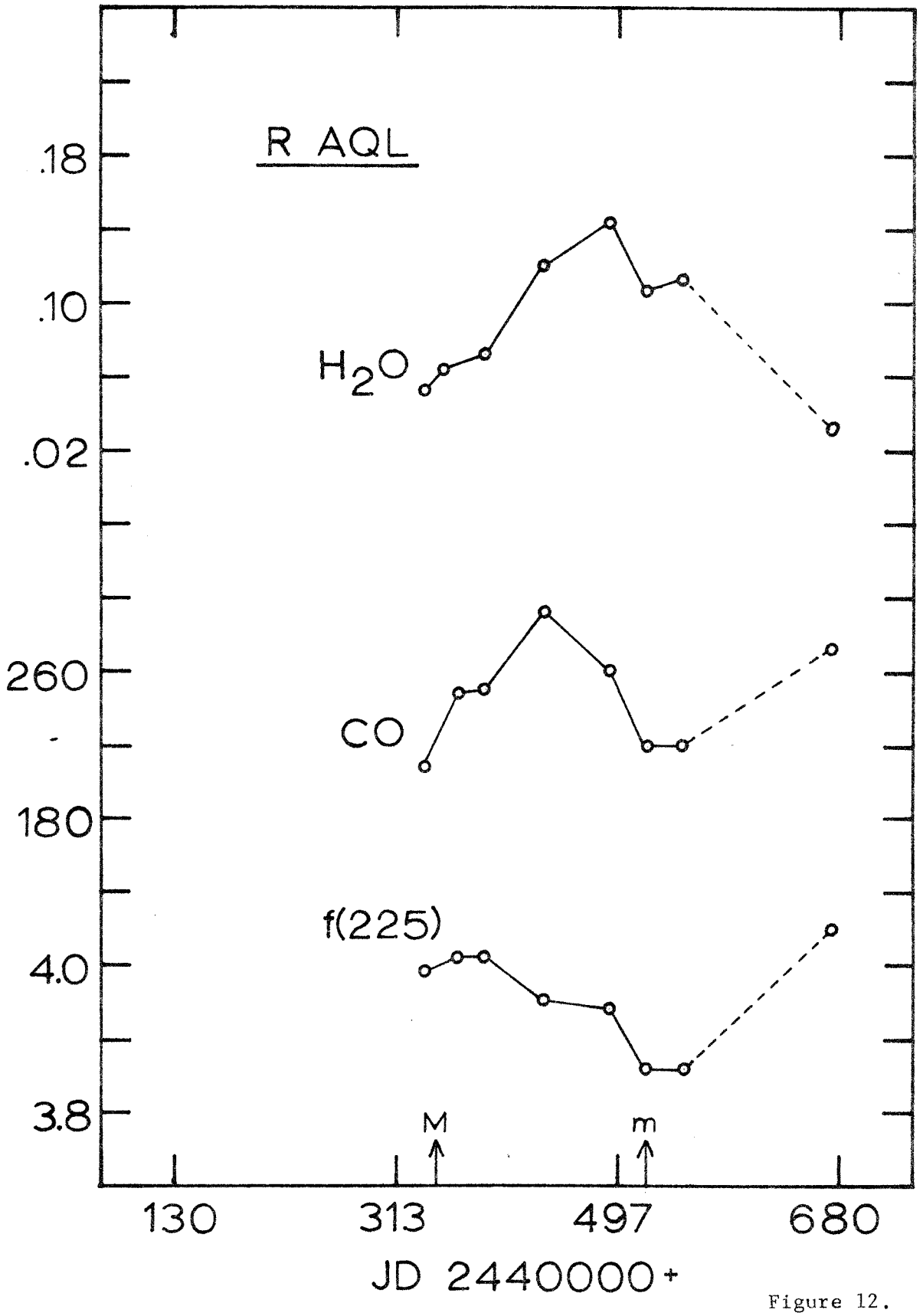
R AQL
.18
.10
.02
H_2O
260
CO
180
f(225)
4.0
3.8
M
m
130
313
497
680
JD 2440000+

Figure 12.

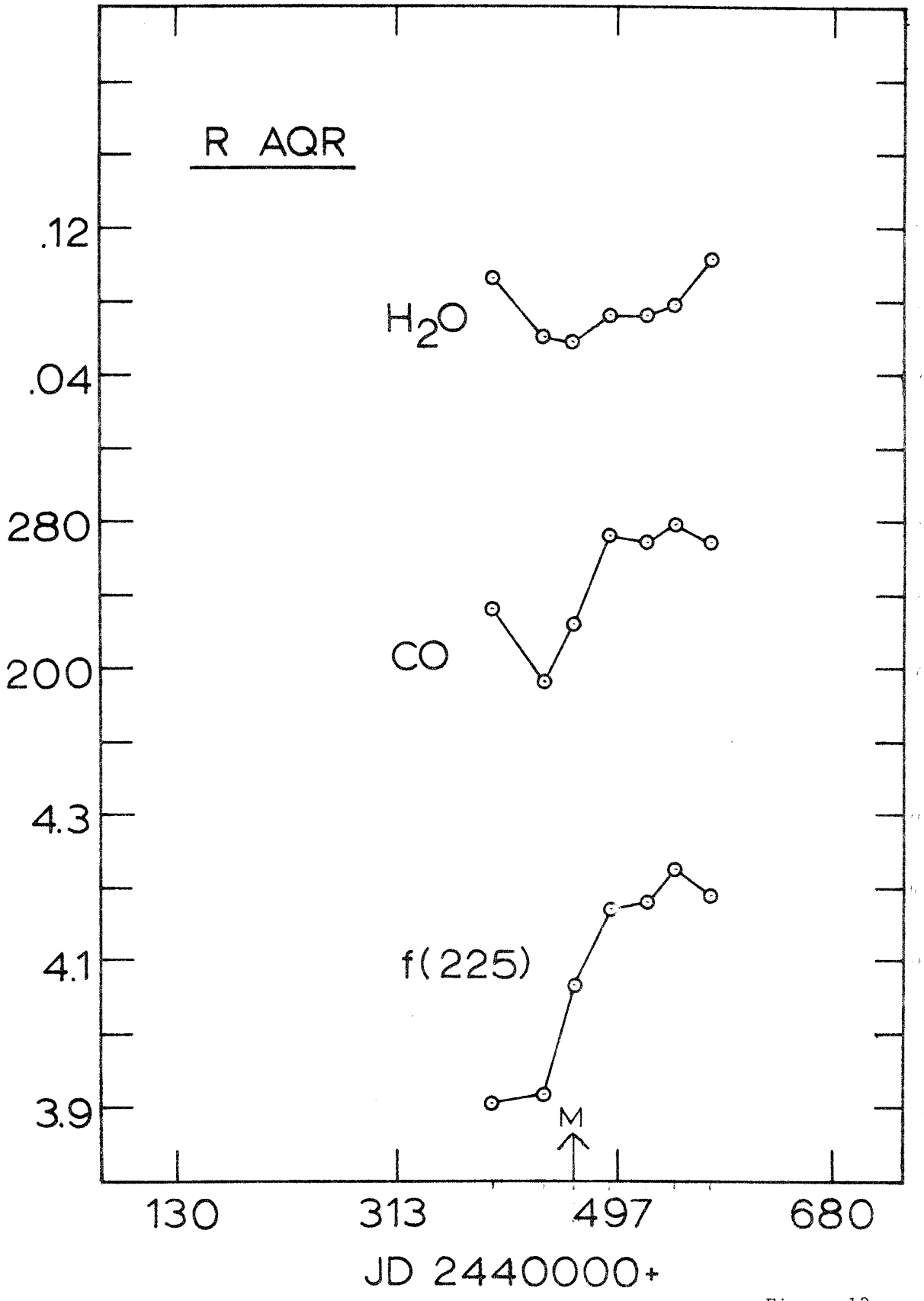
R AQR
.12
.04
H2O
280
200
CO
4.3
4.1
f(225)
3.9
M
130
313
497
680
JD 2440000+

Figure 13.

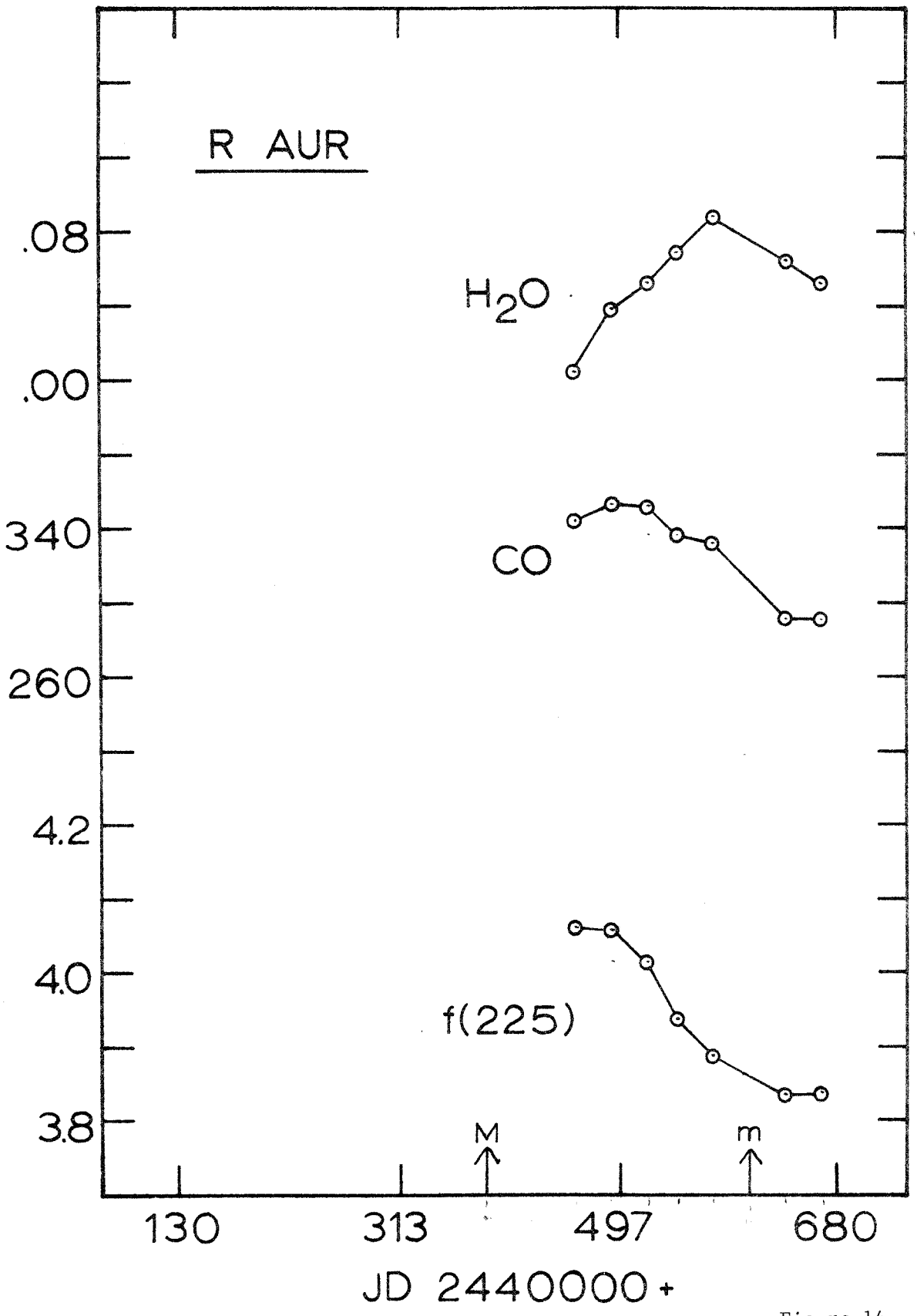
R AUR
.08
.00
340
260
4.2
4.0
3.8
H2O
CO
f(225)
M
m
130
313
497
680
JD 2440000+

Figure 14.

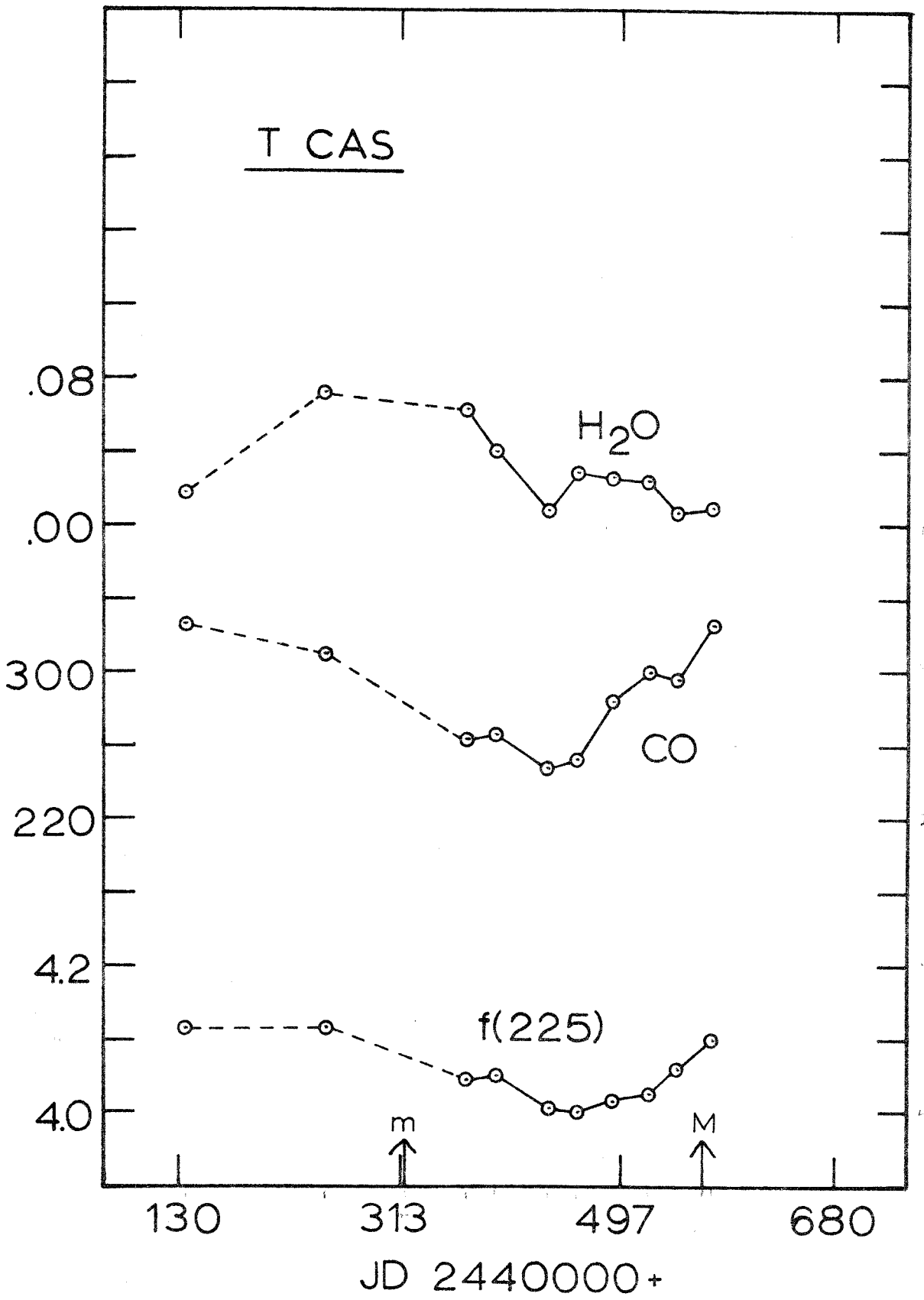
T CAS
.08
.00
300
220
4.2
4.0
H_2O
CO
f(225)
m
M
130
313
497
680
JD 2440000+

Figure 15.

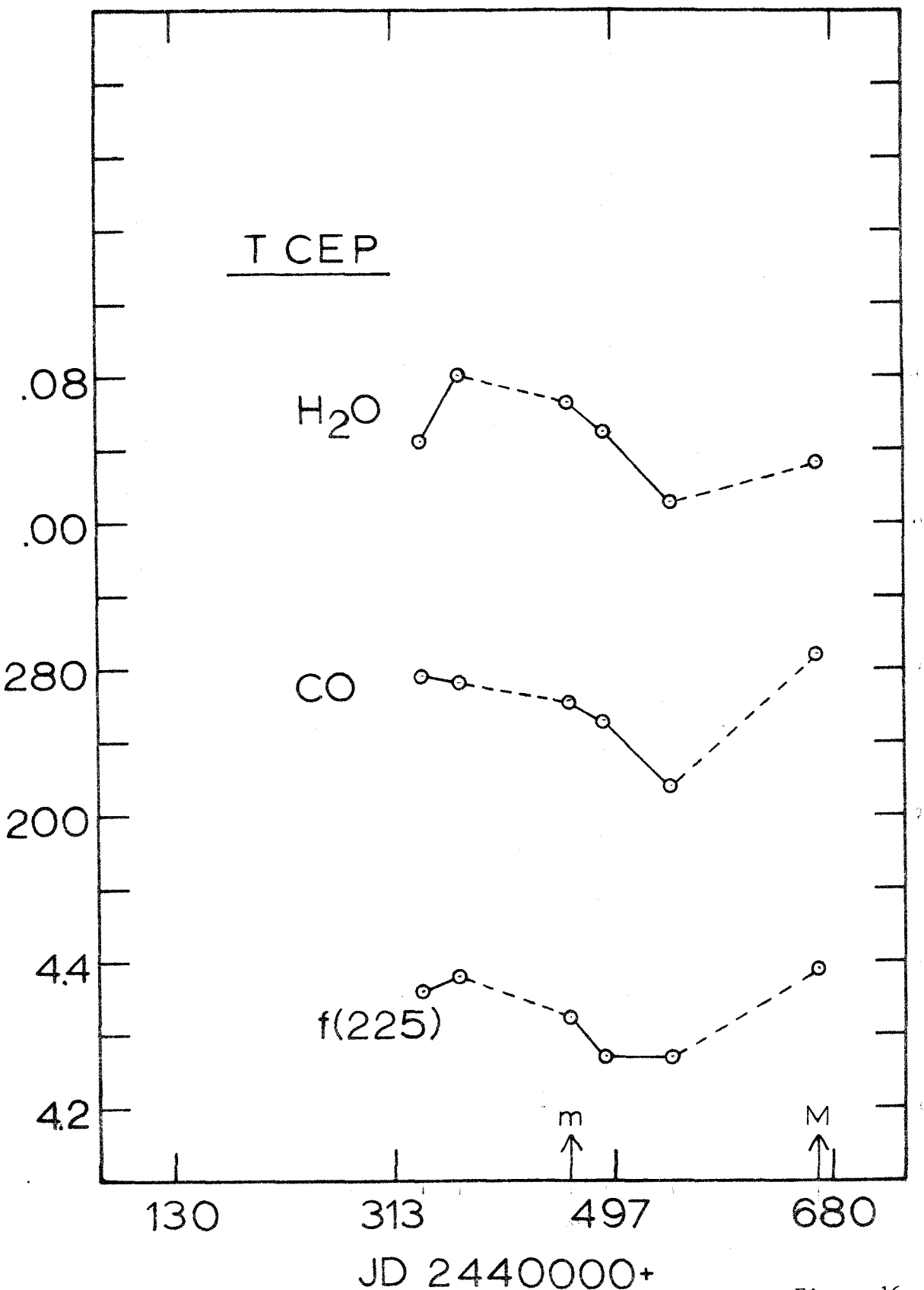
T CEP
.08
.00
280
200
4.4
4.2
H_2O
CO
f(225)
m
M
130
313
497
680
JD 2440000+

Figure 16.

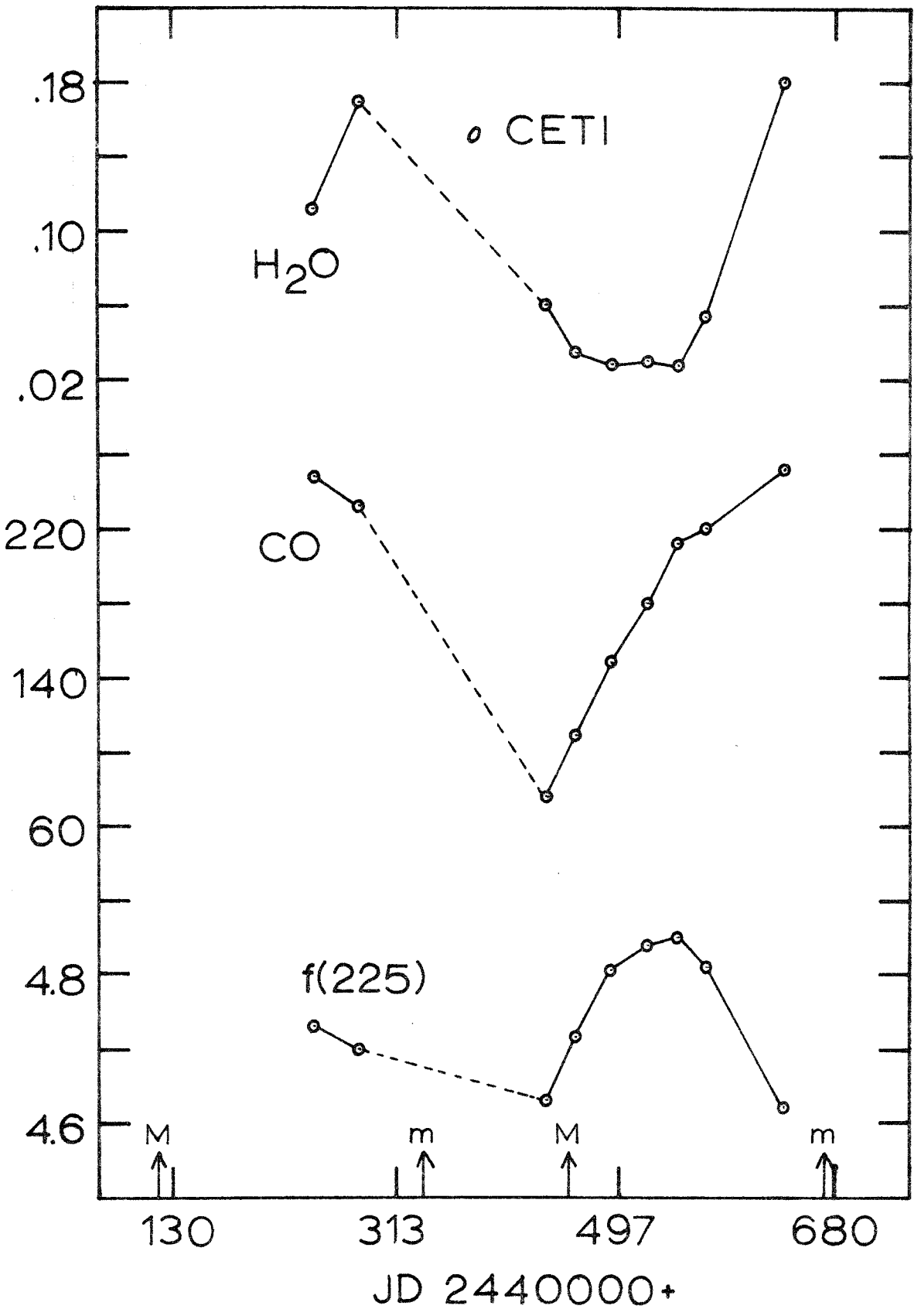
.18
.10
.02
220
140
60
4.8
4.6
o CETI
H2O
CO
f(225)
M
m
M
m
130
313
497
680
JD 2440000+

Figure 17.

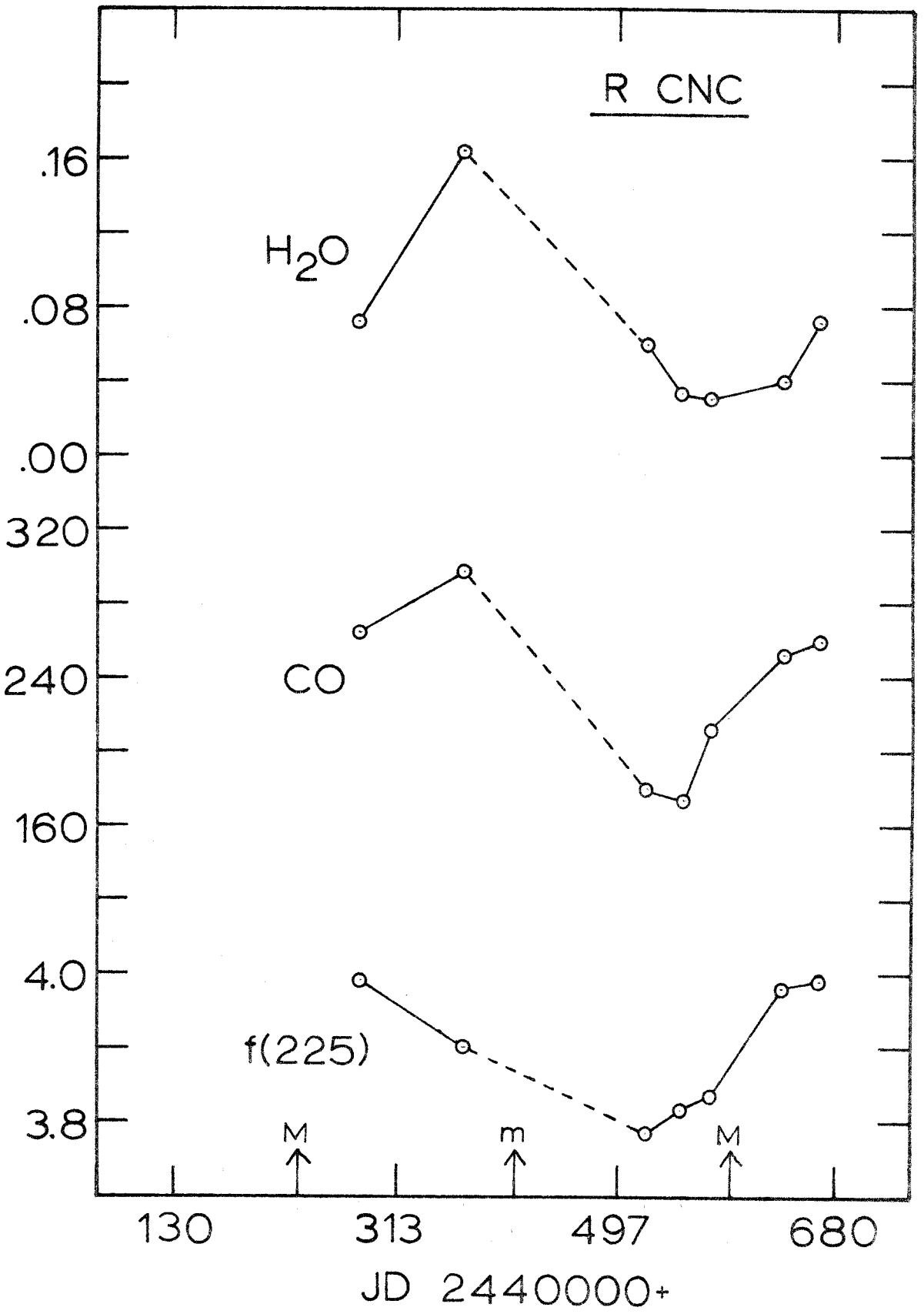
R CNC
.16
H_2O
.08
.00
320
CO
240
160
4.0
f(225)
3.8
M
m
M
130
313
497
680
JD 2440000+

Figure 18.

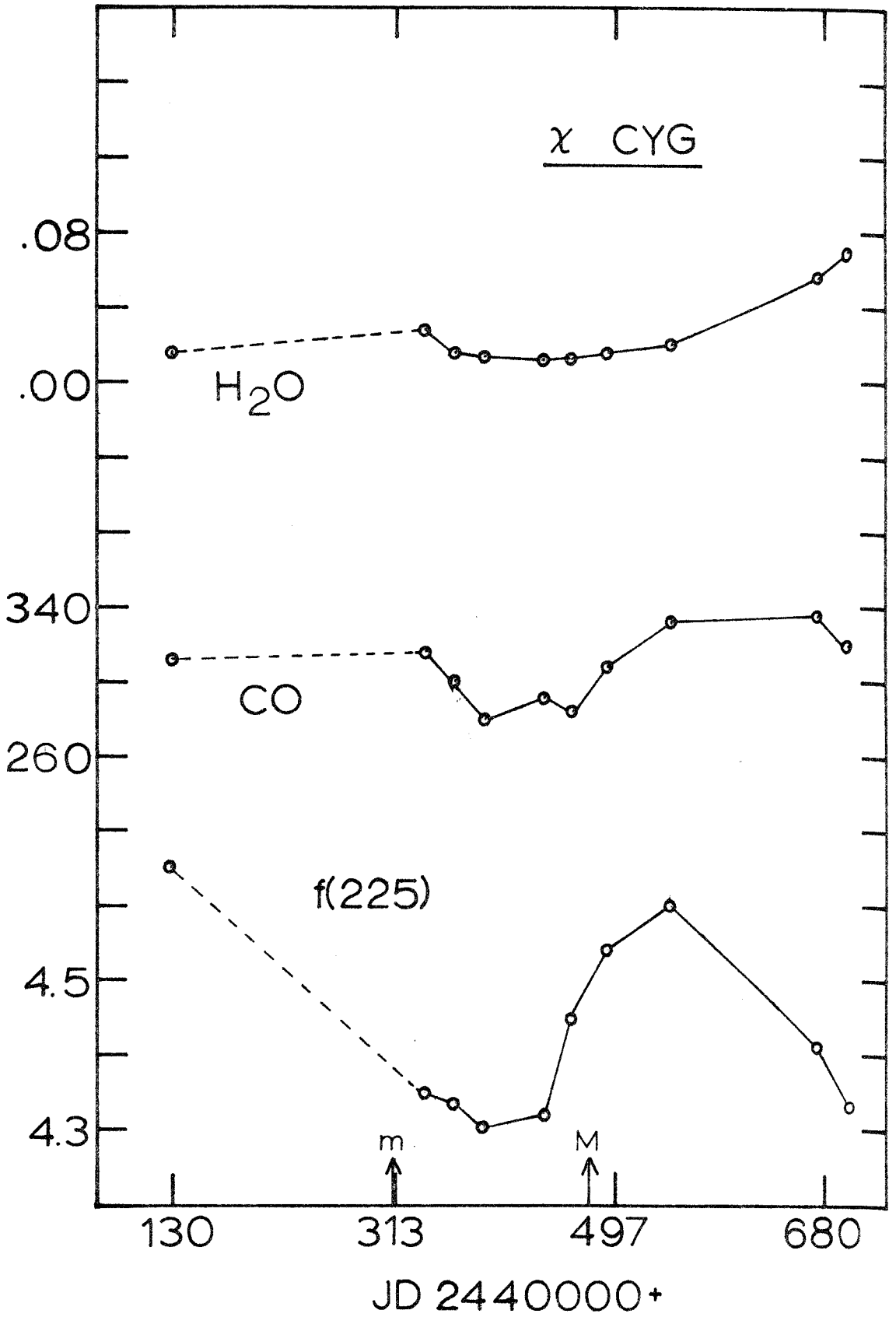
χ CYG
.08
.00
H2O
340
CO
260
f(225)
4.5
4.3
m
M
130
313
497
680
JD 2440000+

Figure 19.

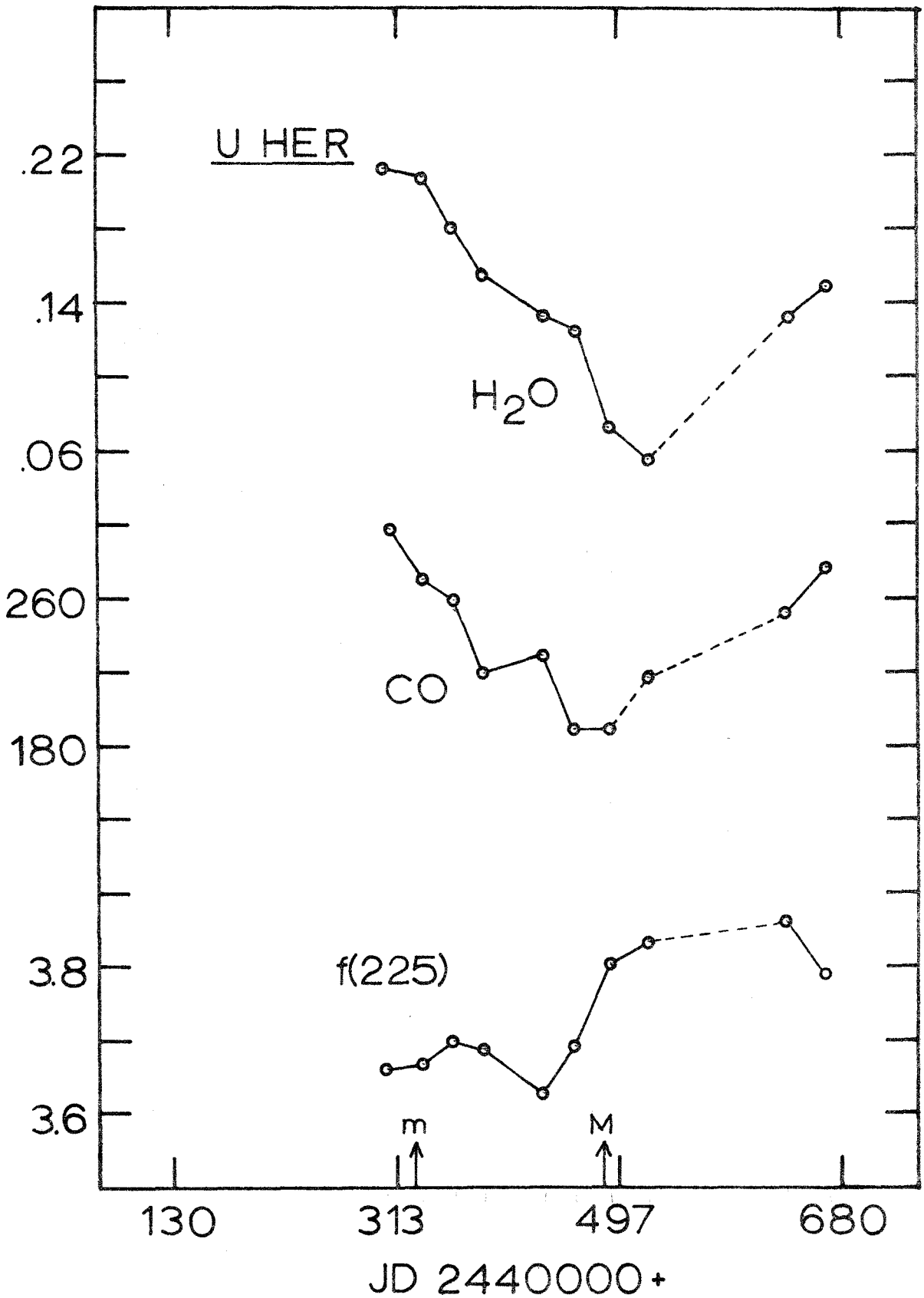
U HER
.22
.14
.06
H_2O
260
180
CO
3.8
3.6
f(225)
m
M
130
313
497
680
JD 2440000+

Figure 20.

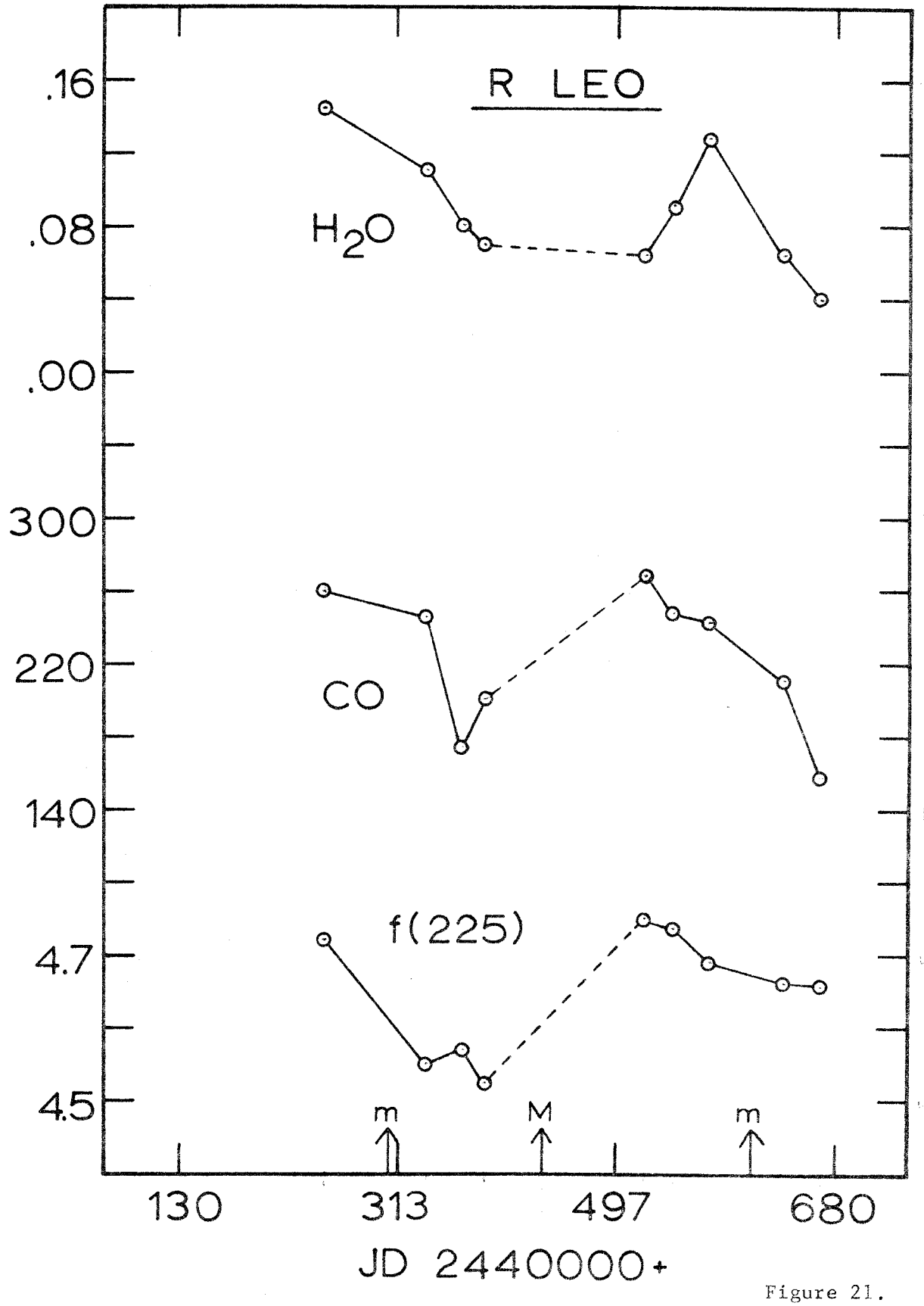
R LEO
.16
.08
.00
H_2O
300
220
140
CO
4.7
4.5
f(225)
m
M
m
130
313
497
680
JD 2440000+

Figure 21.

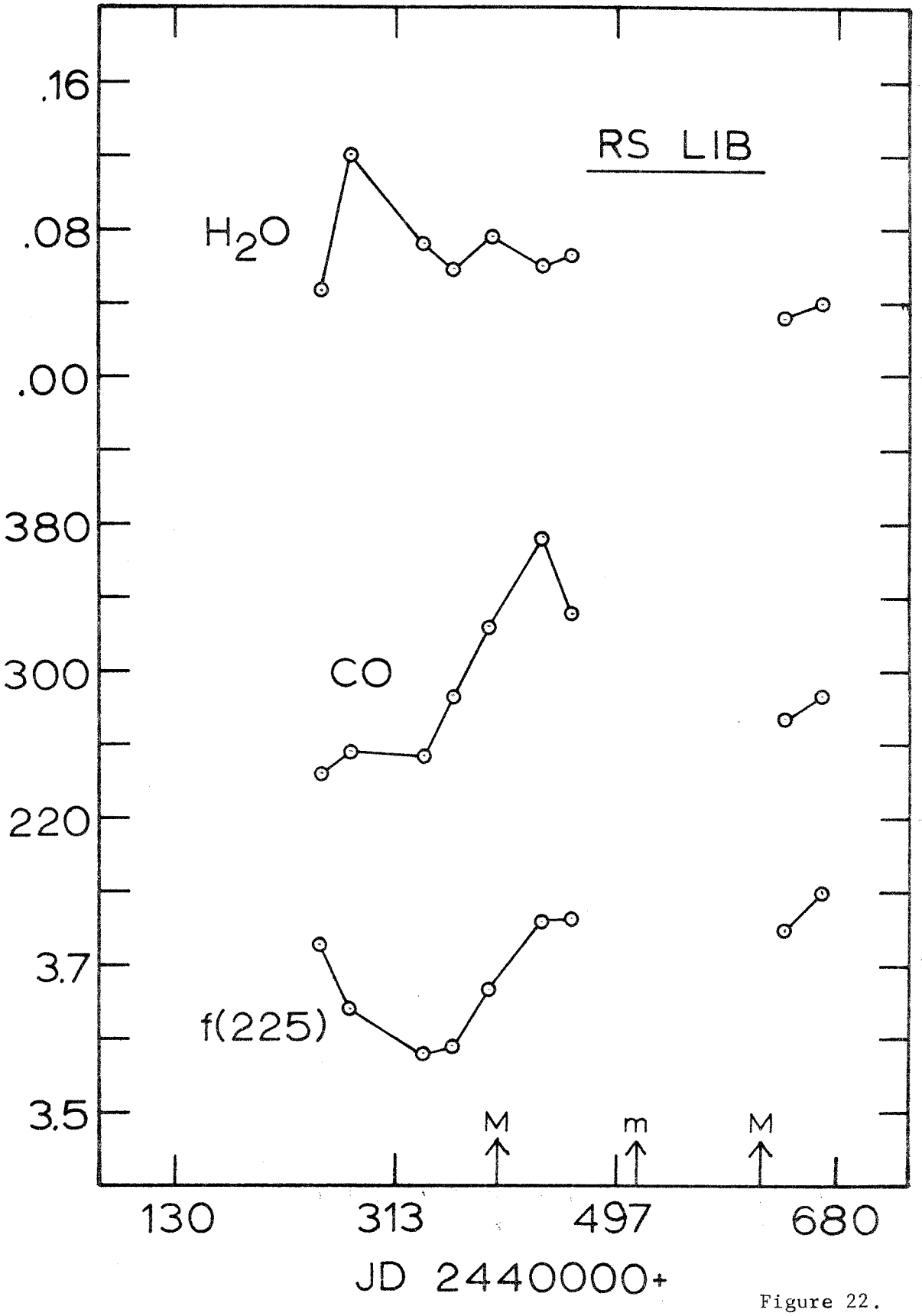
RS LIB
H2O
CO
f(225)
.16
.08
.00
380
300
220
3.7
3.5
M
m
M
130
313
497
680
JD 2440000+

Figure 22.

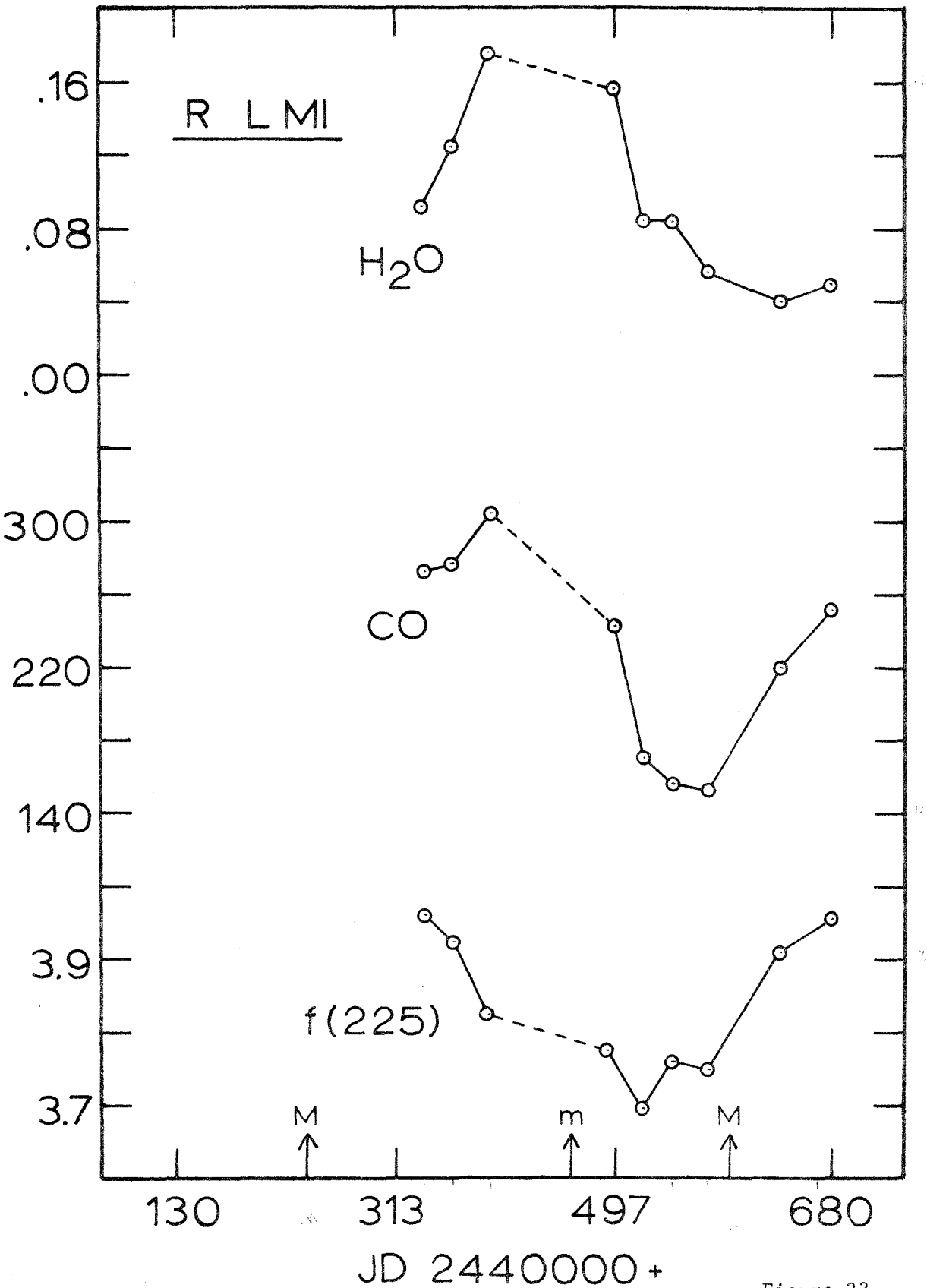
R LMI
.16
.08
.00
H_2O
300
220
140
CO
3.9
3.7
f(225)
M
m
M
130
313
497
680
JD 2440000+

Figure 23.

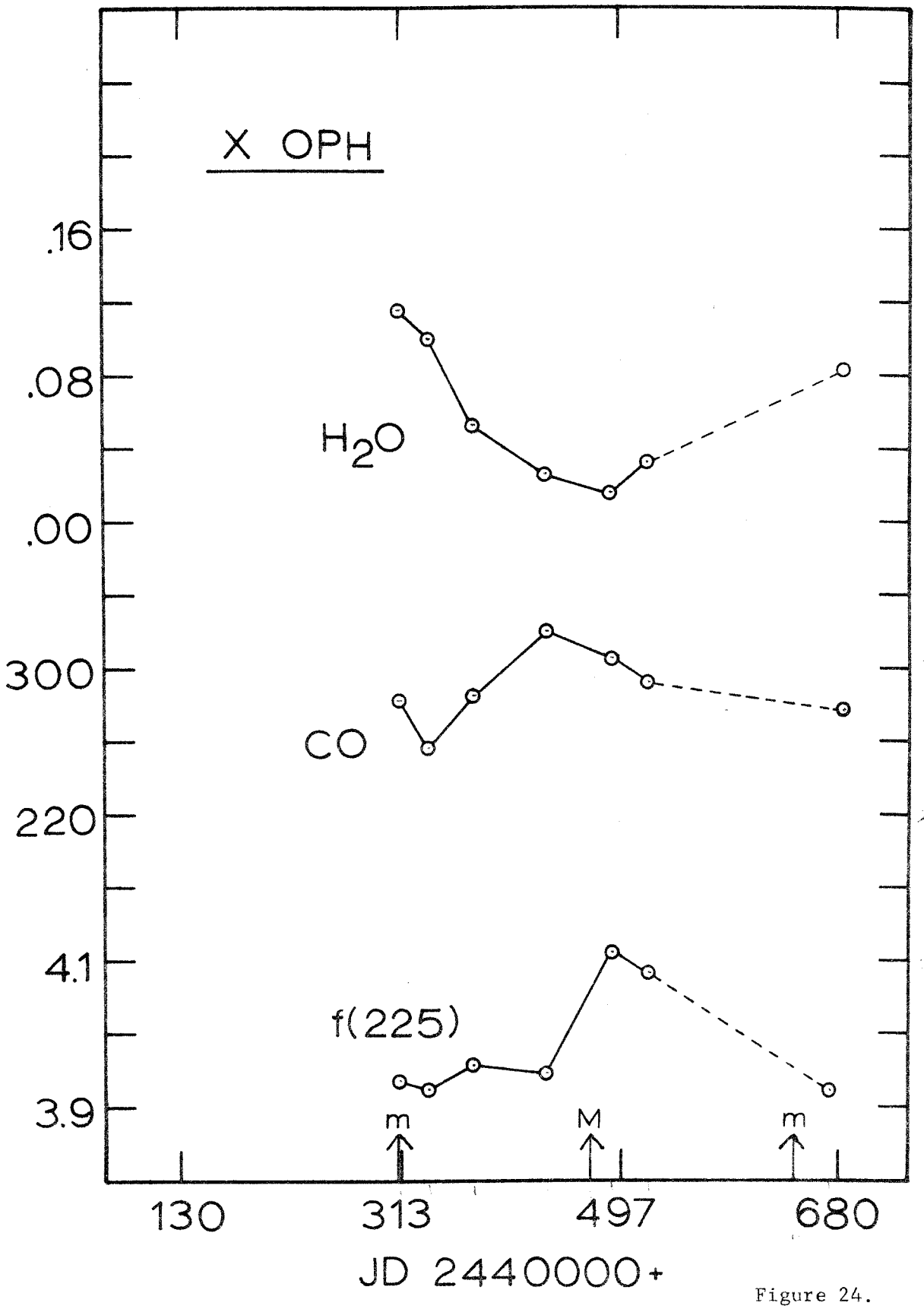
X OPH
.16
.08
.00
300
220
4.1
3.9
H2O
CO
f(225)
m
M
m
130
313
497
680
JD 2440000+

Figure 24.

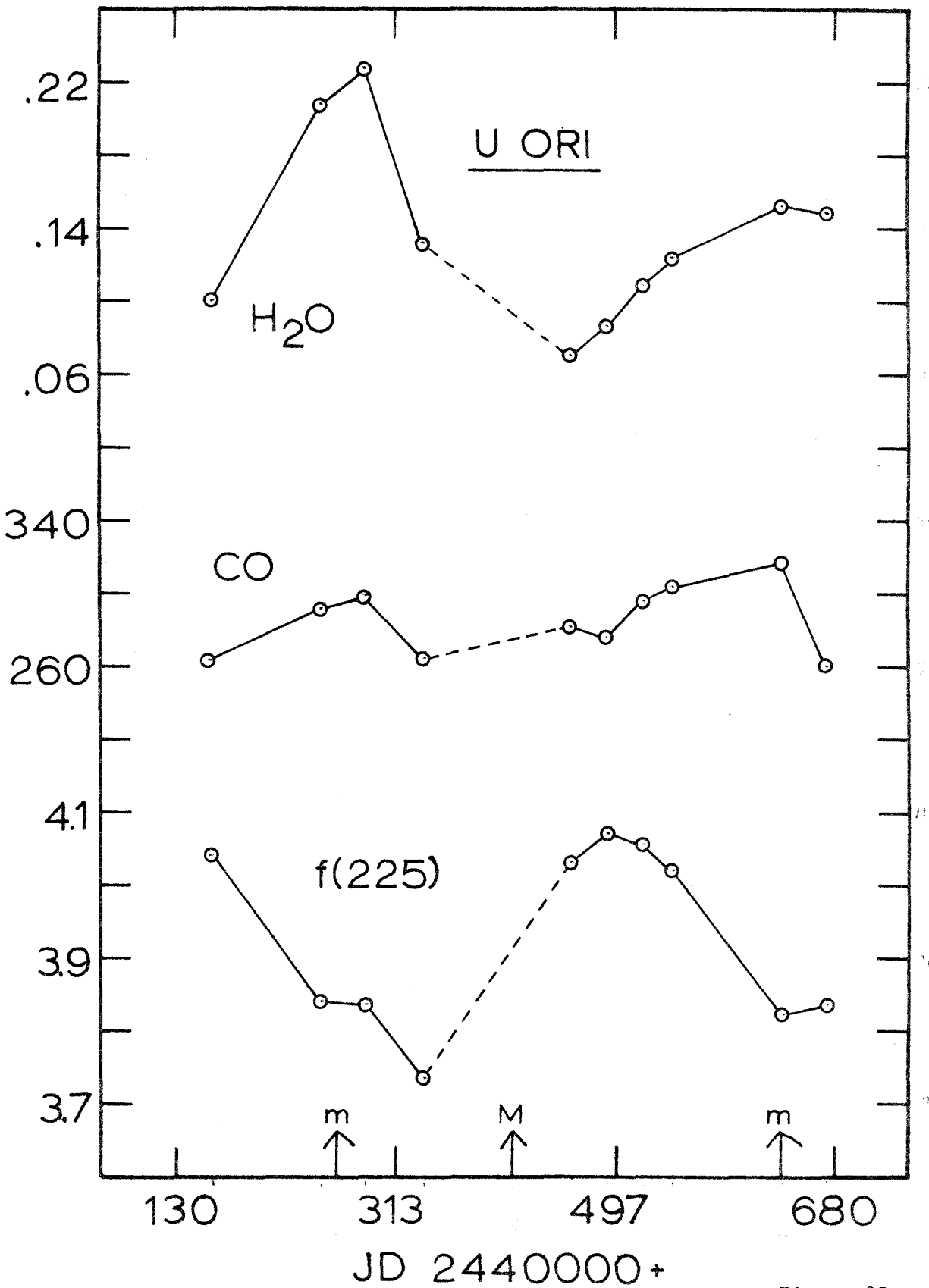
U ORI
H2O
CO
f(225)
.22
.14
.06
340
260
4.1
3.9
3.7
m
M
m
130
313
497
680
JD 2440000+

Figure 25.

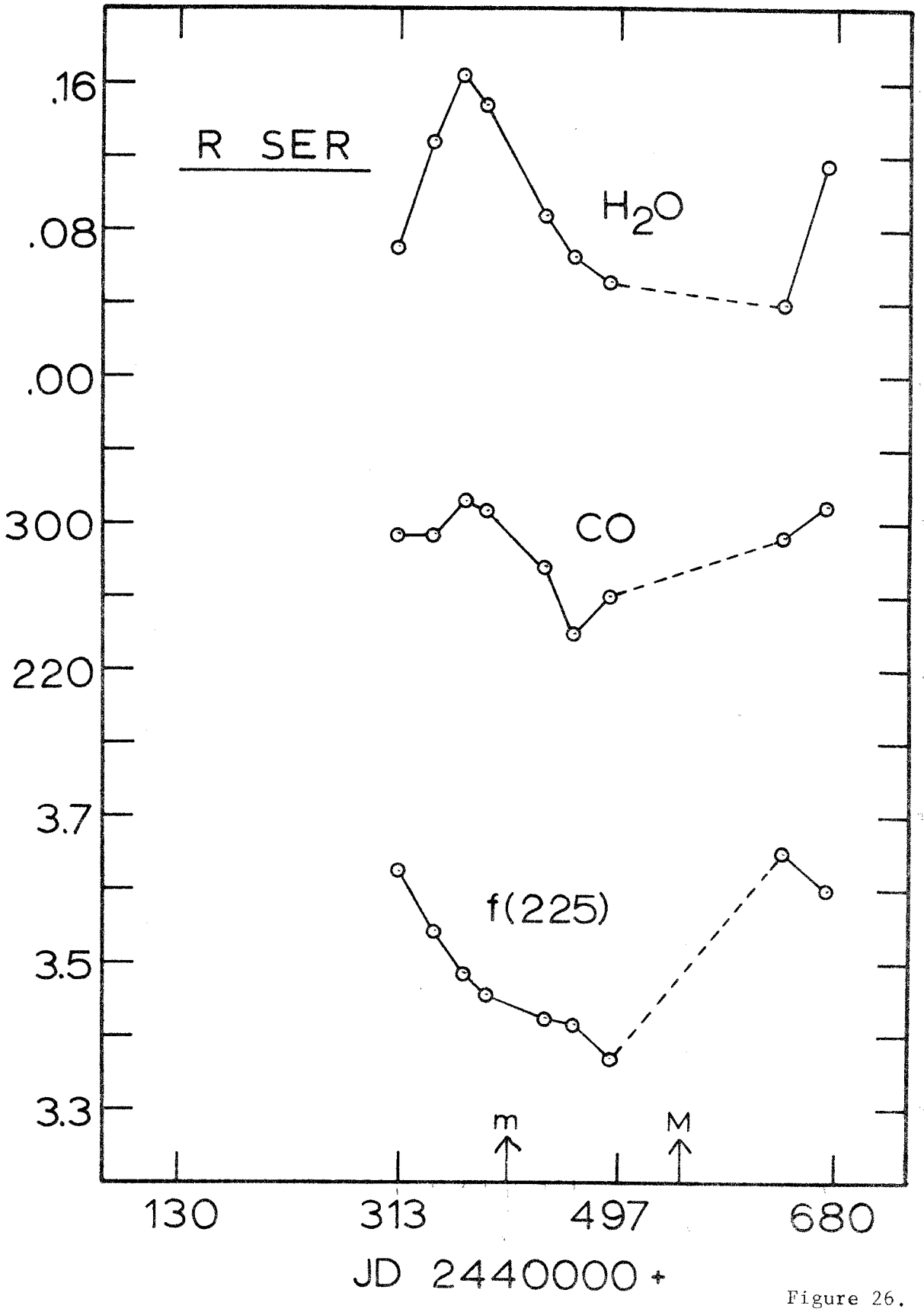
.16
.08
.00
300
220
3.7
3.5
3.3
R SER
H2O
CO
f(225)
m
M
130
313
497
680
JD 2440000 +

Figure 26.

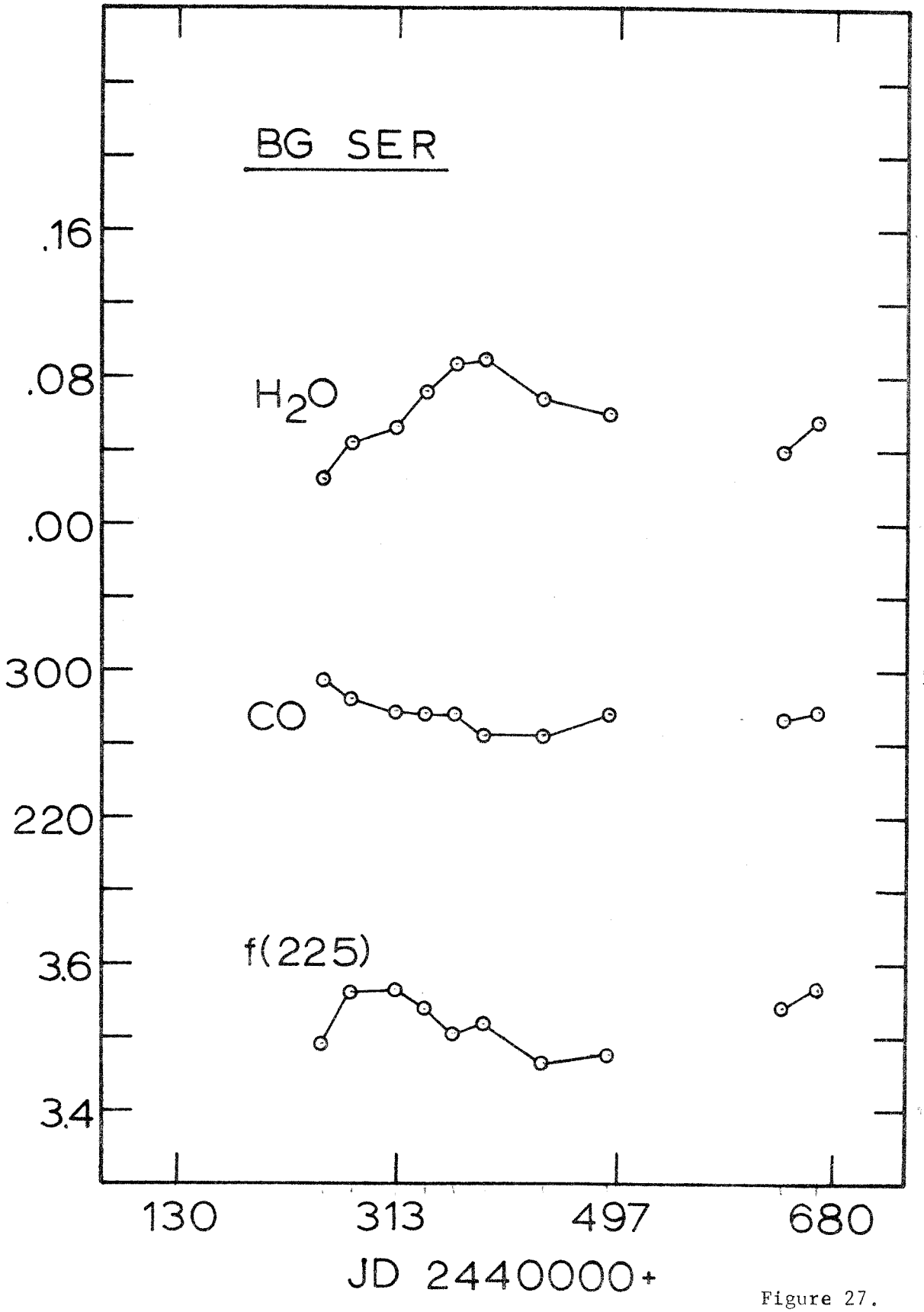
BG SER
.16
.08
.00
300
220
3.6
3.4
H2O
CO
f(225)
130
313
497
680
JD 2440000+

Figure 27.

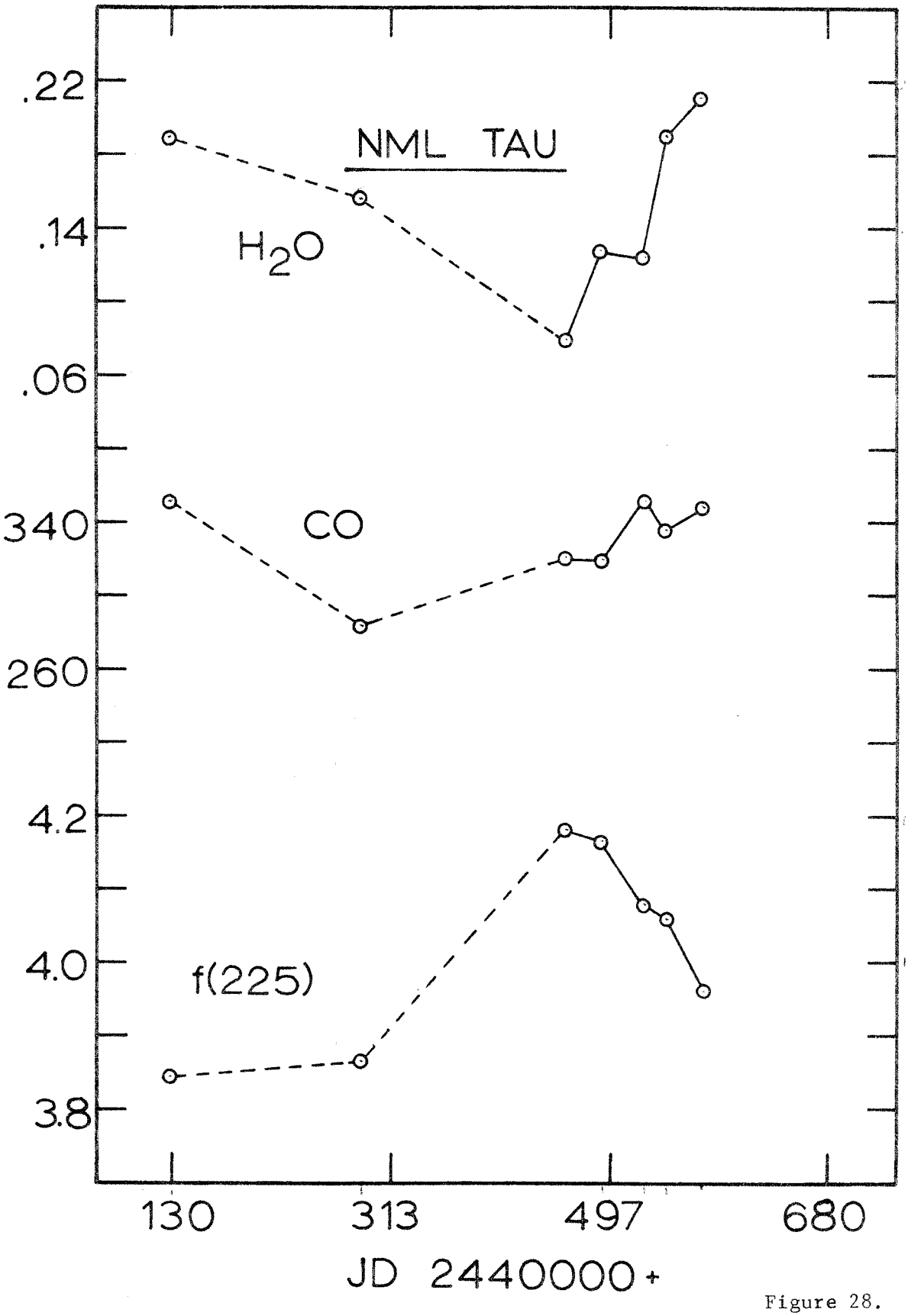
.22
.14
.06
NML TAU
H2O
340
260
CO
4.2
4.0
f(225)
3.8
130
313
497
680
JD 2440000+

Figure 28.

The following series of spectra have been selected to illustrate several of the points made in the text. The legend on the bottom of each gives, in order, the name of the star, the date, the telescope, wavelength, the slit size, and the amplifier gain. The rest is irrelevant for the present purpose. In particular, note the following comparisons: RT Vir with χ Cyg on 27 April 1969; χ Cyg in November and June 1969 which are times of maximum f(225), W(CO) and minimum f, W respectively; U Ori, November 1969, NML Tau, September 1969 and W And, the first two being close to and at f(225) maximum respectively; U Ori, March 1969, September 1969, and NML Tau, December 1969, the first being at maximum WV, the second at maximum f(225) and minimum WV, the third being near maximum WV and W(CO); R Cnc, May and December 1969, maximum and minimum WV respectively; the MS stars R Aur and T Cas at maximum W(CO) and RS Lib at an intermediate value of W(CO). Finally, there is the complete series of spectra obtained for o Ceti, Mira.

Fig. 29. - A series of spectra of U Her with the phase with respect to visual maximum indicated. The left hand scale is designed to show the changing brightness. The units are log F_λ(W/cm^2/micron) + C where C = 17.00.

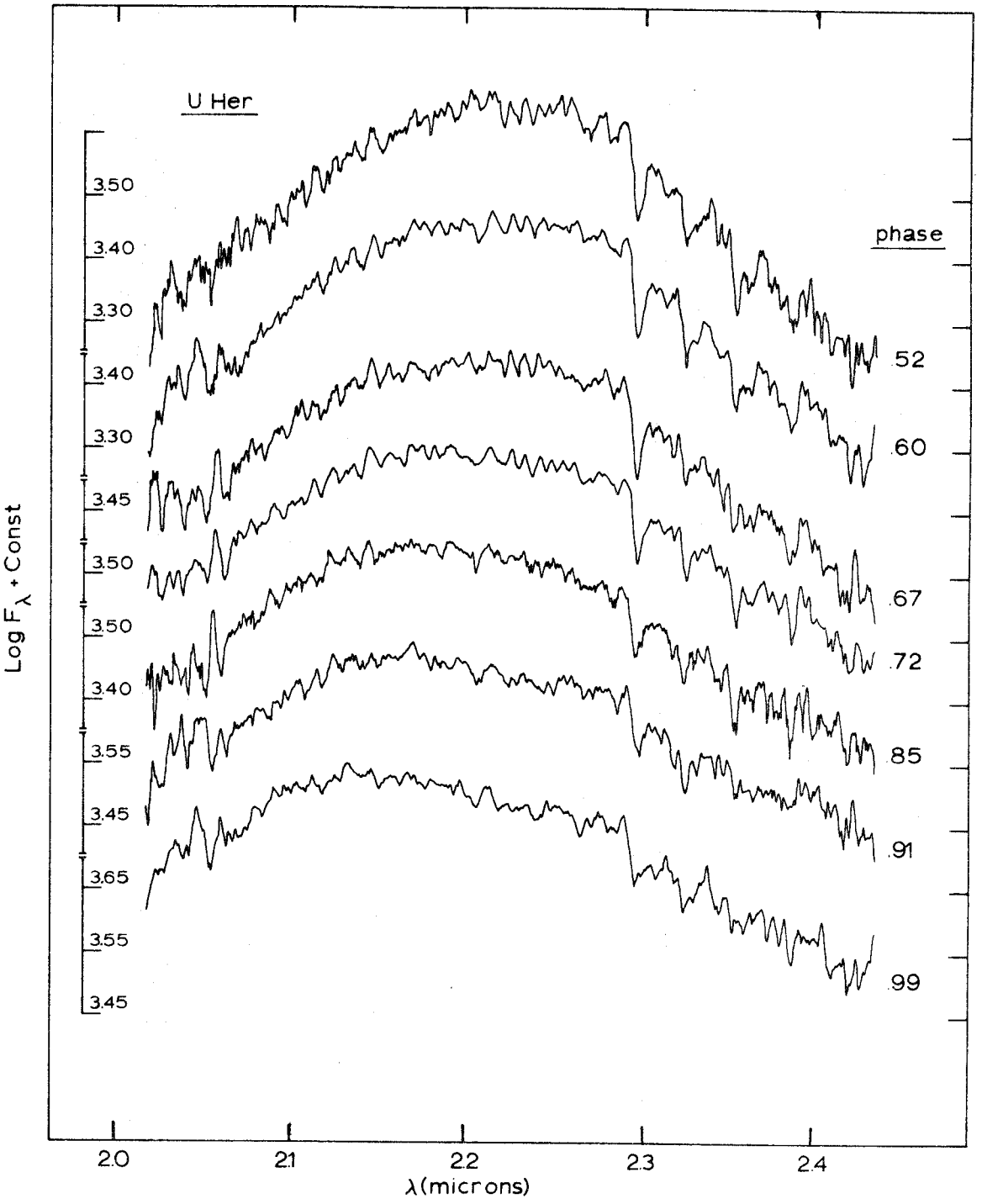
U Her
3.50
3.40
3.30
3.40
3.30
3.45
3.50
3.50
3.40
3.55
3.45
3.65
3.55
3.45
phase
.52
.60
.67
.72
.85
.91
.99
Log F_λ + Const
2.0
2.1
2.2
2.3
2.4
λ(microns)

Figure 29.

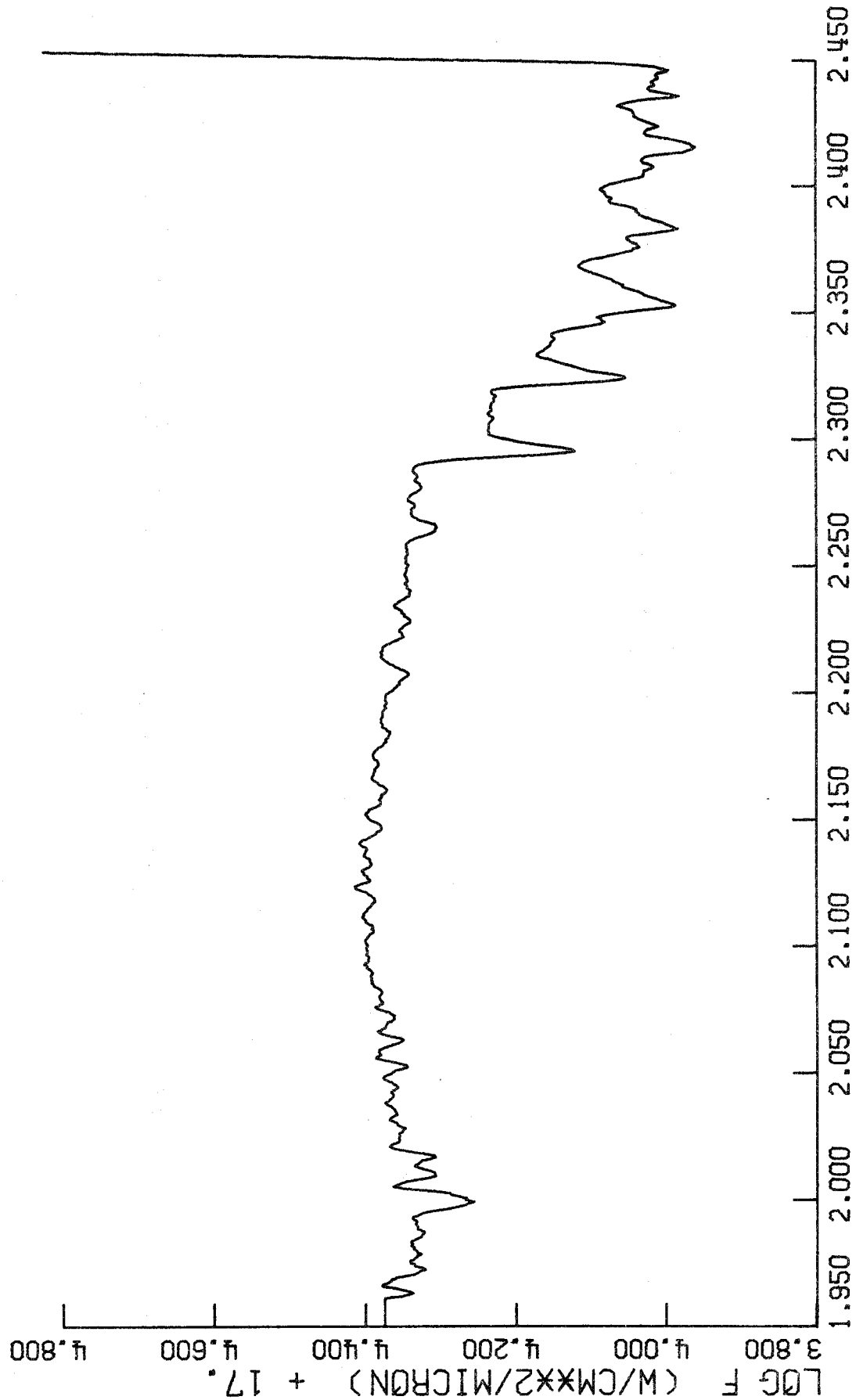
LOG F (W/CM**2/MICRON) + 17.
3.800
4.000
4.200
4.400
4.600
4.800
1.950 2.000 2.050 2.100 2.150 2.200 2.250 2.300 2.350 2.400 2.450
CHI CYG 27 APR 69 60 0.5 6 50 0.5 2 SCANS A LYR

Figure 30.

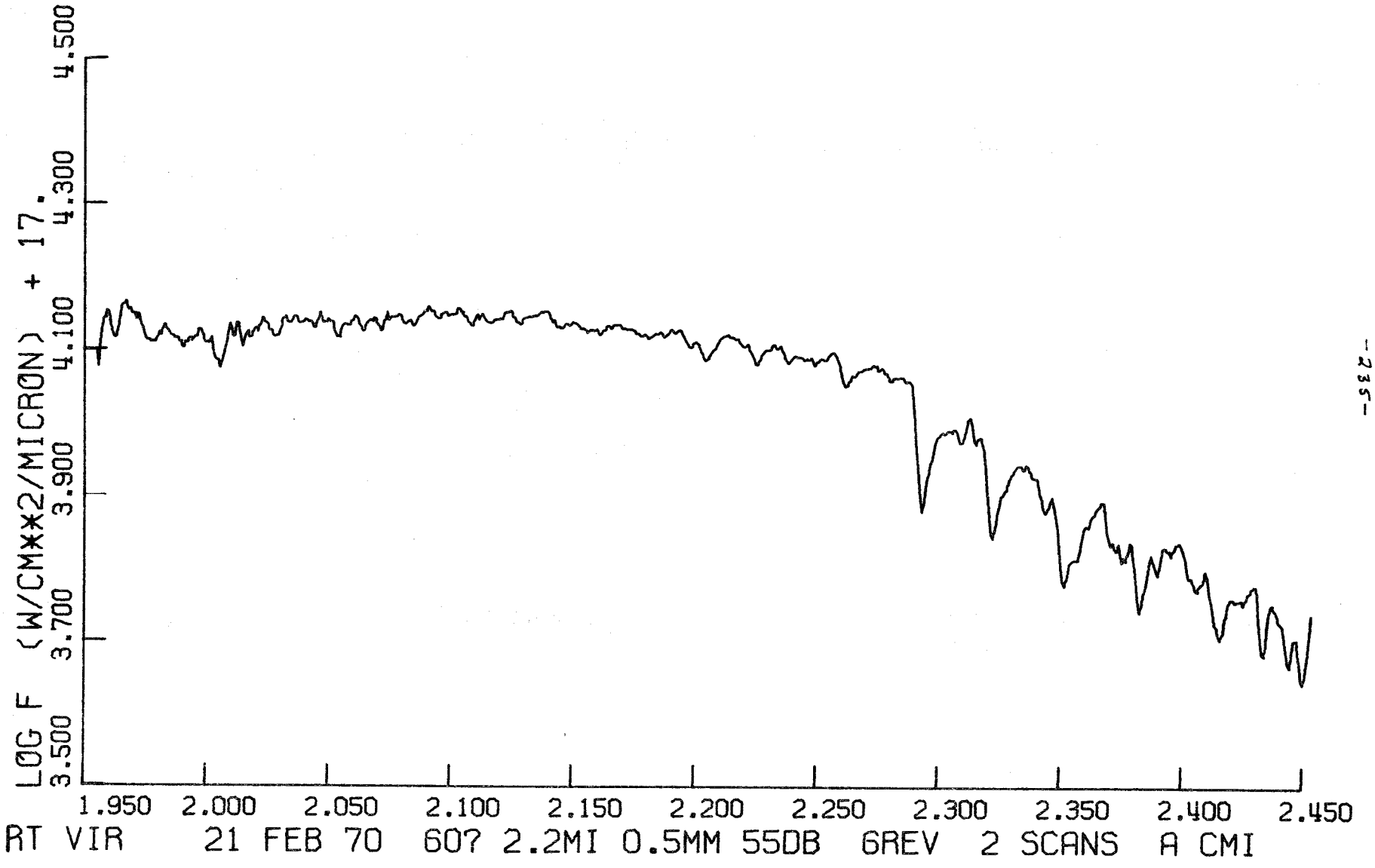
LOG F (W/CM**2/MICRON) + 17.
4.500
4.300
4.100
3.900
3.700
3.500
1.950
2.000
2.050
2.100
2.150
2.200
2.250
2.300
2.350
2.400
2.450
RT VIR 21 FEB 70 60? 2.2MI 0.5MM 55DB 6REV 2 SCANS A CMI

Figure 31.

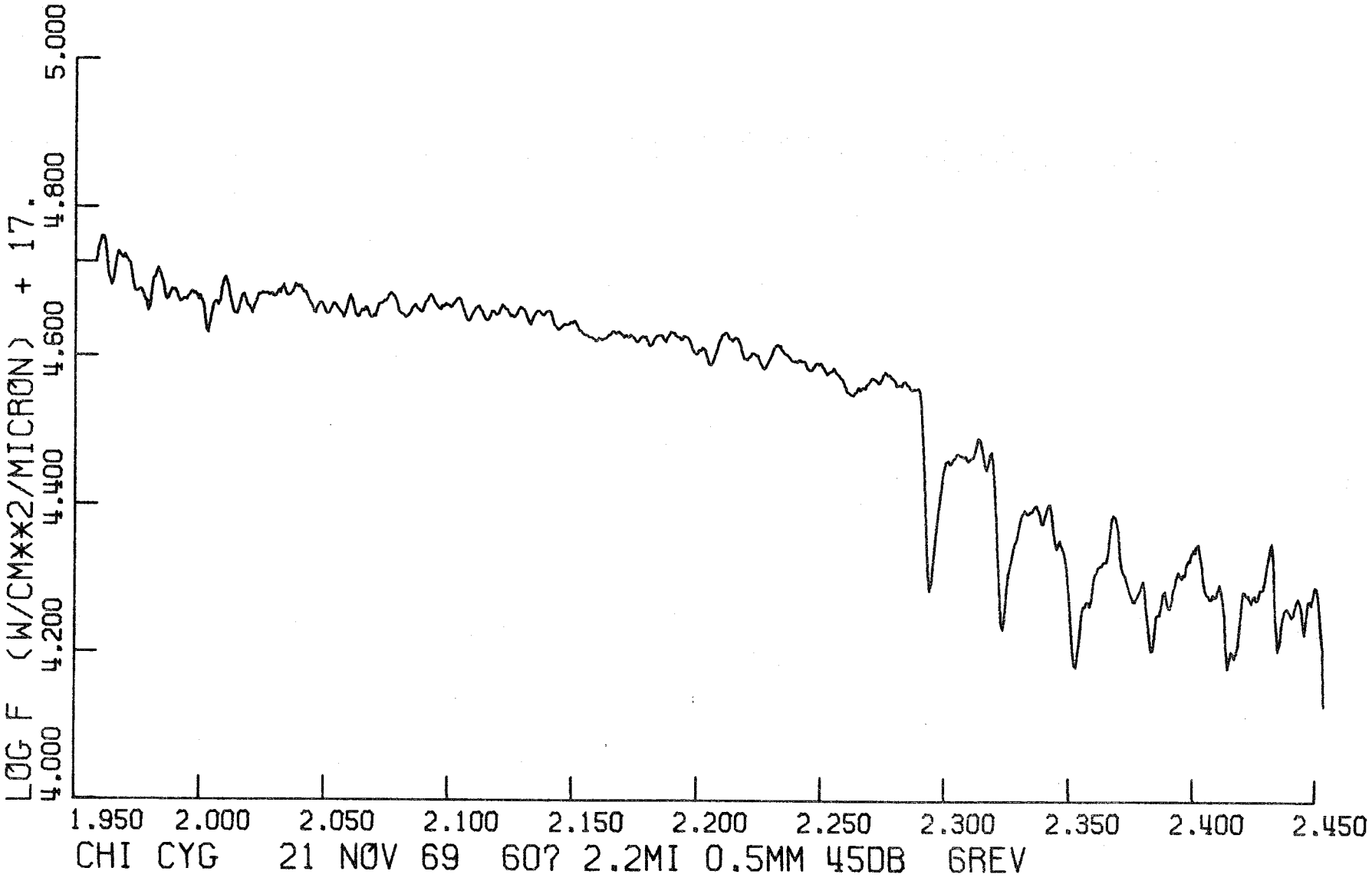
LOG F (W/CM**2/MICRON) + 17.
5.000
4.800
4.600
4.400
4.200
4.000
1.950
2.000
2.050
2.100
2.150
2.200
2.250
2.300
2.350
2.400
2.450
CHI CYG 21 NOV 69 607 2.2MI 0.5MM 45DB 6REV

Figure 32.

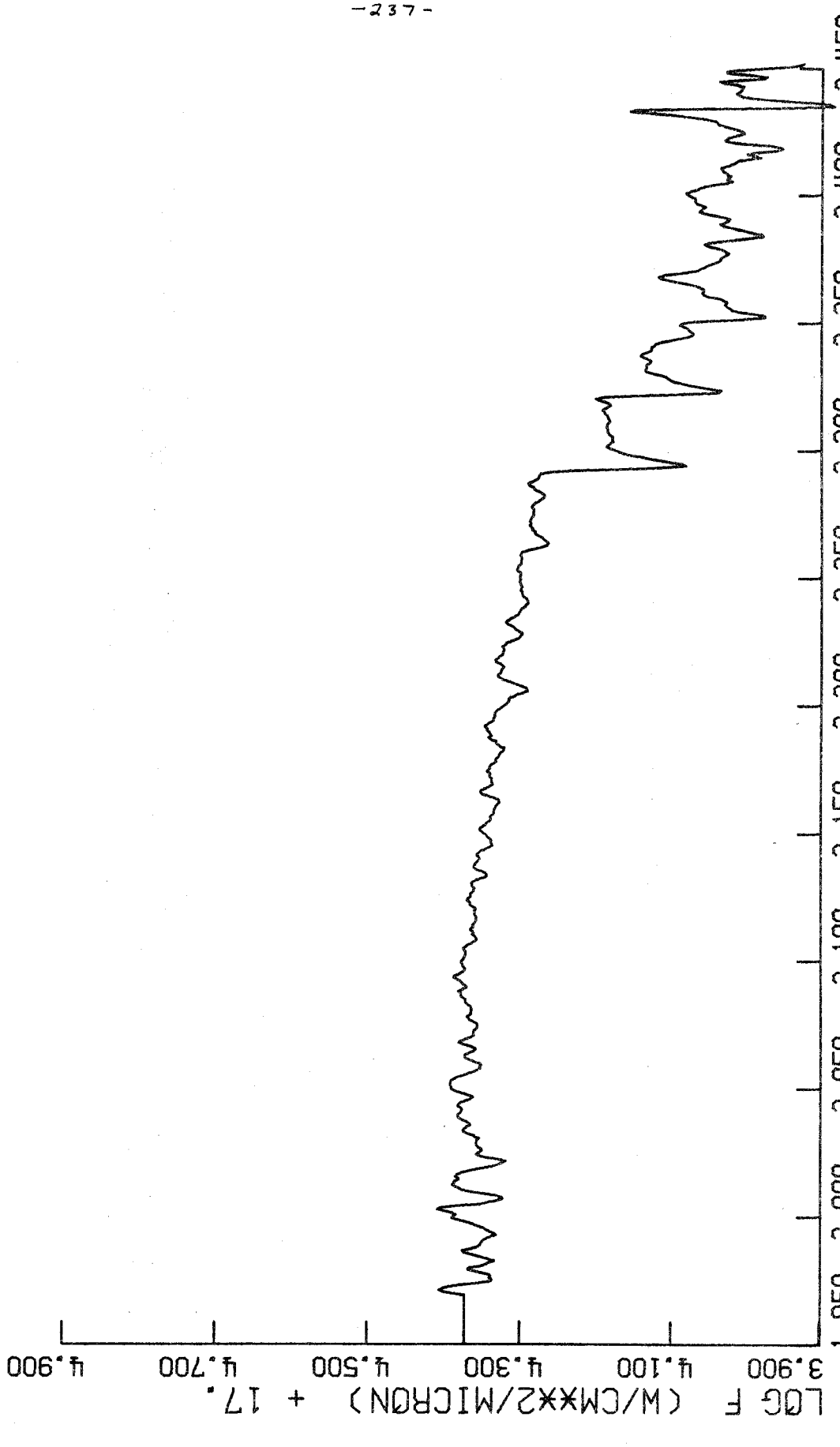
CHI CYG 13 JUN 69 100? 2.2MI 0.5MM 400B 6 REV 2 SCANS A LYR
1.950 2.000 2.050 2.100 2.150 2.200 2.250 2.300 2.350 2.400 2.450
LOG F (W/CM**2/MICRON) + 17.
3.900 4.100 4.300 4.500 4.700 4.900

Figure 33.

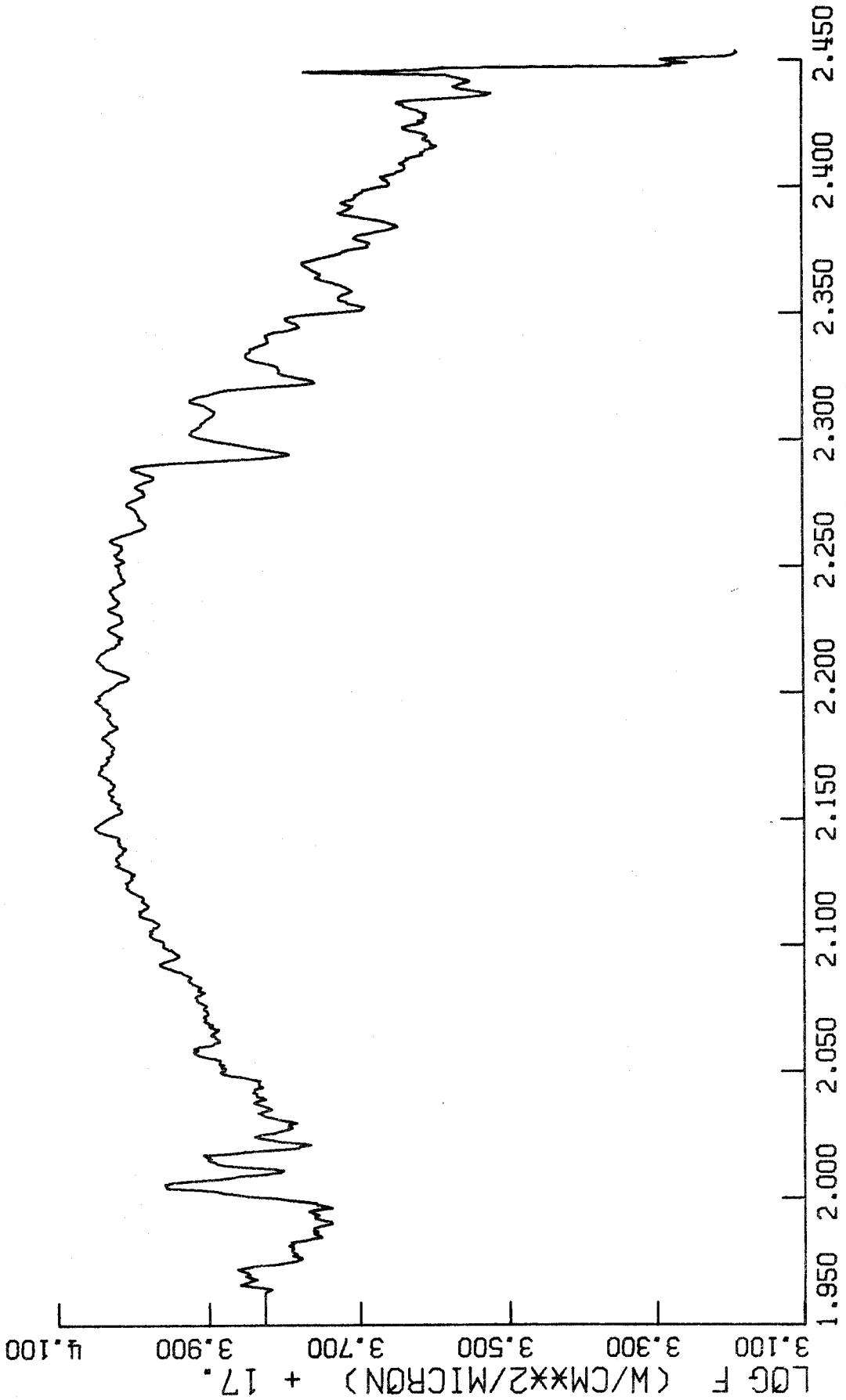
U ORI 21 NOV 69 60? 2.2MI 0.5MM 55DB 6REV
1.950 2.000 2.050 2.100 2.150 2.200 2.250 2.300 2.350 2.400 2.450
LOG F (W/CM**2/MICRON) + 17.
3.100 3.300 3.500 3.700 3.900 4.100

Figure 34.

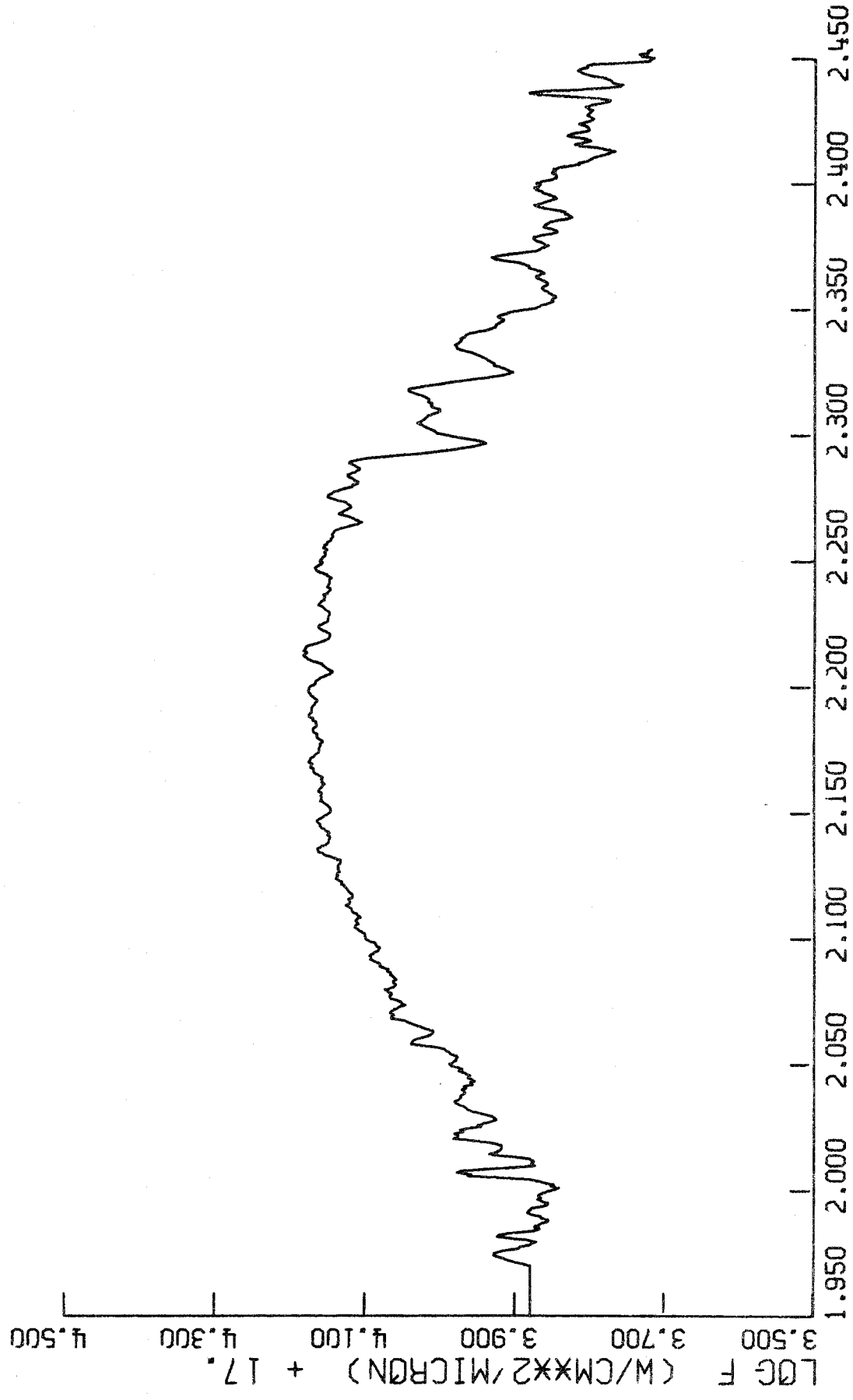
LOG F (W/CM**2/MICRON) + 17.
3.500
3.700
3.900
4.100
4.300
4.500
1.950 2.000 2.050 2.100 2.150 2.200 2.250 2.300 2.350 2.400 2.450
NML TAU 26 SEP 69 60? 2.2MI 0.5MM 500B GREV

Figure 35.

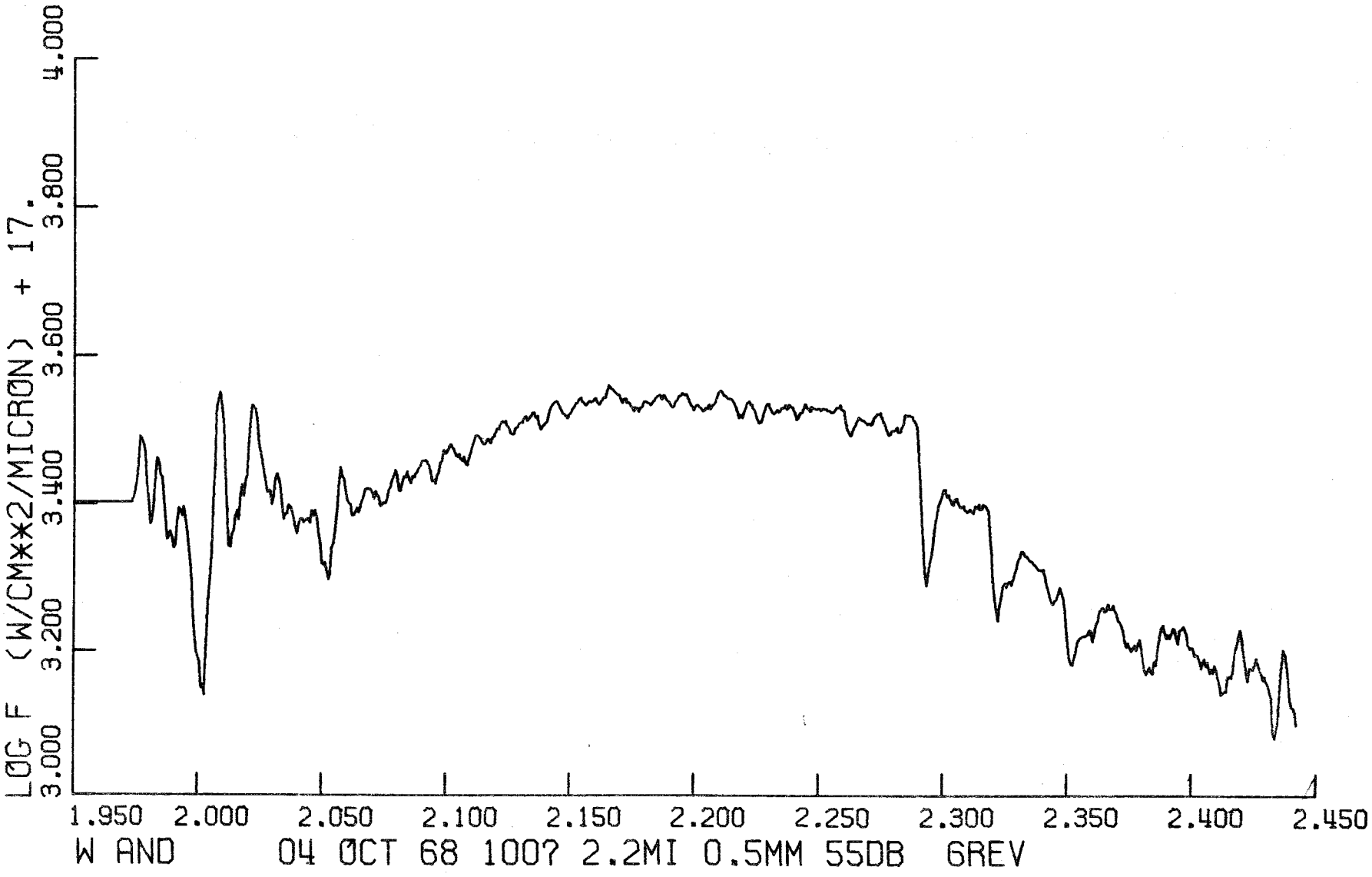
LOG F (W/CM**2/MICRON) + 17.
4.000
3.800
3.600
3.400
3.200
3.000
1.950
2.000
2.050
2.100
2.150
2.200
2.250
2.300
2.350
2.400
2.450
W AND 04 OCT 68 1007 2.2MI 0.5MM 55DB 6REV

Figure 36.

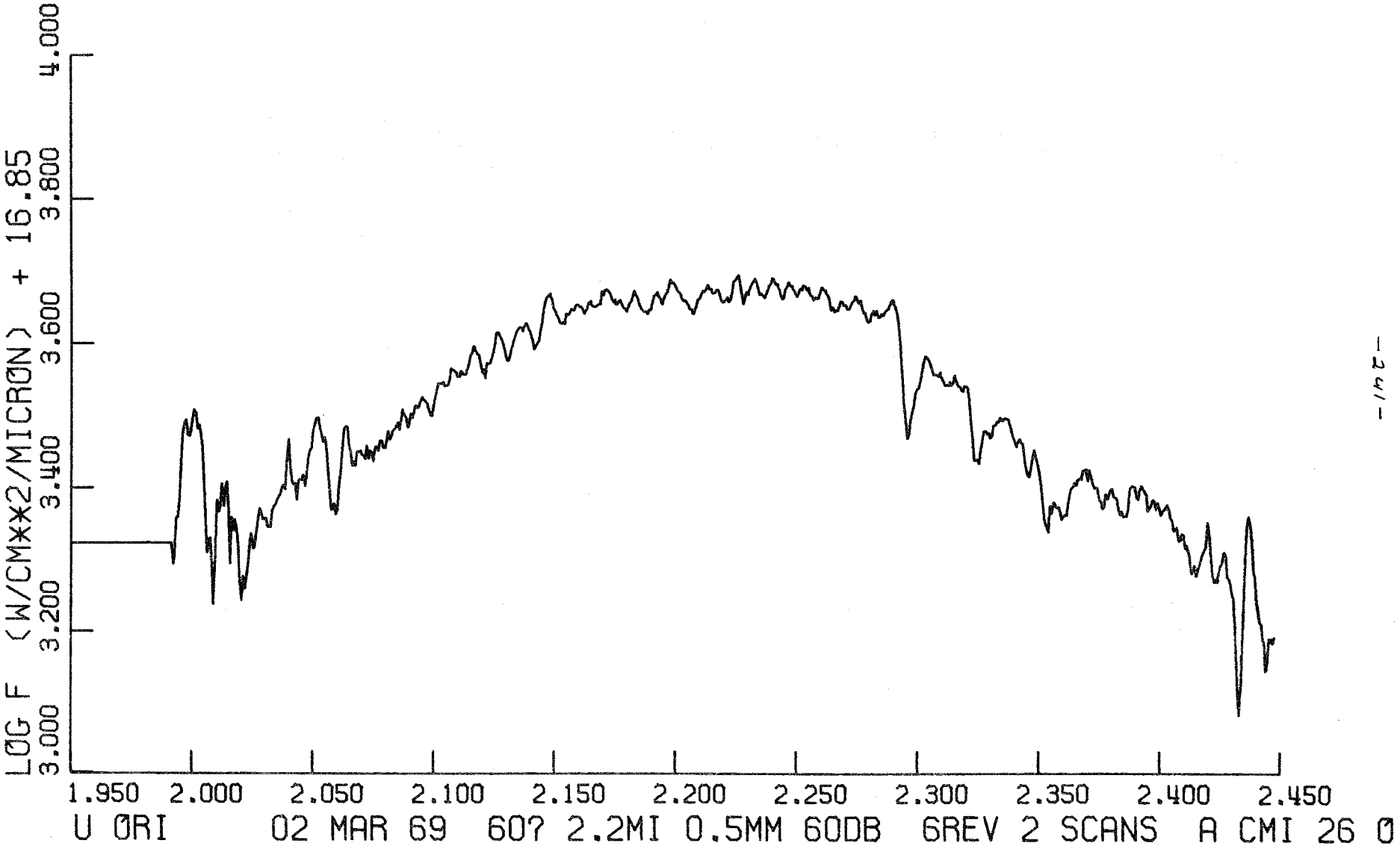
LOG F (W/CM**2/MICRON) + 16.85
4.000
3.800
3.600
3.400
3.200
3.000
1.950
2.000
2.050
2.100
2.150
2.200
2.250
2.300
2.350
2.400
2.450
U ORI 02 MAR 69 60? 2.2MI 0.5MM 60DB 6REV 2 SCANS A CMI 26 0

Figure 37.

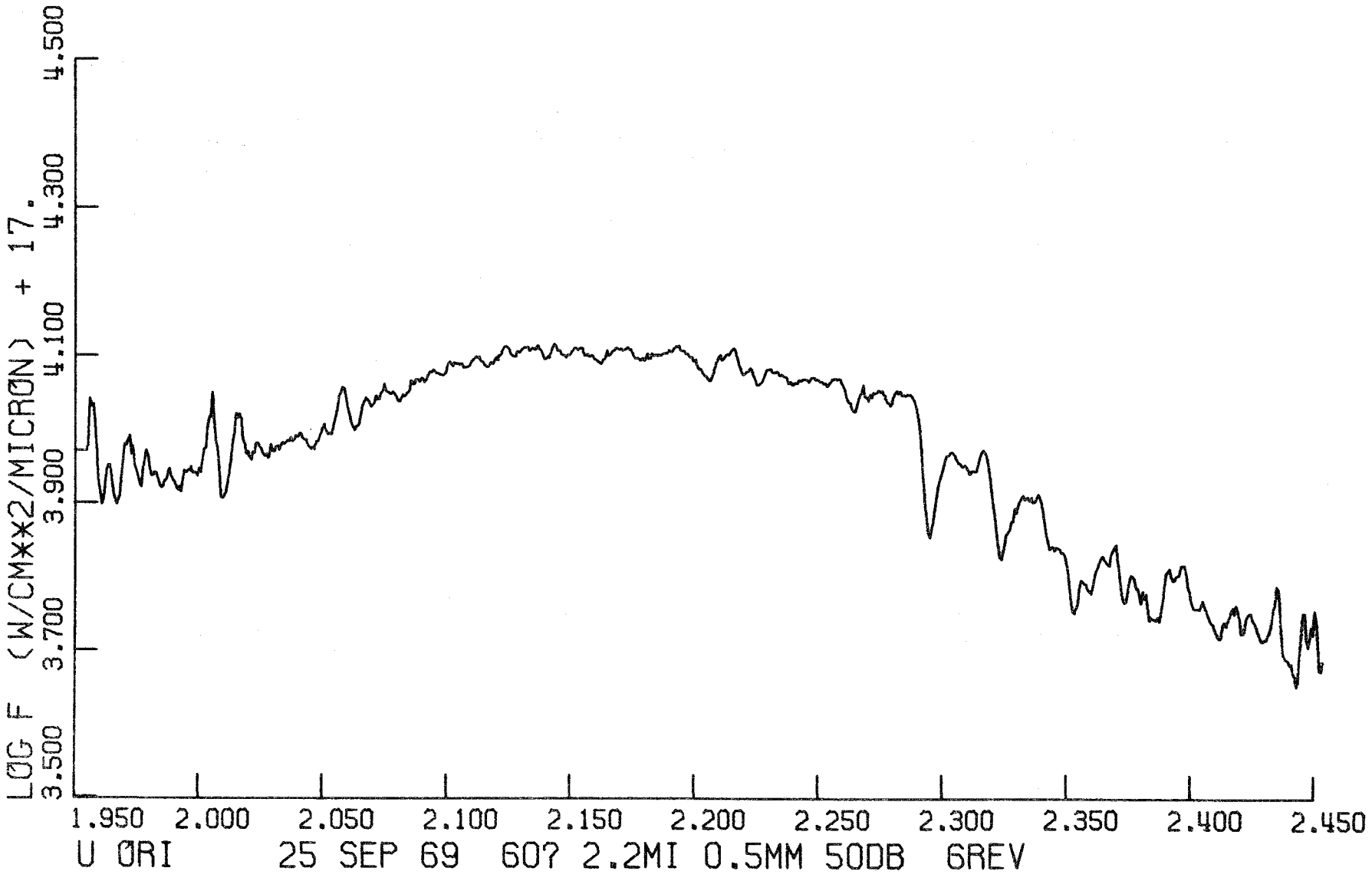
LOG F (W/CM**2/MICRON) + 17.
4.500
4.300
4.100
3.900
3.700
3.500
1.950
2.000
2.050
2.100
2.150
2.200
2.250
2.300
2.350
2.400
2.450
U ORI 25 SEP 69 60? 2.2MI 0.5MM 50DB 6REV

Figure 38.

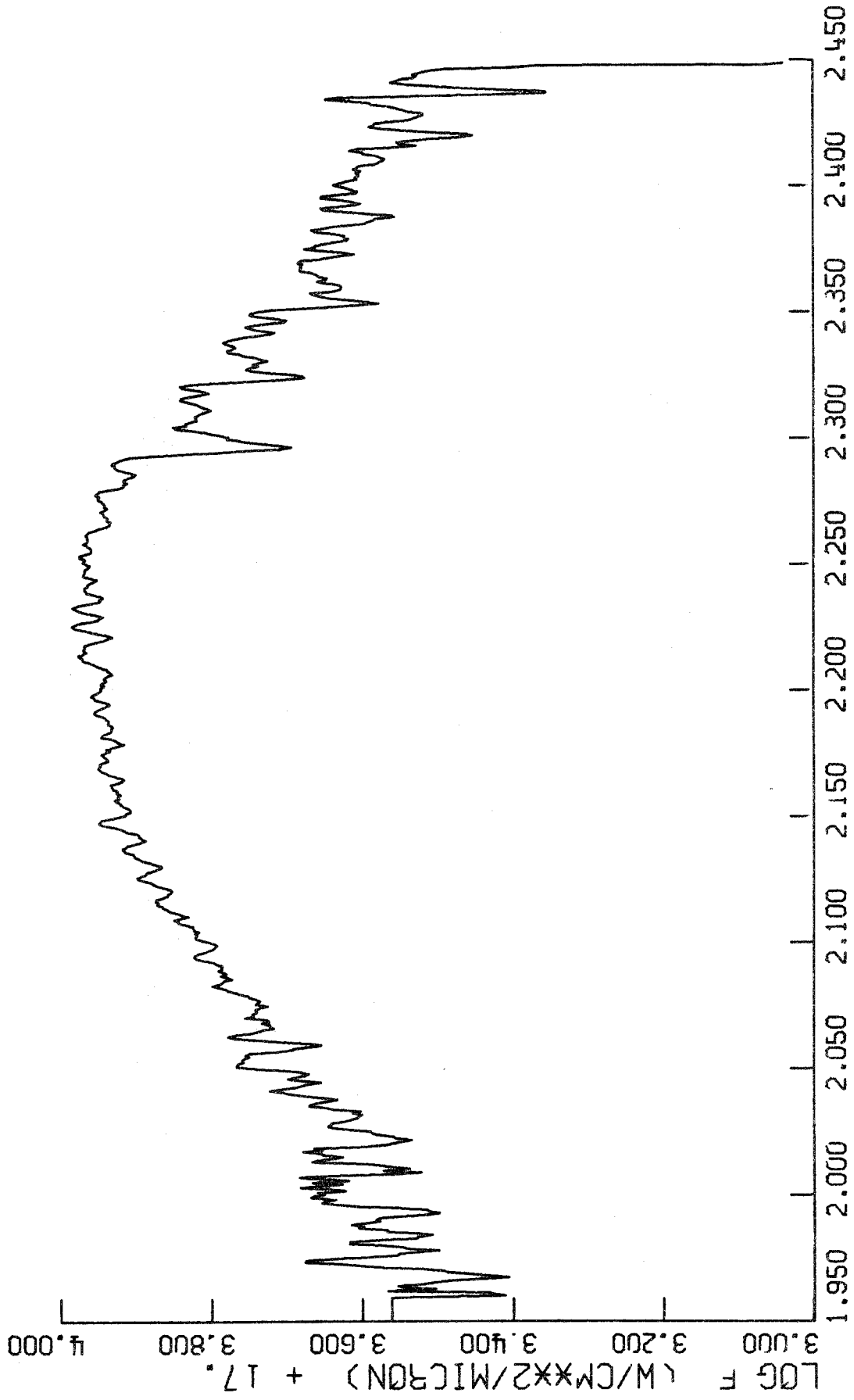
LOG F (W/CM**2/MICRON) + 17.
3.000
3.200
3.400
3.600
3.800
4.000
1.950
2.000
2.050
2.100
2.150
2.200
2.250
2.300
2.350
2.400
2.450
NML TAU 20 DEC 69 60? 2.2MI 0.5MM 550B 6REV

Figure 39.

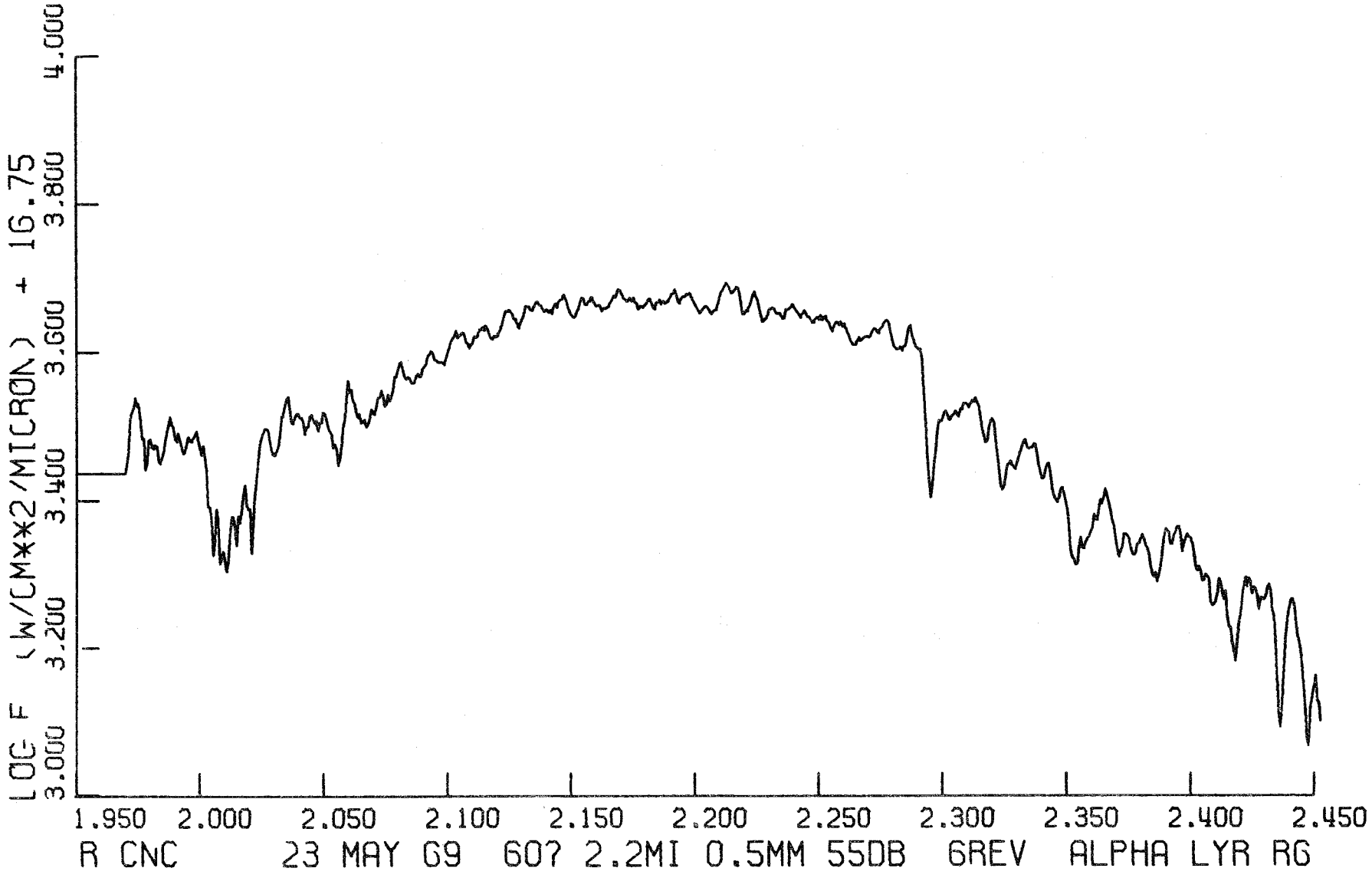
LOG F (W/CM**2/MICRON) + 16.75
4.000
3.800
3.600
3.400
3.200
3.000
1.950
2.000
2.050
2.100
2.150
2.200
2.250
2.300
2.350
2.400
2.450
R CNC 23 MAY 69 607 2.2MI 0.5MM 55DB 6REV ALPHA LYR RG

Figure 40.

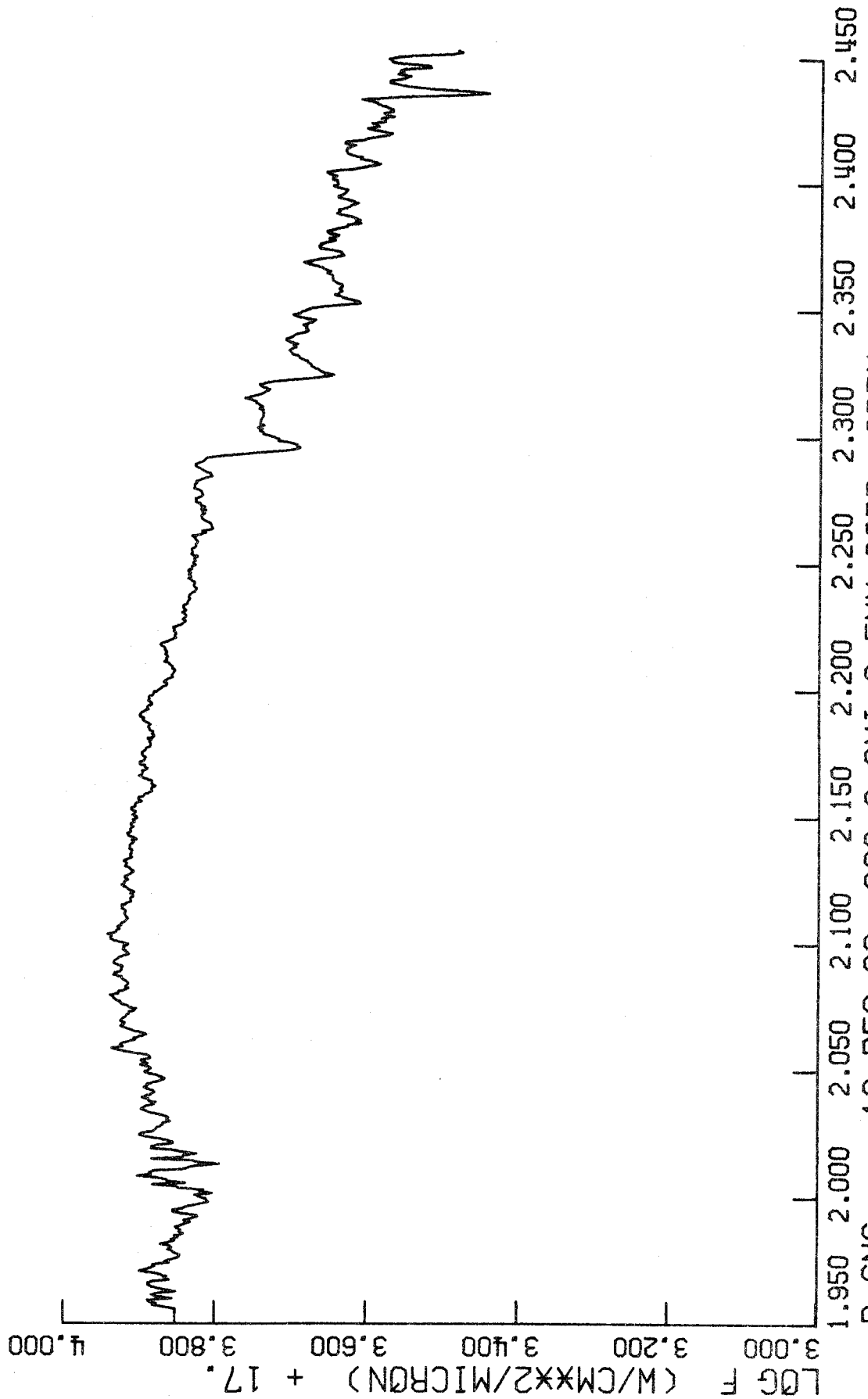
LOG F (W/CM**2/MICRON) + 17.
3.000
3.200
3.400
3.600
3.800
4.000
1.950
2.000
2.050
2.100
2.150
2.200
2.250
2.300
2.350
2.400
2.450
R CNC 18 DEC 69 60? 2.2MI 0.5MM 60DB 6REV

Figure 41.

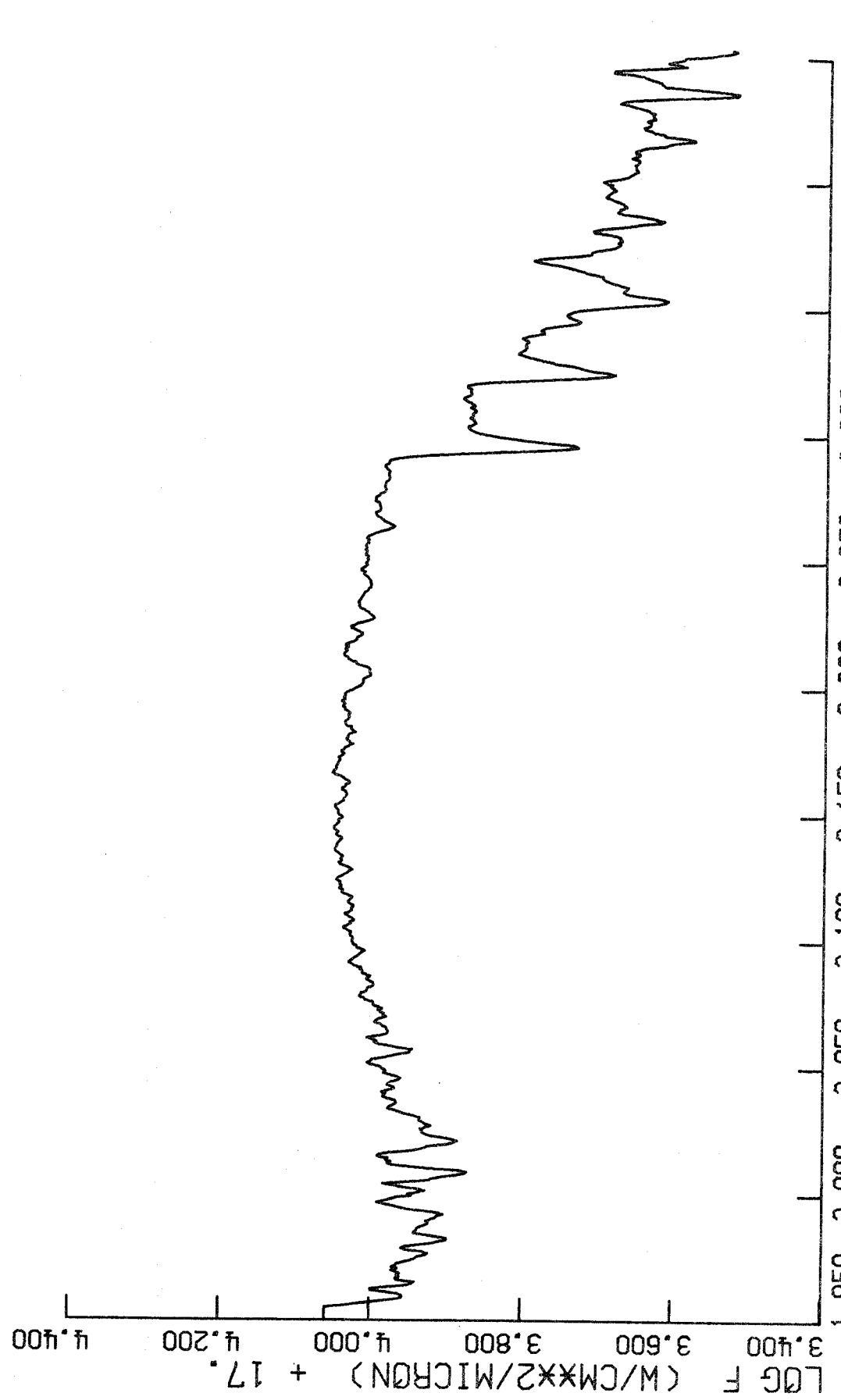
R AUR 26 OCT 69 60? 2.2MI 0.5MM 500B 6REV A CMI
1.950 2.000 2.050 2.100 2.150 2.200 2.250 2.300 2.350 2.400 2.450
LOG F (W/CM**2/MICRON) + 17.
3.400 3.600 3.800 4.000 4.200 4.400

Figure 42.

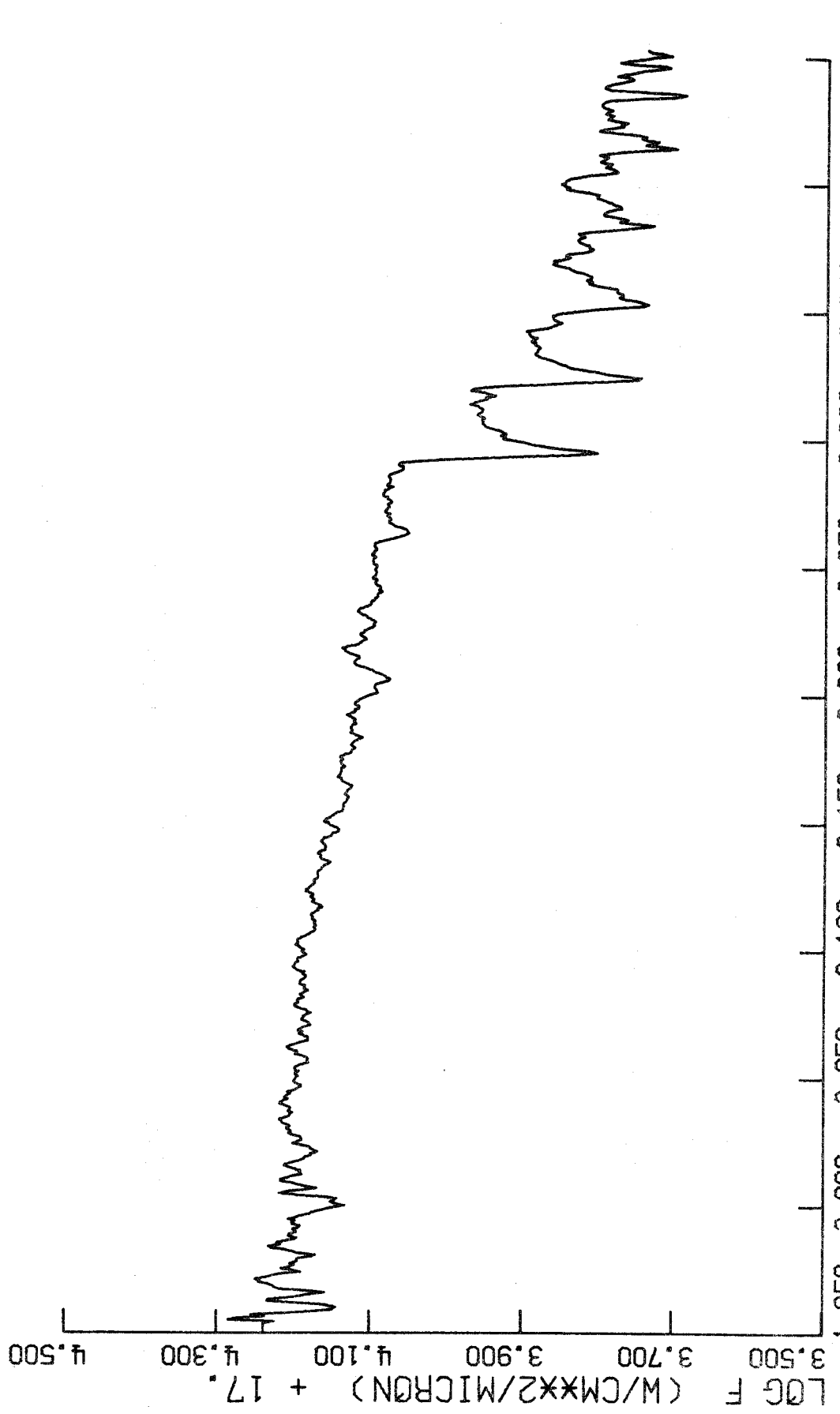
LOG F (W/CM**2/MICRON) + 17.
3.500
3.700
3.900
4.100
4.300
4.500
1.950 2.000 2.050 2.100 2.150 2.200 2.250 2.300 2.350 2.400 2.450
T CAS
20 DEC 69 60? 2.2MI 0.5MM 550B 6REV

Figure 43.

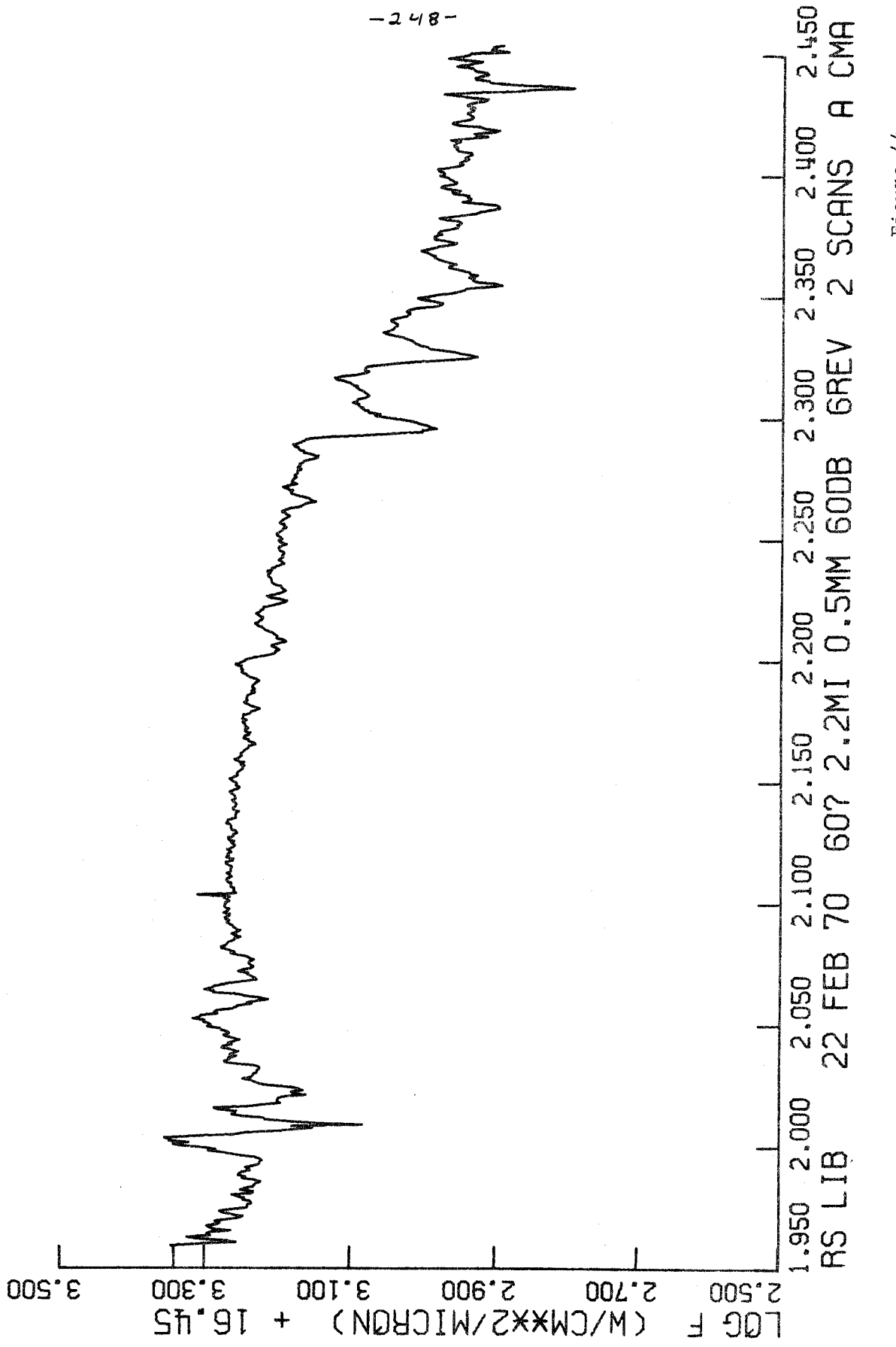
LOG F (W/CM**2/MICRON) + 16.45
2.500
2.700
2.900
3.100
3.300
3.500
1.950 2.000 2.050 2.100 2.150 2.200 2.250 2.300 2.350 2.400 2.450
RS LIB 22 FEB 70 60? 2.2MI 0.5MM 60DB GREV 2 SCANS A CMA

Figure 44.

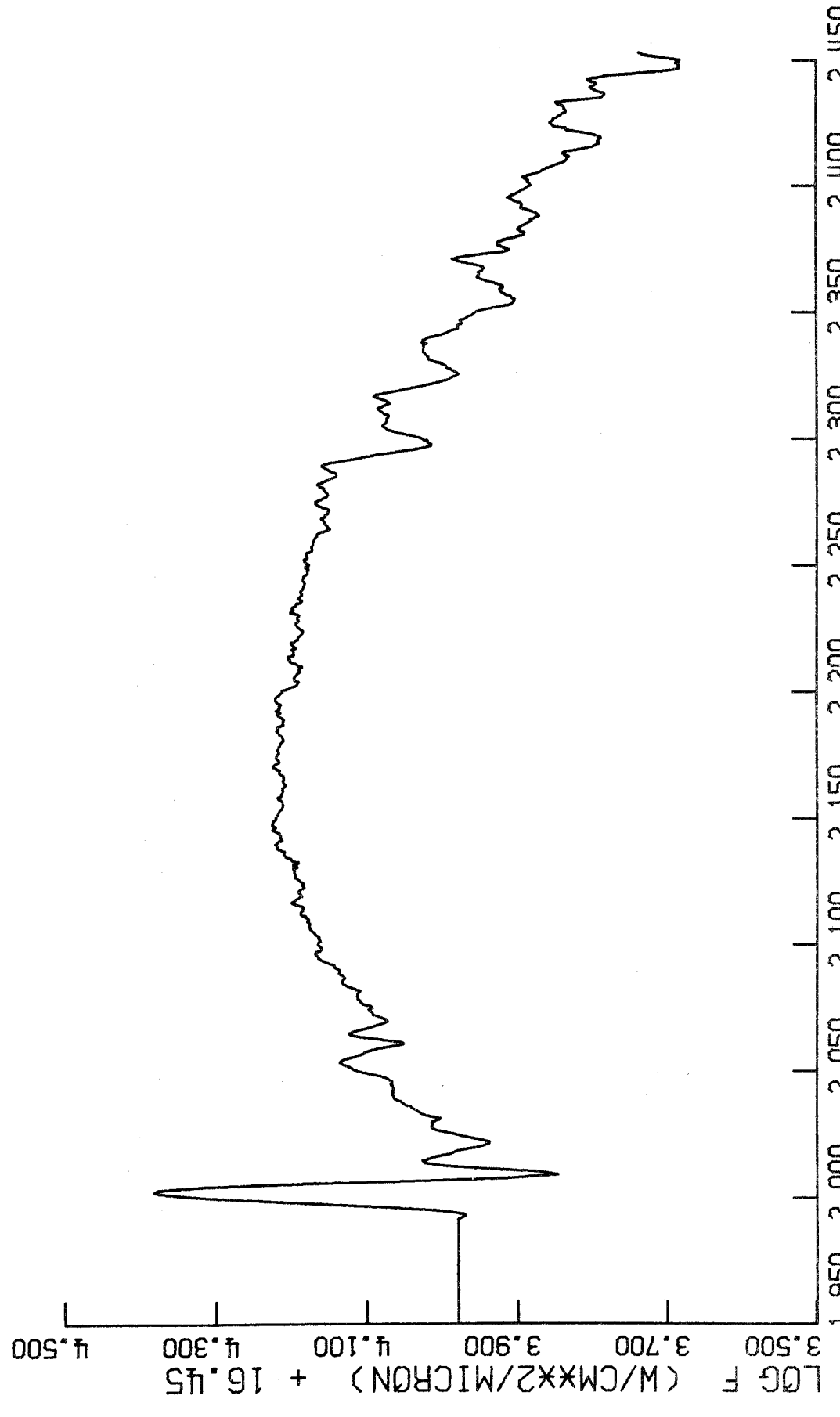
LOG F (W/CM**2/MICRON) + 16.45
3.500
3.700
3.900
4.100
4.300
4.500
1.950 2.000 2.050 2.100 2.150 2.200 2.250 2.300 2.350 2.400 2.450
MIRA 30 JAN 69 60? 2.2MI 0.5MM 40DB 6REV 2 SCANS A CMA

Figure 45.

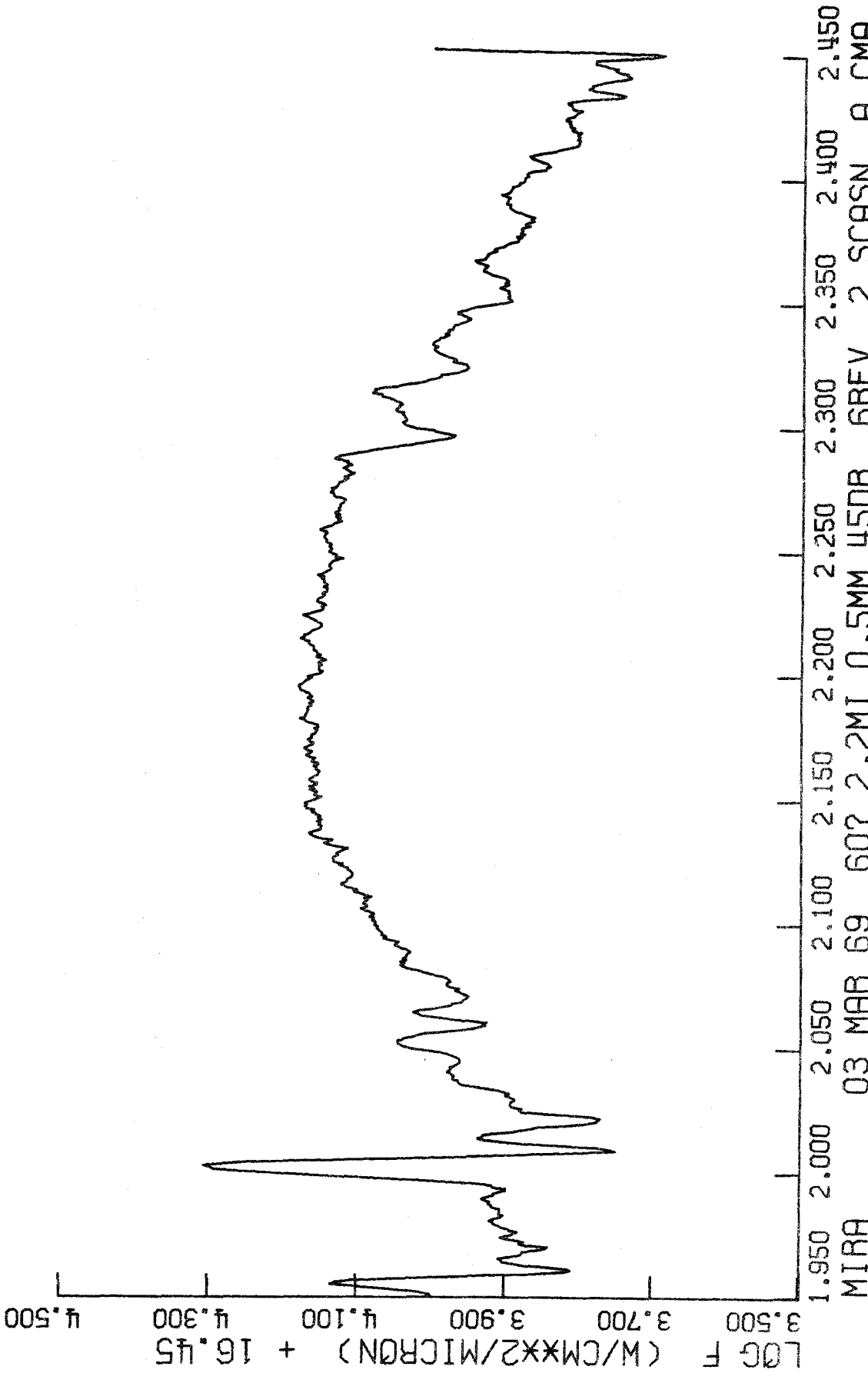
LOG F (W/CM**2/MICRON) + 16.45
3.500
3.700
3.900
4.100
4.300
4.500
1.950
2.000
2.050
2.100
2.150
2.200
2.250
2.300
2.350
2.400
2.450
MIRA 03 MAR 69 60? 2.2MI 0.5MM 45DB 6REV 2 SCASN A CMA

Figure 46.

MIRA 02 AUG 69 1007 2.2MI 0.5MM 30DB 6REV
1.950 2.000 2.050 2.100 2.150 2.200 2.250 2.300 2.350 2.400 2.450
LOG F (W/CM**2/MICRON) + 17.
4.000 4.200 4.400 4.600 4.800 5.000

Figure 47.

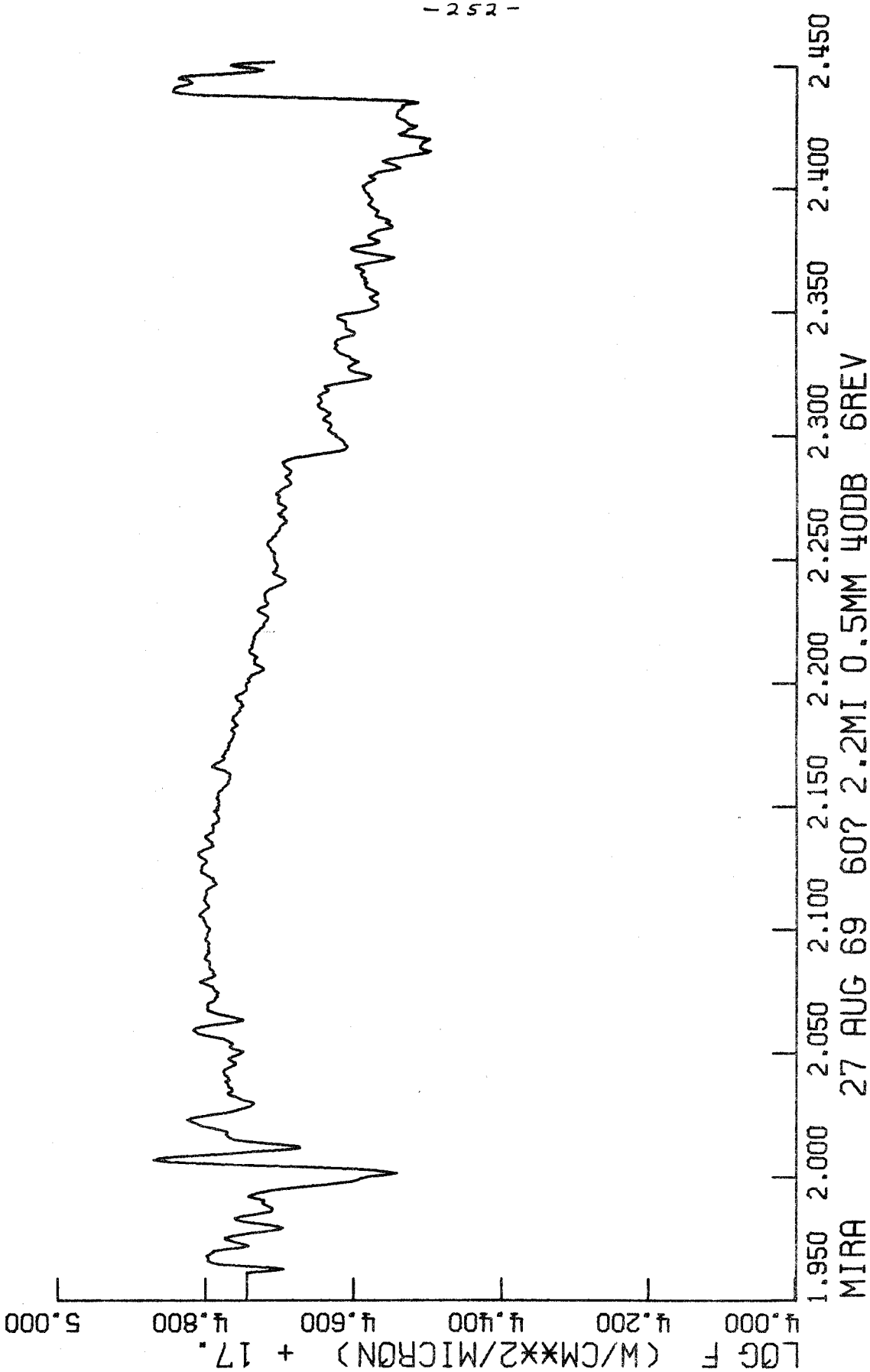
LOG F (W/CM**2/MICRON) + 17.
4.000
4.200
4.400
4.600
4.800
5.000
1.950
2.000
2.050
2.100
2.150
2.200
2.250
2.300
2.350
2.400
2.450
MIRA 27 AUG 69 60? 2.2MI 0.5MM 40DB 6REV

Figure 48.

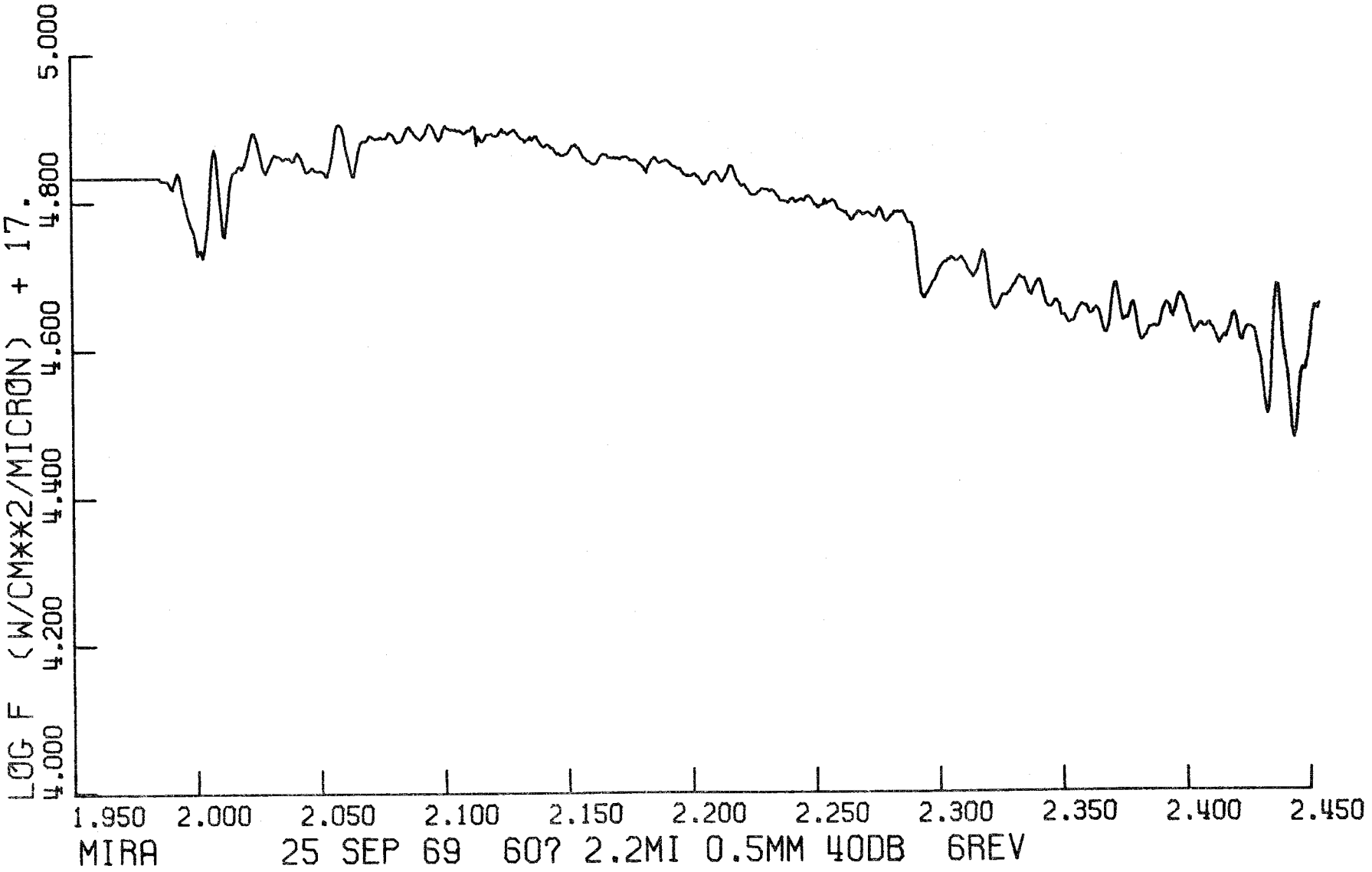
LOG F (W/CM**2/MICRON) + 17.
4.000
4.200
4.400
4.600
4.800
5.000
1.950
2.000
2.050
2.100
2.150
2.200
2.250
2.300
2.350
2.400
2.450
MIRA 25 SEP 69 60? 2.2MI 0.5MM 40DB 6REV

Figure 49.

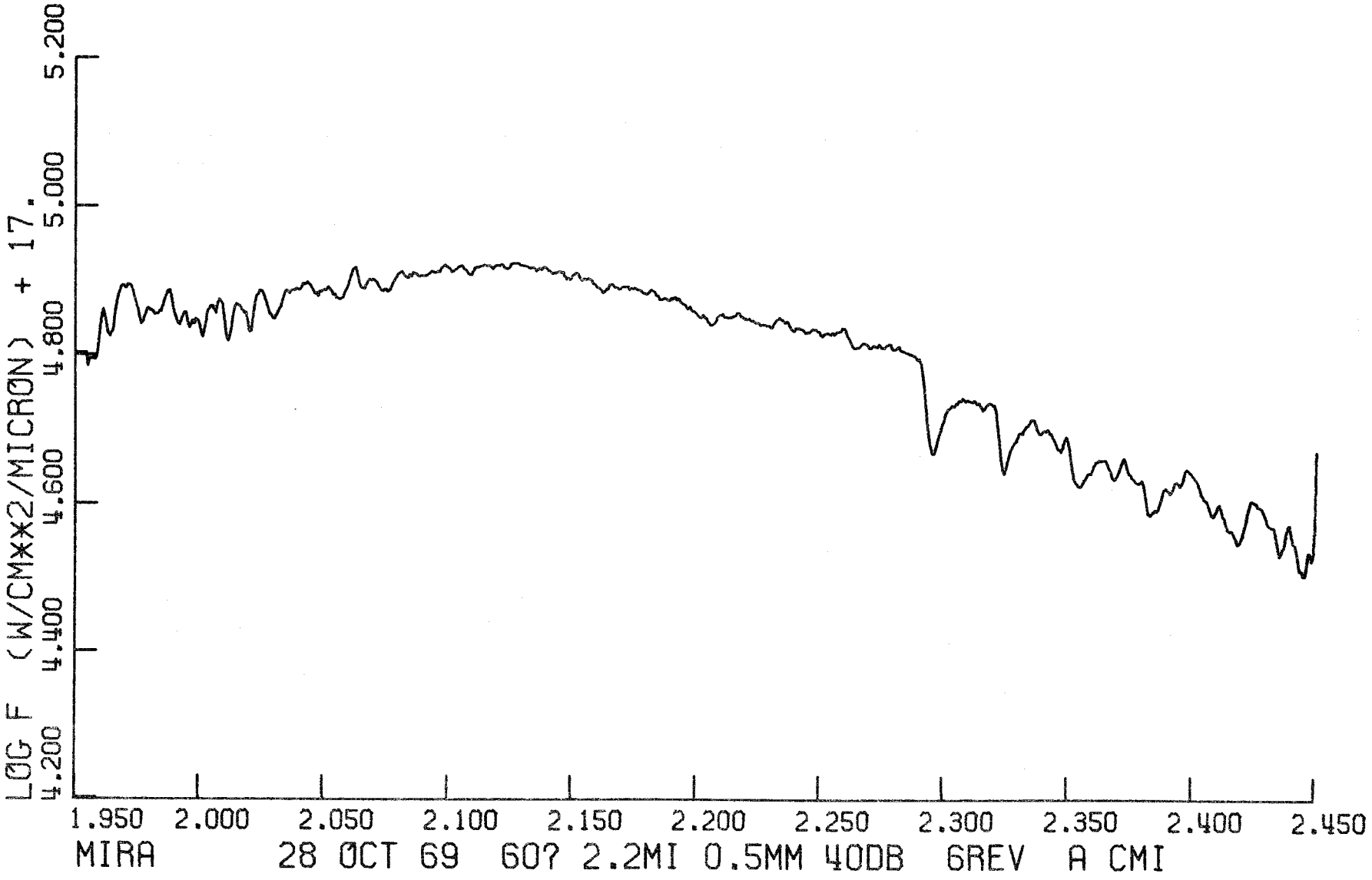
LOG F (W/CM**2/MICRON) + 17.
4.200
4.400
4.600
4.800
5.000
5.200
1.950
2.000
2.050
2.100
2.150
2.200
2.250
2.300
2.350
2.400
2.450
MIRA 28 OCT 69 60? 2.2MI 0.5MM 40DB 6REV A CMI

Figure 50.

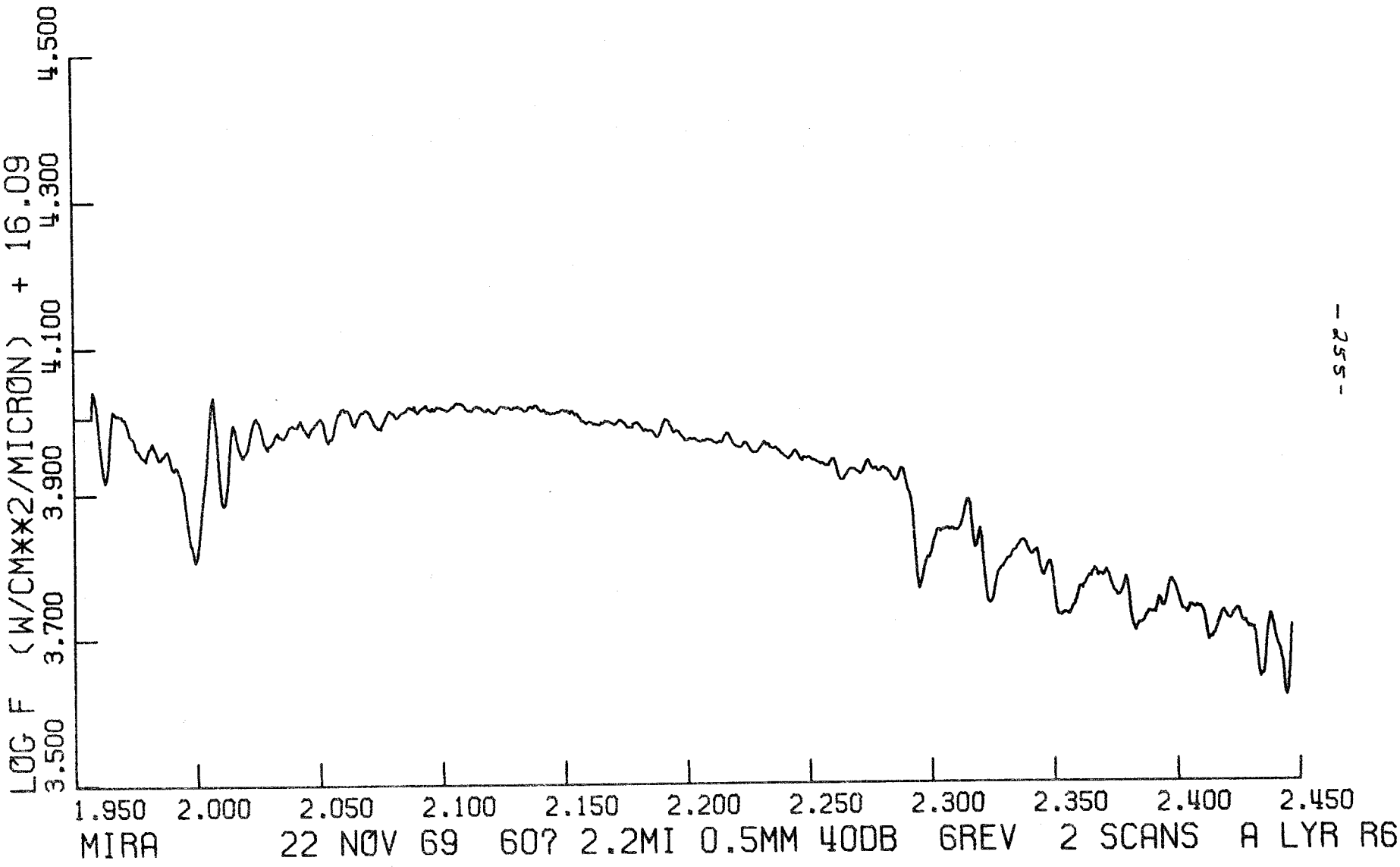
LØG F (W/CM**2/MICRØN) + 16.09
3.500
3.700
3.900
4.100
4.300
4.500
1.950
2.000
2.050
2.100
2.150
2.200
2.250
2.300
2.350
2.400
2.450
MIRA 22 NØV 69 60? 2.2MI 0.5MM 40DB 6REV 2 SCANS A LYR R6

Figure 51.

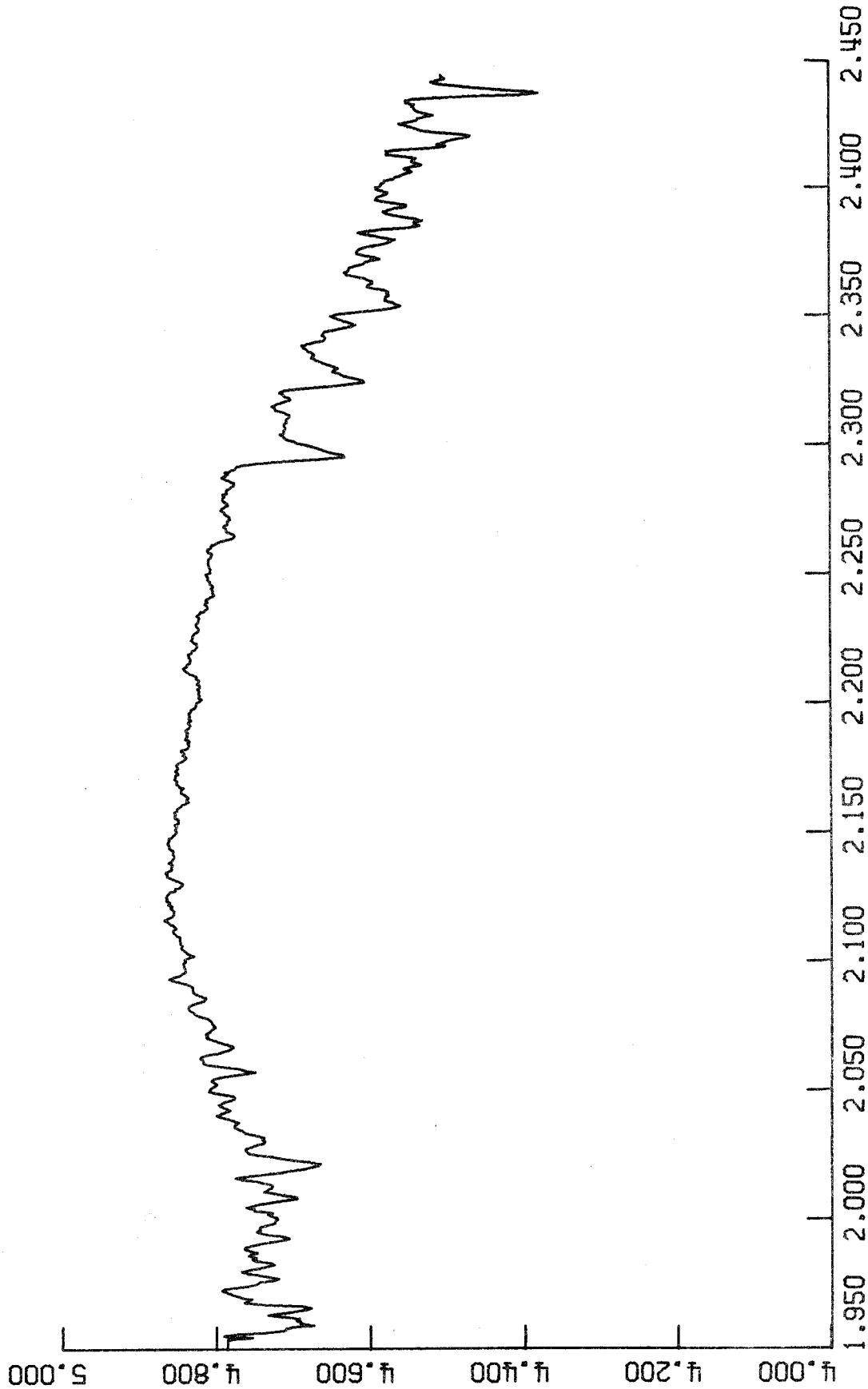
LOG F (W/CM**2/MICRON) + 17.
4.000
4.200
4.400
4.600
4.800
5.000
1.950
2.000
2.050
2.100
2.150
2.200
2.250
2.300
2.350
2.400
2.450
MIRA 20 DEC 69 60? 2.2MI 0.5MM 40DB 6REV

Figure 52.

LOG F (W/CM**2/MICRON) + 16.45
3.500
3.700
3.900
4.100
4.300
4.500
1.950 2.000 2.050 2.100 2.150 2.200 2.250 2.300 2.350 2.400 2.450
MIRAER 22 FEB 70 60? 2.2MI 0.5MM 40DB 6REV 2 SCANS A CMA

Figure 53.

REFERENCES

Auman, Jr., J. R. 1969, Ap. J., 157, 799.

_____. 1970, talk given at Conference on Late-Type Stars, Tucson.

Barbaro, G., Dallaporta, N., and Nobili, L. 1966, in Colloquium on Late-Type Stars, ed. M. Hack (Trieste), 368.

Blanco, V. M. 1964, in Galactic Structure, ed. A. Blaauw and M. Schmidt (Chicago: University of Chicago Press).

Cannon, R. D. 1970, M. N. R. A. S., 150, 111.

Conti, P. S., Greenstein, J. L., Spinrad, H., Wallerstein, G., and Vardya, M. S. 1967, Ap. J., 148, 105.

Deutsch, A. J. 1960, in Stellar Atmospheres, ed. J. L. Greenstein (Chicago: University of Chicago Press).

Deutsch, A. J., and Merrill, P. W. 1959, Ap. J., 130, 570.

Faulkner, J. 1966, Ap. J., 144, 978.

Feast, M. W. 1963, M. N. R. A. S., 125, 27.

Fix, J. D. 1969, M. N. R. A. S., 146, 51.

Frogel, J. A. 1970, Ap. J. (Letters), 162, L5.

Fujita, V. 1970, Interpretation of Spectra and Atmospheric Structure in Cool Stars (Tokyo: University of Tokyo Press).

Fujita, Y., Yamashita, Y., Kamijo, F., Tsuji, T., and Utsumi, K. 1964, Publ. Dom. Astroph. Obs., 12, 293.

Gehrz, R. D., and Woolf, N. J. 1970, Ap. J. (Letters), 161, L213.

_____. 1971, Ap. J., to be published.

Gillett, F. C., Merrill, K. M., and Stein, W. A. 1971, Ap. J., to be published.

Goon, G., and Auman, Jr., J. R. 1970, Ap. J., 161, 533

Gorbatskii, V. G. 1961, Soviet A. J., 5, 192.

Greene, T. F. 1969, Ap. J., 157, 737.

_____. 1970, Ap. J., 161, 365.

Herzberg, G. 1945, Infrared and Raman Spectra of Polyatomic Molecules (New York: D. Van Nostrand Co.).

Hyland, A. R., Becklin, E. E., Frogel, J. A., and Neugebauer, G. 1971, Ap. J., to be published.

Iben, Jr., I. 1965, Ap. J., 142, 1447.

_____. 1966, Ap. J., 143, 483.

_____. 1967, Ap. J., 147, 650.

_____. 1968, Ap. J., 154, 581.

Johnson, H. L., Coleman, I., Mitchell, R. I., and Steinmetz, D. L. 1968, Comm. Lun. and Planet. Lab., 7, 83.

Johnson, H. L., and Méndez, M. E. 1970, Astron. J., 75, 785.

Joy, A. H. 1954, Ap. J. Suppl., 1, 39.

Kamijo, F. 1962, P. A. S. J., 14, 271.

_____. 1963, P. A. S. J., 15, 440.

Keeley, D. 1970, Ap. J., 161, 657.

Keenan, P. C. 1954, Ap. J., 120, 484.

Kippenhahn, R. 1966, in Colloquium on Late-Type Stars, ed. M. Hack (Trieste), 319.

Kunde, V. G. 1968, NASA Technical Note, NASATN D-4798.

Landau, L. D., and Lifshitz, E. M. 1959, Fluid Mechanics (London: Pergamon Press).

Maehara, H. 1968, P.A.S.J., 20, 77.

McCammon, D., Münch, G., and Neugebauer, G. 1967, Ap.J., 147, 575.

Mendoza, V., E. E. 1967, Bol. de los Obs. Ton. y Tac., 4, 114.

Merchant, A. E. 1967, Ap.J., 147, 606.

Merrill, P. W. 1940, Spectra of Long Period Variable Stars (Chicago: University of Chicago Press).

_____. 1952, Ap.J., 116, 18.

_____. ibid., 337.

_____. ibid., 344.

Merrill, P. W., Deutsch, A. J., and Keenan, P. C. 1962, Ap.J., 136, 21.

Merrill, P. W., and Greenstein, J. L. 1956, Ap.J. Suppl., 2, 225.

_____. 1958, P.A.S.P., 70, 98.

Merrill, P. W. 1960, in Stellar Atmospheres, ed. by J. L. Greenstein (Chicago: University of Chicago Press).

Michaud, G. 1970, Ap.J., 160, 641.

Noyes, R. W., Gingerich, O., and Goldberg, L. 1966, Ap.J., 145, 344.

Pettit, E., and Nicholson, S. B. 1933, Ap.J., 78, 320.

Schadee, A. 1968, Ap.J., 151, 239.

Smak, J. 1964, Ap.J. Suppl., 91, 141.

_____. 1966, Ann. Rev. Astr. and Ap., 4, 19.

Spinrad, H., and Newburn, Jr., R. L. 1965, Ap.J., 141, 965.

Spinrad, H., Pyper, D. M., Newburn, Jr., R. L., and Younkin, R. L. 1966, Ap.J., 143, 291.

Spinrad, H., and Vardya, M. S. 1966, Ap. J., 146, 399.

Spinrad, H., Kaplan, L. D., Connes, P., Connes, J., and Kunde, V G. 1971, to be published.

Terrill, C. L. 1969, Astron. J., 74, 413.

Tsuji, T. 1964, Ann. Tokyo Obs., 9, 1.

_____. 1966, P. A. S. J., 18, 127.

_____. 1968, Astron. J., 73, S120.

Vardya, M. S. 1966, M. N. R. A. S., 134, 347.

Wallerstein, G. 1966, Ap. J., 143, 823.

Weymann, R. 1962, Ap. J., 136, 476.

_____. 1963, Ann. Rev. Astr. and Ap., 1, 97.

Wickramasinghe, N. C. 1968, Ap. J., 140, 273.

Wilson, O. C. 1960, in Stellar Atmospheres, ed. by J. L. Greenstein (Chicago: University of Chicago Press).

Wing, R. F. 1966, in Colloquium on Late-Type Stars, ed. M. Hack (Trieste), 205.

Wing, R. F., Spinrad, H., and Kuhi, L. V. 1967, Ap. J., 147, 117.

Wisniewski, W. Z., and Johnson, H. L. 1968, Comm. Lun. and Planet. Lab., 7, 57.

Woolf, N. J., Schwarzchild, M., and Rose, W. K. 1964, Ap. J., 140, 833.

Young, L. A. 1966, Avco Everett Research Laboratory, AMP L88.